Impact of EGFR pathway inhibition on immunogenicity of head and neck squamous cell carcinoma

Justine de Azevedo

UNIVERSITÉ DE STRASBOURG

ÉCOLE DOCTORALE DES SCIENCES DE LA VIE

THESIS presented by :

DE AZEVEDO Justine

soutenue le: **08 Juillet2022**

INSERM U1113 – IRFAC - Strasbourg

Impact of EGFR inhibition on the immunogenicity of head and neck squamous cell carcinoma

Discipline/ Specialty: Molecular and Cellular Aspect of Biology

THESIS DIRECTORS:

JUNG Alain	Researcher ICANS, ICANS, Strasbourg

JURY MEMBERS :

BADOUAL Cécile	external reporter	PR PUPH, INSERM, university of Paris Descartes Sorbonne Paris-cité
GHIRINGHELLI François	external reporter	PR PUPH, INSERM, university of Bourgogne
CERALINE Jocelyn	internal examiner	MCUPH, IGBMC, university of Strasbourg

Dédicace à Amandine !

Remerciements

Ma thèse arrive à son terminus après presque 4 ans d'effort. Ce projet n'aurait pu aboutir sans le soutien d'une équipe soudée et toujours présente en cas de problèmes. L'étalage de sentiments n'est vraiment pas mon point fort cependant, je vais tout de même tenter d'exprimer mes remerciements même si je pense n'arriver qu'à émettre 10% de mon ressenti.

Dans un premier temps, je remercie les membres de mon jury qui ont accepté de juger mon travail de thèse. Sans vous, ma thèse ne pourrait entamer son étape finale. Je vous suis reconnaissante du temps que vous avez accordé à ce travail et espère vous présenter un travail de qualité agréable à décortiquer. Je vous remercie également du délai supplémentaire que vous m'avez alloué pour le rendu du manuscrit.

J'espère t'avoir rendu la monnaie de ta pièce, Alain, toi qui as déjà dû lutter pour que je puisse réaliser mon stage de M2 dans cette équipe. Nous avons ensuite passé l'épreuve du concours de l'école doctorale et enfin 4 ans de galères. Merci de ta prise en charge toujours bienveillante et de m'avoir toujours soutenue dans les différentes épreuves que j'ai pu traverser. Tu as su me redonner confiance après mes échecs et constamment voir le positif dans mon travail. Merci encore de ton implication dans l'écriture et la correction de cette thèse et il y avait du travail !

Alain n'a pas été seul dans mon encadrement, malheureusement ou heureusement pour moi, Christian et Georg ont ajouté leur expertise. Cela a conduit à des débats plus que des réunions sur les trajectoires données à ce projet. Georg, merci pour ton expertise sur les immunofluorescences et pour ton empathie. Christian, merci pour ton implication dans le projet, tes idées et toutes ces réflexions. J'ai particulièrement amélioré mon argumentaire grâce à toi. Un grand merci à vous trois d'avoir été conciliants avec mon caractère pas forcément facile à gérer. Avec le recul, je me rends compte des progrès que j'ai fait grâce à vous, notamment sur les présentations orales, que ce soit au niveau du support comme au niveau du discours.

Merci à Jean-Nöel de m'avoir acceptée dans son unité, et un grand merci à son équipe pour l'aide humaine et matérielle apportée sur ce projet. Merci particulièrement à Isabelle et, Elisabeth qui ont su répondre à toutes mes demandes. Nathalie, je te remercie particulièrement pour le domptage du cytomètre en flux.

Un énorme merci à Chloé Terciolo d'avoir pris le temps de relire ma thèse, et ce, dans un délai assez court. Un grand merci à Pierre pour le cetuximab.

Un merci particulier à Aurélie qui m'a formée sur la manipulation des souris et les injections et sans qui je n'aurais pu réaliser mes expériences *in-vivo* en toute quiétude. Merci aussi pour ton humour et ta bonne humeur constante ainsi que ton écoute toujours disponible.

Je remercie bien évidemment toute l'équipe STREINTH qui a partagé mes hauts et mes bas et remercie Christophe pour l'ambiance musicale ainsi que Erwan pour son soutien.

Merci maman Véronique d'avoir été l'avocat des petits étudiants, de toujours avoir été là pour moi. Tu m'as appris beaucoup de choses et j'ai trouvé en toi une excellente alliée. Tu as été disponible à chaque fois, accessible et de bon conseil. Tu ne m'as jamais laissée dépasser les limites, me montrant quand j'avais raison mais aussi quand j'avais tort, ce qui m'a permis de toujours rester en bons termes avec tout le monde. Merci pour toutes ces discussions, ces rires et ces conseils.

Cyril, si j'étais reine de Westeros, tu serais ma Main du roi. Tu as été celui qui m'a formée sur la culture cellulaire et le MTT et puis tu es devenu mon binôme. La partie *in-vivo* de ce projet, je te la dois, de par ton travail sur les lignées murines et ton aide avec les souris. Merci. Sans toi, je ne sais pas comment j'aurais pu réaliser cette partie. Mais tu as aussi été un excellent homme à tout faire, science, informatique, organisation, ornithologie … Tellement de cordes à ton arc. Je ne sais pas comment tu as fait pour travailler avec moi si désorganisée, c'est certainement ta gentillesse qui a fait tenir notre duo. J'espère te laisser un souvenir aussi agréable que celui que tu me laisses.

Il y a eu des doctorantes et un doctorant après moi. Jana, je te remercie du travail fourni pour l'article. Chloé, Sevda, Mingyi merci d'avoir animé mon bureau pour les derniers mois de ma thèse. Je vous souhaite à tous de réussir tous vos projets et j'espère refaire de nombreuses sorties avec vous.

Il y a eu des doctorantes en même temps que moi, Aimée et Ava, nous avons commencé ensemble en M2 et avons fini ensemble 4 ans plus tard. Dommage que la covid nous ait pris plusieurs mois et avec ça de nombreuses sorties potentielles. Cela dit, on s'est bien amusées et j'espère que vous réaliserez tous vos désirs.

Enfin, il y a eu des doctorantes avant moi. Susanna, je te remercie pour ton aide au microscope et dans la relecture et mise en forme de cette thèse. C'est surtout en dehors du travail que nous avons surtout réalisé nos folies. Des aventures, on en a vécu trop pour toutes les compter. Merci pour ton aide dans l'adoption et l'arrivée de Rocket et ton soutien quand ses problèmes de santé se sont déclarés. Tu as été la seule à comprendre mes blagues sur les deux minutes du peuple et JDG et la seule à avoir partagé ce trait de ma personnalité. Qu'est-ce qu'on a ri en voiture ou à 22h encore au labo pour finir tes manips ! Je te souhaite de t'épanouir complètement et que tu trouveras ta voie. On se voit bientôt en Finlande !

Anaïs, d'abord un énorme, énorme merci pour m'avoir laissée envahir : ta paillasse, ton bureau, ta voiture et ta piscine ! Tu as été là pour me former, puis tu as partagé tes connaissances et ton expertise. Tu n'as pas hésité à t'embarquer avec moi dans des expériences nouvelles et je t'en suis reconnaissante. Tu as été une alliée redoutable durant ma thèse aussi bien sur mon projet professionnel que dans mes projets personnels. J'espère que tu réaliseras tout ce dont tu as envie.

Et puis il y a eu cette personne qui a commencée en stage de M2 avec moi et qui depuis ne m'a plus lâchée. Amandine, j'ai autant eu envie de te tuer que de te serrer dans mes bras. Toutes ces questions qui m'ont mis hors de moi mais qui pouvaient aussi mettre tout mon travail en doute, me permettant alors d'améliorer significativement la qualité de ce dernier. Toutes ces petites prises de tête qui ont menées vers des réponses claires et ont parfois données un sens à tous ces résultats. Tu as été avec moi dès le début du M2 et jusqu'au bout de la thèse. Durant ces 4 ans, tu as été mon agenda, ma calculatrice, mon binôme, ma relectrice et enfin ma partenaire de désespoir. Avoir eu quelqu'un qui vivait la même chose que moi au même moment a été un vrai plus. Mais s'il te plaît Amandine prends confiance en toi, tu n'as pas autant besoin de l'avis des autres, lance-toi ! Par contre, ne change pas ton côté social, car tu as été celle qui a compensée mon manque de sociabilité, et tu m'as servi d'intermédiaire et de bouclier lors d'événements regroupant plein d'inconnus. Tu as défini tes projets depuis un bon moment, alors j'espère que tu deviendras chef de projet dans une entreprise pharmaceutique, que tu te marieras, que tu deviendras propriétaire et enfin fonderas une famille, dans cet ordre !

Matthias et Eva, vous m'avez bousillé bien des week-ends à jouer toute la nuit aux jeux vidéo comme aux jeux de société. On s'est mis dans des états lamentables durant nos balades de 4h dans les bois, à marcher dans l'eau, couper à travers bois, monter et descendre les côtes sauvages. Que dire des sorties Disney, Europa Park, convention et autres qui nous ont mis sur les rotules. Et tellement d'autres sorties ou idioties accompagnées de fous rires mémorables. Merci de m'avoir détournée de ma thèse pour mieux y retourner. Votre soutien a été sans faille durant toutes ces années. Vous me connaissez assez pour savoir que je suis bien incapable de vous montrer toute ma reconnaissance.

Un grand merci à toute ma famille qui m'a toujours soutenue et encouragée dans cette aventure. Je remercie particulièrement mes parents qui m'ont permis de faire des études. Étant une famille pudique, je n'étalerai pas ici toute l'affection que je leur porte, ils en sont de toute façon bien conscients.

Une pensée particulière pour ma grand-mère, moi aussi mémère, je suis bien triste que tu ne vois pas la fin de mon doctorat.

Table of contents

ABBREVIATIONS **1**

SPOILERS **9**

A. MODULATION DE L'IMMUNOGÉNICITÉ DES CARCINOMES ÉPIDERMOÏDES DE LA TÊTE ET DU COU PAR INHIBITION DE L'EGFR **ERREUR ! SIGNET NON DÉFINI.**

1. Analyse des mécanismes cytotoxiques impliqué dans la réponse au co-traitement ... ***Erreur ! Signet non défini.***

2. Mesure la capacité du cetuximab à induire la MCI dans des modèles cellulaires de CETC, in vitro et in vivo ***Erreur ! Signet non défini.***

a. In vitro ..... **Erreur ! Signet non défini.**

b. in vivo ..... **Erreur ! Signet non défini.**

3. Impact du cetuximab sur l'expression de points de contrôle ..... ***Erreur ! Signet non défini.***

B. SCIENTIFIC PUBLICATIONS: 33

INTRODUCTION **35**

CHAPTER I **37**

A. HEAD AND NECK SQUAMOUS CELL CARCINOMA 39

1. Generalities *39*

a. Epidemiology and risks factor 39

b. Carcinogenesis 39

c. Tumor suppressor mutations 39

d. Oncogenic alterations 43

e. Molecular classification of HNSCC 45

f. Biomarkers and survival 47

B. TREATMENTS 49

1. Surgery *49*

2. Radiotherapy *51*

3. Cisplatin *51*

a. Stress response to radiotherapy and chemotherapy 53

4. Cetuximab *57*

a. Cetuximab induces cell cycle arrest 59

b. Cetuximab induces apoptosis 61

c. Cetuximab impact metastasis progression 63

d. Cetuximab induces ADCC 63

CHAPTER II **67**

A. TUMOR MICROENVIRONMENT 69

B. Immune cells.. 71

1. Natural killer ... *71*
2. B lymphocytes ... *75*
3. Dendritic cells ... *77*
4. Macrophage ... *79*
5. Lymphocytes T ... *81*
C. IMMUNE CHECKPOINT ... 87
1. PD-1 / PD-L1 ... *89*
2. CD80, CD86 / CTLA-4 ... *89*
3. TIM-3 / GALECTIN-9 ... *89*
4. LAG-3 / MHC II ... *91*
5. TIGIT / CD155-CD112 ... *91*
6. Immune checkpoint in TME ... *91*

CHAPTER III ... **99**

A. IMMUNOGENIC CELL DEATH ... 101
1. DAMPS ... *101*
a. Calreticulin ... 101
b. ATP ... 101
c. Type-I interferons ... 103
d. HMGB1 ... 103
B. IMMUNE RESPONSE ... 105
C. INDUCERS OF ICD ... 109
1. Pathways inducing ICD ... *109*
a. ER Stress ... 109
b. Autophagy ... 111
2. Type II inducers ... *113*
a. Photodynamic Therapy (PDT) ... 113
b. Pathogens infection ... 113
3. Type I inducers ... *115*
a. Radiation and Chemotherapy ... 115
b. Cetuximab ... 115
D. ICD AND HNSCC ... 117

OBJECTIVES ... **119**

RESULTS ... **125**

ARTICLE ... **127**

COMPLEMENTARY RESULTS **157**

A. RESULTS 159

B. MATERIAL AND METHODS 169

DISCUSSION **173**

A. IMPACT OF THE EXTREME REGIMEN ON HNSCC CELL IMMUNOGENICITY THROUGH DAMPS EMISSION AND THE INDUCTION OF ICD 175

B. IMPACT OF THE EXTREME REGIMEN ON HNSCC CELL IMMUNOGENICITY THROUGH THE REGULATION OF THE EXPRESSION OF ICP 177

C. GENERAL CONCLUSIONS 187

BIBLIOGRAPHY **191**

ARTICLE ANNEX **215**

Figure contents

Figure 1: Generalities about HNSCC. 38
Figure 2: Schematic and simplified representation of HNSCC carcinogenesis. 40
Figure 3: Simplified representation of the 3 main signaling pathways.regulated by EGFR activity. 42
Figure 4: Induction of apoptosis by radiotherapy and cisplatin. 54
Figure 5: Cetuximab impact. 60
Figure 6: Cetuximab induction of ADCC. 62
Figure 7: Simplified schematic representation of the immune system. 68
Figure 8: Composition of the Tumor microenvironment (TME) 84
Figure 9: Immune cell death (ICD) 100
Figure 10: Complementary results 1 158
Figure 11: Complementary results 2 160
Figure 12: Complementary results 3 163
Figure 13: Complementary results 4 165
Figure 14: Complementary results 5 167

Table 1 :Complementary: List of oligonucleotides primers used for RT-qPCR gene expression assays 171

Abbreviations

5-FU: 5-Fluorouracil

ADCC: antibody-dependent cell-mediated cytotoxicity

ALDH1: aldéhyde déshydrogénase 1 de type H1

APC: antigen-presenting cells

AREG: amphiregulin

ATF6: activating transcription factor 6

ATG: autophagy-related *protein*

ATM: ataxia telangiectasia mutated

ATP: adenosine triphosphate

ATR: ataxia telangiectasia and Rad3-related

BAK: BCL2 Antagonist/Killer 1

BAT3: HLA-B associated transcript 3

BAX: Bcl-2–associated X

BCL-2: B-cell lymphoma 2

BCR: B-Cell Receptor

BID: BH3 Interacting Domain Death Agonist

BIP: binding immunoglobulin protein

CAF: cancer-associated fibroblasts

CARL: calreticulin

CCR: C-C chemokine receptor type

CD: cluster differentiation

CDKN2A: cyclin-dependent kinase inhibitor 2A

CHOP: C/EBP homologous protein

CTLA4: cytotoxic T-lymphocyte-associated protein 4

CXCR: C-X-C motif chemokine receptors

DAMP: damage-associated molecular pattern

DC: dendritic cells

DDB2: DNA damage-binding protein 2

DNA: Deoxyribonucleic acid

DR: death receptors

DSB: double-strand break

EGF: epidermal growth factor

EGFR: epidermal growth factor receptor

Eif2α: Eukaryotic Initiation Factor 2

EMT: epithelial-mesenchymal transition

ER: endoplasmic reticulum

EREG: epiregulin

ERK: extracellular signal-regulated kinases

Fab: fragment antigen-binding

FAS: fas cell Surface death receptor

FASL: FAS ligand

Fc: fragment crystallizable region

FDA: food and drug administration

FDXR2: ferredoxin reductase *gene 2*

FOXP3: forkhead box P3

HLA: human leukocyte antigen

HMGB1: high mobility group box 1

HNSCC: head and neck squamous cell carcinoma

HPV: human papillomavirus

HR: homologous recombination

iCAF: immune CAF

ICD: immune cell death

IDO-1: indoleamine 2,3-dioxygénase

IFN: interferon

IFNAR: interferon-α/β receptor

IgG1: immunoglobulin G1

IL: interleukin

IR: irradiation

IRE-1: Inositol-requiring enzyme 1

IRP2: iron regulatory protein 2

IS: immune system

ITAM: immunoreceptor tyrosine-based activation *motif*

ITIM: immunoreceptor tyrosine-based inhibitory *motif*

ITSM: immunoreceptor tyrosine-based Switch Motif IT

JAK: janus kinase

LAG3: lymphocyte-activation gene 3

LAMP: lysosomal-associated membrane protein 1

LCK: lymphocyte-specific protein tyrosine kinase

LN: lymph nods

LRP1: Lipoprotein Receptor-Related Protein 1

LT CD8$^+$: Lymphocytes T CD8$^+$

MDM2: murine double minute 2

MDMX: murine double minute 4

MHC: major histocompatibility complex

MICA: MHC class I polypeptide–related sequence A

MPO: myeloperoxidase

MPTP: mitochondrial permeability transition pore

MTOR: mammalian target of rapamycin

MYD88: Myeloid differentiation primary response 88

NHEJ: Non-Homologous End-Joining

NER: nucleotide excision repair

NF-κB: nuclear factor-kappa B

NK: natural killer

NKG2D: natural killer group 2D

OS: overall survival

OSCC: oral squamous cell carcinoma

OCT4: octamer-binding transcription factor 4

P2X7: P2X purinoceptor 7

P2Y2: P2Y purinoceptor 2

PAMP: pathogen-associated molecular pattern

PBL: peripheral blood lymphocyte

PD-1: Programmed cell death protein 1

PDCD1: Programmed cell death protein 1 gene

PD-L1/2: programmed death-ligand 1/2

PERK: PKR-like ER protein kinase

PI3K: phosphoinositide 3-kinase

PRR: Pattern recognition receptor

PS: phosphatidylserine

PTEN: Phosphatase and TENsin homolog

PUMA: p53 upregulated modulator of apoptosis

R/M: relapse/metastasis

RAF: rapidly accelerated fibrosarcoma

RAGE: receptor for advanced glycation endproducts

RB: retinoblastoma

RNA: ribonucleic acid

RNA-seq: RNA sequencing

ROS: reactive oxygen species

RPS27L: ribosomal protein S27 like:

Sc RNA-seq: single-cell RNA sequencing

SH2: Src Homology 2

SHP2: SH2 domain-containing tyrosine phosphatase-2

SIRNA: small interfering RNA

SNAP: synaptosomal-associated protein

SOX2: sex determining region Y-box 2

SSB: simple strand break

STAT: Signal Transducers and Activators of Transcription

TAA: tumor-associated antigen

TAM: tumor-associated macrophages

TCR: T cell receptor

TGF: transforming growth factor

Th: T helper

TIGIT: T cell immunoreceptor with Ig and ITIM domains

TIM-3: T-cell immunoglobulin and mucin containing protein-3

TKD: tyrosine kinase domain

TLR: toll-like receptor

TLT-2: TREM-like protein 2

TME: tumor microenvironment

TNF: *Tumor necrosis factor*

TNM: tumor node metastasis

TP53: tumor protein 53

TP63: tumor protein 63

TP73: tumor protein 73

TRAIL: TNF-related apoptosis inducing ligand

TREM: Triggering receptor expressed on myeloid cells

Treg: Lymphocyte T regulatory

TYK2: Non-receptor tyrosine-protein kinase

UPR: unfolded protein response

VAMP: vesicle-associated membrane proteins

XBP1: X-box binding protein 1

ZAP70: Zeta-chain-associated protein kinase 70

ZMAT3: Zinc Finger Matrin-Type 3

Spoilers

A. Modulation de l'immunogénicité des carcinomes épidermoïdes de la tête et du cou par inhibition de l'EGFR

Les carcinomes épidermoïdes de la tête et du cou (CETC) définissent un groupe hétérogène de tumeurs malignes qui se développent aux dépens de l'épithélium des voies aérodigestives supérieures (cavité orale, pharynx et larynx). Les principaux facteurs de risque sont la forte consommation de tabac et d'alcool et l'infection par les papillomavirus humains (HPV). Les CETC sont le 6ème cancer le plus fréquent dans le monde, avec plus de 600 000 cas diagnostiqués chaque année. La majorité des CETC sont diagnostiqués à un stade localement avancé (c'est-à-dire quand les structures/tissus locaux sont envahis). La prise en charge de ces tumeurs de haut grade est multimodale et associe la chirurgie, la radiothérapie et la chimiothérapie à base de sels de platine. Dans le cadre des CETC, le sel de platine utilisé est le cisplatine. La radiothérapie et le cisplatine induisent des dommages à l'ADN provoquant l'apoptose des cellules, mais ils peuvent également conduire à ce résultat par l'induction d'un stress oxydatif ou l'augmentation des signaux de mort. Ces deux thérapies sont administrées séparément mais la combinaison radio/chimiothérapie peut être proposée pour les stades les plus avancés. Ces thérapies montrent leurs limites dans le contexte d'apparition de mutations entrainant une perte de fonction des effecteurs de l'apoptose tels que la protéine p53, créant ainsi des résistances aux traitements. Malgré ces modalités de traitements agressifs, le pronostic des CETC ne s'est que marginalement amélioré au cours des 3 dernières décennies, avec une survie globale à 5 ans restant inférieure à 45-50%.

Le cetuximab, un anticorps monoclonal dirigé contre l'EGFR (récepteur du facteur de croissance épidermique), est la seule thérapie ciblée bénéficiant d'une AMM (Autorisation de Mise sur le Marché) pour le traitement des CETC localement avancés. En clinique, le cetuximab est proposé en association avec la radiothérapie ou en association la chimiothérapie et le 5-FU dans le protocole nommé EXTREM, chez les patients en situation récurrente ou métastatique. L'ajout du cetuximab a permis un gain modéré de la survie globale et sans progression.

L'utilisation de cette thérapie ciblée est motivée par une surexpression de l'EGFR dans 90% des CETC. L'EGFR est un récepteur tyrosine kinase activé par autophosphorylation à la suite de sa liaison avec le ligand. Les voies en aval de l'EGFR sont : la voie PI3K/Akt, la voie des MAPKinase, et la voie JAK/STAT, qui régulent positivement le cycle cellulaire et négativement l'apoptose. Le cetuximab se lie à l'EGFR avec plus d'affinité que le ligand naturel, l'EGF (facteur de croissance épidermique), empêchant ainsi l'activation du récepteur. Le cetuximab provoque également l'endocytose de l'EGFR. Tous ces mécanismes mènent à une inhibition des voies en aval de l'EGFR qui a pour conséquences un arrêt de

la prolifération et une induction de l'apoptose. Cependant, l'effet principal du cetuximab serait dû à la cytotoxicité à médiation cellulaire dépendante des anticorps (ADCC) provoquant la lyse de la cellule « marquée » par le cetuximab. Le cetuximab est un anticorps IgG1 dont la partie constante est reconnue par des cellules immunitaires, comme les cellules natural killer et provoque alors la sécrétion de protéines cytotoxiques appelées granzymes et perforines.

Un microenvironnement tumoral est l'environnement dans lequel évoluent les cellules cancéreuses et se compose de divers types cellulaires, dont notamment les cellules immunitaires issues de la réponse anti-tumorale. Cette réponse anti-tumorale est médiée par le système immunitaire qui identifie les cellules cancéreuses comme du « non-soi ». En effet, les cellules cancéreuses produisent des néo-antigènes qui sont reconnus et activent les cellules immunitaires. Ces néo-antigènes apparaîssent suite à des mutations génétiques engendrant l'apparition de protéines différentes ou surexprimées par exemple. Cette réponse immunitaire permet l'élimination de la tumeur. Cependant, la réponse inflammatoire qui découle de cette activation peut être bénéfique au développement tumoral grâce aux nombreux signaux de croissance sécrétés. La réponse anti-tumorale va alors engendrer une pression de sélection sur la tumeur sélectionnant les cellules cancéreuses peu immunogènes donc peu activatrices du système immunitaire. Les cellules cancéreuses peu immunogènes utilisent différents mécanismes pour échapper au système immunitaire comme la diminution de néo-antigènes ou l'expression de points de contrôle immunitaire. Les points de contrôle immunitaire sont des couples ligands-récepteurs dont la liaison inactive les cellules effectrices du système immunitaire. Les cellules cancéreuses détournent ce mécanisme et expriment ces points de contrôle immunitaire afin d'échapper à la réponse anti-tumorale.

Plus récemment, les immunothérapies ciblant des points de contrôle immunitaire ont été développées. L'enjeu de ces approches thérapeutiques innovantes est de lever l'inhibition que les cellules cancéreuses exercent sur les cellules immunitaires présentes dans le microenvironnement tumoral, permettant ainsi de rétablir leur activité cytotoxique anti-tumorale. Les immunothérapies permettent donc de remobiliser le système immunitaire du patient pour éliminer la tumeur. Des essais cliniques ont validé l'efficacité de ces nouvelles stratégies thérapeutiques chez des patients souffrants d'un CETC Ainsi, les anticorps monoclonaux pembrolizumab et nivolumab (dirigés contre PD-1 ; Programmed Cell Death 1) ont été approuvés par la FDA pour le traitement des patients atteints de CETC localement avancés en rechute après utilisation de chimiothérapie à base de cisplatine. En effet, les essais cliniques ayant évalué l'efficacité des immunothérapies démontrent une diminution significative d'environ 20% du risque de

décès, 12 mois après traitement. En revanche, une réponse tumorale partielle (diminution du volume tumoral >50%) ou totale (fonte tumorale complète) n'est observée que chez moins de 20 % des patients. La dérégulation de la présentation des antigènes tumoraux par le complexe majeur d'immunohistocompatibilité ainsi qu'un microenvironnement hypoxique et/ou immunosuppresseur serait à l'origine des résistances innées ou acquises des CETC aux immunothérapies.

Pour améliorer l'efficacité des immunothérapies, deux pistes peuvent être suivies : i) identifier des marqueurs prédictifs de réponse permettant d'affiner la sélection des patients mais limitant le bénéfice de ces innovations thérapeutiques aux seuls patients éligibles ; ii) augmenter la proportion des tumeurs répondant aux immunothérapies, soit en ciblant d'autres points de contrôle immunitaire, soit en augmentant l'immunogénicité des cellules cancéreuses. Cette augmentation de l'immunogénicité peut être induite par une mort cellulaire particulière appelée mort cellulaire immunogène (MCI).

La MCI est un processus cellulaire qui permet le recrutement et l'activation de cellules présentatrices de l'antigène, telles que les cellules dendritiques, qui à leur tour activent des cellules immunitaires effectrices (ex. lymphocytes T, macrophages). La MCI stimule ainsi l'élimination de cellules altérées (ex. cellules infectées, cellules cancéreuses).

Les cellules subissant la MCI émettent plusieurs « signaux de danger », appelés DAMP (Danger Associated Molecular Patterns), qui sont impliqués dans les étapes initiales de l'activation du système immunitaire, à savoir le recrutement, la maturation et l'activation des cellules dendritiques, suivies de l'activation des lymphocytes T cytotoxiques.

Les principaux DAMP décrits à ce jour sont : la translocation membranaire de la calréticuline qui agit comme signal « mange-moi » ; le relargage extracellulaire de HMGB1, responsable de l'inflammation, et de l'ATP, qui agit comme signal « trouve-moi »; et l'induction d'une réponse interféron (IFN) de type I qui agit par chimiotactisme. Ces DAMP sont reconnus par des récepteurs spécifiques présents sur les cellules dendritiques et entraînent leur activation et migration vers les ganglions lymphatiques. Les cellules dendritiques vont alors activer les lymphocytes T $CD8^+$ en leur présentant un antigène associé à la tumeur (AAT). Une fois activés, les lymphocytes T $CD8^+$ vont proliférer et migrer sur le lieu d'inflammation et détruire les cellules tumorales présentant le AAT.

L'émission des DAMP et l'induction de la MCI, dans différents modèles tumoraux, ont été décrites en réponse à des chimiothérapies à base d'oxaliplatine ou d'anthracyclines telles que la doxorubicine. Un lien fonctionnel a été établi entre l'induction de la MCI et le stress du réticulum endoplasmique (RE). Le stress du RE intervient à l'occasion de l'accumulation de protéines mal repliées, et assure la protéostase

ou induit la mort cellulaire si ses capacités sont dépassées par l'intermédiaire de protéines membranaires du RE (IRE1α, PERK, PDI), de plusieurs voies de signalisation et de facteurs de transcription (CHOP, ATF6, ATF4, XBP1) . De manière intéressante, l'émission des DAMP peut être induite par le stress du RE et la phosphorylation du facteur eucaryote d'initiation de la traduction 2α (eIF2α), qui est impliqué dans la protéostase, est un marqueur de la MCI.

Une étude récente a démontré que le cetuximab provoque la MCI de cellules de cancer colique ou rectal, à savoir la translocation membranaire de la calréticuline suivie de la phagocytose des cellules cancéreuses par des cellules dendritiques. De plus, l'injection de cellules traitées par le cetuximab à des modèles murins immunocompétents induit une réponse immunitaire protectrice anti-tumorale dépendante des lymphocytes T cytotoxiques (vaccination), suggérant l'induction d'une MCI *in vivo* par le cetuximab.

En plus de cette capacité du cetuximab à induire une MCI, il pourrait également avoir des effets sur l'expression des points de contrôle immunitaire, cibles des immunothérapies. En effet, l'EGFR et la voie de signalisation PI3K/Akt/mTOR sont impliqués dans la régulation de l'expression transcriptionnelle du gène codant le point de contrôle immunitaire PD-L1 et l'inhibition de l'EGFR peut réprimer cette expression. Enfin, d'autres points de contrôle peuvent être impliqués dans l'anergie de la réponse immunitaire ou prendre le relais de PD-L1 en réponse à son inhibition.

Ainsi, on ignore à l'heure actuelle dans quelle mesure l'inhibition de la voie de l'EGFR peut moduler l'immunogénicité des cellules et potentialiser les immunothérapies, et cela, au travers de l'induction de la MCI ou de la modulation de l'expression de cibles des immunothérapies.

Ma thèse formule donc l'hypothèse que le traitement des CETC par le cetuximab peut provoquer une MCI, impacter l'expression de points de contrôle immunitaire et, de ce fait, potentialiser les immunothérapies inhibant les points de contrôle immunitaire.

L'influence de l'inhibition de la voie de l'EGFR ou encore l'effet de la combinaison entre le cisplatine et le cetuximab sur l'immunogénicité tumorale n'ont pas été caractérisés. Une compréhension globale de l'adaptation des cellules tumorales au traitement est donc indispensable pour choisir les immunothérapies les plus pertinentes en fonction de l'expression de leurs cibles et favoriser le transfert de cette combinaison thérapie ciblée/immunothérapie vers la routine clinique. Ainsi, les objectifs de ma thèse sont : de comprendre les **mécanismes impliqués dans la réponse toxique** au cetuximab seul ou en combinaison avec le cisplatine, de mesurer la **capacité du cetuximab à induire la MCI** dans des modèles cellulaires de CETC, *in vitro* et *in vivo,* et finalement d'analyser l'**impact d'un traitement par le cetuximab sur l'expression de points de contrôle immunitaire.**

À cette fin, mon travail de thèse a évalué la capacité du cetuximab à induire l'émission des DAMP (translocation membranaire de la CALR, relargage extracellulaire de HMGB1, réponse IFN de type I) dans des modèles cellulaires de CETC *in vitro* et a déterminé la capacité du cetuximab à induire une MCI fonctionnelle *in vivo*, à travers des expériences de vaccination grâce à l'utilisation de modèles syngéniques de CETC. Enfin, j'ai analysé l'impact d'un traitement par le cetuximab sur l'immunogénicité des cellules de CETC et notamment sur l'expression de points de contrôle immunitaire.

1. Analyse des mécanismes cytotoxiques impliqués dans la réponse au co-traitement

L'ensemble des résultats obtenus au cours de mes travaux de thèse repose sur l'exploitation de deux lignées cellulaires HPV-négatives et portant un allèle muté de *TP53*. D'une part, la lignée cellulaire SQ20B est utilisée comme prototype de lignée de CETC résistante au cetuximab (établie à partir d'une tumeur du larynx) et, d'autre part, la lignée cellulaire CAL27 est utilisée comme modèle de CETC sensible au cetuximab (établie à partir d'une tumeur de la langue). La dose minimale de cetuximab permettant son efficacité maximale *in vitro* est de 2.5 µg/mL pour les deux lignées cellulaires. À cette concentration, le cetuximab provoque une diminution de la prolifération cellulaire de respectivement ~10% et ~30% chez les cellules SQ20B et CAL27. Les doses inhibitrices de la combinaison cetuximab/cisplatine ont été déterminées avec une dose fixe de cetuximab (2.5µg/ml) et différentes doses de cisplatine. La combinaison est plus cytotoxique que le cisplatine seul dans la lignée CAL27 mais l'ajout du cetuximab a l'effet inverse dans la lignée SQ20B avec une baisse de la cytotoxicité par rapport au cisplatine seul. Pour la suite de l'étude, le cetuximab a été utilisé seul (2.5µg/ml), le cisplatine a été utilisé seul aux IC_{50} , IC_{75}, et IC_{90} tout comme la combinaison cetuximab/cisplatine.

L'analyse de l'impact du cetuximab, du cisplatine, seuls ou combinés, a été réalisée par cytométrie en flux après marquage à l'iodure de propidium (IP) et à l'annexine V (AV) et montre un arrêt en phase G2 du cycle cellulaire, particulièrement à l'IC_{75} du cisplatine seul ou combiné dans les deux lignées. La proportion de cellules en début d'apoptose (IP-AV+) est augmentée seulement après 48h de traitement avec le cisplatine dans les deux lignées. La proportion de cellules en fin d'apoptose (IP+AV+) est augmentée de façon dose-dépendante dans la lignée SQ20B dans chaque condition de traitement. Par ailleurs, la lignée CAL27 montre une augmentation plus importante. Ainsi, le cetuximab seul ou combiné au cisplatine, montre un arrêt en phase G2 du cycle cellulaire et suggère la mise en place d'une apoptose. Afin de confirmer la mise en place de l'apoptose, une analyse du clivage de la caspase 3 a été

réalisée par western blot. Un signal correspondant au clivage de la caspase 3 est obtenu dans toutes les conditions, avec une intensité différente selon les doses utilisées, excepté lors du traitement avec le cetuximab,. Ainsi, l'apoptose observée en cytométrie en flux semble passer par le clivage de la caspase 3 dans le cas du traitement au cisplatine seul ou du co-traitement. Ce mécanisme semble avoir une cinétique différente selon le temps de traitement. Une induction de la caspase 3 clivée est détectée à 24h pour l'IC_{75} et une forte induction avec l'IC_{90}, mais après 48h de traitement, la tendance est inversée avec une induction plus forte à l'IC_{75} qu'à l'IC_{90}.

En conclusion, nos observations sont cohérentes avec le fait que le traitement des cellules CETC par le cisplatine seul ou combiné au cetuximab altère la viabilité cellulaire *via* l'inhibition du cycle cellulaire et l'induction de l'apoptose, avec un impact biologique plus important dans les cellules CAL27 par rapport aux cellules SQ20B.

Afin d'étudier les bases moléculaires de l'induction de l'apoptose, nous avons étudié l'expression des membres de la famille p53 composée de p53, p63 et p73. La protéine p53, en particulier, est impliquée dans la cytotoxicité et l'apoptose des cellules induites par les sels de platine. Le facteur de transcription p53 est impliqué dans l'arrêt du cycle cellulaire et dans la mise en place de l'apoptose à la suite de dommages à l'ADN.

Cette étude de la famille p53 débute par l'analyse par RT-qPCR de 4 gènes de réponse à p53 suite aux différentes traitements : *FDRX*2, *DDB2, ZMAT3*, et *RPS27*L. Ainsi, l'expression de ces gènes de réponse à p53, n'est pas impactée par les différents traitements dans les deux lignées. Par la suite, j'ai étudié l'impact des différentes conditions de traitement sur l'expression de p53, p63 et p73 au niveau protéique par western blot.

Conformément aux rapports précédents et compte tenu du fait que les lignées cellulaires CAL27 et SQ20B sont connues pour porter un gène muté *TP53*, la protéine p53 est exprimée à des niveaux élevés, indépendamment des traitements génotoxiques.

Le gène codant p73 et celui pour p63 nommés respectivement *TP73* et *TP63*, encodent deux isoformes distinctes. Les formes avec un domaine de transactivation, nommées TAp73 et TAp63, sont considérées comme étant des suppresseurs de tumeur et les formes dépourvues de domaine de transactivation nommées ΔNp73 et ΔNp63 sont considérées comme pro-tumorales. Un épissage alternatif en 3' ajoute en plus des deux isoformes TA et ΔN, de nombreux autres variants.

Après 24h de traitement, dans l'analyse par western blot de la protéine p73, deux signaux sont détectés : une bande « haute » et une bande « basse », correspondant à deux isoformes que nous

supposons être TA et ΔN. L'anticorps utilisé contre p73 n'est pas spécifique d'une isoforme, c'est pourquoi nous ne pouvons certifier à quelle isoforme correspond le signal. Dans la lignée CAL27, la bande « haute » n'est pas détectée en absence de traitement. En revanche, son signal est augmenté par le traitement au cetuximab seul ou combiné au cisplatine, et, dans une moindre mesure par le cisplatine seul. Le signal de la bande « basse » est le plus intense et est également augmenté par le cetuximab seul ou combiné. À l'inverse, dans la lignée SQ20, le signal le plus intense correspond à la bande « haute » et les deux isoformes sont présentes dans la condition sans traitement. Le cetuximab seul ou la combinaison cetuximab/cisplatine diminuent le signal de la bande « haute ». Par ailleurs, l'intensité de la bande « basse » n'est pas impactée par les différents traitements.

Concernant p63, après 24h de traitement, deux bandes sont également observées avec une forte intensité du signal pour la bande « haute ». Les deux isoformes détectées sont fortement diminuées par l'IC_{90} du cisplatine et l'IC_{75} et l'IC_{90} du co-traitement dans la lignée CAL27. La lignée SQ20B montre des résultats similaires auxquels s'ajoutent une diminution de p63 lors du traitement avec l'IC_{75} du cisplatine seul.

Comme le traitement des cellules CETC par le cisplatine semble impliquer l'induction d'une apoptose dépendante de la caspase 3, du moins dans une certaine mesure, et que le cisplatine affecte l'expression des membres de la famille p53, nous nous sommes demandés si l'utilisation d'une molécule réactivatrice de p53 améliorerait la cytotoxicité du traitement. À cet effet, les deux lignées cellulaires ont été traitées avec 50µM d'un réactivateur de p53, nommé PRIMA MET, seul ou combiné aux différents traitements. Le test MTT utilisé pour mesurer la cytotoxicité de ces conditions ne montre pas d'amélioration avec l'ajout de PRIMA MET lors du traitement des deux lignées.

Pour conclure, les traitements à base de cisplatine, seul ou en combinaison avec le cetuximab, impactent l'expression de p63 et p73 mais pas celle de p53 ni de ses gènes de réponse, dans les deux lignées.

Ces résultats suggèrent que l'apoptose induite dans les lignées CAL27 et SQ20B par les traitements avec le cisplatine et la combinaison avec le cetuximab pourrait partiellement être indépendante de p53.

2. Mesure la capacité du cetuximab à induire la MCI dans des modèles cellulaires de CETC, *in vitro* et *in vivo*

a. In vitro

L'investigation de l'induction de la MCI commence par l'étude de l'emission des DAMP. Une isolation des protéines membranaires, par une technique basée sur l'utilisation de la Sulfo-NHS-SS-Biotine marquant les protéines membranaires et la précipitation par des billes couplées à la streptavidine, a permis de mettre en évidence la relocalisation membranaire de la calréticuline. Dans la fraction membranaire, la présence de la calréticuline a été détectée lors du traitement au cetuximab seul ou du co-traitement avec le cisplatine à l'IC_{90}, pour les deux lignées cellulaires.

L'analyse du relargage extracellulaire de la protéine HMGB1 par les cellules SQ20B et CAL27 a été réalisée à partir du milieu de culture. Dans la lignée CAL27, un relargage de HMGB1 se met en place fortement après 48 h de traitement au cetuximab seul ou combiné au cisplatine à l'IC_{50} alors qu'à l'IC_{75} du co-traitement, le relargage est faible. Le cisplatine seul induit plus modestement le relargage de HMMGB1 à l'IC_{50} et plus faiblement encore à l'IC_{75}. À l'inverse, dans la lignée SQ20B, le cetuximab n'induit pas ce relargage et ce sont les IC_{75} du cisplatine et du co-traitement qui permettent un relargage plus important de HMGB1.

Enfin l'étude de gènes de réponse à l'IFN de type I, montre un impact significatif après 48h de traitement sur l'expression des gènes *CXCL9* et *CXCL10* dans la lignée CAL27 et du gène *CXCL8* dans la lignée SQ20B. Dans la lignée CAL27, l'expression de *CXCL9* est augmentée par le cetuximab et le cisplatine mais c'est le co-traitement, en particulier l'IC_{75}, qui induit la plus forte augmentation. Tout comme *CXCL9*, *CXCL10* voit son expression augmentée par le cetuximab, mais plus fortement par le cisplatine seul. Le co-traitement entraîne une forte augmentation de *CXCL10* à l'IC_{75}. Dans la lignée SQ20B, le cetuximab n'a pas d'effet contrairement au cisplatine qui augmente légèrement l'expression de *CXCL8*. Le cisplatine à l'IC_{75} seul ou en combinaison à l'IC_{50} et IC_{75} induit la même augmentation sur l'expression de *CXCL8*.

Ainsi, mes résultats montrent que le cetuximab seul ou en combinaison avec le cisplatine, induit l'émission de DAMP impliqués dans la régulation de la MCI et que ce phénomène dépend à la fois du type cellulaire, et de la dose de traitement utilisée.

Le cetuximab, seul ou en combinaison avec le cisplatine, est capable d'induire l'émission de DAMP, première étape de la MCI, et serait donc capable d'activer une réponse immunitaire contre les cellules cancéreuses de CETC.

b. In vivo

Pour certifier la mise en place d'une MCI, et donc l'activation de système immunitaire, une expérience de vaccination sur des animaux immunocompétents est obligatoire.

Pour confirmer *in vivo* la mise en place de la MCI, une lignée murine stable exprimant un EGFR humain, hEGFR MOC2-C1, a été mise au point. Cette lignée a été générée par transduction rétrovirale de cellules MOC-2 à l'aide d'un plasmide d'expression du hEGFR et de la sélection à la puromycine. Plusieurs clones ont été obtenus dont le clone MOC-2-phEGFR-C1, qui s'est révélé exprimer la protéine hEGFR d'après les analyses par western blot et immunocytofluorescence.

Dans un premier temps, comme pour les lignées CETC, l'analyse cytotoxique des traitements a été réalisée sur le clone MOC-2-phEGFR-C1 pour obtenir les IC_{50} et IC_{75} des différents traitements et une analyse par western blot a montré une induction de la caspase 3 clivée avec les IC_{75} du cisplatine et du co-traitement après 24h de traitement.

Concernant la MCI, l'IC_{50} et l'IC_{75} du co-traitement suffisent à induire la relocalisation membranaire de la calréticuline analysée par l'utilisation de la Sulfo-NHS-SS-Biotine, marquant les protéines membranaires, et la précipitation par des billes couplées à la streptavidine.

Enfin, contrairement aux lignées de CETC, le relargage de HMGB1 est plus important avec le cisplatine seul ou en combinaison à l'IC_{75}.

Ainsi, le cetuximab, seul ou combiné au cisplatine, induit la première étape de la MCI à savoir l'émission de DAMP.

Enfin, la vaccination est réalisée en deux temps sur des souris C57B/L6. Premièrement, les cellules hEGFR-MOC2-C1 traitées *in vitro* durant 24 et 48h sont injectées sur le flanc droit des souris. Ces cellules sont mourantes et ne donnent pas de tumeur mais servent à vacciner l'animal grâce à l'émission de DAMP et donc la mise en place de la MCI. Deuxièmement, 7 jours après la première injection, sur le second flanc, sont injectées les cellules hEGFR-MOC-C1 saines. Si la vaccination a lieu, alors la formation de tumeurs est empêchée ou réduite par le système immunitaire.

Les résultats indiquent la mise en place d'une vaccination et donc d'une MCI lors de l'immunisation avec des cellules traitées au cetuximab, avec 0/12 souris développant une tumeur. Cette immunisation est présente, mais plus faible, avec les IC_{50} du cisplatine avec 4/12 souris développant une

tumeur et 2/12 souris développant une tumeur pour le co-traitement. La vaccination semble dose-dépendante puisque les IC_{75} ne présentent aucune vaccination. Les souris traitées avec les IC_{75} du cisplatine et du co-traitement et développant des tumeurs, 10/12 et 12/12 respectivement, sont aussi nombreuses ou presque que dans le groupe du contrôle négatif (11/11) .

Un impact trop important par des doses trop élevées semble inhiber l'effet protecteur des traitements. L'induction de DAMP ne semble pas corréler parfaitement à l'induction de la MCI. En effet, le co-traitement à l'IC_{75} induit fortement la relocalisation membranaire de la calréticuline et le relargage de HMGB1 mais ne semble pas avoir un effet protecteur chez l'animal. Le cetuximab induit la relocalisation membranaire de la calréticuline et faiblement le relargage de HMGB1 mais permet tout de même une activation du système immunitaire et donc une mise en place de la MCI. Pour terminer, le cisplatine à l'IC_{50} induit seulement le relargage de HMGB1, mais cela suffit à vacciner l'animal.

Une explication pourrait résider dans l'induction de la caspase 3 clivée. En effet, en cas d'apoptose, la caspase 3 clivée induit l'expression, vers le milieu extérieur, des phosphatidylsérines (PS). Les PS sont reconnues par les macrophages pour permettre la phagocytose des corps apoptotiques. Durant l'apoptose, le système immunitaire n'est pas activé car la reconnaissance des PS entraîne une sécrétion de cytokines anti-inflammatoires par les macrophages. Ainsi, une trop forte induction de caspase 3 clivée serait responsable d'une diminution de la réponse immunitaire et, par conséquent, pourrait donc être un frein à la mise en place de la MCI.

En conclusion, nous avons montré que le cetuximab, seul ou en combinaison avec le cisplatine, est capable d'améliorer l'immunogénicité des cellules murines et humaines de CETC par l'exposition de DAMP comme la relocalisation membranaire de la calréticuline, qui est connue pour fournir un fort signal "mange-moi" aux phagocytes du système immunitaire. Il est intéressant de noter que seules les conditions de traitement cellulaire *ex vivo* permettant la libération de DAMP et le clivage modéré de la caspase 3 (cetuximab seul, le cisplatin, et la combinaison à l'IC_{50}) semblent pouvoir déclencher une réponse immunitaire anti-tumorale chez les animaux immunocompétents.

3. Impact du cetuximab sur l'expression de points de contrôle

De manière à compléter mon analyse de l'impact du co-traitement par le cisplatine et le cetuximab sur l'immunogénicité des cellules cancéreuses, j'ai analysé l'expression de plusieurs points de contrôle immunitaire. L'expression de ces points de contrôle immunitaire au niveau transcriptionnel a été analysée et montre une forte expression de *CD47* et *CD276* dans les deux lignées mais sans impact des

traitements. Un autre point de contrôle étudié est *IDO-1*, dont l'expression n'est détectée que dans la lignée CAL27 et est peu impactée par les traitements. Enfin *PD-L1* et son homologue *PD-L2* sont plus faiblement exprimés. L'étude s'est concentrée sur *PD-L1*, par le fait qu'il soit le ligand associé à la cible de l'immunothérapie anti-PD-1, approuvée pour le traitements des CETC.

Cette analyse a été menée à bien après des traitements de 24, 48, et 72h avec le cetuximab seul, et le cisplatine seul ou combiné à l'IC_{50} et l'IC_{75}. Au niveau transcriptionnel, aucun traitement n'a montré d'impact significatif sur l'expression de *PD-L1* dans la lignée SQ20B. Dans la lignée CAL27, le cetuximab n'a pas d'effet sur l'expression de *PD-L1* mais le cisplatine seul induit fortement son expression. La combinaison du cetuximab et du cisplatine induit l'expression de PD-L1 de manière significative après 48h de traitement.

Au niveau protéique, les résultats diffèrent et mettent en évidence des effets distincts du cetuximab dans les deux lignées cellulaires. En effet, l'expression protéique de PD-L1 est augmentée dans les cellules SQ20B en réponse au cetuximab et après traitement au cisplatine, et ce, dès 24h de traitement. En revanche, l'expression de PD-L1 est diminuée à la suite du traitement par le cetuximab dans les cellules CAL27 par rapport aux cellules non traitées. De plus, le cetuximab induit également une diminution de l'expression de PD-L1 lorsqu'il est utilisé en combinaison avec le cisplatine par rapport à la condition cisplatine seul dans la lignée CAL27 après 24 et 72h de traitement, mais seulement à 48h dans la lignée SQ20B. Ainsi, mes résultats suggèrent que le cetuximab est capable de moduler l'expression de PD-L1 de manière différentielle en fonction du contexte cellulaire et impacte donc potentiellement l'immunogénicité des cellules tumorales à travers la régulation de points de contrôle immunitaire.

En conclusion, le cetuximab serait capable d'induire une MCI et induirait ainsi l'activation du système immunitaire à l'encontre des cellules cancéreuses mais semble également avoir un impact sur l'expression de points de contrôle immunitaire. De par ces deux mécanismes, le cetuximab pourrait influencer l'immunogénicité des tumeurs CETC, d'une part, en rendant leur microenvironnement plus favorable à une réponse immunitaire anti-tumorale et d'autre part, en sensibilisant les tumeurs aux immunothérapies à travers l'augmentation de l'expression de PD-L1. Le cetuximab conserverait également ses effets sur la MCI lorsqu'il est combiné avec du cisplatine à faible dose.

B. Scientific publications:

Jana MOURTADA1,#, Christelle LONY1,#, Anaïs NICOL2, **Justine DE AZEVEDO**, Cyril BOUR1, Christine MACABRE, Patrick RONCARATI, Sonia LEDRAPPIER, Philippe SCHULTZ, Bohdan WASYLYK, Michaël HERFS, Christian GAIDDON, Alain C. JUNG ΔNp63 favors an anti-tumor immune landscape via expression of diffusible factors and improves the prognosis of patients with Human Papillomavirus-related oropharyngeal cancers. En soumission ESBO

Justine DE AZEVEDO[1], Jana MOURTADA[1], Cyril BOUR[1,2], Véronique DEVIGNOT[1], Philippe SCHULTZ[3], Christian BOREL[4], Erwan PENCREACH[1,5], Georg MELLITZER[1], Christian GAIDDON[1], Alain C. JUNG[1,2] The cytotoxicity of the EXTREME regimen is associated with the modulation of Head and Neck cancer cell immunogenicity and the induction of an anti-cancer immune response.

Badie, A, **De Azevedo, J**. Pencreach, E. Gaiddon, C Impact of chemotherapy standards and their combination with HDAC inhibition on the immunogenicity of gastric cancer. In progress

Introduction

Every adventure requires a first step. Trite, but true, even here.
Cheshire cat, Alice in Wonderland

.

Chapter I

A

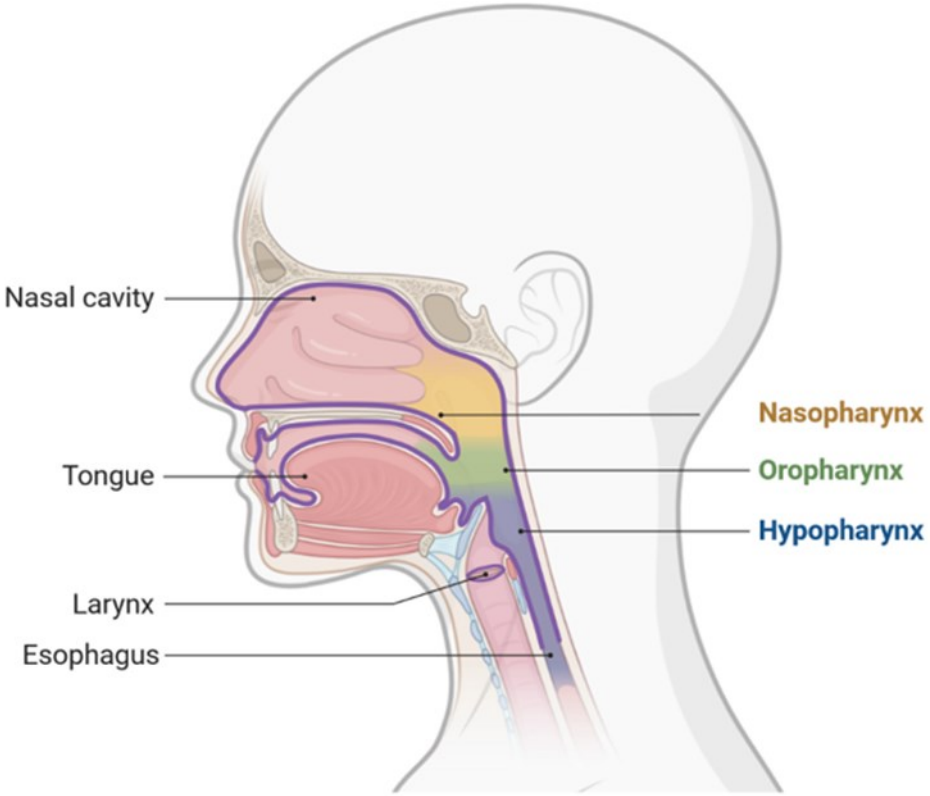

B

Chung *et al*	De Cecco *et al*	Molecular Signature	Prognostic	Percentage of tumors
Atypical	HPV-like	HPV siganture	+++	24
	Immunoreactive	Up-regulation of immune response	++	
Classical		**EGFR amplification** **P53 mutation** Oxydative stress	--	18
Basal	Hypoxia	Hypoxia pathways	--	31
	Defense response	Enrichement in immune response	++	
Mesenchymal		EMT transition	---	27

Figure 1: Generalities about HNSCC.

A. HNSCC grows from the epithelium of the upper aerodigestive tract including the sinonasal tract, oral cavity, pharynx, and larynx. B. Proposed molecular classification of HNSCC tumors according to their alterations, each group is associated with a prognosis. *HNSCC, head and neck squamous cell carcinoma; HPV, human papillomavirus; EGFR, epidermal growth factor receptor; EMT, epithelial-mesenchymal transition*

A. Head and neck squamous cell carcinoma

1. Generalities

a. *Epidemiology and risks factor*

Head and Neck Squamous Cell Carcinomas (HNSCC) are heterogeneous tumors that arise from the mucosal epithelium in the oral cavity, larynx, pharynx, and sinonasal tract [1] **(Figure 1A)**. HNSCC are the sixth most common cancer worldwide with 890 000 new cases in 2018 [2]. The major risks factors for developing HNSCC are tobacco and alcohol use which expose epithelium to different mutagens that lead to DNA adducts, fragment of DNA covalently bound to a chemical, inducing somatic mutations [3]. These two risk factors have a synergistic effect and increase the odds of developing HNSCC by 35 if consumed in excess [1], [4]. Another main risk factor is human papillomavirus (HPV) infection, which represents 70% of oropharynx tumors. Patients with HPV-positive tumor have better prognostic and better survival than patients with HPV-negative tumor. For all HNSCC, the sex ratio of these cancers is 2 or 4 men for 1 woman [5].

HNSCC are diagnosed by medical imaging, like Magnetic Resonance Imaging, and the disease progression is evaluated by the TNM stage where T represents the “tumor size”, N is the number/size/localization of nymph lodes affected, and M represents the presence of metastasis [6]. The management of the patient depends on the TNM stage, which correlates with cancer progression. The TNM leads to stage classification according to the progression of the disease; stage I and II are depending on the tumors size and are free of lymph node (LN) invasion. As soon as LN are affected, tumors are classified as stage III. Stage IV corresponds to metastases presence. In studies, the denomination “locally advanced” corresponding to stage III to IV and “R/M” corresponding to relapse and/or presence of metastases are commonly used as they represent the most common conditions in HNSCC [7].

b. *Carcinogenesis*

Cancer development is based on driver mutations, including loss of tumor suppressor gene function and oncogenic gain-of-function. Different genomic anomalies, such as deletions, and conversely amplifications but also somatic mutations allow the emergence of aberrant cells with cancerous characteristics. HNSCC tumors are no exception to this rule and contain numerous genetic alterations.

c. *Tumor suppressor mutations*

The histological progression from healthy head and neck epithelium to hyperplasia (increased cell proliferation), dysplasia (abnormal cells development), and carcinoma is determined by genetic

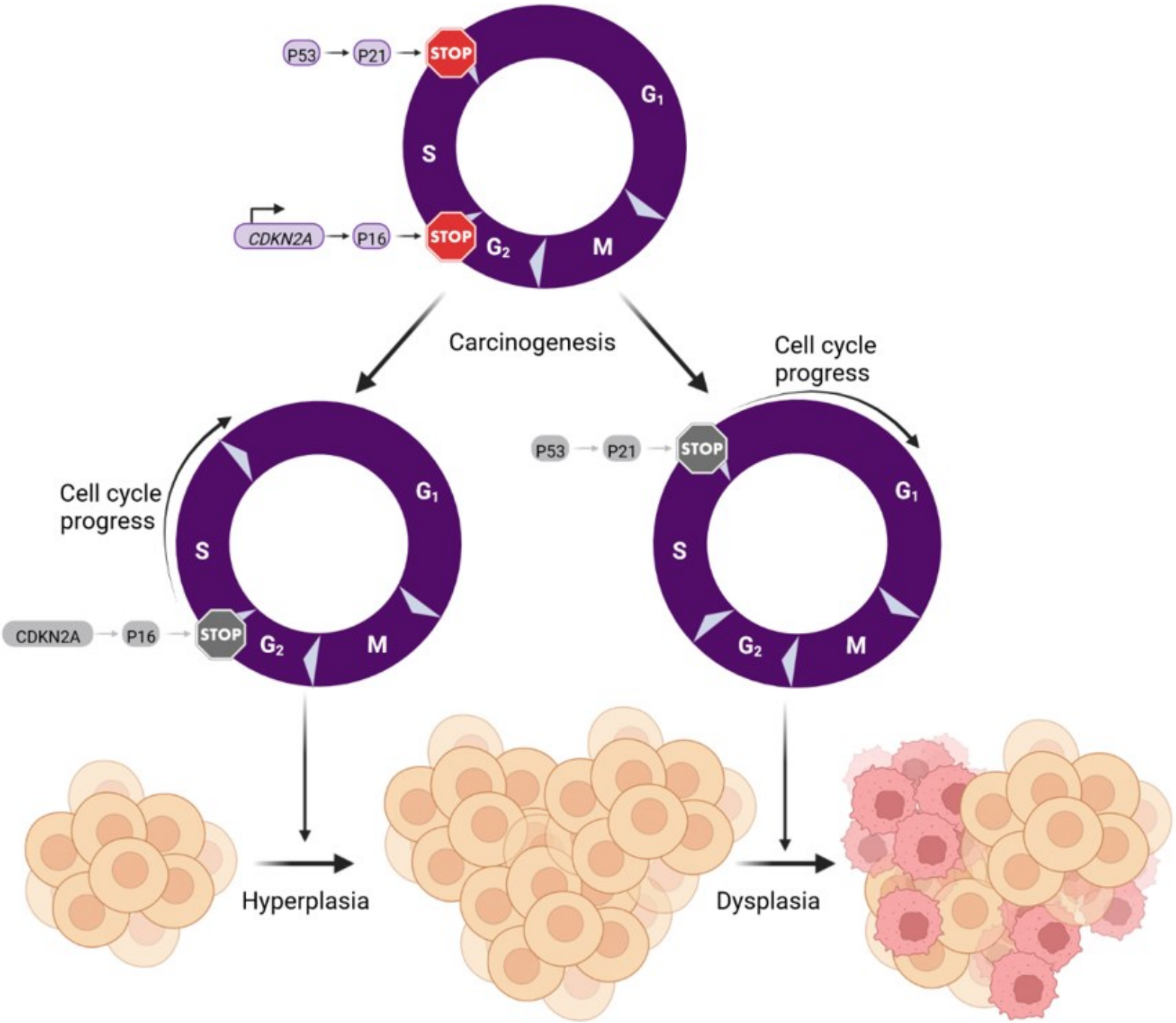

Figure 2: Schematic and simplified representation of HNSCC carcinogenesis.

CDKN2A gene encodes for p16 protein which blocks cell cycle in G_2 phase. The transcription factor p53 induces p21 expression which blocks cell cycle in S phase. The loss of the CDKN2A gene through genetic alterations prevents the transcription of p16 and creates a runaway cell cycle. This leads to dysplasia which is characterized by uncontrolled cell proliferation. In a second step, the loss of function of p53 prevents the induction of p21 and thus the negative regulation of the cell cycle. High proliferation is conducive to the appearance of genetic alterations. It is following the loss of p53 that tumor cells appear among the proliferating cells forming hyperplasia. *CDKN2A, cyclin-dependent kinase inhibitor 2A*

alterations **(Figure 2)**. The loss of Cyclin-Dependent Kinase inhibitor 2A *(CDKN2A)* could be the driver of the first step of HNSCC formation called hyperplasia [1]. The loss of the tumor suppressor gene called *CDKN2A* encoding p16 protein, which is implicated in the cell cycle, concerns 22% of HNSCC tumors [1]. The cell cycle is ruled by different proteins like cyclin and cyclin-dependent kinase and cell cycle checkpoints that stop the cycle if the DNA presents abnormalities. Protein p16 is one of the cell cycle checkpoints that blocks cyclin-dependent kinase and cyclin D actions. The action of p16 blocks the cells in G1 and thus prevents the progression in the S phase [8].

Progression from hyperplasia to dysplasia is triggered by the loss of function of the transcription factor p53 due to the loss of the chromosomal region coding for p53. The gene *TP53* is a tumor suppressor mutated in more than 72% of HNSCC [1] and associated with poor overall survival (OS) [9]. p53 also called the "guardian of the genome" due to its multiple actions on cell-cycle arrest, apoptosis, senescence, DNA repair, and metabolism, makes it an important tumor suppressor [10]. This transcription factor responds to cellular stress like DNA damage or oncogene activation [5]. In unstressed physiological conditions, p53 is regulated by Murine Double Minute 2 (MDM2), a ubiquitin ligase. When genotoxic stress (DNA damages by mutagens agents like UV, radiation, mutagens) occurs, p53 undergoes post-translational modifications (acetylation, phosphorylation) that block its interaction with MDM2, stabilize its expression, and thus its activation. Interestingly, p53 could activate several positive or negative feedback loops like the expression of Ribosomal Protein S27 like *(RPS27L)* which will take the place of p53 in the direct interaction with MDM2 [11]. Once in the nucleus, p53 induces expression of target genes involved in cell cycle arrest or genes inducing apoptosis [10]. After DNA damage, the cell will first try to repair the damages, the cell cycle is then stopped. To do so, p53 induces p21 expression which is a cell cycle inhibitor and thus blocks the cell in the S phase. The effect of p53 on DNA repair mechanisms depends on DNA Damage-Binding protein 2 (*DDB2)* gene expression, among others. If the amount of damage exceeds the DNA repair ability of the cell, p53 induces caspase-dependent apoptosis by activating gene expression of *PUMA*, *BAX,* and *ZMAT3*, but also through induction of *Fas*. Finally, p53 could also affect the iron homeostasis by modulating Ferredoxin Reductase *gene 2 (FDXR2)* expression and this loop is important in tumor suppression. FDRX2 targets Iron Regulatory Protein *2 (*IRP2) but in the case of FDRX2 depletion, IRP2 is increased and represses p53, moreover, FDRX2 depletion induces deregulation of iron homeostasis and then iron accumulation that leads to DNA damage as well as oncogene activation and so to the appearance of cancer cells [12]. This illustrates the important role of p53 in cellular homeostasis and the deleterious effects of its loss of function.

p53 is part of the p53 family including two other transcription factors, p63 and p73 encoded by *TP63* and *TP73* genes respectively. They share functional homologies with p53 like cell cycle arrest and

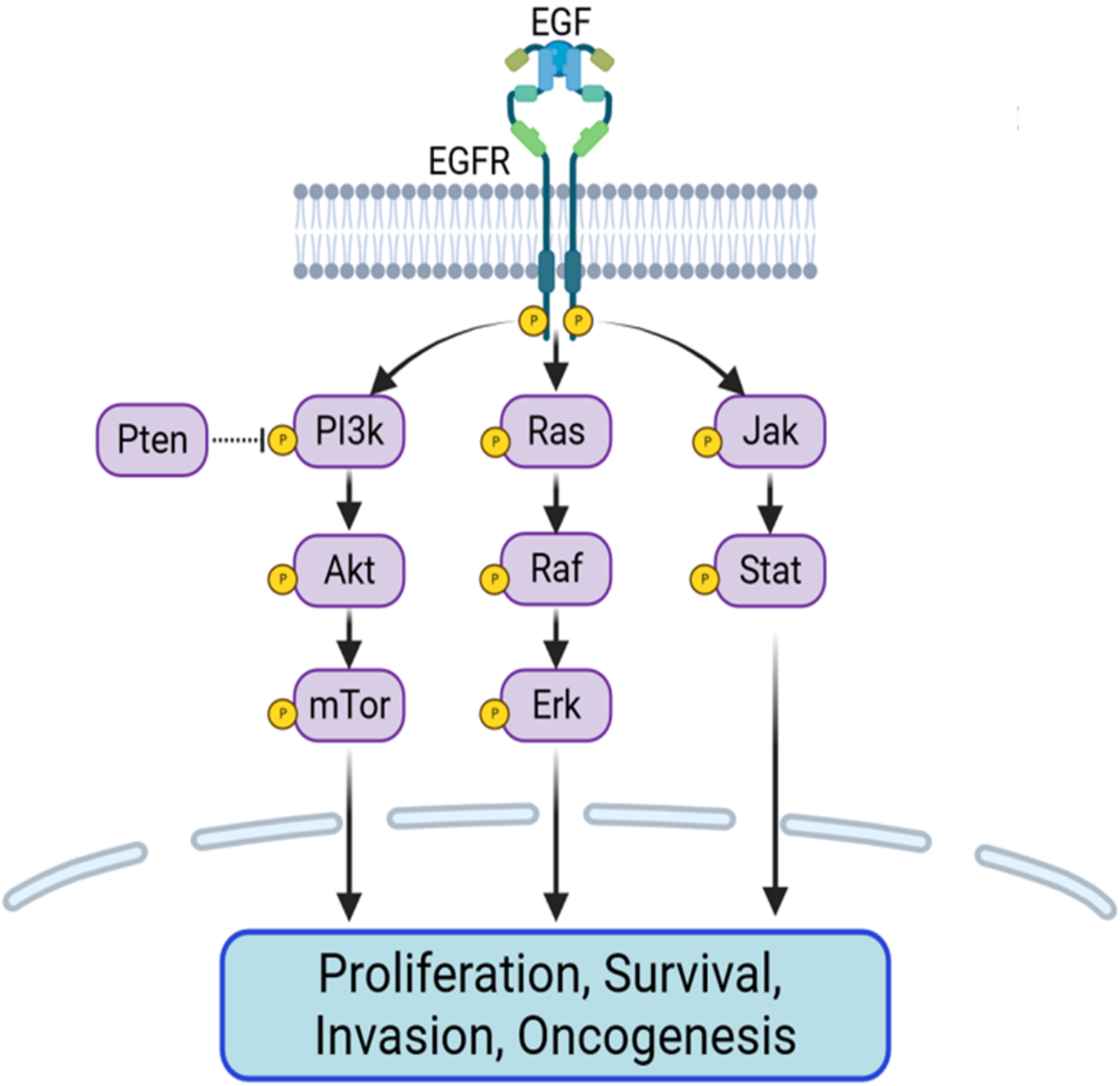

Figure 3: Simplified representation of the 3 main signaling pathways.regulated by EGFR activity.

After binding to its ligand, EGF, EGFR dimerizes and autophosphorylates at its tyrosine kinase domain. This activation of the receptor leads to the activation of 3 protein kinase pathways.

The PI3K/AKT/mTOR pathway is induced by the phosphorylation of PI3K by the receptor, PI3K phosphorylates AKT which then induces the mTOR pathway. mTOR induces proliferation and protein synthesis. This pathway has a negative regulator, PTEN, which prevents the phosphorylation of PI3K.

The MAPKinase pathway consists of RAS, RAF, and finally ERK, and their activation also depends on their phosphorylation. ERK induces cell cycle progression and angiogenesis.

And finally, the JAK/STAT pathway is induced by the phosphorylation of Jak which phosphorylates STAT leading to the expression of genes involved in survival and invasion.

Overexpression of EGFR or one of these pathways is involved in oncogenesis through the expression of survival, proliferation, and angiogenesis genes.

apoptosis regulation properties when cells present genotoxic stress, but p63 seems also implicated in epidermal morphogenesis and keratinocyte differentiation while p73 is implicated in neurogenesis. *TP63* and *TP73* produce proteins with p53-agonistic or p53-antagonist function through functional diversity residing in the genetic architecture [13]. Indeed, *TP63* and *TP73* genes possess two alternative promoters that generate two protein isoforms corresponding to forms with a transactivation domain (TA) called TAp63 or TAp73 and another form lacking this domain called ΔNp63 or ΔNp73. An alternative splicing in 3' allows the synthesis of isoforms with different C-ter regions adding more variants [14]. TA isoforms are considered as a tumor suppressors whereas ΔN isoforms are considered to be oncogenic [14]. Similar to p53, the p63 and p73 proteins are regulated by MDM2 but they more strongly interact with another ubiquitin ligase, MDMx [15]. In HNSCC, p73 is less expressed than p53 and p63 [13]. The impact of p73 on HNSCC progression needs further investigation, with the only current conclusion being that TAp73 function is abolished in these tumors leading to stem cell-like properties of cancer cells through the expression of *NANOG*, *SOX2,* and *OCT4* [1]. In contrast, *TP63* is amplified or overexpressed in 80% of HNSCC [5]. Specifically, the dominant form expressed is ΔNp63 which plays an important role in HNSCC pathogenesis by regulating cell survival and suppression of senescence [1]. The TAp63 isoform is downregulated [13].

d. Oncogenic alterations

The amplification of Epithelium growth factor receptor (EGFR) is the most common alteration in HNSCC and it's found in 80% to 90% of HNSCC. Unfortunately, it is associated with poor prognosis [1]. EGFR or ErbB1/HER1 is a transmembrane receptor of the ErbB/HER tyrosine kinase receptor family [16]. Its principal ligand is the Epithelium Growth Factor (EGF) but also Transforming growth factor-α (TGF-α), Amphiregulin (AREG), and Epiregulin (EREG) [17] for example. The homo- or hetero-dimerization of EGFR monomers is caused by ligand binding. This dimerization leads to activation of the receptor by auto-phosphorylation of the intracellular tyrosine kinase domain (TKD). Afterward, TKD recruits adaptor proteins such as Src homology 2 (SH2) [18]. Three principal pathways, based on phosphorylation cascades, are activated by EGFR: the RAS/RAF/MEK/ERK or MAPkinase pathway, the PI3K/AKT/mTOR pathway, and the JAK/STAT pathway **(Figure 3)**. Each pathways modulate different cellular processes including proliferation, cell survival, and angiogenesis. The MAPK pathway enables cell proliferation, whereas the PI3K/ATK pathway is implicated in cellular survival, proliferation, and metabolism, and the JAK/STAT pathway induces growth factors production, cell migration, and cell survival [19]. Some of the EGFR pathway actors are mutated in HNSCC in a minor portion, such as PI3K gene amplification (16%) or a mutation (14%), or gain-of-function mutation for RAS/HRAS (4%) [1]. The Phosphatase and TENsin homolog (PTEN) is a negative regulator of EGFR pathways. PTEN antagonizes PI3K action and thus

inhibits the downstream pathway [20]. Unfortunately, PTEN loss of function occurs in 30% of HNSCC tumors [1]. Thus, taken together, EGFR pathway alterations represent a significant proportion of patients.

Multiple genetic abnormalities are required to progress from dysplasia to carcinoma. A full understanding of this process requires more study [1].

In addition to the driver mutations that allow the transformation of healthy cells into cancerous cells, HNSCC tumors present numerous genomic alterations which have been identified with genomic analyses, and several molecular classifications have been proposed to obtain more homogeneous groups with a particular signature. The classification of HNSCC is intended to associate a prognosis and possibly a therapeutic response to each group. Thus, a personalized therapy could be set up according to the group in which the patient is.

e. Molecular classification of HNSCC

First, Chung *et al* proposed a classification into 4 molecular or "gene-expression" groups based on the transcriptomic analysis of 60 HNSCC [21]. Almost ten years later, Walter *et al* confirmed this classification in a larger cohort (138 HNSCC) and gave each group a name: atypical, classical, basal, and mesenchymal but also added prognostic value to the classification [22] **(Figure 1B)**. Finally, in 2015, the cancer genome atlas used 279 HNSCC to complete each group with new gene alterations and analyzed the distribution of each group [23].

- The atypical group is marked by HPV positive signature, has the second-worst OS [22], and represents 24% of HNSCC [23]. Interestingly, if the survival analysis is restricted to atypical HPV-negative tumors, the atypical group presents the worst prognostic [22].

- The classical group includes tumors with gene alterations associated with oxidative stress, thus this group includes tumors from patients with heavy smoking history [23]. This group also includes other alterations such as *EGFR* amplification, *CDKN2A* loss, and *TP53* mutations [19]. This group represents 18% of the tumors[23] and is associated with the worst prognosis[22].
- The basal group contains HNSCC with *HRAS* mutation [23], high expression of TGF-α and EGF receptor, and high expression of *TP63* [22]. It represents 31% of HNSCC [23] and has a the better OS [22].

- Finally, the mesenchymal group has an epithelial-mesenchymal transition (EMT) signature [23]. EMT is the process by which epithelial cancer cells lose polarity and cell-cell adhesion,

- and gain migratory and evasive properties. Thanks to this transition, cancer cells can detach themselves from their support and migrate to distant sites to generate secondary tumors. Then, they will make a reverse transition called mesenchymal-epithelial transition, and allow the development of metastases [24]. The alteration of the innate immunity genes has been described in this group with an augmentation of natural killer (NK) cells and a low frequency of Human Leukocyte Antigen (HLA) class I mutation [23]. This group represents 27% of HNSCC [23] and patients in this group have a higher risk of developing metastases [22].

EGFR amplification is present in 90% of HNSCC, thus EGFR amplification is found in the classical group but also in the basal group. The same goes for *TP53* alteration which includes 70% of HNSCC, so *TP53* alterations are found in every group except for the atypical group, where they are less frequent [23].

The last classification of HNSCC has been proposed in 2015 by De Cecco *et al* **(Figure 1B)**, who expanded it to include the immune response, among other things, resulting in a final classification into 6 clusters. Their study is based on the TGCA and includes 1386 tumors.

- Two groups are identical in all studies: mesenchymal and classical.
- In this study, the atypical group is divided into two clusters defined by HPV positive signature and "immunoreactive". "Immunoreactive" group expressed up-regulation of the immune system, as Interferon (IFN) response.
- The basal group is also separated into two clusters, "hypoxia" and "defense response". The group named "Hypoxia" includes activation in the hypoxia pathways, and the "defense response" group includes enrichment in the immune response.

The OS prognostic depends on the cluster. HPV positive cluster shows better outcomes which is consistent with the fact that HPV positive patients have a better prognosis. The group associated with good immune response, "immunoreactive" and "defense response" shows the second better outcome while clusters associated with hypoxia and oxidative stress, cluster 5 and the classical group, have the worst OS. Finally as expected the mesenchymal group or cluster is associated with the progression of disease and metastases and shows the worst outcome [25].

f. Biomarkers and survival

Despite the improvement in our understanding of the genomic alterations and the molecular classification of HNSCC tumors, this tool is not used in clinical management. Furthermore, the prognosis for these groups is based on the TGCA data and requires a more patient-inclusive analysis, including clinical trials for a stronger correlation. For now, these molecular groups do not show a strong correlation with the clinic.

Still, the HNSCC classification needs to be validated in patient cohorts before it can be used as a robust tool for stratifying patients and should identify actionable therapeutic targets for each group, and/or prognostic/predictive biomarkers.

In summary, HNSCC tumors are a group of heterogeneous tumors with genomic alterations such as EGFR overexpression in >80% of cases and *TP53* mutation in ~70% of cases.

Despite a better understanding of HNSCC tumors through the identification of genomic alterations, carcinogenesis, or the classification of tumors with specific molecular signatures, the survival of HNSCC patients remains very poor. Indeed, the 5-year survival is only 45%, and HNSCC caused 450 000 deaths in 2018 worldwide. The poor survival is explained by different factors. Notably, it is due to a late detection at locally advanced stages. Indeed only one third of patients are detected at an early stage [6]. Another factor is tumor relapse, which occurs in nearly 65% of patients [26]. Recurrent patients could also present metastases mainly in lungs, bones, and liver [7]. The last factor is the treatment failure.

B. Treatments

There are three main therapeutic options for HNSCC: surgery, radiation therapy, and chemotherapy administrated alone or in combination. Treatments options depend on several factors including the tumor stage:

Stage I and stage II are early stages, corresponding to a small tumor without invasion of neighboring tissues [27], the usual treatment is surgery or radiation [28].

For later stages (stage III and stage IV) characterized by larger tumors, invasion of LN, and presence of metastasis, [27], a combination of treatments is proposed: radiation and chemotherapy together, or consecutively as the last resort [28]. In case of relapse, and particularly in the stage R/M locally advanced, palliative treatment is set up and consists of radiotherapy or chemotherapy both coupled with a targeted therapy [28].

1. Surgery

Surgery is the main treatment of HNSCC and the most effective. It consists of the total resection of the tumor. Surgery possibilities rely on the anatomical subsite, tumor size, and functional considerations. In the early stages, surgery alone provides an 80% success rate in curing HNSCC. Surgery is particularly used for oral cavity tumors. For the larynx and pharynx, due to their location, surgery is more complex; however, improvements have been made to restrict resection or reconstruction techniques. Whenever possible, surgery will be attempted [1].

2. Radiotherapy

Radiotherapy is preferable for organ preservation thus it remains the main treatment for HNSCC management. Patients who respond best to radiotherapy are those with HPV^+ tumors, the cause of which has not yet been totally elucidated but could be explained by the presence of wild type p53. As surgery, in the early stages, radiotherapy alone provides an 80% success rate in curing HNSCC [1].

Radiotherapy uses ionizing radiation (IR) that are electromagnetic energy that directly ionizes atoms or molecules. The IR are directed to the area of the tumor, where they trigger water ionization, which generates reactive oxygen species (ROS), such as superoxide anion and hydrogen peroxide. ROS induce oxidative stress, damage cell integrity via the oxidation of lipids and proteins, cause mitogenic stress by deregulation of mitochondrial activity, and also various damage: IR, therefore, triggers growth arrest and DNA repair mechanism thanks to its ability to induce DNA double-strand breaks (DSB) and single-strand breaks (SSB) [29]. Radiotherapy can induce approximately 1000 SSB and 1 Gy (Gray, unit of ionizing radiation) of γ-radiation can induce 30DBS. The standard fractionating dose is 2Gy/cycle which causes about 3000 DNA lesions while only 40 DBS are sufficient to induce cell death [28]

In general, patients with HNSCC can receive 60Gy of IR divided into 2Gy sessions [28].

Radiotherapy does not only target the cancer cells but will cause damage to all the tissues IR passes through. Side effects of radiotherapy include fibrosis leading to hardening of the affected tissues, but also xerostomia, thyroid damage, and sometimes osteoradionecrosis which may lead to tooth extraction. In addition, a narrowing of the pharynx or esophagus can be caused by radiotherapy and lead to nutritional problems [30].

3. Cisplatin

Chemotherapy is a treatment based on a chemical compound that eliminates highly proliferating cells, which is the case with cancer cells. Platinum-based compounds are part of chemotherapy and, cisplatin is the most used to treat HNSCC [5] and remains the favored systemic agent in this cancer [29]. It is generally used as the second line of therapy. Indeed, treatment with cisplatin associated with radiation is given on patients with stage III or IV, and in case of relapse [28]. The combination of cisplatin and radiotherapy is recommended for the preservation of the larynx and used in first line of treatment only in this case [31].

Cisplatin is used to control tumor progression when the patient cannot be operated on immediately. Neoadjuvant chemotherapy is used to reduce the size of the tumor, especially in cases of

airway obstruction or when the patient cannot be irradiated. Cisplatin is an alternative for patients who are refractory to radiation [1].

Cisplatin comprises a platinum atom surrounded by two chlorine atoms and two ammoniac atoms. It enters the cells through copper membrane transporters 1 and 2. In the cell, cisplatin is metabolized, and the chlorine atoms are displaced by a water molecule. The result of these molecular changes is a hydrolyzed product that can react with nucleophile groups such as nucleic acid. Once in the nucleus, cisplatin establishes a covalent bond with the N7 reactive center of the guanine base preferentially. It will then result in the formation of DNA adducts including monoadduct, intrastrand adducts, and interstrand crosslinks [32]. This will cause genotoxic stress. Cisplatin is also able to induce oxidative stress but the mechanism involved is not yet fully understood in HNSCC. It seems that reversing oxidative stress abrogates cisplatin toxicity meaning oxidative stress is important in cisplatin cytotoxicity [33]. Cisplatin also induces oxidative stress by accumulation in mitochondrial leading to ROS generation [32], [34]. To conclude, cisplatin can induce cell death through DNA damages and oxidative stress.

Cisplatin is administrated alone at a concentration of 100mg/m^2 every 3 weeks. For the patient who cannot tolerate high doses of cisplatin, weekly administration of 40mg/m^2 shows a similar response [1]. At last, a low dose every week seems to be more effective than a high dose of cisplatin every three weeks [35].

Like radiotherapy, the cytotoxicity of cisplatin is not specific to cancer cells and affects healthy cells. The main side effects of cisplatin are nephrotoxicity, neurotoxicity, a decrease in the number of immune cells produced in the bone marrow, and possibly hearing loss [36].

a. Stress response to radiotherapy and chemotherapy

Radiotherapy and cisplatin induce similar effects, DNA damages, and oxidative stress, thus the mechanisms of response to these two treatments share similarities.

The DNA damage response involves different mechanisms to repair the different damages induced by cisplatin and radiotherapy. The mechanism involved will depend on the type of lesions.

SSB are detected by Ataxia Telangiectasia and Rad3-related protein (ATR) and DBSs are detected by Ataxia Telangiectasia Mutated (ATM). ATM and ATR activate p53 by inhibiting the negative regulator of p53, MDM2. Once activated, the transcription factor p53 induce cell cycle arrest and DNA reparation [28] **(Figure 4)**.

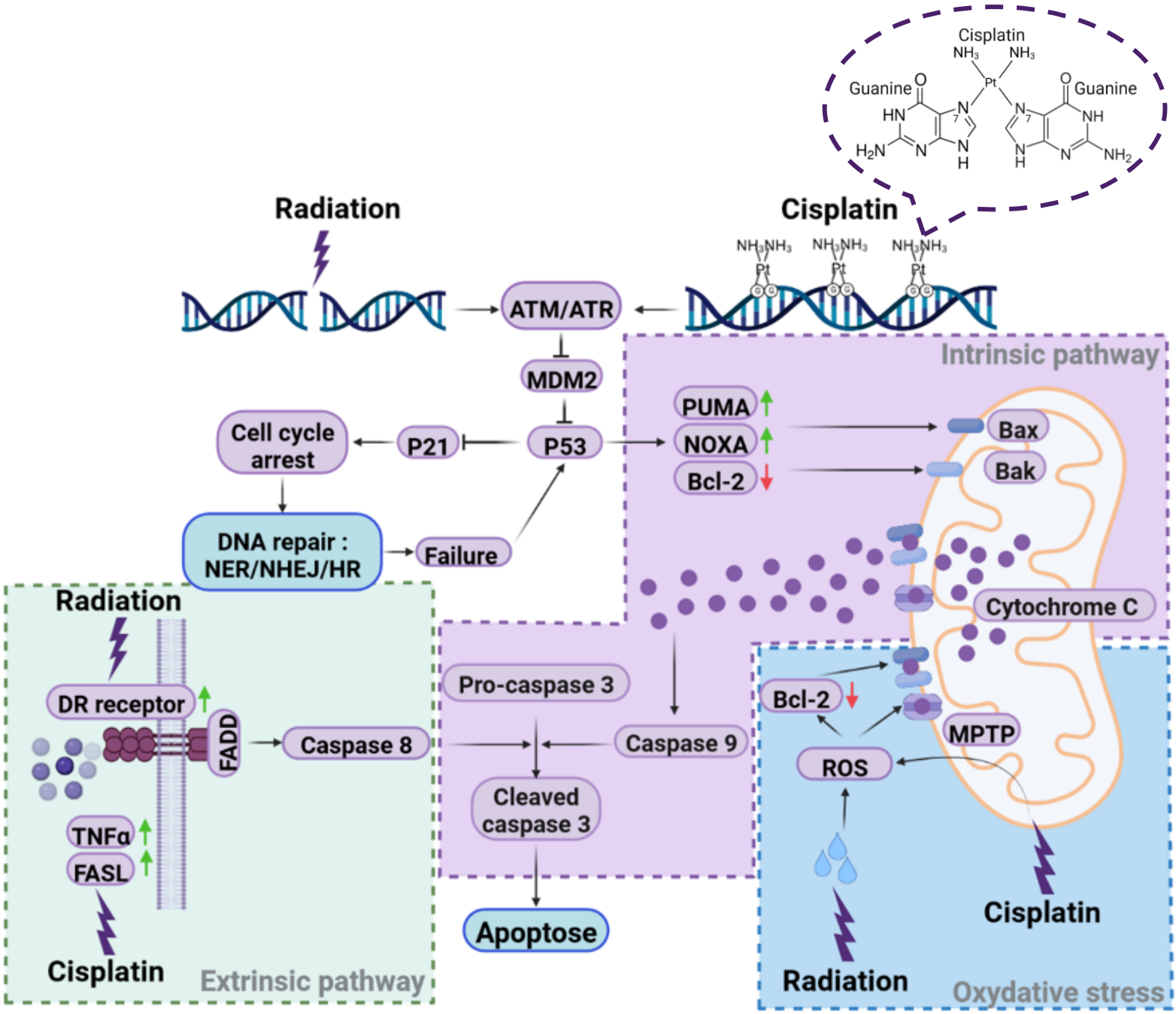

Figure 4: Induction of apoptosis by radiotherapy and cisplatin.

Radiotherapy and cisplatin induce DNA damage detected by ATM/ATR sensors. These will inhibit MDM2 releasing the transcription factor p53. Fist P53 induces cell cycle arrest via p21 to repair the DNA damages. p53 induces the **intrinsic pathway (purple)** of apoptosis if the DNA damage repair fails.p53 induces the intrinsic pathway of apoptosis by inducing the expression of the pro-apoptotic factors Noxa, and Puma and by decreasing the anti-apoptotic factor Bcl-2. It releases Bax and Bak proteins that form heterodimers at the mitochondrial membrane and allows the release of cytochrome C. Cytochrome C activates caspase 9 which cleaves caspase 3 inducing apoptosis.

Radiation therapy and cisplatin can also induce the **extrinsic pathway (green)** of apoptosis. Radiation therapy increases the expression of death receptors (DR) and cisplatin increases the expression of ligands: FasL and TNF-α. Once the ligand and its receptor are bound, the FADD moiety activates caspase 8 which cleaves caspase 3.

The last pathway induced by Radiation therapy and cisplatin is **oxidative stress (blue)** through ROS production via water ionization and mitochondrial damage, respectively. ROS decrease Bcl-2 and cause the opening of mitochondrial permeability transition pore (MPTP), which allows the release of cytochrome C and activation of caspases resulting in apoptosis.

NER, nucleotide excision repair; NHEJ, non-homologous end joining; HR, homologous recombination;

Cell cycle arrest is induced by the expression of the p53 target gene p21. The cyclin-dependent inhibitor p21 blocks cyclin-CDK complex activities. This inhibition results in hypo-phosphorylated Retinoblastoma (RB) that blocks RB-E2F complex formation and so repressed cell cycle genes expression. The cell is blocked in the S phase until DNA reparation [37].

The main DNA damage caused by cisplatin is DNA adduct. In consequence, the Nucleotide Excision Repair (NER) pathway is activated by the cell. NER pathway is complex machinery composed of multiple proteins from the XP family (XPA, XPC, and XPE) that recognize DNA damage, excise nucleotide, and close the gap. Excision Repair Cross-Complementing 1 (*ERCC-1)* and ERCC-4 (XPF) are endonucleases that form a complex to remove the cisplatin adducts. Thus ERCC-1 and ERCC-4 have a key role in cisplatin resistance. The elimination of cisplatin adduct is the rate-limiting step of the NER process [32].

The response to DBS induced by radiotherapy involves two different mechanisms: Homologous Recombination (HR) and Non-Homologous End Joining (NEHJ) [28], [36]. HR needs a homologous DNA sequence from sister chromatids so HR only takes place in late S/G2 phase when chromatids are available. The complex MRN (MRE11-RAD50-NBS1) recognizes DSBs and activates ATM kinase which initiates the full DNA damage response. To simplify, the HR steps require 5' to 3' resection of broken ends mediated by nuclease CtIP, research of homologous sequence via RAD51 nucleoprotein, strand invasion, recognition, and finally ligation. NEHJ is a simple mechanism that can occur during each phase of the cell cycle but mostly on G0 and G1. KU70/80 complex and DNA-PKcs process the broken ends and XRCC4-ligase4 ligate the ends together [38].

If DNA damage cannot be repaired or if it is too abundant, apoptosis will be induced by three independent pathways:

- The intrinsic pathway of apoptosis **(Figure 4, purple box)**. The factor p53 induces pro-apoptotic BH3-only protein PUMA and NOXA that inhibits the pro-survival protein Bcl-2 and MCL-1, respectively. The diminution of Bcl-2 and MCL-1 that localize in the outer mitochondria membrane prevents them from binding to the pro-apoptotic proteins Bax and Bak which can then form a monomer in the outer membrane of mitochondria. This monomer allows the release of cytochrome C that induce cleavage of caspase 9 which in turn cleaves caspase 3 and induces apoptosis [29], [32], [36], [39].

- Another way to induce apoptosis, without necessarily involving DNA damage and p53, is oxidative stress due to ROS generation induced by cisplatin [39] and radiotherapy [40] **(Figure 4, blue box)**. Radiation induces oxidative stress through water ionization that leads to water molecules

decompositions in ROS [28]. Cisplatin induces ROS via mitochondrial damage but the mechanism remains unclear [36], it seems that cisplatin disrupts the respiratory chain and thus causes ROS generation [41]. ROS trigger a decrease of Bcl-2 expression and an increase of Bax expression without p53 implication. ROS also triggers the opening of mitochondrial permeability pores (MPTP) [41]. In both ways, ROS induces the release of cytochrome C that cleaved caspase 3 and induces apoptosis [40].

- Finally, the extrinsic pathway of apoptosis does not involve p53, it is not the main pathway induced by treatments **(Figure 4, green box)**. This pathway depends on the Death Receptors (DR). Radiotherapy increase the number of DR [28] and cisplatin increase DR ligands expression such as TNF-α, and FasL [36], [41]. The association between the DR and its ligand recruits the Fas-associated death domain protein, and the pro-caspase 8 to form the death-inducing signaling complex. This complex, like in the intrinsic pathways, cleaved caspase 3 and lead to apoptosis [42].

Alterations of these pathways, like p53 loss-of-function and on the contrary overexpression of anti-apoptotic protein such as Bcl-2, increased DNA mechanisms repair, ROS detoxification by increasing glutathione or resistance to Fas signaling, lead to resistance against apoptosis signals and then decreased the efficiency of radiotherapy and cisplatin [29], [32].

The numerous alterations, especially p53 loss of function, but also increased of DNA repair mechanism, increased of anti-apoptotic protein expression, and decreased of pro-apoptotic proteins, lead to the appearance of resistance to traditional therapies, radiotherapy and chemotherapy have limited effects and do not allow total recovery. To improve the therapeutic efficiency of HNSCC, targeted therapies based on recurrent and targetable alterations have been developed. Indeed, molecular analysis has shown an increase in EGFR in 90% of HNSCC tumors, and HNSCC seems to be addicted to EGFR pathway [17] meaning that the malignant phenotype depends on the constitutive activity of EGFR pathway [43] so EGFR has become an interesting target in the fight against these cancers.

4. Cetuximab

Cetuximab is a chimeric human-murine monoclonal antibody used as targeted therapy against EGFR, approved by the FDA in 2006. Cetuximab is used on recurrent patients, metastatic patients, and patients not eligible for cisplatin or radiation [1]. The patient is administrated with one first loading dose (400 mg/m^2) of cetuximab and then by weekly doses (250 mg/m^2) [44]. Unfortunately, overexpression of EGFR is not a prognostic marker of cetuximab response and in monotherapy, only 13% of patients respond to the treatment [29].

Cetuximab is frequently used in combination with traditional treatment. As a matter of fact, it is a radio-sensitizer [1] through inhibition of the PI3K/AKT/MAPK pathways that leads to increased apoptosis mediated by DNA damage. The EXTREM protocol is a combination of cetuximab, cisplatin, and the 5-FU anti-metabolite, and is classically used on recurrent or R/M patients. In clinical trials, this protocol shows a gain in median OS of three months (10.1 months vs 7.4 months) against chemotherapy alone [45]. The EXTREME protocol is the standard treatment for recurrent/metastatic HNSCC, especially for patients who cannot receive chemotherapy [46].

Unfortunately, many resistance mechanisms exist against cetuximab, like EGFR mutations, as well as mutations in factors downstream of the EGFR, particularly PI3K and RAS mutations, that can lead to constitutive activation of EGFR pathways, therefore blocking the cetuximab effect [47]. Another mechanism of resistance is the overexpression of ErbB receptors to compensate for the inhibition of EGFR [5].

This antibody competes with the EGF and binds to the extracellular domain III of EGFR with a higher affinity. Thus, cetuximab blocks the ligand-receptor interaction, therefore, inhibiting the kinase-dependent signal transduction by the intracellular domain. EGFR tyrosine kinase could also dimerize with other TKI from the erbB family but the binding of cetuximab to EGFR also prevents it. Another mode of action of cetuximab is the internalization of the receptor. This internalization blocks EGFR signaling and is followed by degradation of the EGFR in lysosomes and thus downregulation of EGFR [19]. Finally, Cetuximab, or c225, is a chimeric IgG1 antibody with a human Fc region (fragment crystallizable region), and murine Fab (fragment antigen-binding) [19]. The Fc region is an invariable region that interacts with the immune system while the Fab region is a variable region that binds the antigen.

With its action on the receptor, cetuximab inhibits the downstream signaling pathway. Since cetuximab prevents EGFR activation, there is no activation of downstream pathways, MAPkinase, and PI3K/AKT/mTOR, and therefore no transcription of target genes or activation of target proteins [19] leading to cell cycle arrest and apoptosis.

a. Cetuximab induces cell cycle arrest

The effect of cetuximab on the cell cycle could be explained by the inhibition of PI3K/AKT/mTOR and MAPKinase pathways **(Figure 5)**.

In the PI3K/AKT/mTOR pathways, the principal action of Akt is the mTOR activation that increased Cyclin D1 expression responsible for the induction of G1/S phase transition [48]. By inhibiting PI3K/AKT/mTOR pathways, cetuximab decreases Cyclin D1 expression, and thus the cell cycle arrest.

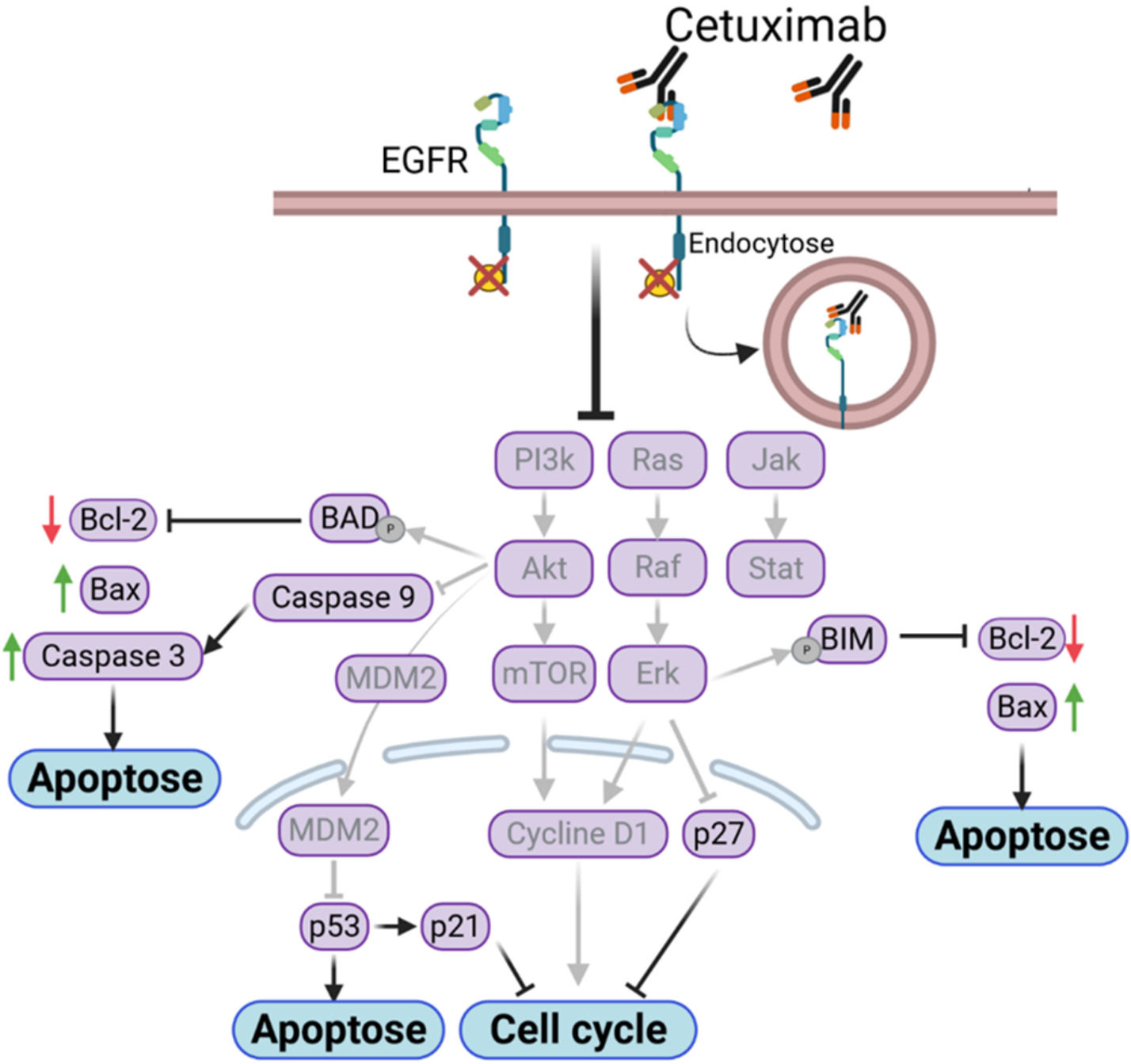

Figure 5: Cetuximab impact.

Cetuximab inhibits the binding of EGF to EGFR and also causes endocytosis of the receptor, so EGFR cannot be phosphorylated and activated. Thus the upstream pathways are not activated and cannot induce cell proliferation and survival.

Inhibition of the **RAS/RAF/ERK** pathway releases the negative regulator of the cell cycle, p27, and leads to cycle arrest. Erk inhibition induces the dephosphorylation of pro-apoptotic factor Bim leading to its activation. In return, BIM inhibits Bcl-2 and induces apoptosis through Bax increase

Inhibition of the **PI3K/AKT/mTOR** pathway inhibited the induction of the cell cycle driver, cyclin D1.

Inhibition of Akt has several apoptotic effects. Akt can no longer phosphorylate the pro-apoptotic factor Bad which then sequesters Bcl-2 and prevents its inhibitory action on Bax, Bax is thus increased and can trigger the mechanism of apoptosis. Akt also has an inhibitory effect on caspase 9, once Akt is inhibited, caspase 9 can induce apoptosis. And finally, Akt allows the translocation to the nucleus of MDM2 which will inhibit p53, the inhibition of Akt allows the induction of p53 and thus the arrest of the cell cycle via p21 and apoptosis.

EGF, epidermal growth factor; EGFR, epidermal growth factor receptor

The inhibition of the MAPKinase leads to the inhibition of the transcription of the genes that encode C-Jun and C-Fos. C-Jun and C-Fos are known to form the complex Activator Protein-1, which is responsible for the transcription of the G1 phase driver Cyclin D1 [48].

In addition, inhibition of MAPKinase by cetuximab overcomes inhibition of the cell cycle inhibitor p27 through inhibition of ERK, the final effector of MAPKinase pathways [48]. The cell cycle inhibitor p27KIP1 binds to CDK to block the interaction domain between CDK and cyclin, and on the other hand prevents ATP binding to the catalytic site of CDK [49], [50]. It has been observed that cetuximab caused an arrest in the G1 phase of the cell cycle on oral squamous cell carcinoma (OSCC) via the decrease of the activity of the Cyclin-Dependent Kinases 2 (CDK2) through upregulation of cell cycle inhibitor p27KIP1 (kinase inhibitor). CDK2 associates with cyclin E to stimulate the progression from the G1 phase to the S phase of the cell cycle.

b. *Cetuximab induces apoptosis*

Moreover, the mechanism behind the induction of apoptosis by cetuximab is not clearly established.

However, cetuximab has an impact on pro-apoptotic gene expression and proteins on colorectal cancer cell lines. Cetuximab increased the expression of pro-apoptotic gene *p21*, *p27,* and *p57,* and increased autophagy gene *LC3A*, *BECN1,* and Autophagy-Related protein *ATG44* [51]. Cetuximab is also able to induce activation of caspase 3, caspase 8, and caspase 9 responsible for apoptosis [52]. Cetuximab also induces expression of Bax [53] and decreases Bcl-2 [54] like in the intrinsic pathways of apoptosis on colorectal cancer and epithelial cell lines, respectively.

The hypothesis for induction of apoptosis by cetuximab is through the inhibition of PI3K/AKT/mTOR and MAPKinase pathway that overcome pro-apoptotic factors inhibition. MAPKinase pathway negatively regulates apoptosis by phosphorylation of pro-apoptotic factor BIM leading to its ubiquitination and degradation [48] **(Figure 5)**. Akt also negatively regulates apoptosis by phosphorylation of pro-apoptotic factor BAD but also inhibits the activity of caspase 9, and finally, Akt induces translocation in the nucleus of MDMD2 to inhibit p53 activity [48]. The capacity of cetuximab to inhibit PI3K/AKT/mTOR lifts the inhibition of apoptosis.

Taken together, Cetuximab treatment leads to cell proliferation arrest by blocking EGFR activation and therefore non-activation of downstream pathways, and cetuximab also induces apoptosis.

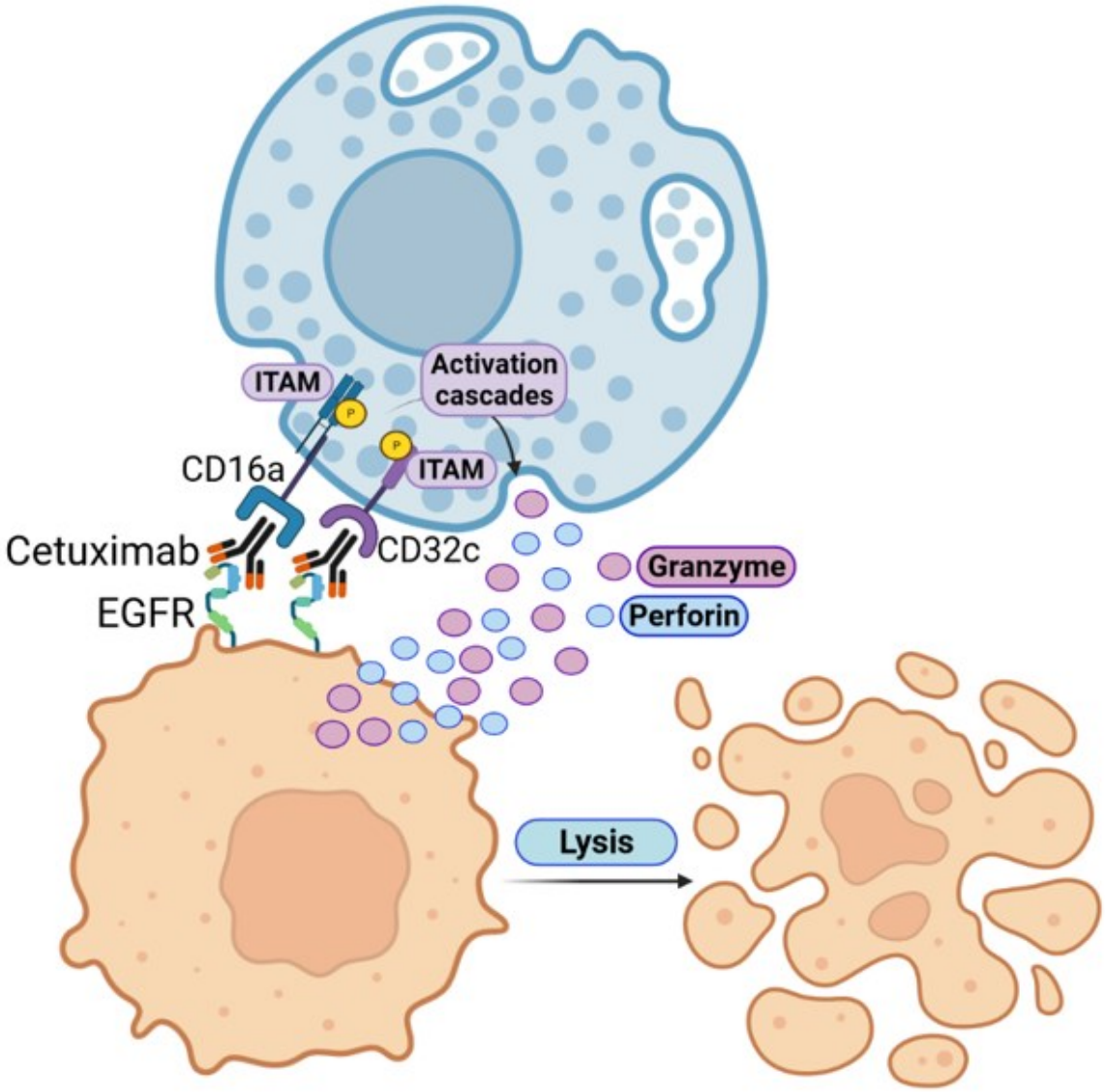

Figure 6: Cetuximab induction of ADCC.

Cetuximab is an antibody with a murine variable part that binds to EGFR and the constant part can be recognized by certain immune cells, in particular, natural killers (NK) to cause Antibody-dependent cell-mediated cytotoxicity (ADCC). ADCC is a specific mechanism causing lysis of antibody-tagged cells.

The CD16a and CD32c receptors present on the surface of the NK recognize and bind the constant part of cetuximab bound to the cancer cell, this induces phosphorylation of the ITAM motif present in the intracellular part of these receptors. This phosphorylation of ITAM allows, via a signaling cascade, the release of perforin and granzyme in the synapse between the NK and the cancer cell. Perforin creates pores in the membrane of the cancer cell allowing the entry of granzymes which will have a cytotoxic effect.

Thus, ADCC allows the lysis of cancer cells recognized by NKs thanks to cetuximab.

c. *Cetuximab impact metastasis progression*

Cetuximab also has an effect on angiogenesis and metastasis development. Cetuximab decreases the production of the VEGF by cancer cells, responsible for the creation of new blood vessels. VEGF expression is regulated by the MAPKinase pathway activation, suggesting that the cetuximab effect on VEGF expression depends on the inhibiting of the EGFR pathway on bladder cancer, HNSCC, and squamous cell carcinoma [50]. Cetuximab also decreases the production of IL-8 on human intestinal microvascular endothelial cells [50] which has an angiogenic effect through its interaction with CXCR1/2 [55]. The metastases inhibition mediated by cetuximab is also thought to be due to a decreased expression of matrix metalloproteinase-9 [56]. Matrix metalloprotease-9 cleaves cell surface proteins releasing the cells from their anchorage in the matrix allowing the migration of cells to other sites in the body.

d. *Cetuximab induces ADCC*

Thus, Cetuximab has several cell effects via the regulation of the activity of several signaling pathways and the expression of different factors in cancer cells. However, it has been proposed that the primary mechanism of action of cetuximab relies on antibody-dependent-cell-mediated cytotoxicity (ADCC) **(Figure 6)**.

The ADCC is a mechanism involving the immune system by which the antibody-bound cell is lysed by cytotoxic immune cells. Cetuximab is able to induce ADCC thanks to his human Fc and its IgG1 isotype. Interestingly, cetuximab is also known to induce ADCC in lung cancer cells and leukemia cell lines [57], [58]. Remarkably, cetuximab induces ADCC at low doses that do not allow inhibition of cell proliferation, with a minimum effective concentration of 0.25µg/ml [57]. ADCC mediated by cetuximab can even take place without the EGFR inhibition effect [58]. Furthermore, cetuximab induces ADCC independently of the mutational status of the receptor downstream pathways [58]. ADCC correlates with the level of EGFR expression [58] but it can still be detected with weak EGFR levels of expression [57]. The main immune cells implicated in cetuximab-mediated ADCC are $CD3^{-}CD56^{+}$ cells corresponding to NK cells [57]. The ADCC can be improved *in vitro* by the addition of IL-2 which permits a better NK activation [57].

In the case of IgG1 antibodies, like cetuximab, NK cells are the most implicated cells in ADCC. NK cells are immune cells from the innate immune system that can recognize the Fc region of the antibody. CD32c and CD16a expression on NK will bind to the antibody Fc region, leading to immunoreceptor tyrosine-based activation motifs (ITAM) phosphorylation and signal transduction. The result of this signal is a release of cytotoxic granules (granzyme and perforin), TNF signaling, and finally

cell lysis [59]. Other cells like monocyte or $CD8^+$ lymphocyte T cytotoxic (LT $CD8^+$ cytotoxic) are also implicated in ADCC. Furthermore, LT $CD8^+$ cytotoxic depletion in animal models diminished cetuximab-mediated ADCC [60]. Thus, cetuximab-mediated ADCC depends on innate immunity through NK implication and on adaptative immunity through LT $CD8^+$ cytotoxic [19].

Other antibodies against EGFR have been developed and approved for the management of patients, like the fully humanized panitumumab antibody [19]. However, panitumumab did not show a better response than cetuximab and failed to induce ADCC, probably due to the fact that it is an IgG2 isotype and not an IgG1 isotype like cetuximab. Cetuximab-induced ADCC is more effective if the number of immune cells, such as NK cells or LT $CD8^+$ cytotoxic is high. This evidence shows the importance of the immune infiltrate in the tumor microenvironment in the therapeutic efficacy of cetuximab.

Chapter II

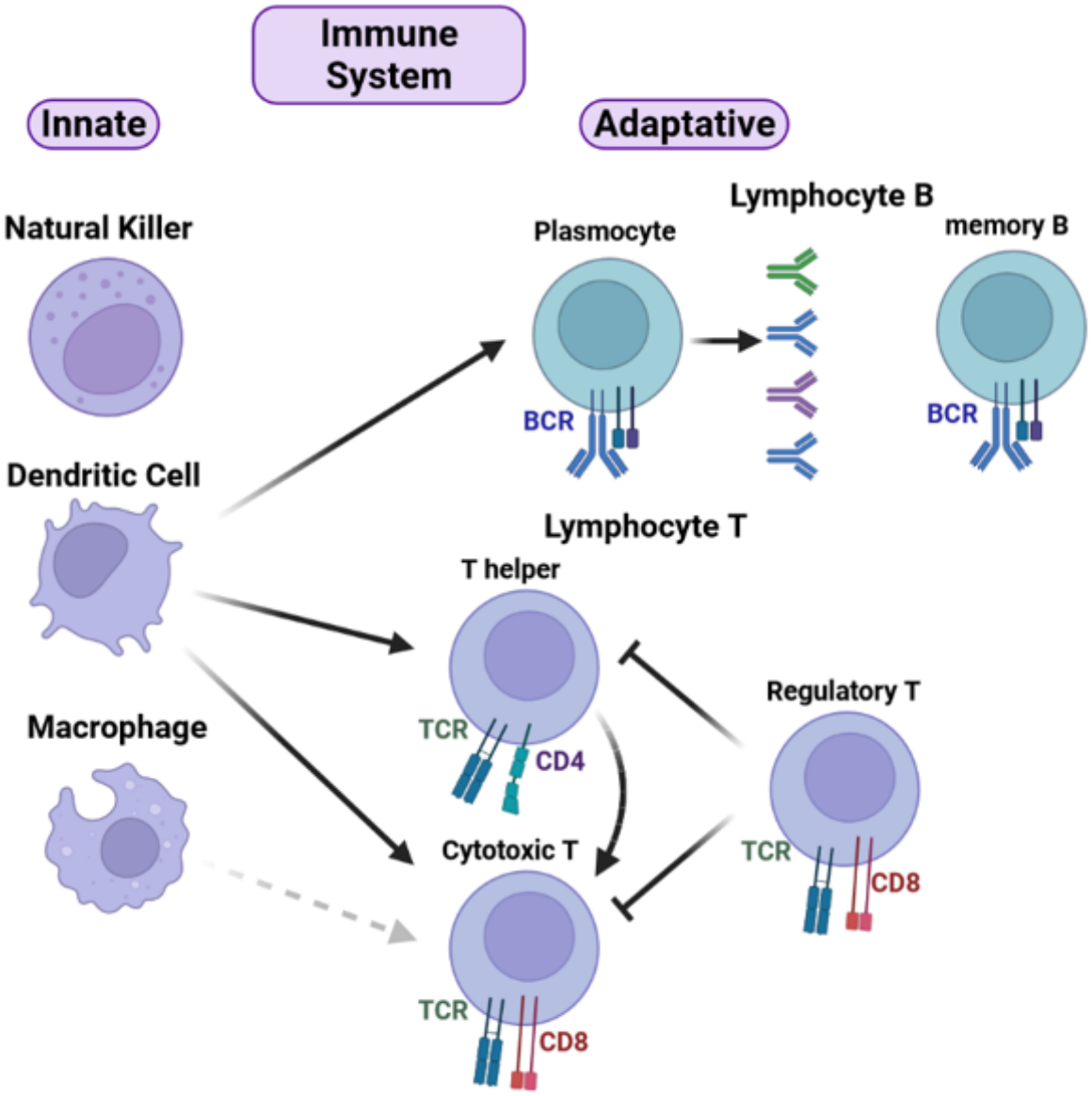

Figure 7: Simplified schematic representation of the immune system.

The immune system recognizes antigens considered as 'non-self', i.e., foreign to the body. This can be a pathogen (bacteria, virus). The immune system also recognizes neoantigens that have appeared as a result of genetic alterations (mutated proteins, overexpression of proteins, expression of embryonic proteins) that are strongly present in tumor cells. The immune system is composed of two parts, an innate part that intervenes rapidly and without specificity and an adaptive part that is slower and specific to an antigen. These two systems work in cooperation. In the innate part, the natural killers secrete cytotoxic proteins. Macrophages phagocyte cells infected by pathogens or presenting non-self antigens. Macrophages can also present antigens to activate cytotoxic T-cells and are therefore considered to be antigen-presenting cells. Dendritic cells are antigen-presenting cells that will activate B and T lymphocytes by presenting them with a specific antigen, thus creating an adaptive response. B lymphocytes are involved in the immune response and produce antibodies. B lymphocytes can also form an immune memory that remains dormant and allows for faster activation when the danger reappears. Finally, T cells are activated by dendritic cells. There are two categories of T cells, CD4 and CD8. The CD4 T cells are the T helper cells that help to activate the CD8 T cells. The CD8 T cells form the cytotoxic T cells that lyse the target cells and the regulatory T cells that inhibit the immune system.

A. Tumor microenvironment

The tumor microenvironment (TME) is defined as the cellular environment in which the tumor develops. It is composed of different cell populations: malignant cells, fibroblasts, mesenchymal cells, endothelial cells, and immune cells [61]. All subsets of non-malignant cells form the stroma [62]. Tumor cells constantly interact with other cells in the TME and benefit from the release of pro-tumor signals, so the TME is often favorable to tumor progression. But it can also contain elements that inhibit tumor development. This balance between pro-and anti-tumor elements will determine the progression of the tumor and thus the prognosis of the patient. [62].

One of the key elements of TME is immune cell infiltration because of the immune response against cancer cells. The immune system (IS) is made up of several cell types that make up the innate and adaptive IS. The role of the IS is to protect the organism against external (pathogens) and internal (cancerous cells) dangers. The cells communicate with each other allowing their mutual activation giving a certain complexity to the IS **(Figure 7)**.

The IS plays a major role in carcinoma development, and notably, a chronic inflammatory environment favors the development of tumor cells [63]. Inflammation is a defense mechanism to a dangerous/harmful stimulus such as tissue injury, pathology, or cell damage. Through cytokine and chemokine production, inflammation allows the recruitment of immune cells to eliminate damaged/dangerous cells. Unfortunately, these signals also have pro-tumor effects such as the cytokine IL-6 or TNFα, which have proliferative and anti-apoptotic effects on tumor cells [64]. Today, chronic inflammation is considered as a hallmark of cancer and is associated with 25% of them [65][66].

During tumor initiation, tumor cells are recognized by the IS as non-self and are then eliminated. Indeed, at the neoplasia stage, tumors carry many mutations and this gives rise to peptides harboring tumor-associated antigens, abnormal expression of a ubiquitous protein, expression of a protein normally associated with a particular tissue, expression of viral/bacterial material, or expression of embryological signals. All these neo-antigens are recognized by the IS as non-self [67]. During this phase of immunosurveillance, both innate and adaptative immunity are involved. Innate immunity intervenes quickly whereas adaptive immunity can take several days to be set up. However, it is more specific to pathogens like bacteria, virus, and parasites, thanks to a phenomenon of selection of cells reactive to this pathogen. This selection allows the establishment of an immune "memory" by maintaining dormant cells specific to this pathogen [68]. To avoid lysis, malignant cells develop immunosuppressive mechanisms, like the production of anti-inflammatory molecules like IL-10 or IL-4 [69], decreased neoantigen expression and presentation, and also the expression on their surface of immune checkpoints [67].

All these mechanisms cause selection pressure for less immunogenic malignant cells and tumor escape from the IS control.

HNSCC TME is highly infiltrated with a subset of immune cells in general and this infiltration could be associated with prognostic depending on the type of infiltrated cells [1]. The advent of single-cell RNA sequencing has made it possible to accurately analyze the composition of the TME. This technique requires the isolation of viable individual cells by limiting dilution, fluorescence-activated cell sorting, microfluidic, and other approaches. Once the cells are isolated, RNA sequencing is performed. The final step is the data processing by many bioinformatic tools to separate relevant signals from background noise [70]. So, single-cell RNA-sequencing allows the identification of every cell composing the TME based on their specific gene expression profiles.

Single-cell RNAseq has been used in a few studies to understand the heterogeneity of the TME of HNSCC in order to better understand how each cell type can influence the tumor ecosystem and tumor progression as well as patient prognosis. These studies focus particularly on the immune cells. First, they identified immune cells constituting the TME [71], and the state of activation in which they are [72]. Then they analyzed the interaction between the immune cells and the non-immune cells through the analysis of the expression of ligand and their respective receptor [71], [73] but also through the correlation between immune cells infiltration and non-immune cells infiltrations like fibroblast, endothelial cells, etc. Finally, the tumor progression is analyzed through a comparison between the composition of the primary tumor and the next stage of LN invasion [62], [75]. All this data, expressions of immune cells and their states of activation, their interactions with the tumor, and the changes of the TME between primary tumor and LN, allow a prognosis to be associated with each immune cell type. These studies have been based on a cohort analyzed by Puram *et al* [72] (GEO: GSE103322) on OSCC obtained from a cohort of 18 patients and the isolation and analysis of ≈ 6000 cells. This cohort is composed of treatment-naïve patients, 5 of these patients present LN metastasis samples, and 15 patients present Peripheral Blood Leukocytes (PBL) samples. Cells had been distinguished by $CD45^+$ (immune cells) and $CD45^-$ (epithelial and stromal cells).

B. Immune cells

1. Natural killer

NK cells are part of the innate IS and play a crucial role in immunosurveillance by eliminating tumor cells and controlling tumor growth [76]. The NK activation is regulated by a balance between activating and inhibitory signals. Activation signal is given by the binding of a ligand, UL16 binding protein1-6, with its receptors Natural killer Group 2D (NKG2D) on NK surface.

The inhibitory signal depends on the MHC class I (MHC-I) expressed by the target cells and the inhibitory receptor, like NKG2A or inhibitory killer cell immunoglobulin-like Receptor on NK surface [77]. NK cells target malignant cells because they lack MHC-I and so they lack the ligand for inhibition signal. But this only signal isn't sufficient, NK also recognizes ligands such as MHC I polypeptide-related sequence A (MICA) present at the tumor cell surface through the NKG2D receptor. NKGD2 seems to play a key role in immune surveillance, as mice lacking this receptor are more prone to cancer development. The malignant cell lysis mediated by NK relies on two mechanisms: the liberation of cytotoxic perforin and granzyme in the synapse between the two cells, and the activation of TRAIL and FasL pathways in cancer cells through the production of TNFα or direct contact between the cells [67].

TNFα, TRAIL, and FasL induce the extrinsic apoptosis pathway but Granzyme and perforin release has also a crucial role in IS cytotoxicity. The perforin forms a pore in the cell membrane and allows the entry of ions, water, small molecules, and enzymes [78]. Granzymes are proteases with different intracellular effects that lead to apoptosis. Granzyme B induces caspase-dependent apoptosis via mitochondrial changes. For example, Granzyme B cleaves the BH3-only protein Bid which interacts with Bax and/or Bak and induces the release of cytochrome C. This cytochrome C release can also be induced by the inactivation of Bcl-2 by granzyme B. Conversely, Granzyme A does not activate pro-apoptotic factors, but generates single-stranded DNA cuts, as well as it disrupts the inner mitochondria membrane leading to ROS generation. Apoptosis induced by granzyme A is caspase-independent, in fact, Granzyme A activates a DNase that produces SSB in the DNA. The mechanism of granzymes C/H/K and M are not yet fully understood. Granzyme C/H/K seems to have a similar effect to granzyme A, and granzyme M induces caspase and mitochondria-independent apoptosis [79].

In the sc-RNA seq performed on the cohort of 18 patients described above, NK cells had been identified by the canonical markers KLRD1, NCAM1, or CD94 [74], [80]. The differential expression of *GNLY*, *NKG7*, *CD160*, *GZMB*, and *CCL3* genes was also used as markers for the identification of NK cells [62]. NK cells are also identified by these markers in the PBL [74]. No analyses have been done here on the activated state of NK but the expression of granzyme B could be the marker of an activated state of NK since its release when NK is activated. However, CD94 is implicated in self-tolerance, it heterodimerizes with NKG2A receptors to induce a strong inhibitory signal when binding to HLA-E [81]. CD94 expression implicated that an inactive state is also possible.

Not much investigation has been done to understand the interaction between the tumor cells and NK, like the ratio expression of NKG2D/NKG2A and the level of ligands expression, like MICA or HLA-E

respectively ligands of NKG2D and NKG2A [77]. These data could indicate a strong activation or inhibitory signal and so the activated state of NK.

These sc-RNA seq studies have not investigated the specific impact of the NK population on prognosis. Commonly, NK infiltration is a good factor for the patient [82] and is associated with better survival [1].

2. B lymphocytes

B lymphocytes are the only cells of humoral immunity and the only cells that produce antibodies. They have a receptor on their surface, the BCR, which allows the recognition of antigens. To be activated, the lymphocyte must recognize an antigen either directly in the environment or presented by an Antigen-Presenting Cell (APC). Once the BCR-antigen binding is achieved, there is a clonal selection of B lymphocytes specific to this antigen which will then proliferate and differentiate into plasma cells to produce antibodies specific to the antigen. B lymphocytes can also become memory B lymphocytes. These are dormant cells that circulate in the body and initiate a stronger and faster immune response when they recognize their specific antigen [83].

The sc-RNA seq study identified B lymphocytes/plasma B lymphocytes subset on 18 patients based on 4 genes expression: *SLAMF7*, *CD79A*, *BLNK*, and *FCRL5* [72], [80]. The gene expression *CD37*, *CD79B*, *IGHG*, *IGHA1*, and *IGHM* are also used to identify B lymphocytes in this cohort [62]. The portion of B lymphocytes differs among patients with a minimum of 1.35% of tumor fraction to 58.1% of tumor fraction inversely proportional to the fraction of malignant cells which is 60% and 2% for these two respective patients [80].

The interaction between immune cells and malignant cells is measured by the expression of ligands and the corresponding receptors. B lymphocytes represent a small portion of immune infiltration but they show strong interaction with the tumors with 40 interactions found when ligands are expressed by malignant cells and corresponding receptors by B lymphocytes and 15 interactions in the other way[72]. Unfortunately, the names of the ligand-receptor pairs analyzed are not specified, only TGFB3-TGFBR2, FGF7-FGR2, and C-X-C motif ligand 12 (CXCL12) interaction with C-X-C motif chemokine Receptor 7 (CCR7) has been described and are implicated in EMT [72]. However, EMT negatively correlates with B lymphocytes [84] supposing that most of the B lymphocytes interactions observed by Puram *et al* don't include EMT ligands or receptors.

In some patients, B lymphocytes aren't found in the tumor but only in LN metastasis [72]. B lymphocytes LN metastatic infiltration has been associated with good prognostic but the phenotype and activation state have not been studied [85].

B lymphocytes infiltration correlates with better OS [73], [84], [86], and a diminution of the B lymphocytes population correlated with the worst OS [62]. Interestingly, B lymphocytes are associated with oropharynx location, and the molecular group atypical [86]. The atypical subtype is marked by HPV infection, and this infection mainly affects the oropharynx, and B lymphocytes are strongly implicated against pathogen infection [71]. This explains the prevalence of B lymphocytes in the oropharynx. Atypical subgroup has a better OS [22] that could maybe be explained by the infiltration in B lymphocytes.

3. Dendritic cells

Dendritic Cells (DC) are antigen-presenting cells at the interface between innate and adaptive immunity [67]. DC have two distinct states, an immature state, and a mature state. An immature DC can recognize antigens and phagocytose them. DC recognizes danger signals such as Pathogen-Associated Molecular Pattern (PAMP) or Danger-Associated Molecular Pattern (DAMP) through Pattern Recognition Receptors (PRR). Once the antigen is phagocytosed the DC will mature and migrate to the lymph nodes. Maturation of DC allows it to gain mobility properties, such as the expression of the CCR7 receptor which by binding with its ligands CCl221 and CCl19 expressed in the LN allows the migration of DCs towards them [87].DC maturation also increases the expression of the co-stimulatory molecule CD80 and CD86 that activates lymphocytes T and increases the production of pro-inflammatory cytokines and chemokines. Once in the lymph node, the DC will present the antigen to $CD4^+$ T lymphocytes through MHC I and to $CD8^+$ T lymphocytes through MHC II. Thus the DC allows the activation of T lymphocytes [88]. In the context of tumors, the antigen presented by DCs is called Tumor-Associated Antigen (TAA) or Tumor-Specific Antigen. TAA is released by stressed tumor cells or dead/dying cells are also described as “immunogenic” and then TAA is recognized by DC as DAMPs leading to their maturation [89].

DC subsets had been identified on 18 patients by the gene expression of *CD80*, *CD40*, *CD83*, and *CCR7* [71], [72], [80]. DC is also identified by *CD1A*, *CD1C*, *CD207*, and *CCL17*[62]. The DC population differs to no infiltration, to 33.8% of the tumor fraction [80].

DC shows the same level of interaction than B lymphocytes but the correlation between EMT and DC population hasn’t been done [72]. But like B lymphocytes, DC is associated with atypical subgroup, this isn’t surprising as DC are a key component against pathogens infection through their APC function. In contrast, DC infiltration correlates with Cancer-Associated Fibroblasts (CAF) infiltration [75]. CAF are associated with tumor progression and immunosuppression via secretion of IL-6, TNF, and immune checkpoint [63]. The phenotype of DC hasn’t been explored so the impact of DC infiltration is unclear.

However, there is no difference between LN metastasis and the primary site of the tumor concerning the repartition of DC [72] suggesting that DC are not implicated in cancer progression to LN even if it correlates with CAF.

Unfortunately, sc-RNA seq shows no correlation between DC and better survival [72].

4. Macrophage

Macrophages are large cells involved in innate immunity but also in the initiation of the adaptive response [90]. Their functions include defense against pathogens, metabolic function, clearance of cellular debris, tissue repair, and remodeling [91]. Macrophages express many receptors, like Toll-Like Receptor (TLR) that can detect bacteria and viruses, but also apoptotic cells via the detection of Phosphatidyl Serine (PS). PS are expressed at the surface of apoptotic cells and are recognized by the integrin αvβ3 or αvβ5 at the surface of macrophages. After receptor stimulation, the membrane protrusions surround the pathogen or apoptotic cells and absorb them into the phagosome formed by the fusion of cell membranes. In the phagosome, the pathogen or apoptotic cells are attacked by ROS, and free fatty acid produces by phospholipase A2. Thereafter, myeloperoxidase (MPO), azurophilic granule, and hydrolase fuse into the phagosome to degrade pathogen and apoptotic cells. In macrophages, Fe^{2+} ions replace MPO as substrates. Finally, ATPase pumps lower the pH in the phagosome and completes the destruction of pathogen and apoptotic cells. Thanks to the mechanism described above macrophages are able to present peptides from the digested pathogen or apoptotic cells through MHC I to T lymphocyte for activation, giving the macrophage a role of APC [92].

Depending on the expression of various factors, including chemokines and cytokines, growth factors, and transcription factors, macrophages can be polarized into at least two activation states, called M1 and M2. This polarization can be influenced by the environment [93]. M1 phenotype is induced by Th1 cytokines such as colony-stimulating factor and IFN-γ while the M2 phenotype is induced by Th2 cytokines like IL-4, and IL-13. These two phenotypes have different metabolism, M1 relies on glycolysis and M2 relies on oxidative phosphorylation. M1 and M2 macrophages exert opposite functions. M1 macrophage induces pro-inflammatory cytokines (IL-6, IL-12, IL-23) and TNF-α and M2 macrophage induces anti-inflammatory cytokines (IL-10) and Transforming growth factor β (TGF-β) [91]. The opposite effect on inflammation of M1 and M2 macrophages leads to an increase or decreased immune response and so the M1 phenotype is considered anti-tumoral while the M2 phenotype is considered pro-tumoral.

In addition to M1 and M2 macrophages, in cancer TME, another macrophage subpopulation has been described called Tumor-Associated Macrophages (TAM). TAM presents M2 activity but also M1

signature. Currently, TAM are considered a different subpopulation of macrophages. TAM expresses chemokines and cytokines, such as IL-6 and IL-10, that promote tumor development [90].

Macrophage subset has been identified in 18 HNSCC patient via *CD14*, *CD68*, *FCGR2A*, *FCGR3A*, and *CSF1R* [72], [73], [75], [80], [86]. Another study, differentiated the two phenotypes of macrophage [62] , through the use of CD163 which is a markers of M2 macrophages [94]. Macrophages represents between 0% to 14.18% of fraction tumor cells [80].

Macrophages are among the immune cells that interact most with the tumor, with about 60 interactions [72]. This can be explained by the versatility of these cells which recognize pathogens, danger signals, apoptotic bodies, and antigen presentation, so they can form numerous interactions with a wide variety of cell types. Macrophages interact with others cells and are negatively impacted in their numbers by keratinocytes [84]. M2 correlates with Immune CAF (iCAF). This could be explained by the expression of CXCL12 by iCAF which recruits M2 through the CXCR4 receptor [84]. Finally, Macrophage infiltration also correlates with the expression of IFN-γ which is a cytokine produced by activated macrophages [84].

The difference in macrophage infiltration between LN metastasis and primary site is unclear. One study shows no difference between LN metastasis and primary site in terms of macrophage infiltration [72]. In one other study, M1 macrophages represent 90% of macrophages in primary site and 95% in LN while M2 macrophages represent 8% and 3% respectively. M2 macrophages decreased in LN while M1 macrophages increased. On the contrary, the TAM population hasn't been identified precisely while a high level of TAM and M2-like TAM has been observed in LN and is associated with poor prognosis [95].

On other hand, cholesterol metabolism is enriched in LN metastasis and the outflow of cholesterol from the macrophage membrane reverses the anti-tumor function of these cells. So cholesterol metabolism could explain the difference in M1 and M2 presence in LN metastasis [62].

Interestingly, it has been shown that $CD163^+$ macrophages, *i.e*. M2 macrophages, are involved in tumor progression [91]. But here, no impact of macrophage infiltration on prognostic value [84], [86].

5. Lymphocytes T

T lymphocytes (LT) are immune cells of the adaptive immunity that express the T Cell Receptor (TCR). They are classified into two groups according to whether they express the co-receptor CD4 or CD8. The $CD4^+$ lymphocytes are a population of cells called "helper" (Th) or "conventional" ($CD4^+$conv) that allow the modulation of the IS. For example, Th1 lymphocytes, which differentiation is regulated by IL-12, produce IFN-γ and TNF, which have pro-inflammatory functions and support the cytotoxic function of Lymphocytes T $CD8^+$ (LT $CD8^+$) cytotoxic and macrophages. The differentiation of Th2 lymphocytes is

regulated by IL-4, and they support the function of B lymphocytes. However, Th lymphocytes can negatively regulate the IS by differentiating into regulatory T (Treg) lymphocytes under the influence of TGF-β and IL-2. Treg lymphocytes express IL-10 and TGF and inhibit immune cell functions [69], [96]. Treg lymphocytes express a particular factor, Forkhead box P3 (FOXP3) that decreases the production of IL-2 needed for the differentiation of $CD4^+$ lymphocytes in Th lymphocytes. Treg lymphocytes also increase the production of immune checkpoints [97].

LT $CD8^+$ cytotoxic are effector cells that trigger the lysis of target cells. LT $CD8^+$ cytotoxic are activated by an APC presenting them an antigen associated with MHC I, which is recognized by the LT $CD8^+$ cytotoxic TCR. Once the activation signal is given, LT $CD8^+$ cytotoxic migrates to the site of infection. The TCR recognizes the antigen presented this time by the MHC I of the target cell. Perforin and granzyme are then released and the target cell is lysed. The LT $CD8^+$ cytotoxic also induce apoptosis through the expression of FAS on their membrane [98].

Therefore, LT $CD8^+$ cytotoxic have the ability to recognize and clear cancer cells. To survive and progress, tumor cells decrease the expression of MHC I recognized by LT $CD8^+$ cytotoxic but also express LT $CD8^+$ cytotoxic inhibitory signals as immune checkpoints. In TME two LT $CD8^+$ cytotoxic subsets are differentiated: the classical LT $CD8^+$ cytotoxic with the normal function of killing the cell and inactivated LT $CD8^+$ cytotoxic commonly called exhausted $CD8^+$LT [67].

In a cohort of 18 HNSCC patients, the population of T lymphocytes was distinguished by the expression of *CD4*, *CCR7*, *TCF7* for $CD4^+$; *CD8*, *Granzyme A/B/M/K*, *perforin* for LT $CD8^+$ cytotoxic, exhausted $CD8^+$LT has been identified by immune checkpoint expression (*PD-1*, *LAG3*, *TIGIT*, *CTLA4*), and finally, Treg lymphocyte has been identified by *FOXP3* and *CD25* expression [71], [72], [75], [80], [86]. $CD4^+$ lymphocyte represents up to 40% of the cells composing the tumors , LT $CD8^+$ cytotoxic up to 20.3%, exhausted $CD8^+$LT up to 31%, Treg lymphocyte up to 16.9% [80].

The analysis of the interaction between ligands expressed by malignant cells and receptors expressed by T lymphocytes shows 60% of interaction. On the others way, ligands expressed by T lymphocytes and receptors expressed by malignant cells show 20% of interaction [72]. T lymphocytes aren't correlated with EMT signature [84] meaning T lymphocytes aren't implicated in EMT, we can suppose that the interaction detected between T lymphocytes and cancer cells should not involve EMT ligands-receptors. Likewise, T lymphocytes activity in the immune defense against pathogens could explain that T lymphocytes infiltration correlates with atypical subtype and oropharynx location, consistent with HPV infection which reveals the immune response induced by virus infection [80], [86]. On the contrary, another way to reduce immune cell infiltration is to block the tumor's access to immune cells. Keratinization is the production of keratin protein by cells and could affect the rigidity of the tumors

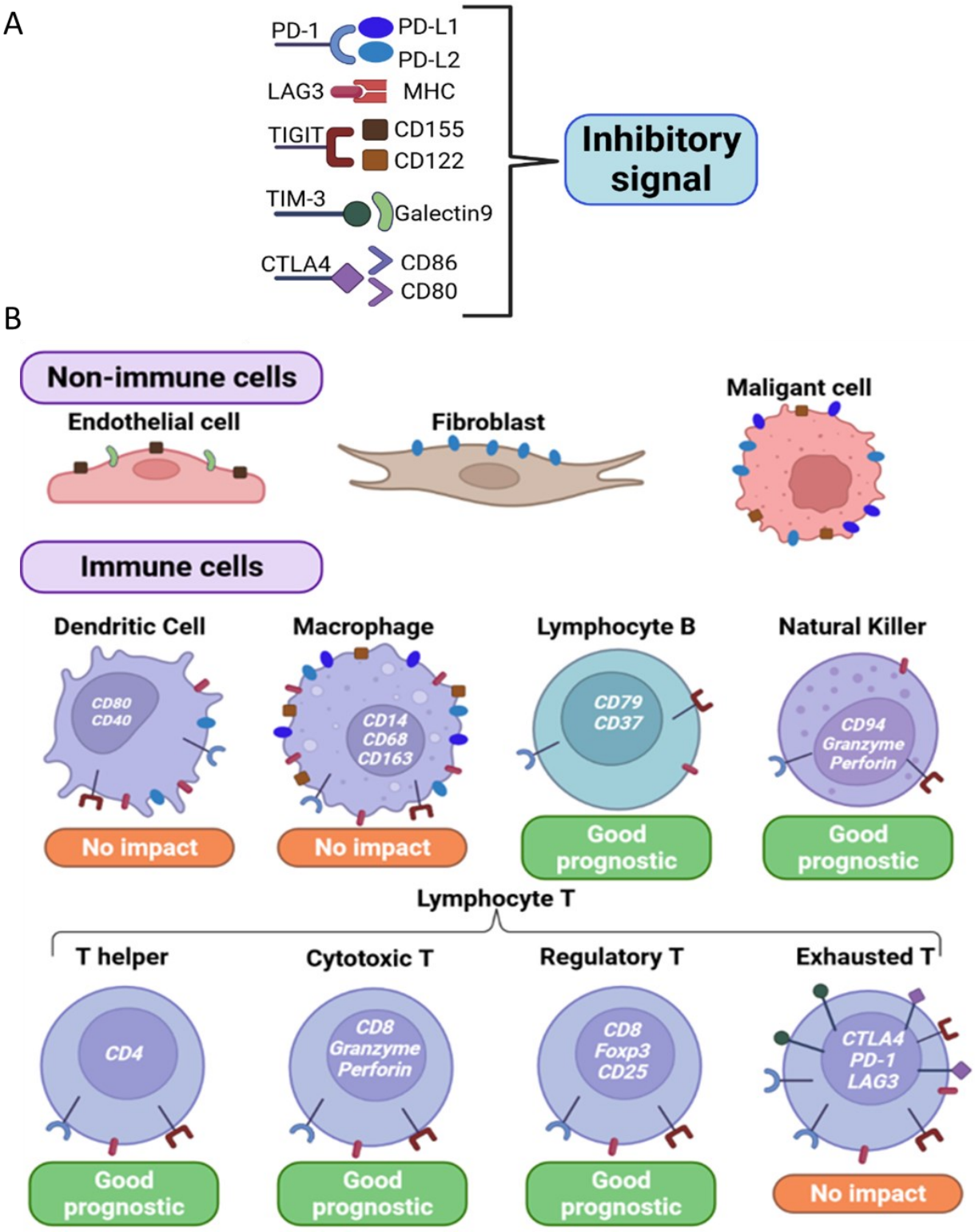

Figure 8: Composition of the Tumor microenvironment (TME)

A. Representation of the most studied immune checkpoint pairs. immune checkpoints are pairs of ligands and receptors that inhibit immune activity. Some immune checkpoint receptors can have two ligands. B. Single-cell RNA-seq studies have identified different cell types that compose the TME based on the expression of specific genes. These studies have made it possible to associate the expression of immune checkpoints with each cell type. They also associated or not a prognosis according to the type of immune cells infiltrating the tumor. This figure schematizes their results.

infiltration by some cells. T lymphocytes are decreased by the tumor keratinization [84].

Because exhausted $CD8^+$ LT express immune checkpoint Programmed death cell 1 (PD-1) which is a target of immunotherapy, one study analyses the change in the T lymphocytes population after anti-PD-1 treatment. Interestingly, after treatment, there is a renewal of the T lymphocyte population due to the recruitment of new T lymphocytes. In this study, the immune response engaged by anti-PD-1 therapies is due to new cytotoxic $CD8^+$LT infiltration, and blocking the PD-1 inhibitory signal of exhausted $CD8^+$LT cells would not be able to change them to cytotoxic $CD8^+$LT [71].

There is no difference in T lymphocyte infiltration between LN metastasis and primary site [72]. In another study, LN metastasis is highly infiltrated by T lymphocytes, especially by LT $CD8^+$ cytotoxic, and presents a better inflammatory signature and high cytokine expression. Exhausted $CD8^+$ LT are less frequent in LN metastasis [62].

T lymphocyte infiltration is associated with better outcomes [84], [86]. Consistently, clustering analyses based on differential gene expression have shown that HNSCC molecular subtypes enriched with T lymphocyte-specific gene expression are also associated with improved OS [73]. Taken individually, Th1 lymphocytes which support LT $CD8^+$ cytotoxic activity are associated with better survival [73]. $CD4^+$ lymphocytes correlate with the better OS, followed by cytotoxic $CD8^+$LT. But the better OS has been observed in the tumor with high infiltration of Treg lymphocytes even if their principal known function is immunosuppressive. The hypothesis explaining this OS is the infection by the oral microbiota. Microbial flora could be translocated from the upper aerodigestive tract to HNSCC tissues, as proposed in the colon. This translocation of microbial leads to inflammation which is a favorable environment for cancer development. To counteract this effect, Treg lymphocytes decreased the inflammation and thus have a good impact and protect against inflammation-mediated cancer cell growth. The hypothesis is that Treg lymphocyte infiltration is a good prognostic because they decrease the inflammation favorable to cancer development [86].

These studies show the heterogeneity of immune cells and the impact of each immune cells population taken individually **(Figure 6B)**.

However it is necessary to take into consideration that the TME is rarely infiltrated by only one population of immune cells, furthermore, immune cells communicate with each other, for example, DC activates T lymphocyte, Treg lymphocyte regulate LT $CD8^+$ cytotoxic, $CD4^+$ lymphocyte interacts with DC and LT $CD8^+$ cytotoxic. The immune infiltration is a complex system implicating many factors. This is why some studies have preferred to stratify tumors according to the infiltration of the TME, defined as “high” or “low immune infiltrate”, independently of the nature and the proportion of immune cells.

Afterwards, tumors with high infiltration of active immune cells, such as LT $CD8^+$ cytotoxic, are classified as "hot" tumors. Conversely, tumors with high infiltration of regulatory cells, such as Treg lymphocytes, are classified as "cold" tumors [99].

High infiltration of immune cells including NK, DC, and T lymphocytes correlates with an improved OS as well as high infiltration of B lymphocytes and DC, and macrophages are associated with a better OS. These tumors also present an upregulation of antigen presentation and enhance the presentation of antigen and thus maintains the activation of immune cells [73]. The TME with high infiltration of immune cells such as LT $CD8^+$ cytotoxic and NK cells would be more favorable for anti-tumor activity. However, these immune cells need to be active in the TME to have a destructive effect on the tumor, which is not always the case. Indeed, the immune cells can be inhibited by different mechanisms, notably the expression of immune checkpoints.

C. Immune checkpoint

Immune Checkpoints (ICP) are molecules that play a key role in the modulation of the immune response and T lymphocytes activity. They are ligand-receptor couples with either stimulating or inhibitory functions **(Figure 8A)**. ICP's principal physiological function is to regulate lymphocyte T activity to avoid autoimmunity or damage to healthy tissue by excessive inflammation [100]. To understand the function of ICP, it is necessary to understand the mechanisms of T lymphocyte activation. T lymphocytes are activated through two signals: one depending on the TCR and the CD4/CD8 co-receptors and the second depending on the CD80/86 co-stimulatory molecule [100]. ICP impact the second signal.

Schematically, concerning the activation of LT $CD8^+$ cytotoxic, an antigen presented by APC via MHC I is recognized by a complex involving the TCR and the CD8 and CD3 co-receptors. This binding of antigens to the TCR/CD8/CD3 complex leads to the phosphorylation of the LCK Src family protein tyrosine kinase, that in turn phosphorylates ITAM in the CD3 intracellular region. Phosphorylated ITAMs further recruit the protein tyrosine kinase ZAP70 [101]. The antigen recognition by TCR/CD8 and activation of CD3 and ZAP70 constitute the first signal required for LT $CD8^+$ cytotoxic activation [102]. The second signal is given by a co-stimulatory ligand CD80/86 on APC cells that binds to CD28 receptors on T lymphocytes. This binding leads to PI3K activation [102]. Both signals lead to the activation of three major signaling pathways: Ca^{2+}-calcineurin, the MAPKinase signaling pathway, and nuclear factor-κB (NF-κB) resulting in survival, proliferation, migration, cytokine production, and effector function [101].

ICP interfere with these stimulatory signals and inhibit activation of LT $CD8^+$ cytotoxic by competing with CD28 as ligands of CD80/CD86 or by dampening the signaling pathway triggering the activation of the TCR.

1. PD-1 / PD-L1

PD-1 or CD279 is a type I transmembrane receptor encoded by the *PDCD1* gene and is expressed on activated T and B lymphocytes membrane. It is known to bind to Programmed Death-ligand 1 (PD-L1) (also called CD274 or B7H1) and its homolog PD-L2 (also known as CD273 or B7DC), which are types I transmembrane protein expressed in endothelial cells, APC and activated lymphocytes. PD-L1 expression is limited outside immune cells but can be found in the heart, lung, placenta, and liver. PD-L2 expression is limited to DC and macrophages [103].

PD-1 possesses an intracellular domain containing an Immunoreceptor Tyrosine-based Inhibitory Motif (ITIM) and immunoreceptor Tyrosine-based Switch Motif (ITSM). The binding of PD-L1/2 with PD1 activates ITIM and ITSM domains that recruit SHP2 to deliver an inhibitory signal. PD-1 activation blocks the phosphorylation of ZAP70, inhibits the MAPKinase pathways, and then stops the activation of T cells [103].

2. CD80, CD86 / CTLA-4

Cytotoxic T Lymphocyte Antigen 4 (CTLA 4) is a type I transmembrane protein expressed on DC, T lymphocytes, and mostly on Treg [103]. CTLA 4 possesses a cytoplasmic tail with tyrosine residues and a proline-rich domain. When this domain is unphosphorylated, CTLA4 is endocytosed to maintain immune cell activity [104]. CTLA 4 outcompetes CD26 and binds to CD80/86 ligands, leading to phosphorylation of his cytoplasmic tail. As PD-1, CTLA a recruits SHP2 resulting in dephosphorylation of CD3 and then inhibition of ZAP70 activation and MAPKinase pathway leading to cell-cycle arrest and decrease of cytokine production [104].

3. TIM-3 / GALECTIN-9

T cell Immunoglobulin-3 (TIM-3) is a type I transmembrane protein with a cytoplasmic tail. The particularity of TIM-3 cytoplasmic tail is the absence of an inhibitory domain but it harbors five conserved tyrosine residues. TIM-3 is a specific marker of Th1 but it is also expressed on other T lymphocytes, including Treg, as well as NK, macrophages, and DC. TIM-3 binds to the C-type lectin galectin 9. The binding of galectin 9 to the IgV domain of TIM-3 causes Th1 cell death. TIM-3-Galectin 9 binding induces intracellular calcium flux and phosphorylation of two tyrosine residues of TIM-3 cytoplasmic tail, which triggers the release of the intracellular adapter protein Bat3 and allows the binding of SH2 domain-containing Src kinases and inhibits TCR signaling by competition. By decreasing TCR signaling, TIM-3 inhibits T cell activities.

But TIM-3 can also have the opposite effect, i.e., a stimulation effect on T cells. In unbound TIM-3, the tyrosine residues are not phosphorylated and Bat3 is anchored to its cytoplasmic tail. In that configuration, Bat3 recruits LCK and preserves or even promotes T cell activation [105].

4. LAG-3 / MHC II

Lymphocyte-Activation Gene 3 (LAG-3) or CD223 is an immunoglobulin composed of an Ig-like domain and type I transmembrane domain and is structurally similar to the CD4 receptor. LAG-3 binds to MCH II with higher affinity than CD4 and then LAG-3 engaged with CD3 negatively regulates T lymphocyte activities [105]. Cytoplasmic tail of LAG-3 is essential since its abrogation deletes the inhibitory function of LAG-3 but the mechanism remains unclear [106]. The signaling pathways induced by the binding of LAG-3 are unclear. The cytoplasmic tail of LAG-3 doesn't harbor any classic inhibitory motif like other ICPs. Among three signal regions, the KIEFLE motif seems to be crucial for the transduction and inhibitory function of LAG-3. LAG-3 reduces T lymphocyte proliferation and cytokine production [105].

5. TIGIT / CD155-CD112

T cell Immunoreceptor with Ig and ITIM domain (TIGIT) is composed of extracellular IgV domains, a type I transmembrane region, and a cytoplasmic tail with ITAM and Immunoglobulin Tail Tyrosine (ITT)-like domain. TIGIT is expressed on NK cells, T cells, Th, and Treg. TIGIT binds with high affinity to CD155 and weak affinity to CD112. These two ligands are expressed on APC. TIGIT binding to CD155 inhibits T lymphocytes proliferation, cytokine production, and TCR signaling but the exact mechanism of TIGIT action hasn't been studied at the protein level in T lymphocytes. In contrast in NK cells, the phosphorylation of tyrosine residue ITAM and ITT-like motifs allows the binding of two adaptor proteins Grb2 and β-arrestin2. These two adaptors recruit SH2 domain-containing inositol-5-phosphatase to TIGIT cytoplasmic tail and that recruitment inhibits MAPKinase and NF-κB pathways resulting in NK cells inhibition. Moreover, TIGIT also promotes survival and maintenance in T cells via induction of anti-apoptotic molecules and receptors for pro-survival cytokine [105].

6. Immune checkpoint in TME

Cancer cells hijack the ICP mechanism: they express ICP at the cell surface, therefore, provoking LT $CD8^+$ cytotoxic anergy and escaping the immune system. ICP-blocking immunotherapies have been developed to counteract the functional effect of ICP expression on malignant cells and restore a cytotoxic anti-tumor immune response. Classically, these immunotherapies target the ligand or the receptor of an ICP couple and block their interaction allowing to remove the inhibition of the immune cells.

ICP ligands were studied by sc-RNA seq in parallel with immune cell identification and their expression was associated with a specific cell type. This could help in the choice of immunotherapy to be administered depending on the target expressed. The authors also tried to associate a prognosis with the expression of ICP. As a reminder, the cohort is composed of 18 treatment-naive patients, 5 LN metastasis samples, 15 PBL samples, and the isolation and analysis of ≈ 6000 cells [72].

ICP receptors PD-1, TIGIT, LAG3, and TIM-3 are expressed by all immune cells at various levels [72], [74] so all immune cells can be inhibited **(Figure 8B)**. ICP expression depends on the TME, tumors with high inflammation present a higher level of LAG3 expressed on DC and especially on macrophages. In general, *PD-1*, *LAG-3*, *TIGIT,* and *CTLA4* expression are markers of exhausted $CD8^+$LT cells and were used to distinguish this subset of cells in the TME in a cohort of 18 HNSCC patients. However, the expression of each ICP was found to be heterogeneous between patients [71], [72], [80], [86]. This different expression could explain the variable responses to the same immunotherapy and emphasizes the choice of therapy according to the level of expression of the therapeutic target. T lymphocytes present the most interaction with the malignant cells [72], and that could be explained by the many interactions involving ICP. In this cohort, the expression of both PD-1 and CTLA4 was decreased in LN metastasis compared to the primary tumor. Interestingly, exhausted $CD8^+$LT are less present in LN metastasis [62], reinforcing the role of ICP expression in the inhibition of cytotoxic $CD8^+$LT. Indeed, PD-1 and CTLA4 expression inhibit T lymphocytes activation leading to exhausted $CD8^+$LT in the primary tumor site while in the absence of PD-L1 and CTLA4, cytotoxic $CD8^+$LT are dominant in LN metastasis.

The level of ligands expression present depends on the cell type **(Figure 6B)**. Macrophages present a high level of PD-L1, PD-L2, and CD122, while DC expressed high level of PD-L2 [74]. The expression of ICP ligands is mostly associated with immune cell type meaning that the inhibition of T effector is principally achieved through other immune cells. Macrophages seem to be the immune cell population with the most ICP expression and are the most implicated in the inhibition of the IS in the TME. Specifically, PD-1/PD-L1 interactions seem to be mainly mediated by macrophages in 8/12 patients, TIM-3/Galectin 9 interactions mediated by macrophages were found in 10/12 patients, and only 2/10 patients present this interaction with $CD8^+$ lymphocytes[74]. It is possible that macrophages expressing a high level of ICP are TAM. TAM immunosuppressive action is supported by the expression of ICP, notably PD-L1 and CTLA-4 ligands [107]. The ICP expression on TAM could explain the association of TAM with bad prognostic [95].

But the ICP ligands can also be expressed by non-immune cells as PD-L2 expressed by fibroblast, endothelial cells expressed galectin9, and endothelial cells expressed CD155. These cells

through the expression of ICP can inhibit IS, notably TIGIT interaction is facilitated by non-immune cells in addition to DC and macrophages [74].

These studies based on sc RNA-seq show the heterogeneity of the TME in immune cell infiltration and ICP expression. It also demonstrated that immune infiltration influences the prognosis of the patient through their state of activation or inhibition linked with the interaction or not with ICP. A better view of the immune population in TME, as well as ICP level expression, could guide the choice of immunotherapies.

The tumor with high inflammation could be a signature of high expression of ICP and so they could be more responsive to immunotherapies targeting ICP receptors.

Immunotherapy against PD-1 and PD-L1 called nivolumab and pembrolizumab has recently been approved by FDA for the treatment of recurrent/metastasis HNSCC. Nivolumab is an anti-PD-1 monoclonal IgG4 antibody and pembrolizumab is an anti-PD-1 monoclonal antibody [100]. In clinical trials, patients show complete and long-lasting responses. Unfortunately, the overall response occurs only in 18% [108]. Strikingly, these clinical trials have shown that the level of PD-1 and PD-L1 expression does not correlate with response to treatment. Some patients with high PD-1 expression do not respond to treatment, while some patients with no PD-1 expression do [100]. Currently, no available biomarker has been found for immunotherapies response.

However, these studies are limited by the small number of patients analyzed, with a maximum of 18 patients. Many more patients must be included to link an immune infiltrate to a prognosis. Larger scale studies are therefore necessary before establishing the immune infiltrate or ICP expression as a clinically useful biomarker. Furthermore, IS is a very complex system with many interactions between immune cells but also between non-immune cells. These interactions also need proximity between cells showing the importance of the spatial architecture of the TME. Finally, the phenotype and activated state of each immune cells is a key factor in the induction or the inhibition of immune response against malignant cells. For example, the ratio of $CD8^+$LT cytotoxic to Treg lymphocytes is important in the prognosis and in the response to immunotherapies since it will be difficult to elicit an immune response if the ratio is in favor of Treg lymphocytes since the TME will be more in an immunosuppressive configuration.

In addition, inhibition of ICP will have less impact if the TME is poorly infiltrated with effector immune cells compared to tumors with a heavily infiltrated TME. This is why tumors with high inflammation and therefore high presence of immune effector cells have a better prognosis. A more comprehensive view is needed to better understand how variations in the immune repertoire in TME impact response to treatment.

Another factor to consider in the response to immunotherapy is tumor cell immunogenicity. Tumor cell immunogenicity refers to their ability to induce an immune response and includes detection of the tumor as a threat, and antigen presentation but also immune infiltration with active immune cells, like LT $CD8^+$ cytotoxic or DC, and finally a favorable TME to immune response.

However, in the case of a lightly infiltrated and low inflammation TME, it is possible to boost the IS by recreating inflammation and thus restoring anti-tumor immunity. This anti-tumor immunity can be restored by a particular death allowing the activation of the IS called Immune Cell Death (ICD). With ICD, tumor cells become more immunogenic and thus activate the immune response.

Chapter III

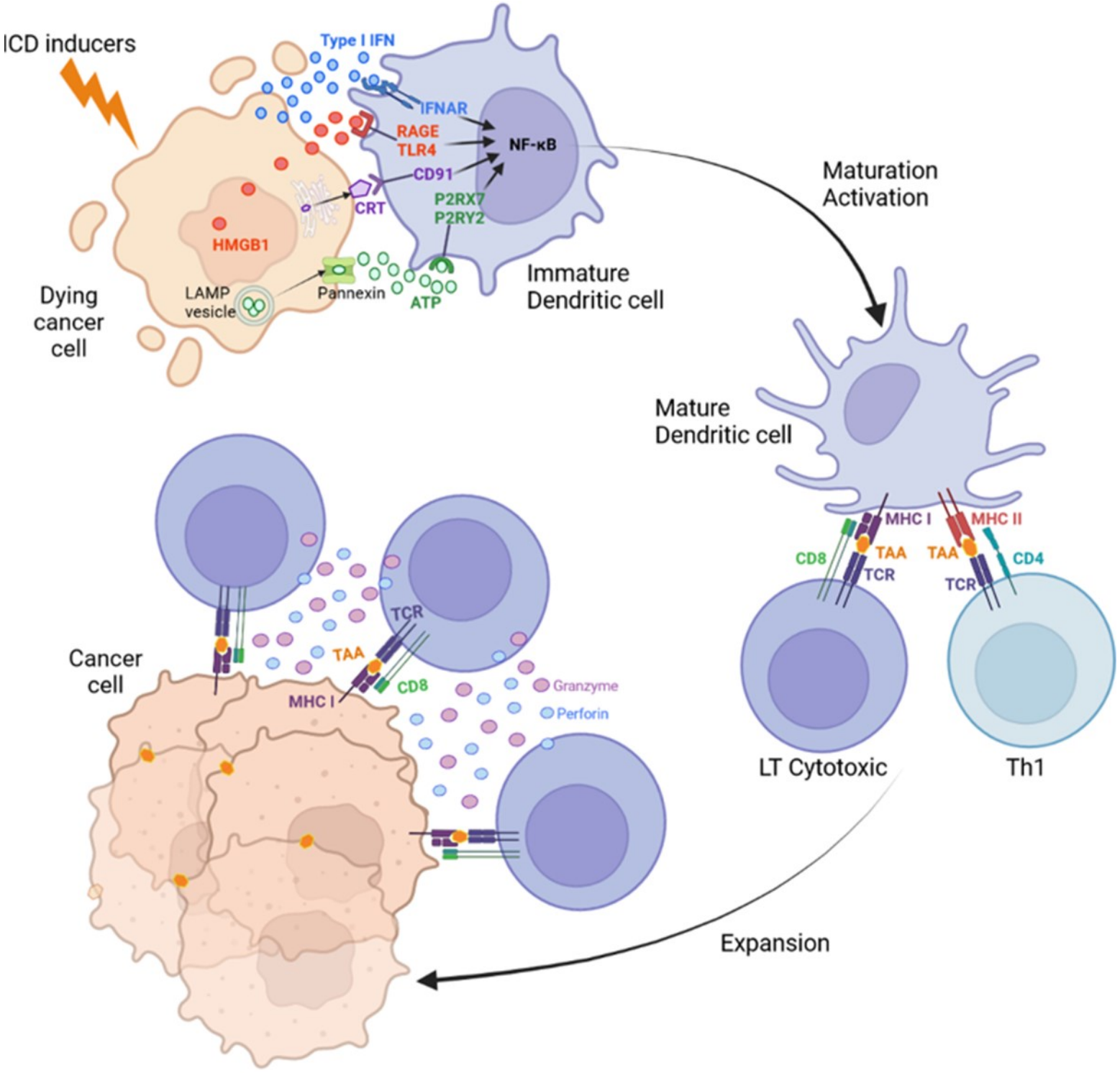

Figure 9: Immune cell death (ICD)

ICD is a cell death that leads to the release of DAMPs from the dying tumor cell inducing inflammation and immune cell recruitment. Membrane exposure of calreticulin (CRT) acts as an “eat me” signal, ATP is a "find me" signal released in the extracellular medium, HMGB1 is a chromatin constitutive protein released during membrane rupture, and finally, the IFN type I induction release inflammatory cytokines. The recognition of DAMPs by receptors on DC cells induces the activation of the NF-κB pathway allowing the maturation and migration of DCs. The mature DC migrates and activates cytotoxic LT cytotoxic by presenting them with a TAA. $CD8^+$ T lymphocytes proliferate and migrate to the site of inflammation. Lt cytotoxic recognize the cells presenting the TAA and therefore the tumor cells still viable, and release perforin and granzyme leading to the lysis of the tumor cells. The activation of ICD allows the elimination of tumor cells by the immune system.

CRT, calreticulin; IFN, interferon; DC, dendritic cell; TAA, tumor associated-antigen; LT cytotoxic,$CD8^+$ T lymphocytes

A. Immunogenic cell death

ICD is a particular cell death that involves the activation of the IS. Precisely, ICD is a "form of programmed death cell that can activate the adaptative immune response in immunocompetent syngeneic host" [109]. This death cell results in the emission of danger signals or DAMP, and then activation of the immune response [110]. In the case of cancer, the ICD induction leads to the development of anti-tumor immunity and even immune memory against cancer cells **(Figure 9)**.

1. DAMPS

DAMPs are molecules or proteins expressed on the cell surface, secreted, or passively released in the extracellular space [111]. They act as a danger signal, are recognized by APCs, and also provoke inflammation [110]. The emission of DAMPs allows the establishment of an inflammatory environment favorable to the induction of an immune response. The major DAMPs are Calreticulin (CARL), ATP, HMGB1, and type 1 interferons.

a. Calreticulin

CARL is a chaperon protein of the Endoplasmic Reticulum (ER) [109] that is translocated to the cell surface at the onset of apoptosis. [112]. CARL is a 46kDA Ca^{2+} binding protein with different activities such as Ca2+ homeostasis and regulation of protein synthesis. CARL also plays a role in immunity when exposed to the cell surface by being the dominant signal for phagocytosis [113] and acts as an "eat-me" signal [110]. CARL expression is induced by ER stress [111]. During ICD, CARL is translocated from the ER to the Golgi apparatus where it is enveloped in a vesicle. This vesicle migrates to the plasma membrane with which it fuses via SNAP and VAMP proteins, exposing the CARL to the cell surface. CARL is translocated with another protein, the Protein Disulfide-Isomerase A3 or Erp57 [114]. The deletion of Erp57 stops CARL translocation demonstrating the essential role of Erp57 in CARL exposure [111]. CARL seems to be the key DAMP for ICD, indeed in absence of CARL, even the presence of other DAMPs is not sufficient to induce ICD [115]. On the other hand, the restoration of CARL exposure allows the ICD [116], [117].

b. ATP

Adenosine Triphosphate (ATP) is a nucleotide. The hydrolysis of ATP provides the energy needed for the good function of the cell. For example, ATP serves as a substrate for protein kinases, DNA synthesis, and synaptic transmission in the brain [118]. During ICD, ATP is released in the extracellular environment. ATP act as a chemoattractant [119] also called "find-me" signal [120]. One of the main mechanisms responsible for ATP release is autophagy [121]. Indeed, the inhibition of autophagy actors

like Atg5, Atg7, or Beclin-1 significantly reduces ATP release and limits ICD [112]. ATP accumulates in an autolysosome called Lysosomal-Associated Membrane Protein 1 (LAPM1). LAMP1 vesicles migrate to the plasma and release ATP through pannexin channel 1 which is opened by a caspase-mediated mechanism [112]. Deficient autophagy, ATP production, or lack of pannexin channel opening lead to the decrease in ATP release and thus the failure of ICD. Restoring ATP concentration by any source, like the injection of ectonucleotidase inhibitors, restores ICD [112]. ATP is an important DAMP since limiting ATP availability in the extracellular space significantly reduces ICD [118].

c. *Type-I interferons*

Type-I IFN are pro-inflammatory cytokines particularly implicated in the immune response against pathogens, but also implicated in innate and adaptative immune cell activities. Pathogens are endocytosed by the targeted cells and degraded allowing the release of danger signals, PAMP. The recognition of PAMP by Pattern Recognition Receptor (PRR) drives the production of type-I IFN [121]. During ICD, type-I IFN expression leads to autocrine or paracrine signaling by binding to type-I IFN receptor (IFNAR) present in the surface cells. IFNAR is a heterodimeric receptor composed of IFNAR1 and IFNAR2, the type-I IFN binding leads to activation of receptor-associated kinase TYK2 and JAK which then phosphorylate the transcription factor STAT1. Then STAT1 homodimerizes and binds to Gamma-Activated Sequences (GAS) inducing pro-inflammatory gene expression [122] like the chemoattractant CXCL10. ICD can't occur without IFNAR, cells lacking IFNAR or mice IFNAR$^{-/-}$ can' be protected via ICD but can be restored by CXCL10 administration [123], [124].

This binding leads to the expression of chemokine CXCL10 which is a strong chemoattractant [110]. By this action, type-I IFN increases the resistance of neighboring cells and stimulated IS [124]. As for the others, DAMPs, the knockout of IFNAR1 inhibits ICD, and recombinant type-I IFN administration restores it [111].

d. *HMGB1*

High Mobility Group Box 1 (HMGB1) is a non-histone chromatin-binding protein possessing two homologous DNA-binding domains. HMGB1 function depends on its localization. In the nucleus, HMGB1 is implicated in the maintenance of nucleosomes, DNA repair, recombination, and transcription. In the extracellular environment, HMGB1 act as an inflammatory molecule [110]. HMGB1 can be released passively by injured cells, necrotic cells, or during the late stage of apoptosis. HMGB1 extracellular function is dictated by its oxidative states. Three cysteine residues, located in the DNA-binding of HMGB1, are sensitive to oxidation. When HMGB1 is completely oxidized, it has no immune function. If the two cysteines, Cys23, and Cys45, are reduced, HMGB1 act as a chemoattractant [125]. Otherwise, the

formation of a disulfide bond between those two cysteines (Cys23 and Cys45) leads to preferential binding to TLR4 receptors and pro-inflammatory cytokine production by immune cells [111]. The association between HMGB1 and TLR4 is critical to induce ICD, indeed mice lacking TLR4 can be protected against tumor cells through ICD [124]. TLR4 agonist rescued the induction of ICD [111].

The kinetic expression of each DAMP is different: CARL exposure occurs in the pre-apoptotic phase, ATP release occurs later and the last DAMP emits is HMGB when membranes are permeabilized [126].

B. Immune response

After DAMPs emission the next step of ICD is the activation of the immune system starting with the activation of APCs and particularly DC. The recognition of DAMPs by specific receptors on the surface of DCs induces their recruitment, activation, and maturation.

Type-I IFN induces autocrine expression of CXCL10 by cells undergoing ICD. CXCL10 binds to CXCR3. CXCR3 is a G protein-coupled receptor present on the surface of many immune cells like NK, T lymphocytes, DC, and macrophages. The CXCL10/CXCR3 axis is critical to the recruitment of immune cells [127].

ATP release in extracellular space has a strong chemotaxis effect [110] and acts as “Find me” signals by interacting with the P2Y2 and P2X7 Purinergic Receptors expressed by DC [124]. Little is known about how P2X7 works. By binding to P2X7, ATP induces the decrease of intracellular K^+ (positively charged potassium ion), by opening the plasma membrane channel. The decrease of K^+ induces the assembly of the inflammasome NLRP3 complex by an undefined mechanism. This results in the activation of pro-caspase 1 which activates the expression of inflammatory cytokines IL-1β and IL-18 [128]. The maturation of DC by P2X7 seems to go by the activation of Nuclear Factor-κB (NFκB) [129] which has a key role in the modulation of immune cells. P2X7 induces, by an unknown mechanism, the expression of CCR7, and CXCR4, two chemokine receptors implicate in chemotaxis to peripheral tissues [129]. P2X7 has the same effect on macrophages with the release of IL-1β and IL-18 leading to inflammation [130].

P2Y2 is a G protein-coupled receptor and is implicated in the recruitment of immune cells by chemotaxis [119]. An absence of this receptor prevents the implementation of the ICD [124]. P2Y2 is expressed by lymphocytes, APC cells, like macrophages, and DC, but the mechanism of chemoattraction of ATP is not yet fully understood. Similarly, little is known about the underlying mechanisms of P2Y2. P2Y2 receptors seem to activate T cells functions through an influx of Na^+ and CA^+ from extracellular

space [131].On macrophages only Ca^{+} intracellular is increased and induces multiple cell responses, such as generation of ROS, generation of Nitric oxide, induction of pro-inflammatory cytokine IL-1β, and IL-18 [131]. This mechanism helps the destruction of the pathogens by the macrophage via acidification. The co-expressed receptors P2Y11 allow the macrophage to escape the P2Y2/ATP mediated killing of pathogens [132]. On DC cells no functional studies explained the mechanism of P2Y2 [131].

HMGB1 release is an inflammatory signal. HMGB1 binds to the Receptor for Advanced Glycation Ends product (RAGE) and the TLR4 leading to NF-κB activation. HMGB1 bindings to RAGE induce activation of Ras, PI3K, and Rho allowing for NF-κB activation. HMGB1 also binds to TLR4 resulting in the recruitment of Myeloid Differentiation primary response 88 (MYD88) and Toll-Interleukin 1 Receptor domain-containing Adaptor Protein. These complex actives Interleukine-1 Receptor-Associated Kinase 1 that induces activation of NF-κB. The key role of TLR4 and myd88 in ICD has been demonstrated by the failure to elicit an immune response in mice defective for TLR4 or Myd88. However, TLR4 agonists restore ICD response [111].CARL is recognized by the main ER chaperon receptor CD91 receptor or Low-Density Lipoprotein Receptor Related Protein 1 (LRP1) [124]. The binding promotes pro-inflammatory cytokine production, like IL-6 and TNF through NFκB activation [133], but mostly CARL enhances the phagocytosis capacity of DC [111]. CD91 binds to CARL and promotes the internalization of the ligand and its associated materials, including antigens, through phagocytosis [134]. After phagocytosis, the ligand-associated material is degraded into peptides in the phagosome and recognized by the MHC II in the late endosome. MHC II migrates to the cell surface to present antigens to other immune cells such as T lymphocytes [135]. CARL/CD91 mediated phagocytosis is important to induce ICD, indeed, lacking CD91 as well as lacking CARL exposition leads to a decrease of ICD causes by reduction of the phagocytosis mechanism [124].

ATP and HMGB1 release, CARL exposure ultimately leads to the activation of NF-κB. NFκB is a family of transcription factors with a critical role in IS. NF-κB induces gene implicated in survival (*Bcl-2*), proliferation (*Cyclin*), inflammation (*IL-1*, *IL-6*) [136]. Other target genes of NF-κB include but are not limited to *CD80* implicated in T lymphocyte stimulation, *MHC* that allow peptide presentation, and *GM-CSF* stimulating macrophage activity[137]. Through its multiple targets, NF-κB induces inflammation, DC maturation, T lymphocyte differentiation, and T lymphocyte activation [136]. And so all these mechanisms induced by DAMPs lead to the induction of immune response. First ATP and type-I IFN act as a chemoattractant and recruits DC in the inflammatory sites. CARL exposition leads to phagocytosis of dying cell debris that is used to present antigen. Finally, CARL exposure and HMGB1 release lead to NF-κB induction and upregulation of MHC II resulting in the switch of DC from an inactive

state to an active state [124]. The DC migrate to the lymphoid organ where they activate T lymphocytes by presenting them with an antigen from the dying cells. After receiving the three signals of activation, TCR/CD8/CD3 and CD80/86/CD28 activating signal and no inhibitory signal from ICP, T lymphocytes differentiate to $CD8^+$ LT cytotoxic migrate to the inflammation site. When $CD8^+$ LT cytotoxic recognize a cell presenting the antigen that has been used to activate them, they release perforin and granzyme molecules causing cell lysis. In this process, DC will also activate the induction of memory immune cells [87]. Thus ICD acts as vaccination with the induction of an immune response against a defined antigen, in the case of cancers a TAA, and the establishment of an immune memory protecting against a future return of the tumor.

C. Inducers of ICD

All mechanisms leading to the induction of ICD have not been completely identified. One of the most likely candidates is ER stress.

1. Pathways inducing ICD

a. ER Stress

ER stress was studied as an ICD inducer due to its responsibility for CARL translocation which plays a crucial role in inducing ICD. ER stress is defined as a cellular response/adaptation to the accumulation of unfolded protein in the ER lumen. To restore proteostasis, and protein homeostasis, and thus decreased the number of unfolded proteins, the Unfolded Protein Response (UPR) is triggered. UPR is regulated by three pathways controlled by ER transmembrane protein sensors including the Inositol Requiring Enzyme -1 (IRE-1), the PKR-like ER protein Kinase (PERK), and the Activating Transcription Factor 6 (ATF6). [138]. In normal conditions, these sensors are inactivated by the Glucose-regulated protein 78 (GRP78)/binding protein (BiP) [110]. In a context of accumulation of unfolded protein, Bip preferentially binds to unfolded proteins, thus releasing the ER stress sensors.

Free IRE-1 excises the intron from the mRNA encoding X-box-Binding protein (XBP1) leading to the splicing of XBP1u mRNA to an active form of XBP1s [139]. XBP1s act like a transcription factor that induces the expression of genes implicated in the degradation of unfolded protein, and ER protein translocation [138].

The release of ATF6 from Bip induces its transit to the Golgi apparatus where ATF6 is cleaved by site- protease. The fragment resulting from this cleavage contains a basic leucine zipper transcription factor called ATF6-p50. In the nucleus, ATF6-p50 induces the gene expression of chaperon, lipid

synthesis, and proteasome-based ER-associated protein degradation. IRE-1 and ATF6 can act simultaneously or even overlap to maintain ER homeostasis [138].

The last pathway takes place after the release of PERK. PERK phosphorylates Eukaryotic translation Initiation Factor 2 subunit-α (Eif2α). Eif2α inhibits protein translation, reducing the protein folding load. Eif2α also induces the expression of a stress-inducible factor ATF4. Then ATF4 can induce expression of GADD34 that acts as feedback that restores protein synthesis by dephosphorylating Eif2α [138].

If the UPR fails to restore proteostasis, the cell enters UPR-mediated apoptosis through the activation of the PERK partway. The Eif2α phosphorylation by PERK leads to activation of ATF4 and one of its targets is the C/EBP Homologous Protein (CHOP). CHOP is a transcription factor that can regulate apoptosis via the BCL2 family. CHOP downregulates anti-apoptotic BCL-2 and upregulates pro-apoptotic BIM causing an increase of BAX/BAK expression [140]. As in intrinsic apoptosis, BAX/BAK release cytochrome C and caspase 3 cleavage.

CARL translocation occurs via PERK pathway. CHOP also induces an apoptotic module composed of caspase 8 and Bap31 that initiates the translocation module based on Golgi trafficking and SNARE-dependent exocytosis [141]. Abolishment of PERK, caspase 8, and Bap31 blocks CARL translocation [142]. CALR translocation via ER stress occurs before cleavage of caspase 3 in the early steps of apoptosis[111].

b. Autophagy

Another way to fight against the accumulation of unfolded proteins is autophagy, which allows the degradation of unfolded protein aggregates that the UPR response can no longer handle [111]. Autophagy activation leads to the release of ATP, an “Find me” signal for immune cells.

Autophagy is a catabolic process that forms a double-membrane vesicle called autophagosomes [143] that traps a cargo formed by damaged organelle, abnormal protein aggregates, and cytoplasmic contents [111]. Autophagy implies ATG proteins and is initiated by protein Beclin-1 to form the phagophore. The elongation of phagophore to autophagosome formation is dictated by the ATG12 and ATG16l1 proteins. Finally, the autophagosome fuses with acidic lysosomes forming the autolysosomes that degrade the cargo. During phagophore expansion LC3 is cleaved by ATG4 and then conjugate with phosphatidylethanolamine to form LC3-II. LC3-II is located in the autophagosome membrane and interacts with cargo receptors leading to its incorporation in autophagosomes [144].

ER stress can also directly induce autophagy. Indeed, Eif2α/ATF4 pathway increases the transcription of autophagy genes implicated in elongation and function of autophagosome *ATG16l1*,

ATG12, and *BECN1* (Beclin-1 gene) [111]. Eif2α/ATF4 pathway also induces upregulate p8 and is downstream target Tribbles homolog 3 responsible for autophagy activation through AKT/mTOR inhibition [111].

It has been speculated that the release of HMGB1 could also induce autophagy by interfering with the mutual inhibition between BECN1 and BCL-2 [118].

Because ER stress seems to have a key role in ICD induction, ICD inducers have been classified into two types, in the type I inducers ER stress is collateral damage but not the principal target while in type II inducers ER stress is the principal target [126].

2. Type II inducers

a. Photodynamic Therapy (PDT)

PDT uses light to activate chemical components that act as a photosensitizer. PDT leads to ROS product causing ER-associated stress and initiating UPR response. For now, hypericin-based PDT is the most effective way to induce ICD [110]. This treatment is accompanied by CARL exposure, ATP secretion, and HMGB1 release. Interestingly, hypericin-base PDT induces CARL exposure depending on PI3K activation, actin skeleton, ER to Golgi transport, and PERK but does not depend on Eif2α phosphorylation [145]. This shows that the mechanism of induction of ICD by ER stress is not yet fully understood.

b. Pathogens infection

Intracellular pathogen infection emits Microorganism-Associated Molecular Patterns recognized by PRR like TLR in the endosomal compartment. Pathogen infection induces ICD via ER stress and autophagy.

An example of induced pathways, TLR7 recruit Myd88, and TRL4 recruit Toll/interleukin-1 Receptor–domain-containing adapter-inducing interferon-β (TRIF). Myd88 and TRIF bind to Beclin-1 inducing autophagy [146]. The recognition of pathogen by TLR induces autophagy and so the release of ATP.

Another example, TLR3 recognizes the dsRNA of virus and induces type-I IFN [111], whileTLR2 and TLR4 recognize bacteria and induce Eif2α and XBP-1 axis [147]. The activation of ER stress can also result in the activation of autophagy [146].

Finally, viral infection can lead to ER stress by the high production of the viral particle, changes in intracellular ionic gradients, and ROS production [146]. Not all sensors capable of activating autophagy after pathogen infection have yet been identified.

The link between ICD and ER stress as well as the link with autophagy has not yet been clearly established in the context of pathogen infections [124].

3. Type I inducers

a. Radiation and Chemotherapy

Radiotherapy and chemotherapy such as oxaliplatin, but not cisplatin, and anthracycline like doxorubicin can induce ICD through similar pathways. ER stress is not the primary target of these therapies but CARL exposure is essential for the ICD induction by these treatments and strictly depends on Eif2α phosphorylation. Platinum compounds such as oxaliplatin induce Eif2α phosphorylation but not cisplatin explaining the inability of cisplatin to induce ICD. ROS production by anthracycline and radiotherapy facilitate the exposition of CARL [148]. ROS could be the trigger of ER stress caused by therapies.

Chemotherapy can also induce autophagy and thus ATP release [145]. ATP release depends on autophagy induced to protect the cell against the DNA damage induced by chemotherapies [150]. The effect of ATP release could be impacted by ectonucleotidases like CD39 and CD73 that reduce the level of extracellular ATP and then reduce its chemoattractant activity [149]. Autophagy could also be induced by ER stress. However, the link between ER stress and autophagy hasn't been explored in ICD-mediated chemotherapies [112].

Type-I IFN response and HMGB1 release have also been detected in ICD induced by chemotherapies [146].

b. Cetuximab

So far, only one study conducted by Pozzi *et al*, has evaluated the ability of cetuximab to induce ICD in colon cancer cells First, they analyzed the CARL emission after cetuximab treatment. Cetuximab induces Eif2α phosphorylation leading to CARL exposure to the cell surface. Secondly, the phagocytosis assay with Cetuximab F(ab'), which cannot bind to the Fc receptor preventing ADCC, increased phagocytosis by DC. Finally, vaccination of immunocompetent mice with colon cancer murine cells expressing human EGFR demonstrated the capacity of cetuximab to induce ICD. They pre-immunize the mice by injection with the Cetuximab F(ab') pre-treated cells leading to DAMP exposition, then rechallenging them after 10 days with an injection of non-treated cells. The treatment with Cetuximab F(ab') shows that the protection is due to ICD and not ADCC [151].

D. ICD and HNSCC

The induction of ICD in HNSCC cells has not been much studied. Data from TGCA indicate an overexpression in HNSCC of DAMP gene CARL, HMGB1, and IFNA1, compared to healthy tissue. The ICD high subtypes, presenting the high expression of the DAMP gene, are associated with favorable clinical outcomes and a high level of immune cell infiltration [152].

In a cohort of 21 patients treated with cisplatin, CXCL10 is decreased, CXCL16 is increased as well as TLR7, TLR9, and IL2R. CXCL10 decrease could imply a decrease of type I response and so a decrease of ICD but in this case, it is associated with good prognostic response to treatment. CXCL16 is produced by DC and macrophage and upregulated during inflammation. The upregulation of CXCL16 shows the inflammatory consequence of cisplatin treatment. IL2R is a mark of T cell activation, and like CXCL16 upregulation, shows the presence of inflammation after cisplatin treatment. Finally, TLR7 and TLR9 high levels translate into an activating immune response against the tumors and their level increased after treatment [153]. Taken together this data shows the inflammation induced by cisplatin and the activation of immune response suggesting that cisplatin could be a potential ICD inducer. This suggestion is supported by the detection by flow cytometry and immunocytofluorescence of CARL after 48h of cisplatin treatment in vitro on three HNSCC cell lines. The same results are observed with oxaliplatin. Cisplatin failed to induce ATP and HMGB1 release may be due to a too short treatment (48h). In vivo experiment by vaccination with Mouse Oral squamous cell 1 (MOC1) shows a weak potential of oxaliplatin and cisplatin to induce ICD. High dose of cisplatin was used with 90% of cytotoxic effect but only 2 mice show protection reflecting the induction of ICD. But the authors still observed a growth delay with cisplatin treatment [154].

Objectives

The only way to achieve the impossible is to believe it is possible.
Alice, Alice in Wonderland.

Carcinoma arising from the epithelium of the upper aerodigestive tract (oral cavity, pharynx, and larynx) forms the head and neck squamous cell carcinoma. This cancer has a 5-year overall survival remaining below 45-50% despite the aggressive treatment modalities based on the use of radiotherapy and platinum-based chemotherapy. Cetuximab, a monoclonal antibody directed against the epidermal growth factor receptor (EGFR), is the only targeted therapy with marketing authorization for the treatment of locally advanced HNSCC. It is proposed in combination with chemotherapy and 5-FU, called EXTREME protocol, in patients with recurrent or metastatic disease, with a moderate gain in overall and progression-free survival.

Re-activating the patient's anti-tumor immunity, a natural defense mechanism against cancer cells seems to be a good therapeutic approach. Immunotherapies targeting immune checkpoints have been developed. The challenge of these innovative therapeutic approaches is to remove the inhibition that cancer cells exert on the immune cells present in the tumor microenvironment, thus allowing the restoration of their cytotoxic anti-tumor activity. Immunotherapies thus remobilize the patient's immune system to eliminate the tumor. Unfortunately, partial or complete tumor response is observed in less than 20% of patients.

Improving the efficacy of immunotherapies may involve increasing the immunogenicity of cancer cells. Indeed, the presentation of danger signals by the tumor, such as neoantigens, as well as the immune infiltration of the microenvironment, strongly influences anti-tumor immunity.

This increase in immunogenicity can be induced by ICD. ICD is a cellular process that allows the recruitment and activation of antigen-presenting cells, such as dendritic cells, which in turn activate effector immune cells (e.g. T cells, macrophages). Cells undergoing ICD emit several DAMPs, which are involved in the initial steps of immune system activation, namely the recruitment, maturation, and activation of DC, followed by the activation of cytotoxic LT $CD8^+$ cytotoxic.

A recent study demonstrated that cetuximab induces ICD of colon or rectal cancer cells, namely membrane translocation of CARL, followed by phagocytosis of the cancer cells by DC. Furthermore, injection of cetuximab-treated cells into immunocompetent mouse models induces a protective anti-tumor immune response and vaccination, suggesting the induction of ICD *in vivo* by cetuximab.

The experimental work I carried out during my thesis, therefore, challenges the hypothesis that cetuximab alone or combined with cisplatin, as in the EXTREME protocol, treatment of HNSCC may induce ICD, impact immune checkpoint expression, and thereby active anti-tumoral response.

The aim of this study is to potentially uncover an optimal treatment strategy combining ICD induction and immunotherapies to reactivate anti-tumoral response in a higher proportion of patients.

The study was separated into three main areas:

The mechanism underlying the effect of cetuximab, alone or in combination with cisplatin, on cycle cell and apoptosis.

The induction of ICD, through the analysis of DAMPs emission, and the activation of the immune system using an *in vivo* vaccination assay.

The regulation of immune checkpoint expression upon treatment with cetuximab. Indeed, ICD-induced immune cells may be inhibited by the remaining tumor cells if they have upregulated immune checkpoints in response to treatment.

Results

It's not about how much we lost, it's about how much we have left.
Tony Stark, Avengers Endgame.

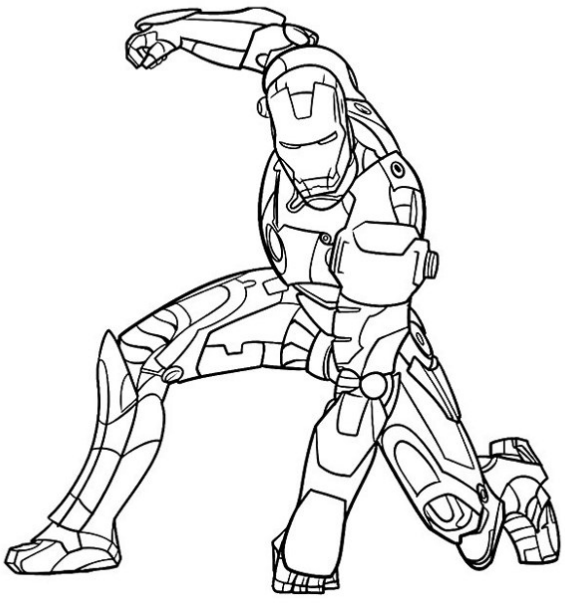

Article

cells

MDPI

Article

The EXTREME Regimen Associating Cetuximab and Cisplatin Favors Head and Neck Cancer Cell Death and Immunogenicity with the Induction of an Anti-Cancer Immune Response

Justine De Azevedo [1], Jana Mourtada [1], Cyril Bour [1,2], Véronique Devignot [1], Philippe Schultz [1,3], Christian Borel [1,4], Erwan Pencreach [1,5], Georg Mellitzer [1], Christian Gaiddon [1,*] and Alain C. Jung [1,2,*]

1 Laboratory Streinth, Université de Strasbourg-Inserm, UMR_S 1113 IRFAC, 67200 Strasbourg, France
2 Laboratoire de Biologie Tumorale, Institut de Cancérologie Strasbourg Europe, 67200 Strasbourg, France
3 Department of Otorhinolaryngology and Head and Neck Surgery, Hôpitaux Universitaires de Strasbourg, 67200 Strasbourg, France
4 Department of Medical Oncology, Institut de Cancérologie Strasbourg Europe, 67200 Strasbourg, France
5 Laboratoire de Biochimie et Biologie Moléculaire, Hôpitaux Universitaires de Strasbourg, 67200 Strasbourg, France
* Correspondence: gaiddon@unistra.fr (C.G.); a.jung@icans.eu (A.C.J.)

Abstract: (1) Background: The first line of treatment for recurrent/metastatic Head and Neck Squamous Cell Carcinoma (HNSCC) has recently evolved with the approval of immunotherapies that target the anti-PD-1 immune checkpoint. However, only about 20% of the patients display a long-lasting objective tumor response. The modulation of cancer cell immunogenicity via a treatment-induced immunogenic cell death is proposed to potentially be able to improve the rate of patients who respond to immune checkpoint blocking immunotherapies. (2) Methods: Using human HNSCC cell line models and a mouse oral cancer syngeneic model, we have analyzed the ability of the EXTREME regimen (combination therapy using the anti-EGFR cetuximab antibody and platinum-based chemotherapy) to modify the immunogenicity of HNSCC cells. (3) Results: We showed that the combination of cetuximab and cisplatin reduces cell growth through both cell cycle inhibition and the induction of apoptotic cell death independently of p53. In addition, different components of the EXTREME regimen were found to induce, to a variable extent, and in a cell-dependent manner, the emission of mediators of immunogenic cell death, including calreticulin, HMGB1, and type I Interferon-responsive chemokines. Interestingly, cetuximab alone or combined with the IC_{50} dose of cisplatin can induce an antitumor immune response in vivo, but not when combined with a high dose of cisplatin. (4) Conclusions: Our observations suggest that the EXTREME protocol or cetuximab alone are capable, under conditions of moderate apoptosis induction, of eliciting the mobilization of the immune system and an anti-tumor immune response in HNSCC.

Keywords: head and neck squamous cell carcinoma; cetuximab; cisplatin; apoptosis; immunogenic cell death

Citation: De Azevedo, J.; Mourtada, J.; Bour, C.; Devignot, V.; Schultz, P.; Borel, C.; Pencreach, E.; Mellitzer, G.; Gaiddon, C.; Jung, A.C. The EXTREME Regimen Associating Cetuximab and Cisplatin Favors Head and Neck Cancer Cell Death and Immunogenicity with the Induction of an Anti-Cancer Immune Response. *Cells* **2022**, *11*, 2866. https://doi.org/10.3390/cells11182866

Academic Editors: Guido Kroemer and Oliver Kepp

Received: 3 August 2022
Accepted: 12 September 2022
Published: 14 September 2022

1. Introduction

Head and neck cancer squamous cell carcinoma (HNSCC) are cancers that arise from the mucosal epithelium of the oral cavity, larynx, and pharynx [1]. The principal risk factors for HNSCC are alcohol and tobacco consumption on the one hand, and Human Papillomavirus (HPV) infection on the other hand. They are the sixth most frequent malignancies with ~700,000 new cases being diagnosed worldwide each year [2]. Due to the fact that most tumors are diagnosed at locally-advanced stages [1], as well as to treatment failure despite recent medical progressions [3], the five-year overall survival of patients with HNSCC is poor (<40–50%) [4]. The management of the majority of patients with HNSCC relies on a multimodal approach that involves surgery (in amenable patients), followed by

adjuvant radiotherapy or platinum-based (e.g., cisplatin or carboplatin, and 5-fluorouracil) chemoradiotherapy [1]. Cetuximab was FDA-approved in 2006 as a targeted therapy for the management of locally advanced recurrent/metastatic (R/M) HNSCC. The rationale of this therapy relies on the overexpression of the Epidermal Growth Factor Receptor (EGFR) in >90% of HNSCC tumors. The EXTREME phase III clinical trial evaluated the efficacy of the combination of cetuximab and platinum-based chemotherapy (using cisplatin or carboplatin,) as a first-line treatment in patients with R/M HNSCC. This clinical trial showed that the combination in the EXTREME protocol of cetuximab with platinum-based chemotherapy improves both disease-free and overall survival [5–7]. Based on this positive outcome, the EXTREME regimen was FDA-approved and became a therapeutic option for the management of patients with R/M HSNCC. The efficiency of the EXTREME protocol could be rationalized by the fact that cells from various molecular subtypes of HNSCC have shown a different degree of response to EGFR blockade [8,9], and that EGFR overexpression has been shown to reduce the cytotoxicity of metal-based drugs [10].

More recently, several immune check-point blocking immunotherapies, which aim to reactivate an anti-tumor immune response, have been approved [11]. Unfortunately, resistance mechanisms to cisplatin and cetuximab are common. They include the overexpression of factors involved in DNA repair or the constitutive, ligand-independent activation of the EGFR pathway, which reduce the benefits of treatments [12]. Furthermore, only a small proportion of patients (<20%) show a tumor response to immune checkpoint-blocking immunotherapies used as monotherapies [13,14]. The immune landscape of the microenvironment (i.e., the nature of immune cells in the microenvironment and their respective proportions) has been proposed to play a role in the tumor response to immune checkpoint inhibiting immunotherapies [15]. Understanding and detecting the variations in the immune cell landscape that can account for a response to immunotherapy is a major goal to improve patient care [16].

The evolution of the cancer immune landscape during tumor progression was previously described by the three Es (Elimination; Equilibrium; Escape) of the cancer immunoediting model [17]. During the "Elimination" phase (when tumor cells are eliminated by the immune cells), tumor-associated antigens (or neoantigens) are up-taken by antigen presenting cells (APCs) like dendritic cells or macrophages phagocyte, which are further cross-presented to cytotoxic CD8+ T lymphocyte (TL) [18,19]. Cytotoxic TLs are the main actors of the anti-cancer immune response: they infiltrate tumors and trigger targeted cell death via the expression perforin and granzymes. Therefore, an "inflamed" or "immuno-suppressive" tumor microenvironment with high infiltration by cytotoxic CD8+ LT is associated with a better patient outcome [20]. Yet, several mechanisms are known to dampen this anti-tumor cytotoxicity and are responsible for the transition from the "Elimination" to the "Equilibrium" and eventually "Escape" phases (during which cancer cells are progressively maintained and escape the immune system). One of these mechanisms relies on the enrichment of the tumor microenvironment with immunosuppressive immune cells (e.g., regulatory T cells (Treg) [21]; pro-tumoral M2 macrophages [22]; myeloid-derived suppressor cells [23]). The microenvironment of HNSCC is known to be frequently "immuno-tolerant" (presence of pro-tumoral M2 macrophages and/or Treg cells) and associated with a poor outcome [11,24]. In addition, cancer cells highjack immune checkpoints to induce cytotoxic LT anergy: for example, the expression of Programmed Death-Ligand 1 (PD-L1) by cancer cells inhibits TLs' cytotoxic activity upon binding with the Programmed Death-1 (PD-1) receptor and allow immune evasion [17]. Increasing tumor immunogenicity and favorizing an immune-suppressive microenvironment to restore anti-tumor activity is therefore proposed to be an interesting option to improve the efficiency of immunotherapies.

One attractive possibility to achieve this could be to trigger an immunogenic cell death (ICD), which is known to induce an immune response [25]. This particular death cell is characterized by the emission of danger-associated molecular patterns (DAMPs) by dying cells, the activation of APCs upon binding of DAMPs to specific receptors as well as tumor

neoantigens uptake, the subsequent activation of a CD8+ TL-based immune response, and the establishment of an immune memory, which eliminates tumor cells [25]. DAMPs are danger signals that are either expressed on the cell surface and act as "eat me" signals for APCs, like the calreticulin (CRT) chaperone protein, or factors that are released in the extracellular space and act as pro-inflammatory chemoattractant signals, like the histone group mobility box (HMGB1) protein [26]. In addition, the secretion of type I interferons also acts as a DAMP and results in the production of the CXCL10 chemokine which is a chemoattractant for cytotoxic TL [27]. It has been shown that several anticancer treatments can induce ICD, such as specific chemotherapies (i.e., oxaliplatin) [28], radiotherapy [28], or even photodynamic therapy [28,29]. In the clinic, inducing ICD in patients could activate an anti-tumor immune response, provoke tumor elimination and provide protection against relapse through an immune memory. Interestingly, cetuximab was shown to induce ICD in colon cancer cells [30].

While cisplatin used alone was previously proposed to modestly induce ICD in HNSCC cell lines [31], the ICD-inducing ability of cetuximab, used either alone or in combination with cisplatin in head and neck cancers, remains to be determined. Therefore, while the protocol EXTREME is used in clinical routine to treat HNSCC patients, its precise impact on the modulation of immunogenicity of HNSCC cells has never been investigated. Based on previous findings showing that cetuximab can elicit ICD in colon cancer [30], we hypothesized that it has similar effects in HNSCC. In addition, we wanted to investigate the precise impact of the EXTREME protocol (i.e., the combination of cetuximab and cisplatin) on cell proliferation and apoptotic cell death, and how this correlates with the induction of ICD. Hence, we first analyzed the biological impact of cetuximab and cisplatin cotreatment on HNSCC cell line models through the analysis of cell cycle and apoptotic cell death. Secondly, we demonstrated the capacity of cetuximab (alone or combined with cisplatin) to induce DAMPs emission. Finally, using prophylactic vaccination of HNSCC syngeneic mouse models, we show that the treatment with cetuximab provides animals with anti-tumor immune protection.

2. Materials and Methods

2.1. Cell Lines and Reagents

The SQ20B cells originate from a laryngeal tumor, express mutated *TP53*, and are a kind gift from Dr. Pierre Bischoff. The CAL27 cell line originates from a carcinoma of the tongue, expresses mutated *TP53*, and is a kind gift from Dr. Sophie Pinel. SQ20B and CAL27 cells were maintained at 37 °C with 5% CO_2 and 90% humidity in Dulbecco's modified Eagle's medium (DMEM; PAN Biotech, Aidenbach, Germany) supplemented with 10% fetal calf serum (FCS; Gibco, Thermofisher, Waltham, MA, USA). The human monocytic leukemia THP-1 cell line was a kind gift of Elisabeth Martin (UMR1113, Strasbourg), and was maintained at 37 °C with 5% CO_2 and 90% humidity in Roswell Park Memorial Institute (RPMI) medium supplemented with 10% fetal bovine serum (Gibco, Waltham, MA, USA). The murine oral carcinoma MOC2 cell line was purchased from Kerafast, Inc, (Boston, MA, USA), and was maintained at 37 °C with 5% CO_2 and 90% humidity in Dulbecco's modified Eagle's medium (DMEM; PAN Biotech, Aidenbach, Germany) supplemented with 10% fetal calf serum (FCS; Gibco, Waltham, MA, USA).

2.2. In Vitro Cell Survival Analysis

A total of 1×10^4 cells were seeded per well in 96–well microplates (Falcon Multiwell, Thermofisher, Waltham, MA, USA), and different concentrations of cisplatin (Mylan: 0; 0.1; 0.5; 1; 2.5; 7.5; 15; 30; 100 µM), cetuximab (Merck; 5 mg/mL) or PRIMA MET were applied for 48 h in 100 µL of fresh medium. For co-treatments, 2.5 µg/mL of cetuximab and/or 50 µM of prima were added to the different concentrations of cisplatin. MTT assay was performed as previously described by replacing the cisplatin solution with fresh medium supplemented with 5 mg/L MTT (Sigma, Saint-Louis, MO, USA) for 1 h [32]. Cells were lysed in DMSO 100% (100 µL/well). Absorbance measurements were performed at 550 nm

with the LB942 Tristar2 Multimode Reader (Berthold Technologies, Bad Wildbad, Germany). The calculation of the IC_{50}, IC_{75}, and IC_{90} was performed with the GraphpadPrism V5.02 software (Graphpad, Software, San Diego, CA, USA) using non-linear regression.

2.3. Annexin V and PI Flow Cytometry

Cell apoptosis analysis was carried out using FITC-Annexin V and propidium iodide (apoptosis detection kit, BD Biosciences, Franklin Lake, WI, USA) according to the manufacturer's instructions. Briefly, cells were seeded in 10 cm Petri dishes and treated with cetuximab +/- cisplatin for 24 h or 48 h. Cells were harvested and counted, diluted in annexin buffer (BD Biosciences, Franklin Lake, WI, USA) at a concentration of 1×10^6 cells per 100 µL, and stained with 10 µL of propidium iodide and 5 µL of FITC-Annexin V. After 15 min of incubation, cells were analyzed in flow cytometer on a BD LSRFortessa™ (BD Biosciences, Franklin Lake, WI, USA) after satisfying QC using CST beads. Acquisition and data analyses have been performed using the BD FACSDiva™ Software.

2.4. Gene Expression Assays

Gene expression assays on cultured cells were performed by extracting total RNA from pelleted cells using a standard TRIZol procedure (TRI Reagent®: TR 118 Molecular Research Center, Cincinnati, OH, USA), according to the manufacturer's instructions. RNA was retro-transcribed using the High-Capacity cDNA reverse transcription system (Applied Biosystems™, Thermofisher, Waltham, MA, USA), and real-time quantitative PCR was performed using the QuantStudio 3 Real-Time PCR system (Applied Biosystems™, Thermofisher, Waltham, MA, USA). *DDB2*, *FDRX2*, *RPS27L*, and *ZMAT3* expression was measured with pairs of specific primers (see Table S1), and *CXCL9* and *CXCL10* expression was measured with TaqMan probes (see Table S2). The expression of genes of interest was normalized to the expression of *TBP*, used as a reference gene, with the $2^{-\Delta\Delta Ct}$ method.

2.5. SDS-PAGE and Western Blot Analysis

Total protein extraction was carried out by homogenizing 1×10^6 cells in 100 µL of 1X Laemmli lysis buffer 6.25 mM Tris (pH 6.8), 1%SDS, 1%DTT, protease, and phosphatase inhibitors, Sigma. A total of 20 or 30 µg of proteins were resolved by 6%–15% SDS-PAGE (depending on protein molecular weight) according to standard methods. For the analysis of HMGB1 release in the extracellular medium, 40 µL of cells culture supernatant, diluted in SDS-PAGE sample buffer (2X Laemmli lysis buffer, 2X DTT), were resolved by 10% SDS-PAGE. Proteins were detected with primary antibodies raised against cleaved Caspase-3, Calreticulin, EGFR, HMGB1, p63, p53, and p73 (see Table S3 for clones, providers, and concentrations). Depending on the host species, blots were probed with secondary antibodies (1/10,000 anti-mouse IgG-HRP linked antibody, Cell Signaling 7076S; 1/10,000 anti-rabbit IgG-HRP linked antibody, Cell Signaling 7074S) Proteins were visualized with enhanced chemiluminescence using the Clarity™ ECL Western blotting Substrate Bio-Rad reagent, according to the manufacturer instructions. Protein-related signals were acquired on a Pxi Imager (Syngene®, Cambridge, United Kingdom). Protein expression (e.g., cleaved Caspase-3, CRT, and HMGB1) was quantified by measuring the SDS-PAGE gel bands using the ImageJ software. In short, and according to the manufacturer's recommendations, a box was drawn in lanes around gel-band signals using the rectangle tool, making sure to include some of the empty gel between lanes and white space outside of the band. The same box was used for all gel-bands on the same blot. Signal acquisition of pixels was converted into peaks by the ImageJ software, and the area of each peak (which correlates with the gel-band signal intensity) was recovered. Each recovered value was normalized to their respective loading control in the same lane (cell "housekeeping" proteins (actin or GADPH) in the case of cleaved caspase-3 or intracellular HMGB1; cell-culture medium Bovine Serum Albumin (BSA) in the case of extracellular expression of released HMGB1). Finally, the protein of interest to loading control ratios were further normalized by setting the value of this ratio to 1 in the negative control

(e.g., non-treated cells). Enrichment of CRT in the membrane protein fraction was evaluated by normalizing the quantification value in a given condition to the quantification value from the same condition in the input.

2.6. Biotinylation and Immunoprecipitation of Cell Surface Proteins

Biotinylation and recovery of cell surface proteins were performed with a method adapted from Gottardi et al. [33], Hanwell et al., and T. Panaretakis et al. [34]. Briefly, cells were grown and treated in 10 cm Petri dishes, were washed three times with ice-cold PBS-$Ca^{2+-}Mg^{2+}$ (PBS with 0.1 mM $CaCl_2$ and 1 mM $MgCl_2$), and placed on ice. Membrane proteins were then biotinylated with 1.25 mg/mL NHS-SS-biotin (Pierce) freshly diluted in biotinylation buffer (10 mM triethanolamine, 2 mM $CaCl_2$, 150 mM NaCl, pH7.5) for 30 min incubation at 4 °C under gentle agitation. Cells were then rinsed and washed in with PBS-$Ca^{2+-}Mg^{2+}$-glycine (100 mM) buffer at 4 °C to quench unreacted biotin. Cells were further rinsed three times with PBS-$Ca^{2+-}Mg^{2+}$, scraped in cold PBS, and pelleted by centrifugation (800 rpm at 4 °C) and total protein was harvested for 45 min in 500 µL of lysis buffer (1%Triton X-100, 150 mM NaCl, 5 mM EDTA, 50 mM Tris pH7.5) containing protease inhibitors. A total of 500 µg of total proteins were incubated for 1 h at 4 °C with packed streptavidin-agarose beads to bind to biotinylated proteins. Beads were then pelleted by centrifugation and aliquots of supernatants were sampled to recover unbound, intracellular proteins. Biotinylated proteins (representing membrane proteins) were eluted from the beads by heating to 100 °C for 5 min in an SDS-PAGE sample buffer. Whole-cell proteins (input), the intracellular and membrane protein fractions were further loaded onto a 4–12% gradient gel (Mini protean TGX, Biorad, Marnes-La-Coquette, France) and analyzed by western blot (see above).

2.7. Immunofluorescence Staining

CAL27 or MOC2 cells were seeded on coverslips and fixed with PFA 4% for 10 min. In addition, MOC2 cells (but not CAL27 cells) were permeabilized with 0.1% Triton X-100 for 20 min at room temperature. For both cell lines, a saturation of aspecific sites was achieved with 5% Normal Goat Serum for 30 min at room temperature. CAL27 were incubated with anti-CRT antibody (1/400; D3E6 Cell signaling) and MOC2 were incubated with anti-EGFR (1/400; D38B1 Cell signaling) overnight at 4 °C. After 3 washes in 1X PBS, coverslips were further incubated with 1/1000 solutions of goat anti-rabbit-alexa488 (A11034 Invitrogen) secondary antibodies. After 3 washes in 1X PBS, nuclei were labeled with a DAPI (4′,6-diamidino-2-phenylindole) solution (1/20,000) for 5 min, and coverslips were mounted in Calbiochem FluorSave™ reagent (Merck Millipore, Darmstadt, Germany). Pictures were taken with a Zeiss Axio Imager M2-Apotome2 fluorescence microscope.

2.8. Generation of hEGFR-MOC2 Clones

MOC2 cells were transduced with lentiviral particles carrying the p-BABE-puro-hEGFR (gift from Dr Di Fiore Pier Paolo) or the empty vectors. Cells were selected with puromycin (8 µg/mL) and checked for ectopic human EGFR expression by western blot. The clone selection was realized by high dilution and seeding of isolated cells. Every clone was then tested by western blot and immunocytofluorecence for the expression of human EGFR.

2.9. Vaccination Assay

All animal experiments were approved by the local ethic comity and the French Ministry of Agriculture under the permit APAFiS#29181. C57BL/6 mice (Janvier labs, Le Genest-Saint-Isle, France) were housed in the certified animal facility (#H-67-482-21). Female mice (8 weeks old) were inoculated in the right flank with 5×10^5 hEGFR-MOC2-C1 cells (treated ex vivo with cisplatin, cetuximab or cotreatment cisplatin plus cetuximab) in 100 µL of DMEM. The injection of hEGFR-MOC2-C1 cells killed by three successive freeze/thaw cycles was used a non-immunogenic cell death inducer (negative control).

After 7 days, a second challenge was carried out by injecting 5×10^5 hEGFR-MOC2-C1 cells in 100 µL of DMEM in the contralateral flank of the same mice. A minimum of 11 animals in the negative control group (Freeze/thaw cycle group) and a maximum of 12 animals in all other treatment groups were used. Tumor growth was monitored over time by measuring the two dimensions with a caliper. Tumor-free survival was analyzed with Kaplan-Meier survival analysis (see below) and log-rank post-test. Tumors were dissected from mice for further investigation of marker expression by immunofluorescence (see below).

2.10. Statistical Analysis

MTT assays results were analyzed with a Mann-Whiney test. For all other data sets, the, the hypothesis of normality (d'Agostino and Pearson test; Shapiro-Wilk test) and homogeneity of variances (Levene test for equality of variances) of data sets were analyzed. If the sample did not meet at least one of these conditions, then a non-parametric test was used (Kruskal Wallis with Dunn post-test). Otherwise, parametric tests were used (Student *t*-test; Anova and Tuckey post-test). The tumor-free survival of mice challenged with a hEGFR-MOC2-C1 cell injection was evaluated with Kaplan-Meier survival analysis (see below) and log-rank post-test. Statistical tests were performed using GraphPad Prism 8. For all analyzes, statistical significance is represented in graphs using asterisks: * $p < 0.05$; ** $p < 0.001$; *** $p < 0.0001$.

3. Results

3.1. Cetuximab and Cisplatin Inhibit HNSCC Cell Cycle and Trigger Apoptotic Cell Death

In order to investigate the underlying mechanisms of the cotreatment with cetuximab and cisplatin used in the EXTREME protocol, we performed cell viability assays using CAL27 and SQ20B cell lines. Cells were exposed to increasing concentrations of cetuximab or cisplatin and the cell survival rate was measured with MTT and used to determine the drugs IC_{50}, IC_{75} and IC_{90} (i.e., concentrations that result in 50%, 75% and 90% of the maximal drug effect, respectively). Survival curves obtained upon cetuximab treatment showed a maximal drop to ~70% of surviving cells in both cell lines (Figure 1A,B). This maximum effect was reached at 2.5 µg/mL, and higher concentrations of cetuximab did not yield more biological effect. Therefore, we performed MTT assays using a co-treatment with cetuximab (2.5 µg/mL) and increasing concentrations of cisplatin. As expected, the addition of cisplatin to cetuximab was more cytotoxic than cetuximab alone (Mann-Whitney $p < 0.01$ in CAL27 cells and $p < 0.05$ in SQ20B cells). The cotreatment appeared slightly more cytotoxic on CAL27 cells compared to cisplatin alone than in SQ20B cells (IC_{50} = 2.4 µM vs. IC_{50} = 3.5 µM, respectively; Figure 1A). Interestingly, in CAL27 cells, cetuximab seems to mostly favor the activity of cisplatin at lower concentrations (Mann-Whitney $p < 0.001$), whereas no difference between cisplatin alone and the combination were observed at higher concentration (for instance, the IC_{75} was similar in both conditions (7.9 µM vs. 7.6 µM; Figure 1A). Intriguingly and in contrast to CAL27 cells, the addition of cetuximab seemed to lower the cytotoxicity of cisplatin in SQ20B cells (IC_{50} = 4.35 µM vs. IC_{50} = 2.9 µM, and IC_{75} = 10 µM vs. IC_{75} = 6.3 µM, respectively; Figure 1B). Consequently, the co-treatment was found to be more effective on CAL27 cells than on SQ20B cells (Figure 1 A,B).

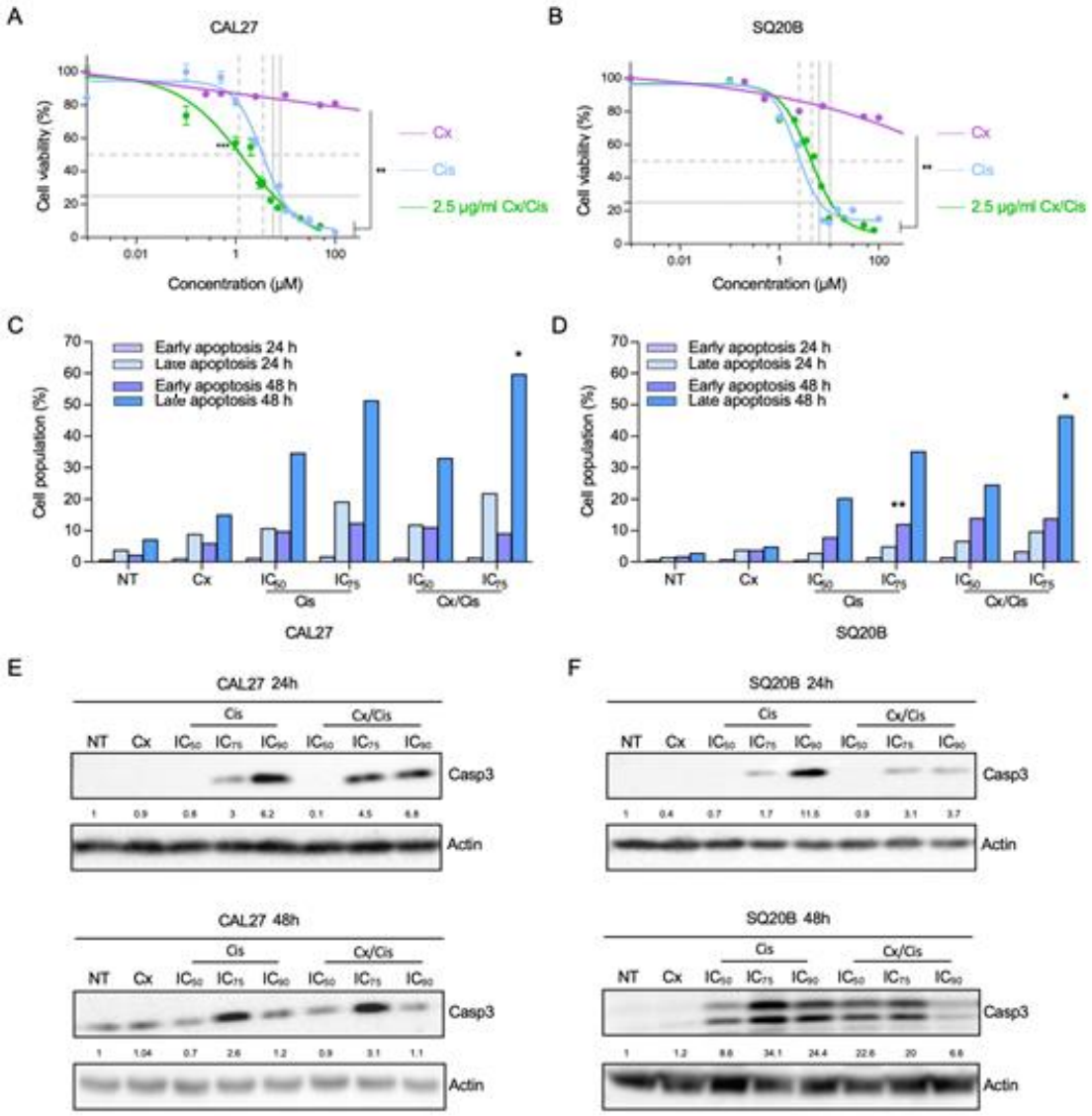

Figure 1. (**A**,**B**). Analysis of CAL27 (**A**) and SQ20B (**B**) cells survival upon treatment with increasing concentrations of cetuximab (Cx; purple line), of cisplatin (Cis; blue line) and of cisplatin +2.5 µg/mL cetuximab (green line), using a MTT-based assay. Mean values from three independent experiments are plotted as sigmoid curves and the cisplatin IC_{50} (dotted grey lines) and IC_{75} (plain grey lines) in the Cis and Cx+Cis conditions are shown. Mann-Whitney *p*-values: * $p < 0.05$; ** $p < 0.01$; *** $p < 0.001$. (**C**,**D**). Annexin V/Propidium Iodide apoptosis assay of CAL27 (**C**) and SQ20B (**D**) cells treated 24 h and 48 h with cetuximab (Cx), cisplatin (Cis) at the IC_{50} and IC_{75} and the Cx/Cis combination. The histograms show the mean number of percentages of early (annexin V-positive, Propidium Iodide-negative; purple) and late (annexin V-positive, Propidium Iodide-positive; purple) cells values from two independent experiments, after 24 h (light colors) and 48 h (dark colors) of treatment. Each treatment condition was compared to its respective non-treated control: ANOVA and Tuckey post-test *p*-values: * $p < 0.05$; ** $p < 0.01$. (**E**,**F**). Western blot analysis of cleaved caspase-3 (Casp3) expression in whole protein extracts from CAL27 (**E**) and SQ20B (**F**) cells treated with cetuximab (Cx), cisplatin (Cis) at the IC_{50}, IC_{75} and IC_{90}, and the Cx/Cis combination for 24 h (upper panels) and 48 h (lower panels). Signals were quantified respectively to the actin loading control and normalized with respect to the non-treated control (quantification results are shown). The blots shown here are representative examples of three independent experiments. Additional independent biological replicates are shown in supporting documents.

Next, we wanted to determine whether the cetuximab and/or cisplatin treatments impact CAL27 and SQ20B cell survival rates by inducing apoptosis or by inhibiting cell proliferation. To this end, cells were fixed, stained with Propidium Iodide (PI) and analyzed by flow cytometry. Upon 48 h of treatment, an increase of the proportion of cells in the G2 phase at the expanse of the G0/G1 phase was observed in both cell lines, and more particularly at the IC_{75} of cisplatin (with or without cetuximab), suggesting a cell cycle halt in G2 (Figure S1A,B). Then, to discriminate between necrosis and apoptosis, cells were stained with an Annexin V probe (AV) and Propidium Iodide (PI) and analyzed by flow cytometry. The percentage of IP− AV+ (early apoptosis) and IP+ AV+ (late apoptosis) cells was determined by flow cytometry, after 24 h and 48 h of treatment with cetuximab +/− cisplatin. Although a trend for the dose-dependent increase of the proportion of cells in early apoptosis (IP− AV+), no significant difference was detected after 24 h of treatment in both cell lines, except upon treatment of SQ20B cells with the IC_{75} of cisplatin (Figure 1C,D; $p < 0.01$). A stronger trend for a dose-dependent increased rate of cells in late apoptosis (IP+ AV+) was observed in SQ20B cells especially after 48 h (Figure 1D), and in CAL27 cells after 24 h and 48 h of treatment with cisplatin+/-cetuximab. Observed differences only reached statistical significance in CAL27 and SQ20B cells treated with cetuximab and the IC_{75} of cisplatin compared to non-treated cells. In addition, this increase was more important in CAL27 cell line (Figure 1C): for instance, the proportions of CAL27 cells in late apoptosis after 48 h of treatment with the IC_{50} and IC_{75} of cisplatin were ~35% and ~50%, respectively, whereas they reach ~20% and ~35% in SQ20B cells. The combination of cetuximab did not synergize with cisplatin, since the proportions of cells in late apoptosis were of the same order of magnitude in both cell lines.

To confirm the induction of apoptosis upon treatments, we analyzed the level of cleaved caspase-3 by western blot in whole protein extracts harvested from CAL27 and SQ20B cells 24 h and 48 h after treatment. Cleaved caspase-3 was observed in CAL27 and SQ20B cells after 24 h treatment with cisplatin at the IC_{75} and IC_{90}, used alone or in combination with cetuximab, in a dose dependent manner (Figure 1E,F, upper panels). After 48 h of treatment of CAL27 cells, the most effective caspase-3 cleavage was observed upon treatment with the IC_{75} of cisplatin +/− cetuximab (Figure 1E, lower panels). At both time points, the cleavage of caspase-3 was similar when cells were treated with cisplatin alone or combined with cetuximab (Figure 1E). In contrast, in SQ20B cells, cetuximab increased the level of cleaved caspase-3 when combined to the IC_{50} of cisplatin for 48 h, whereas it reduced caspase-3 cleavage when combined with higher cisplatin concentration (Figure 1F). In both cell lines and in all experimental conditions, cetuximab used alone did not induce the cleavage of caspase-3 (Figure 1E,F), which is consistent with the low impact of this treatment on cell growth obtained in MTT assays (Figure 1A,B). Hence, altogether, these results show that treatment of HNSCC cells with cisplatin alone or with cetuximab induces caspase-3 cleavage. However, the impact of the addition of cetuximab to cisplatin on caspase3 dependent apoptosis appears to be complex, since it differs and varies in intensity according to several parameters including drug dose, treatment time and cell line.

3.2. p53-Independent Induction of Apoptosis

The p53 family of transcription factors, and especially p53, are well documented mediators of the cytotoxicity induced by DNA damaging drugs, such as cisplatin [35]. Since CAL27 and SQ20B cells were established are from HPV-negative cancers, they both bear a mutated form of p53. CAL27 expresses the mutant H193L p53 that is a gain of function mutant able to interact with YAP [36]. SQ20B harbors a small deletion Tyr126_Lys132del whose impact on p53 activity remains to be established. To understand the contribution of p53 in the effect of the combinatory treatment in CAL27 and SQ20B cells, we first investigated the expression profile of four transcriptional targets of p53 (*FDRX2*, *DDB2*, *RPS27L* and *ZMAT3*) [37] upon treatment with cetuximab+/-cisplatin. No significant impact of the treatments on *DDB2*, *FDRX2*, *RPS27L* and *ZMAT3* gene expression was

observed in CAL27 (Figure 2A) and SQ20B cells (Figure 2B), suggesting that p53 is not activated by the treatment in those cells.

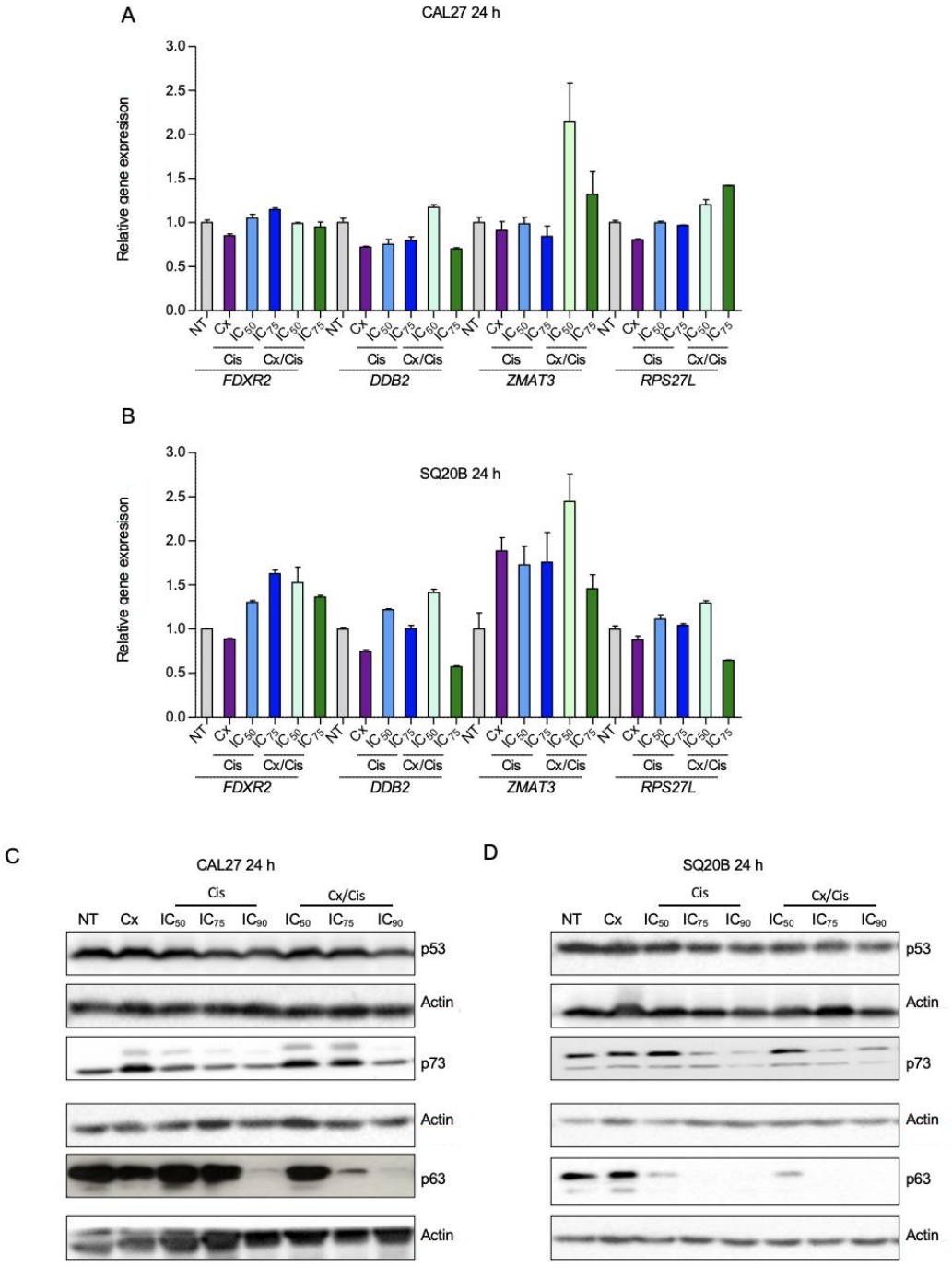

Figure 2. (**A**,**B**). Analysis of the expression of the *FDXR2*, *DDB2*, *ZMAT3* and *RPS27L* genes by RT-qPCR in CAL27 (**A**) and SQ20B (**B**) cells treated for 24 h with cetuximab (Cx), cisplatin (Cis) at the IC_{50} and IC_{75} and the Cx/Cis combination. Data is represented as mean from two independent experiments +SEM. No significant differences were observed between non-treated cells and each treated condition (Kruskal-Wallis and Dunn post-test). (**C**,**D**). Western blot analysis of p53, p73 and p63 expression in whole protein extracts from CAL27 (**C**) and SQ20B (**D**) cells treated with cetuximab (Cx), cisplatin (Cis) at the IC_{50}, IC_{75} and IC_{90}, and the Cx/Cis combination for 24 h. The blots that are shown are representative examples of three independent experiments.

We then analyzed the protein level of p53 by western blot. We found the p53 protein to be expressed at high levels in both cell lines, independently of genotoxic treatments (Figure 2C,D). The high expression level and absence of induction by chemotherapy can be explained by the mutation status of p53 in those cells [35].

p53 mutants have deleterious effects on cells and response to chemotherapy by instating new protein interactions, such as with p63 and p73. These interaction blocks p63 and p73 proapoptotic activity, including in response to chemotherapy [38]. Hence, therapeutic strategies with small molecules aiming at restoring p53 function and inhibiting those neo-interactions have been developed [39,40]. Therefore, we wanted to assess whether in CAL27 and SQ20B cells p63 and p73 were expressed and regulated by the treatment, and whether the p53 reactivator PRIMA-MET could favor the impact of the EXTREME protocol in those cells.

p63 and p73 protein levels were analyzed by western blot. Consistently with the fact that the *TP73* gene encodes multiple isoforms (including a full-length isoform with an N-terminal transactivation domain, called TAp73, and a shorter isoform lacking the N-terminal domain, called ΔNp73), two bands were observed when membranes were probed with an anti-p73 antibody [36]. In CAL27 cells, the lower band showed a stronger expression, which was further increased upon cetuximab and cetuximab/cisplatin treatment. The upper band was not detected in non-treated cells, and the expression of this isoform was induced by cetuximab and the cetuximab/cisplatin co-treatment (especially at the IC_{50} and IC_{75}), and to a lesser extend upon treatment with cisplatin alone (Figure 2C). Unlike what is observed in CAL27 cells, the most expressed p73 isoform is represented by the upper band in non-treated SQ20B cells, although the lower band was observed. Cisplatin treatments at high doses (i.e., IC_{75}; IC_{90}), alone or combined with cetuximab, decreased the expression of the upper isoform of p73. The lower isoform was not affected by the treatments (Figure 2D). We also analyzed the expression of the p63 protein, which is expressed as TA and ΔN isoforms, similarly to p73. p63 was found to be expressed in both CAL27 and SQ20B cells, and the p63-related signal appeared as two bands, the upper band being the more expressed. Strikingly, the expression of both isoforms was strongly downregulated upon treatments of CAL27 with the IC_{90} of cisplatin and the cetuximab/cisplatin (IC_{75} and IC_{90}) cotreatment (Figure 2C). Similar observations were made in SQ20B cells, where both the IC_{75} and IC_{90} of cisplatin alone or in combination with cetuximab strongly decreased the expression of the p63 protein (Figure 2D).

To analyze if p53 signaling can be reactivated, SQ20B and CAL27 cell lines were treated with PRIMA MET (50 μM), a p53 reactivator, in addition to cetuximab and/or cisplatin, and cell viability was assessed using a MTT cell survival assay. The treatments with PRIMA +/− cetuximab were found to be more cytotoxic than cetuximab used alone in both cell lines (Mann-Whitney $p < 0.001$). However, no significant increase in cytotoxicity was observed when PRIMA MET was used in combination with cisplatin and/or cetuximab (Figure 3A,B).

Altogether, these results suggest that mutated p53 has no significant impact on the cytotoxicity induced by the cotreatment. Hence, the apoptosis observed in CAL27 and SQ20B cells is independent of p53. In contrast, p63 and p73 isoforms might be involved, but additional investigations are required to precisely identified which isoforms and their respective function.

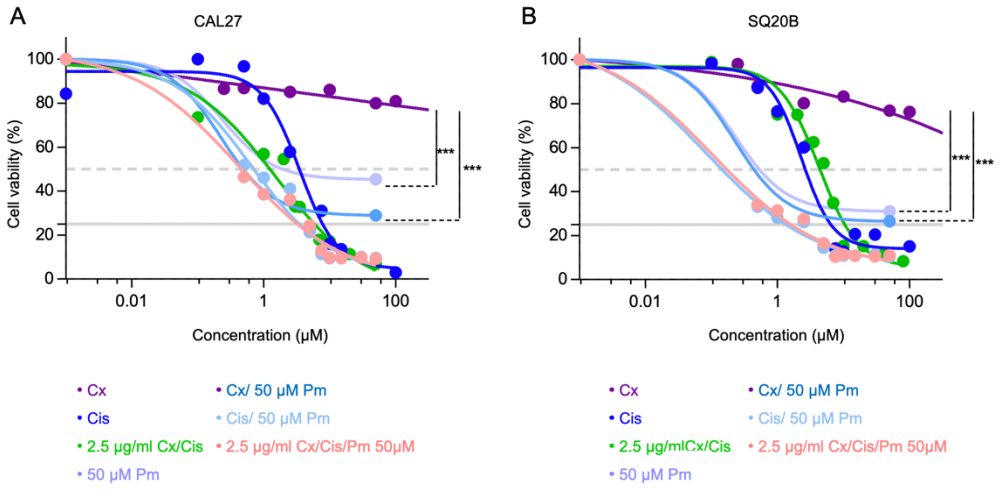

Figure 3. (**A**,**B**). Analysis of CAL27 (**A**) and SQ20B (**B**) cells survival upon treatment with growing concentrations of cetuximab (Cx) +/− 50 µM PRIMA (Pm; dark and light purple lines, respectively), growing concentrations of cisplatin (Cis) +/− 50 µM PRIMA (dark and light blue line, respectively), growing concentrations of cisplatin + 2.5 µg/mL cetuximab +/− 50 µM PRIMA (dark and light green line, respectively), and 50 µM PRIMA alone, using a MTT-based assay. Mean values from 2 independent experiments are plotted as sigmoid curves. The 50% and 25% survival thresholds are shown as a dotted red and plain green lines, respectively. Mann-Whitney *p*-values: *** $p < 0.001$.

3.3. Danger-Associated Molecular Patterns Are Emitted by HNSCC Cells upon Cetuximab and/or Cisplatin Treatment

Using colorectal cancer cell line models, Pozzi and collaborators showed that cetuximab is able to induce an ICD [30]. To explore the capacity of cetuximab to induce ICD in HNSCC, we analyzed the emission of several DAMPs by CAL27 and SQ20B cells upon treatment with cetuximab +/− cisplatin. We first assessed the plasma membrane relocalization of the Calreticulin (CRT) chaperone in CAL27 and SQ20B cells treated with cetuximab, cisplatin or the cetuximab/cisplatin co-treatment. First, based on the literature that describes CRT translocation as an early and essential event of ICD, we chose to assess its expression after 4 h of treatment using the detection of membrane proteins using a non-permeant reactive biotin. Cells were incubated with Sulfo-NHS-SS-Biotin to biotinylate plasma membrane proteins, and streptavidin beads were used to separate membrane-associated proteins from intracellular proteins. Both protein fractions were resolved with SDS-PAGE and analyzed by western blot. Membranes were probed with an anti-EGFR and an anti-GAPDH antibodies, used as positive and negative controls for the membrane fraction, respectively. Probing the blots with an anti-GAPDH antibody was also used as positive control for both the total input and intracellular fraction. Signals corresponding to the EGFR were observed in the three fractions, whereas no signal corresponding to GAPDH were observed in the membrane fraction, both in CAL27 (Figure 4A) and in SQ20B cells (Figure 4B). Membranes were also probed with a specific anti-CRT antibody, and signals corresponding to CRT in the membrane fraction were normalized to CRT signals in the input. Interestingly, the CRT was found to be ~3 and times ~5 more present in the membrane protein fraction of cells treated with cetuximab or the cetuximab/cisplatin IC_{90} combination, in CAL27 and SQ20B cells, respectively (Figure 4A,B). Considering that no changes in CRT expression are observed in the input, this suggest that CRT is translocated from the endoplasmic reticulum to the plasma membrane upon cetuximab treatment. This observation was further confirmed by an immunocytofluorescence analysis of the expression of CRT in non-permeabilized CAL27 cells (Figure 4C). Altogether, these results show that cetuximab used either alone or in combination with cisplatin induce the plasma membrane translocation of CRT in both SQ20B and CAL27 cells.

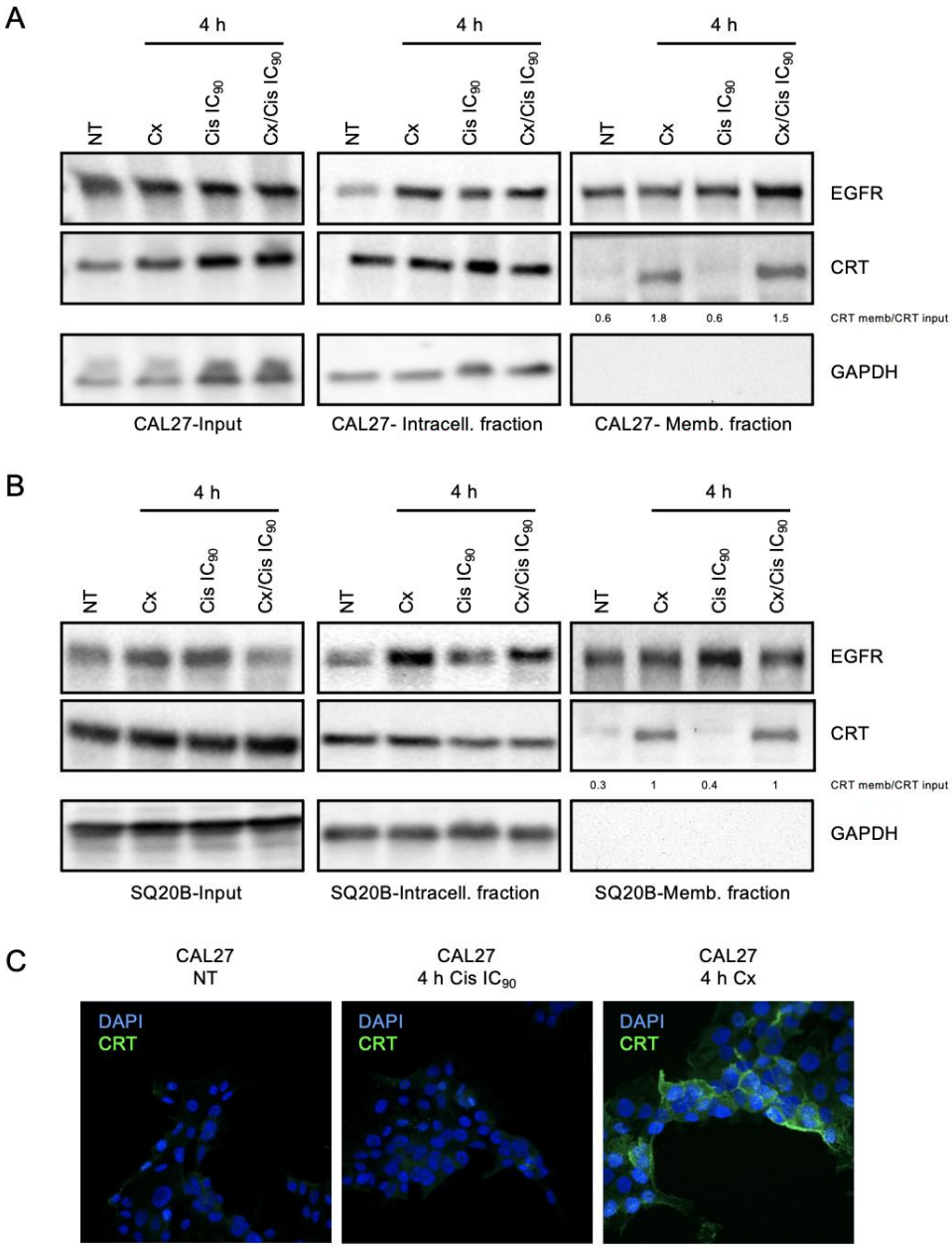

Figure 4. (**A**,**B**). Membrane protein purification and western blot analysis of EGFR, Calreticulin (CRT) and GAPDH expression in the input (left panels), intracellular (middle panels) and extracellular protein fractions of CAL27 (**A**) and SQ20B (**B**) cells treated with cetuximab (Cx), cisplatin (Cis) at the IC_{50}, IC_{75} and IC_{90}, and the Cx/Cis combination for 4 h. The enrichment of CRT in extracellular fractions is shown. The blots that are shown are representative examples of three independent experiments. Additional independent biological replicates are shown in supporting documents. (**C**). Immunocytofluorescent staining analysis of the expression of CRT in non-treated (NT) CAL27 cells (left panel), and CAL27 treated with cisplatin (Cis) at the IC_{90} (middle panel) or cetuximab (Cx; right panel). Nuclei are stained with DAPI. Magnification: X64.

We also investigated the expression of HMGB1, which is known to be released from the nucleus to the extracellular environment at later ICD stages [41]. CAL27 and SQ20B cells were treated with cetuximab +/− cisplatin, and both whole cell proteins and proteins in the cell culture medium were harvested 48 h after treatment, resolved with SDS-PAGE and analyzed by western blot. The level of BSA was used as a loading control of samples of supernatant protein and for normalization. In the CAL27 cell line, HMGB1 was present in

the supernatant upon treatment, in all conditions, with the most important signal observed after treatment with cetuximab and with cetuximab/cisplatin IC_{50}, with an induction fold compared to the untreated control of 8.5 and 8.4, respectively (Figure 5A). The induction of HMGB1 level was higher upon treatment with the IC_{50} of Cisplatin compared to the IC_{75} (Figure 5A). On the contrary, HMGB1 level in the supernatant of SQ20B cells was only triggered with treatments involving cisplatin and, in a concentration-dependent manner (i.e., cisplatin alone and the cisplatin/cetuximab with similar expression patterns; Figure 5B).

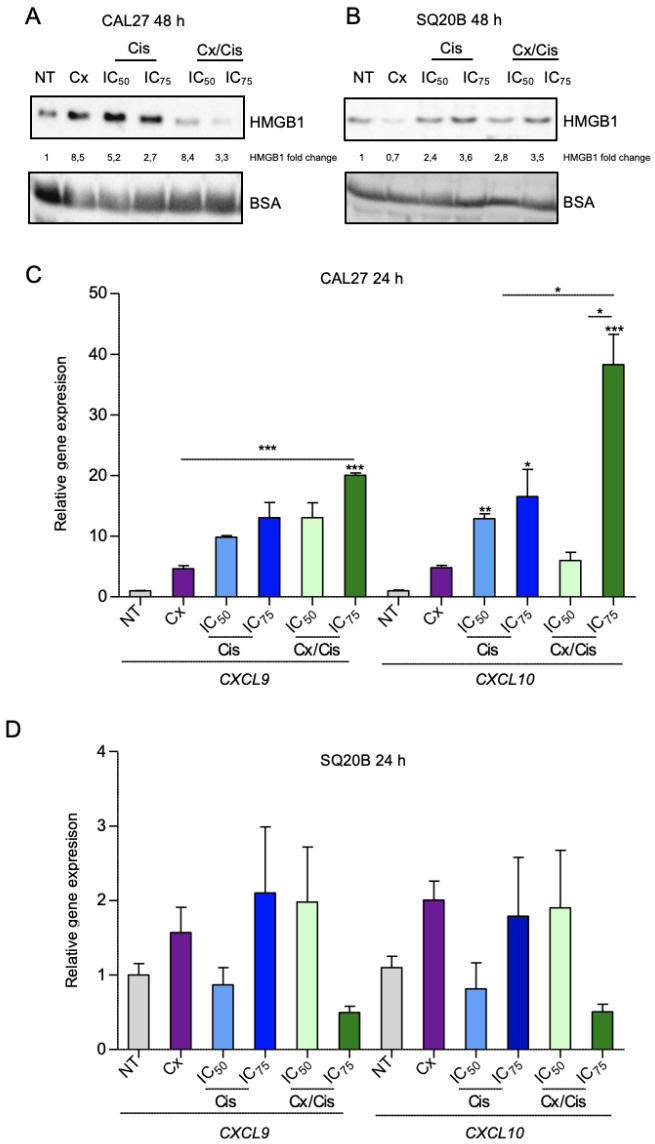

Figure 5. (**A**,**B**) Western blot analysis of the HMGB1 expression in the supernatant from CAL27 (**A**) and SQ20B (**B**) cell cultures harvested 48 h after with cetuximab (Cx), cisplatin (Cis) at the IC_{50} and IC_{75} and the Cx/Cis combination. Signals were quantified respectively to the actin loading control and normalized with respect to the non-treated control (quantification results are shown). The blots that are shown are representative examples of two independent experiments. Additional independent biological replicates are shown in supporting documents. (**C**,**D**). Analysis of the expression of the *CXCL9* and *CXCL10* by RT-qPCR in CAL27 (**C**) and SQ20B (**D**) cells treated for 24 h with cetuximab (Cx), cisplatin (Cis) at the IC_{50} and IC_{75} and the Cx/Cis combination. Data is represented as mean from two independent experiments +SEM. Kruskal-Wallis and Dunn post-test *p*-values: * $p < 0.05$; ** $p < 0.01$; *** $p < 0.001$.

Finally, we analyzed the expression of type I interferon-responsive cytokines using RT-qPCR 24 h after treatment, and namely *CXCL9* and *CXCL10*, that are known to be upregulated by type I interferons [42]. In CAL27 cells, the expression of both *CXCL9* and *CXCL10* was strongly upregulated: a significant ~10-fold induction of *CXCL10* (compared to non-treated control) was observed upon treatment with cisplatin alone. Treatment of CAL27 cells with the cetuximab/cisplatin IC_{75} combination triggered a ~20-fold and ~45-fold induction of *CXCL9* and *CXCL10*, respectively (Figure 5C). Conversely, no statistically significant impact of the treatments on *CXCL9* and *CXCL10* expression was observed in SQ20B cells (Figure 5D). However, the biological impact on treatments of these cytokine gene expression appears more complex. Indeed, a gene expression assay was also carried out 48 h after treatment, and we observed that *CXCL9* and *CXCL10* are downregulated in both cell lines upon cisplatin treatment compared to other conditions (Figure S2B).

Altogether, our observations show that treatment of HNSCC cells with cetuximab induced the emission of DAMPs in a cell-dependent manner: CAL27 cells treated with cetuximab alone or combined with cisplatin appear to be more prone to the emission of DAMPs (CRT plasma membrane translocation; HMGB1 release; induction of type I interferon response) than SQ20B cells. Interestingly, platinum-based chemotherapy alone does not trigger CRT exposure and appears to repress *CXCL9* and *CXCL10* expression 48 after treatment.

3.4. Cetuximab +/− Cisplatin Trigger DAMPs Emission in Murine Head and Neck Carcinoma Cells

To confirm that the cetuximab +/− cisplatin treatment modifies the immunogenicity of HNSCC cells, anti-cancer prophylactic immunizations of mouse syngeneic models were carried out. To this end, we used the MOC2 mouse head and neck carcinoma cell line to generate a stable murine cell line expressing the human EGFR (hEGFR). After retroviral transduction of MOC2 cells using an hEGFR expression plasmid and selection on puromycin, several clones were obtained, one of which (MOC2-phEGFR-C1) was found to express the hEGFR protein (Figure S3). An immunocytofluorescent staining of hEGFR of MOC2-phEGFR-C1 cells showed that the expression of hEGFR is homogeneous in the cell population (Figure 6A). Consistently with what was observed in CAL27 and SQ20B cells, treatment with cisplatin alone or in combination with cetuximab induced caspase-3 cleavage, 24 h (Figure 6B) and 48 h (Figure S4A) after treatment.

Interestingly, the same treatments were also found to trigger the relocalization of CRT to the plasma membrane (Figure 6C). However, unlike CAL27 and SQ20B, the cetuximab/cisplatin co-treatment was able to induce a more robust expression of CRT at the plasma membrane of MOC-2-phEGFR-C1 cells compared to treatment with cetuximab alone (Figure 6C, right panels). Finally, we observed that HMGB1 was released in the extracellular medium, 24 h, and 48 h after treatment with cisplatin alone or in combination with cetuximab, in a dose-dependent manner (Figure 6D), whereas the expression of intracellular HMBG1 was not affected by treatments (Figure S4B).

3.5. Induction of Bona Fide ICD by Cetuximab +/− IC_{50} of Cisplatin

To assess whether the treatment of MOC2-phEGFR-C1 cells by cetuximab and/or cisplatin was able to induce an anti-tumor immune response in vivo, MOC2-phEGFR-C1 cells were first treated ex vivo, and dead cells were injected in the right flank of immunocompetent C57BL/6 mice. The same mice were then challenged seven days after the first immunization, by injecting non-treated living MOC2-phEGFR-C1 cells on the left flank, and the mice progression-free survival was evaluated. An injection of MOC2-phEGFR-C1 cells killed by three consecutive freeze/thaw cycles was used as a non-immunogenic cell death control. Expectedly, tumor progression was observed within 26 days in 11/11 mice that were injected with MOC2-phEGFR-C1 cells killed by freeze/thaw cycles (Figure 7A,B). A similar observation was made for mice in the IC_{75} cisplatin (tumor growth in 10/12 mice) and cetuximab + IC_{75} cisplatin (tumor growth in 12/12 mice) treatment groups. Strikingly, the injection of cells treated with cetuximab, the IC_{50} of cisplatin, or the combination was

able to prevent tumor progression, which was observed in only 1/12, 4/12, and 2/12 mice, respectively (Figure 7A,B). Thus, these observations suggest that the injection of MOC2-phEGFR-C1 cells treated with cetuximab and/or the IC_{50} of cisplatin provides protection against a subsequent tumor challenge.

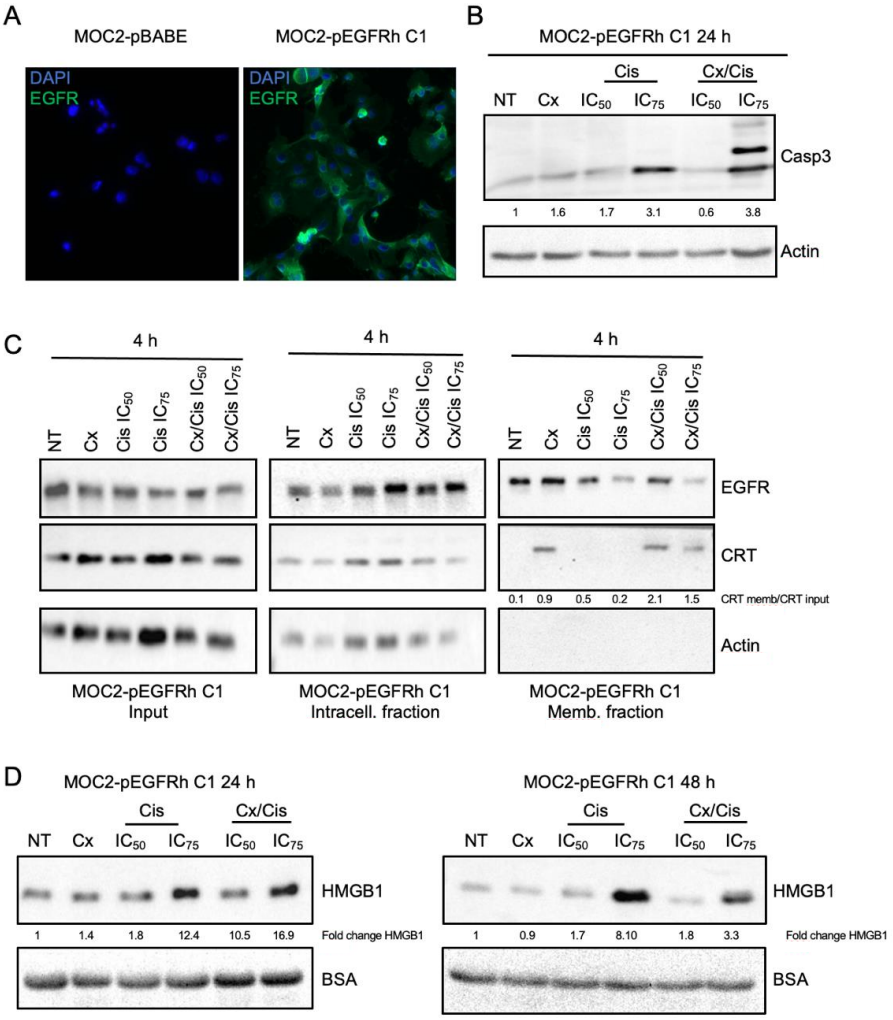

Figure 6. (**A**). Immunocytofluorescent staining analysis of the expression of EGFR in MOC2 cells that were stably transfected with the empty pBABE (left micrograph) and pBABE-hEGFR (right micrograph, MOC2-phEGFR C1 clone) expression plasmid. Nuclei are stained with DAPI. X40. (**B**). Western blot analysis of cleaved caspase-3 (Casp3) expression in whole protein extracts from MOC2-phEGFR C1 cells treated with cetuximab (Cx), cisplatin (Cis) at the IC_{50} and IC_{75}, and the Cx/Cis combination for 24 h. Signals were quantified respectively to the actin loading control and normalized with respect to the non-treated control (quantification results are shown) (**C**). Membrane protein purification and western blot analysis of EGFR, Calreticulin (CRT) and Actin expression in the input (left panels), intracellular (middle panels) and extracellular protein fractions of MOC2-phEGFR C1 cells treated with cetuximab (Cx), cisplatin (Cis) at the IC_{50} and IC_{75}, and the Cx/Cis combination for 4 h. The enrichment of CRT in extracellular fractions is shown. (**D**). Western blot analysis of the HMGB1 expression in the supernatant from MOC2-phEGFR C1 cell cultures harvested 24 h (left panels) and 48 h (right panels) after with cetuximab (Cx), cisplatin (Cis) at the IC_{50} and IC_{75} and the Cx/Cis combination. All blots shown in this figure are representative examples of three independent experiments. Additional independent biological replicates are shown in supporting documents.

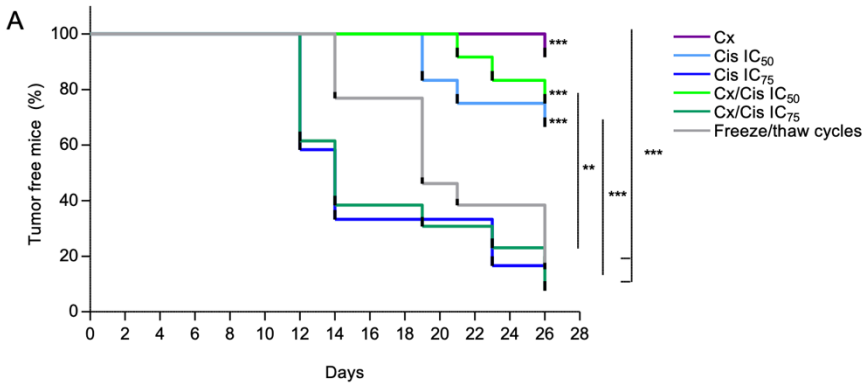

B

Ex vivo treatment	# mice with tumors
Freeze/thaw cycles	11/11 (100%)
Cx	1/12 (8.3%)
Cis IC_{50}	4/12 (33.3%)
Cis IC_{75}	10/12 (83.3%)
Cx/Cis IC_{50}	2/12 (16.7%)
Cx/Cis IC_{75}	12/12 (100%)

Figure 7. (**A**). Kaplan-Meier analysis of the tumor-free survival of MOC2-hEGFR syngeneic mice models vaccinated with ex vivo treated cells. Treatments include cetuximab (Cx), the IC_{50} and IC_{75} of cisplatin (Cis IC_{50}; Cis IC_{75}), the cetuximab and cisplatin combination (Cx/Cis IC_{50}; Cx/Cis IC_{75}) and cells killed by freeze/thaw cycles. Kaplan-Meier *p*-values: ** $p < 0.01$; *** $p < 0.001$. (**B**). Analysis of the number of tumor-free mice. The ex vivo treatment arms, number of treated mice that grew tumors/total number of mice and percentage, and the mean volume of tumors are shown.

4. Discussion

HNSCC is a particularly deadly cancer, with approximately 400,000 cancer-related deaths in 2018 [2]. Cetuximab, which targets EGFR, is the only approved targeted therapy for the management of locally advanced R/M HNSCC. However, Cetuximab is not used as a monotherapy, but is associated with either radiotherapy [1] or platinum-based chemotherapy (EXTREME regimen) [7]. To the best of our knowledge, the molecular mechanisms underlying the cytotoxicity of the EXTREME regimen have not been investigated in detail in HNSCC.

Here we showed that the cetuximab/cisplatin combined treatment displays higher toxicity than both treatments provided alone in the CAL27 cell line. These in vitro observations are consistent with clinical trials, where the EXTREME protocol results in a 3-month increase in the overall survival of patients with HNSCC compared to monotherapies [6]. In addition, similar observations were also made in nasopharyngeal cancer [43] and in colon cancer models [44]. More specifically, the cetuximab/cisplatin combination was shown to block the EGFR pathway via the inhibition of EGRF and ERK phosphorylation in the HCT116 and SW480 human colon cancer cell lines [44]. ERK is a kinase of the MAP Kinase pathway downstream of the EGFR, whose activation leads to cell proliferation. Most interestingly, ERK inhibition seems to be critical for the synergic effect of the cetuximab/cisplatin treatment, since it plays a role in the resistance to cetuximab, which can be overcome by a dual blockade of EGFR and HER3 [44,45]. However, no improved cytotoxicity of the cetuximab/cisplatin was observed in SQ20B cells. We previously have shown that the high basal and cetuximab-induced expression of the Hypoxia Inducible Factor-2α transcription factor in SQ20B cells is responsible for resistance to EGFR-blockage [8]. This could explain the lack of benefit from treatment with cetuximab. In addition, additional unidentified molecular disorders in SQ20B cells could account for the absence of synergy between cisplatin and cetuximab. Thus, the differential cytotoxicity of the cisplatin/cetuximab combination in CAL27 and SQ20B cell lines illustrates that different genetic and molecular backgrounds are likely to dictate cell response to the therapy. Key molecular differences between the

two cell lines that are likely to include the *TP53* mutational status (CAL27 and SQ20B harbor different *TP53* gene mutations, of unknown functional consequences), which might influence the induction of apoptosis upon genotoxic stress, as well as the basal and induced expression level of the Hypoxia Inducible Factor-2 (HIF-2) transcription factor (CAL27 express the lower basal level of HIF-2 that are unaffected by cetuximab treatment, whereas SQ20B expresses higher levels of HIF-2, that is upregulated upon cetuximab treatment), which is responsible for resistance to EGFR blockade in SQ20B cells [8]. These observations also highlight that the response of patients to the EXTREME protocol is likely to vary depending on tumor-specific molecular signatures.

We further analyzed the impact of the EXTREME regimen on both cell cycle deregulation and the induction of apoptotic cell death, which both contribute to cell growth, by using specific markers (iodide propidium/annexin V; cleaved caspase-3). Our observations suggest that the co-treatment induces both a cell cycle arrest in the G2 phase, as well as apoptotic cell death. More particularly, we observed that cisplatin +/− cetuximab triggered caspase-3 cleavage in both CAL27 and SQ20B cells, as well as in MOC2-phEGFR C1 cells. The induction of caspase-3 cleavage and upon cetuximab/cisplatin cotreatment was previously reported in the HCT116 and SW480 colon cancer cell lines, where both molecules seem to synergize [44]. However, the benefit of adding cetuximab to cisplatin with respect to caspase-3 cleavage and the extent of the synergy appears to depend on drug concentration, treatment timing, and treated cell line. Indeed, a mild synergy was observed in CAL27 and SQ20B after 24 h of treatment with the combination of the IC_{50} of cisplatin and cetuximab, whereas a stronger synergy was observed only in SQ20B cells after 48 h of treatment with cetuximab and cisplatin at the IC_{75}. Strikingly, the combination using high doses of cisplatin performed more poorly in SQ20B cells than drugs used alone. This suggests that SQ20B might undergo caspase-3-independent cell death upon treatment with high doses of cisplatin. This also highlights that cell response to genotoxic stress is likely to vary according to both the dose and the duration of treatment, with the induction of different signaling pathways. The level of activation of these pathways is probably dependent on the molecular and genetic background of each cell line. Further detailed analyses of these mechanisms are required to shed more light on the molecular basis of these phenomenon.

The p53 family of transcription factors is involved in DNA damage repair and apoptosis induction upon platinum-derived compound treatment [46]. Importantly, the *TP53* gene is mutated in >80% of HNSCC and plays a major role in tumor initiation and progression and resistance to platinum-based chemotherapy [47]. Interestingly, the role of p53 in the modulation of the tumor immune microenvironment and response to immunotherapy has recently emerged in the literature [48,49]. In addition, it was shown the pharmacological reactivation of p53 by Nutlin-3a induces the release of DAMPs and the activation of ICD [50]. Therefore, in order to gain further insight into the molecular mechanisms associated with the induction of apoptosis by the EXTREME protocol, and its potential correlation to the induction of ICD, we analyzed the expression of the three members of the p53 family (i.e., p53, p63, and p73). The CAL27 and SQ20B cell lines have mutated p53 and consequently, non-treated cells expressed a high level of the p53 protein. Our western blot analysis did not show any modification of the p53 protein expression level upon treatment with cetuximab and cisplatin, alone or combined, and the expression of known p53 target genes was not induced upon treatment, suggesting that p53 might not be involved in the apoptosis of CAL27 and SQ20B cells. The crosstalk between the p53 and the EGFR signaling pathway, and its consequence on therapeutic EGFR blockade has been shown in other cancer models. For instance, both wild-type and mutant p53 have been proposed to regulate *EGFR* transcription [51,52], and inhibition of p53 results in EGFR downregulation in prostate cancer cells [53]. Resistance to cetuximab has been correlated to a loss of p53 expression and an increase of p-ERK expression in H226 lung cancer cells and SCC6 HSNCC [54]. Consistently, p53 was shown to functionally impact the response of H226 cells to EGFR blockade [54], and the restoration of p53 function in p53

null prostate cancer cells stimulates EGFR and Akt phosphorylation and restores sensitivity to cetuximab [55]. We attempted to restore p53 function by treating SQ20B and CAL27 cells with the PRIMA MET reactivator but did not observe any consequences in terms of cell response to cetuximab and/or cisplatin. We cannot rule out that p53 reactivation was not achieved in our hands due to the nature of the mutations present in both cell lines, and additional functional studies about the role of p53 in the response of HNSCC cells to the EXTREME protocol are required.

The *TP73* and *TP63* genes encode two isoforms: one longer isoform called TA, which contains the N-terminal translational domain and displays pro-apoptotic function, and one shorter isoform called ΔN, which lacks the translational domain and has oncogenic activity [56]. Very scarce data is available on the expression and role of p73 in HNSCC. It has been reported to be expressed at lower levels compared to the other member of the p53 family (i.e., p53 and p63) [57]. Two bands were observed in a western blot analysis of p73 and p63 expression in whole protein extracts from CAL27 and SQ20B cells. ΔNp73, which could correspond to the lower band, seems to be the dominant p73 isoform in CAL27 cells. However, a higher band, which could correspond to TAp73, is induced by cetuximab +/− cisplatin at the IC_{50}. This might suggest a modification of the ratio of the p73 isoforms in CAL27 cells, with the induction of the expression of the pro-apoptotic TAp73 isoform (possibly the upper band) upon treatment. Interestingly, a modification of the TA/ΔNp73 (possible the upper and lower band, respectively) ratio is also observed in SQ20B cells, with a reduced expression of the TAp73 isoform upon treatment with higher doses of cisplatin (IC_{75} and IC_{90}). However, formal identification of the bands is required to confirm this hypothesis. TAp73 can induce apoptosis by indirectly regulating p53 target genes [11]. Most interestingly, EGFR signaling blockade by cetuximab has been shown to inhibit AKT and ERK, thus relieving p73 inhibition and subsequent transactivation of PUMA and the induction of mitochondrial stress-related apoptosis [58]. ΔNp63 is the dominant p63 isoform in HNSCC and is known to play a critical role in carcinogenesis and tumor cell survival [57,59]. In our hands, the expression of ΔNp63 was downregulated by high doses of cisplatin, and treatment with cetuximab increased this effect. The effect of the cisplatin +/− cetuximab treatment was found to be more important in SQ20B cells, where it resulted in total inhibition of the expression of ΔNp63. Importantly, ΔNp63 is known to inhibit p73-related apoptosis on HNSCC cells through direct physical interaction and direct binding on response elements if the promoter of *PUMA* [59,60]. Our observations are therefore consistent with the downregulation of ΔNp63 and subsequently lifted inhibition on p73 expression and/or activity upon treatment with cetuximab+/−cisplatin, which might participate in the induction of apoptotic cell death by the EXTREME protocol. Additional functional data are required to test this hypothesis.

In addition to the role that the EXTREME protocol might play in apoptosis, we also investigated whether it was able to induce ICD. Indeed, Pozzi and colleagues have shown that cetuximab is capable to trigger the emission of DAMPs as well as the activation of anti-tumor immunity in colon cancer cells [30]. Consistently with their findings, we found that cetuximab alone or in combination with cisplatin-induced the relocalization of CRT to the plasma membrane in both SQ20B and CAL27 cell lines as early as 4 h after treatment. The CRT chaperone is known to translocate from the ER to the cell surface early during ICD [61], where it is recognized by the CD91 receptor on antigen-presenting (APC) cells and acts as an "eat me" signal [27]. Consistently with the fact that cisplatin is not an ICD-inducer [62], we did not observe CRT relocalization upon treatment with cisplatin. The extracellular release of HMGB1 was triggered upon all treatments in CAL27 cells, and upon treatment with the combination only, in a dose-dependent manner, in SQ20B cells. The extracellular release of the chromatin-associated HMGB1 protein has an immunomodulatory function, including cytokine activity and pro-inflammatory activity, that depends on its oxidation state [63]. In the frame of ICD, HMGB1 is recognized by TLR4 and induces dendritic cell activation, increasing phagocytosis of tumors antigen liberated by dying cells [41]. Although, the mechanism allowing the release of HMGB1 is unknown [27], we observed a correlation

between the presence of HMGB1 in the extracellular medium and the percentage of CAL27 and SQ20B cells in late apoptosis 48 h after treatment, suggesting a potential link between the intrinsic sensitivity of HNSCC cells to the EXTREME protocol and HMGB1 emission. The production of type I interferons (IFNs) is also a feature of cells undergoing ICD. The secretion of type I IFNs activates signaling pathways through their interaction with the Interferon Alpha and Beta Receptor Subunit 1, in an autocrine and paracrine manner, which ultimately triggers the expression of T-cell chemoattractant chemokines CXC motif ligand CXCL9 and CXCL10 [27,64]. Interestingly, the expression of *CXCL9* and mainly *CXCL10* was found to be increased in the CAL27 cell line, upon treatment by cetuximab and/or cisplatin in a dose-dependent manner. This shows that the EXTREME protocol can trigger the secretion of immunomodulatory cytokines in HNSCC cells, although our observation suggests that this effect is likely to be cell-dependent. In conclusion, and consistently with what was shown by Pozzi and collaborators in colon cancer cells [30], we found that cetuximab, alone or with cisplatin, can trigger the emission of several DAMPs (including CRT, HMGB1, and type I IFN response) in HNSCC cell lines, according to different patterns and/or intensity. Further studies will be required to assess whether this heterogeneity of response is also found in human tumors, as well as the relevance it might have with response to the treatment and patient outcome.

In order to validate the immunogenic nature of the treatment of HNSCC cells by cetuximab +/− platinum-based chemotherapy, we performed a vaccination assay using immunocompetent syngeneic models, which is considered to be the gold standard to demonstrate ICD in vivo [26]. To this end, a MOC2 cell line stably expressing the human EGFR was generated. The parental MOC2 cells were derived from a tumor in the oral cavity of a C57BL/6 mouse, and generated aggressive tumors within an immunosuppressive environment [65]. Similar to what was observed in CAL27 and SQ20B cells, MOC2-phEGFR-C1 cells incubated with cisplatin and/or the cisplatin/cetuximab combination displayed apoptosis features (caspase-3 cleavage), and the plasma membrane translocation of CRT and extracellular release of HMGB1. Interestingly, ex vivo treatment of MOC2-phEGFR-C1 cells with either cetuximab, the IC_{50} of cisplatin, or their combination provided mice an anti-tumor protection against a second tumor challenge, whereas treatment with the IC_{75} of cisplatin +/− cetuximab did not. Our results suggest therefore that cetuximab can induce ICD of HNSCC cells, which is consistent with previous observations on murine lung cancer cell line [66] and on murine colon cell line expressing a human EGFR [30]. Surprisingly, we found the immunization effect provided by cisplatin treatment to be depending on drug concentration and does not correlate with the dose-dependent effect we observed in vitro on the emission of DAMPs. This could be explained by the fact that caspase-3 cleaved is induced at higher levels upon treatment with the IC_{75} of cisplatin. Indeed, the activation of caspase-3 stimulates the exposure of phosphatidylserine (PS) on the outer leaflet of cells' plasma membrane. The recognition of PS by specific PS receptors stimulates the uptake of apoptotic corpses by phagocytes of the immune system together while delivering an anti-inflammatory signal (see [67] and references therein). In addition, caspase-3 is known to stimulate the expression of prostaglandin E2, which has immunosuppressive functions [67]. Finally, caspase-3 inhibits signals known as DAMPs, including the IL-33 cytokine as well as intracellular signals that lead to the expression of type I IFNs [67]. Thus, our observations suggest that the induction of the immunogenicity of cancer cells upon cytotoxic treatment could correlate inversely with the intensity of the induction of caspase-3-related cell death, through the number of cells that undergo apoptosis and/or the level of induction of caspase-3 protein.

The lack of correlation between cisplatin concentrations and the immunogenic effect of the treatment in vivo is consistent with clinical data showing that cytotoxic anti-cancer drugs delivered at lower doses with metronomic treatment schedules rather than administrated at their maximum tolerated dose influence the infiltration of treated tumors with immune cells (for review see [68] and references therein): indeed, drugs used at their maximum tolerated dose in order to provide a high cytotoxic effect, whereas lower sub-

optimal doses have been shown to stimulate an anti-tumor effect through the stimulation of the immune system. Interestingly, the intra-tumor deliverance of nano-doses of conventional chemotherapeutic drugs has also been reported to make up the tumor immune landscape [69]. Altogether, this highlights the relative importance of the drug-related induction of apoptotic cell death vs. the emission of ICD mediators, which is more desirable to stimulate the immune system and possibly synergize with immunotherapies. Thus, there might be a subtle balance between treatment-induced stress, which could result in the improvement of cancer cell immunogenicity, and treatment-induced cell death, which potentially hinders cancer cell immunogenicity via immunomodulatory signals.

In conclusion, we have shown that cetuximab (either alone or in combination with cisplatin) is able to enhance murine and human HNSCC cells' immunogenicity through the exposure of CRT, which is known to provide a strong "eat-me" signal to phagocytes of the immune system. However, the impact of cetuximab alone on the release of HMGB1 varies in a cell-dependent manner, while cisplatin (alone or in combination with cetuximab) appears to stimulate HMGB1 release from apoptotic cells. Finally, cisplatin +/− cetuximab appears to trigger a type I IFN response that elicits the expression of CXCL9 and CXCL10 in a cell-line-dependent manner. Interestingly, only ex vivo cell treatment conditions that allow the release of DAMPs and moderate cleavage of caspase-3 (i.e., cetuximab and/or cisplatin at the IC_{50}) appear to be able to elicit an anti-tumor immune response in immunocompetent animals. Further studies are warranted to evaluate whether variations of the EXTREME protocol including the dose of cisplatin are able to trigger ICD and provide a similar effect, and to what extent this can be synergistic with immunotherapies in HNSCC patients.

Supplementary Materials: The following supporting information can be downloaded at: https://www.mdpi.com/article/10.3390/cells11182866/s1: Figure S1. Quantification of the cell cycle distribution data of CAL27 (A) and SQ20B (B) cells treated 24 h (upper histograms) and 48 h (lower histograms) with cetuximab (Cx), cisplatin (Cis) at the IC_{50} and IC_{75} and the Cx/Cis combination. The histograms show the mean number of percentages of cells in S, G2, G1/G0, and early apoptosis (EA; i.e., sub-G1); Figure S2. (A) Western blot analysis of the HMGB1 expression in the supernatant from CAL27 (left panels) and SQ20B (right panels) cell cultures harvested 68 h after with cetuximab (Cx), cisplatin (Cis) at the IC_{50} and IC_{75} and the Cx/Cis combination. Signals were quantified respectively to the actin loading control and normalized with respect to the non-treated control (quantification results are shown). The blots that are shown are re Apresentative examples of three independent experiments. Additional independent biological replicates are shown in supporting documents. (B) Analysis of the expression of *CXCL9* and *CXCL10* by RT-qPCR in CAL27 (left histographs) and SQ20B (right histographs) cells treated for 48 h with cetuximab (Cx), cisplatin (Cis) at the IC_{50} and IC_{75} and the Cx/Cis combination. Data are represented as the mean from one independent experiment +SEM; Figure S3. Western blot analysis of EGFR expression in whole-cell protein extracts from MOC-2 cells transduced with a pBABE-hEGFR expression plasmid after selection of clones on puromycin. EGFR expression is observed in the MOC2-phEGFR C1 clone. The blots that are shown are representative examples of three independent experiments; Figure S4. (A) Western blot analysis of p53 and cleaved caspase-3 (Casp3) expression in whole protein extracts from MOC2-phEGFR C1 cells treated with cetuximab (Cx), cisplatin (Cis) at the IC_{50}, $IC_{75,}$ and IC_{90}, and the Cx/Cis combination for 24 h (left panels) and 48 h (right panels). Casp3 signals were quantified respectively to the actin loading control and normalized with respect to the non-treated control (quantification results are shown). (B) Western blot analysis of the HMGB1 expression in whole protein extracts from MOC2-phEGFR C1 cell cultures treated for 24 h (left panels) and 48 h (right panels) with cetuximab (Cx), cisplatin (Cis) at the $IC_{50,}$ and IC_{75} and the Cx/Cis combination. Signals were quantified respectively to the actin loading control and normalized with respect to the non-treated control (quantification results are shown). Blots. shown are representative examples of two independent experiments. Additional independent biological replicates are shown in supporting documents; Table S1. List of oligonucleotides primers used for RT-qPCR gene expression assays: Gene names, forward and reverse primer sequences are shown; Table S2. List of TaqMan assays used for RT-qPCR gene expression assays: Gene names and TaqMan gene expression assay ID are shown; Table S3. List of antibodies used for western blot analysis; Protein names, antibody providers and used antibody dilutions are shown.

Author Contributions: Conceptualization, A.C.J. and C.G.; methodology, J.D.A. and C.B. (Cyril Bour); validation, J.D.A., J.M., C.B. (Cyril Bour), C.G. and A.C.J.; formal analysis, J.D.A., J.M., C.G. and A.C.J.; investigation, J.D.A., J.M., C.B. (Cyril Bour) and V.D.; resources, E.P.; writing—original draft preparation, J.D.A. and A.C.J.; writing—review and editing, P.S., C.B. (Christian Borel), E.P., G.M. and C.G.; visualization, J.D.A., J.M. and A.C.J.; supervision, C.G. and A.C.J.; project administration, C.G. and A.C.J.; funding acquisition, C.G. and A.C.J. All authors have read and agreed to the published version of the manuscript.

Funding: This research was financially supported by the Centre National pour la Recherche Scientifique (CNRS, France; C.G.), the Conférence de Coordination Interrégionale Grand Est-Bourgogne Franche-Comté de la Ligue Contre le Cancer and the Institut de cancérologie Strasbourg Europe. The Streinth Team is also supported by the Association pour la Recherche sur le Cancer, ITMO Cancer, European action COST Proteocure, the Interdisciplinary thematic Institute InnoVec, the IDEX Excellence grant from Unistra, and the Institut National du Cancer. J.D.A has been financially supported by a PhD fellowship awarded by the Ministère de l'Enseignement Supérieur et de la Recherche. J.M. is financially supported by a PhD fellowship awarded by the French national "Ligue Contre le Cancer".

Institutional Review Board Statement: All animal experiments were approved by the Institutional Animal Care and Use Committee (APAFIS #29181; 8 April 2021). Six weeks-old C57BL/6 female were housed in the certified animal facility (#H-67-482-21). The mice were cared for according to the Institutional Guidelines for Animal Care. Mice were acclimated for two weeks, provided with unlimited access to sterilized food and water ad libitum, and housed with 12 h day/night cycle.

Informed Consent Statement: Not applicable.

Data Availability Statement: Not applicable.

Acknowledgments: We are most grateful to Pierre Bischoff, Sophie Pinel, Elisabeth Martin and Di Fiore Pier Paolo for providing cell lines and reagents. We are grateful to Aurélie Eisenmann for her help regarding the regulatory and technical aspects of animal experimentation. We are grateful to Rob Simmons for editing the manuscript.

Conflicts of Interest: The authors declare no conflict of interest.

References

1. Johnson, D.E.; Burtness, B.; Leemans, C.R.; Lui, V.W.Y.; Bauman, J.E.; Grandis, J.R. Head and Neck Squamous Cell Carcinoma. *Nat. Rev. Dis. Primer* **2020**, *6*, 1–22. [CrossRef]
2. Bray, F.; Ferlay, J.; Soerjomataram, I.; Siegel, R.L.; Torre, L.A.; Jemal, A. Global Cancer Statistics 2018: GLOBOCAN Estimates of Incidence and Mortality Worldwide for 36 Cancers in 185 Countries. *CA. Cancer J. Clin.* **2018**, *68*, 394–424. [CrossRef] [PubMed]
3. Picon, H.; Guddati, A.K. Mechanisms of Resistance in Head and Neck Cancer. *Am. J. Cancer Res.* **2020**, *10*, 2742–2751. [PubMed]
4. Pontes, F.; Garcia, A.R.; Domingues, I.; João Sousa, M.; Felix, R.; Amorim, C.; Salgueiro, F.; Mariano, M.; Teixeira, M. Survival Predictors and Outcomes of Patients with Recurrent and/or Metastatic Head and Neck Cancer Treated with Chemotherapy plus Cetuximab as First-Line Therapy: A Real-World Retrospective Study. *Cancer Treat. Res. Commun.* **2021**, *27*, 100375. [CrossRef]
5. Vermorken, J.B.; Mesia, R.; Rivera, F.; Remenar, E.; Kawecki, A.; Rottey, S.; Erfan, J.; Zabolotnyy, D.; Kienzer, H.-R.; Cupissol, D.; et al. Platinum-Based Chemotherapy plus Cetuximab in Head and Neck Cancer. *N. Engl. J. Med.* **2008**, *359*, 1116–1127. [CrossRef]
6. Rivera, F.; García-Castaño, A.; Vega, N.; Vega-Villegas, M.E.; Gutiérrez-Sanz, L. Cetuximab in Metastatic or Recurrent Head and Neck Cancer: The EXTREME Trial. *Expert Rev. Anticancer Ther.* **2009**, *9*, 1421–1428. [CrossRef]
7. Muraro, E.; Fanetti, G.; Lupato, V.; Giacomarra, V.; Steffan, A.; Gobitti, C.; Vaccher, E.; Franchin, G. Cetuximab in Locally Advanced Head and Neck Squamous Cell Carcinoma: Biological Mechanisms Involved in Efficacy, Toxicity and Resistance. *Crit. Rev. Oncol. Hematol.* **2021**, *164*, 103424. [CrossRef]
8. Coliat, P.; Ramolu, L.; Jégu, J.; Gaiddon, C.; Jung, A.C.; Pencreach, E. Constitutive or Induced HIF-2 Addiction Is Involved in Resistance to Anti-EGFR Treatment and Radiation Therapy in HNSCC. *Cancers* **2019**, *11*, 1607. [CrossRef]
9. Job, S.; de Reyniès, A.; Heller, B.; Weiss, A.; Guérin, E.; Macabre, C.; Ledrappier, S.; Bour, C.; Wasylyk, C.; Etienne-Selloum, N.; et al. Preferential Response of Basal-Like Head and Neck Squamous Cell Carcinoma Cell Lines to EGFR-Targeted Therapy Depending on EREG-Driven Oncogenic Addiction. *Cancers* **2019**, *11*, 795. [CrossRef]
10. Licona, C.; Delhorme, J.-B.; Riegel, G.; Vidimar, V.; Cerón-Camacho, R.; Boff, B.; Venkatasamy, A.; Tomasetto, C.; da Silva Figueiredo Celestino Gomes, P.; Rognan, D.; et al. Anticancer Activity of Ruthenium and Osmium Cyclometalated Compounds: Identification of ABCB1 and EGFR as Resistance Mechanisms. *Inorg. Chem. Front.* **2020**, *7*, 678–688. [CrossRef]
11. Alsahafi, E.; Begg, K.; Amelio, I.; Raulf, N.; Lucarelli, P.; Sauter, T.; Tavassoli, M. Clinical Update on Head and Neck Cancer: Molecular Biology and Ongoing Challenges. *Cell Death Dis.* **2019**, *10*, 540. [CrossRef] [PubMed]

12. Ortiz-Cuaran, S.; Bouaoud, J.; Karabajakian, A.; Fayette, J.; Saintigny, P. Precision Medicine Approaches to Overcome Resistance to Therapy in Head and Neck Cancers. *Front. Oncol.* **2021**, *11*, 614332. [CrossRef] [PubMed]
13. Ferris, R.L.; Blumenschein, G.; Fayette, J.; Guigay, J.; Colevas, A.D.; Licitra, L.; Harrington, K.; Kasper, S.; Vokes, E.E.; Even, C.; et al. Nivolumab for Recurrent Squamous-Cell Carcinoma of the Head and Neck. *N. Engl. J. Med.* **2016**, *375*, 1856–1867. [CrossRef] [PubMed]
14. Seiwert, T.Y.; Burtness, B.; Mehra, R.; Weiss, J.; Berger, R.; Eder, J.P.; Heath, K.; McClanahan, T.; Lunceford, J.; Gause, C.; et al. Safety and Clinical Activity of Pembrolizumab for Treatment of Recurrent or Metastatic Squamous Cell Carcinoma of the Head and Neck (KEYNOTE-012): An Open-Label, Multicentre, Phase 1b Trial. *Lancet Oncol.* **2016**, *17*, 956–965. [CrossRef]
15. Bagaev, A.; Kotlov, N.; Nomie, K.; Svekolkin, V.; Gafurov, A.; Isaeva, O.; Osokin, N.; Kozlov, I.; Frenkel, F.; Gancharova, O.; et al. Conserved Pan-Cancer Microenvironment Subtypes Predict Response to Immunotherapy. *Cancer Cell* **2021**, *39*, 845–865.e7. [CrossRef]
16. Mueller, C.G.; Gaiddon, C.; Venkatasamy, A. Current Clinical and Pre-Clinical Imaging Approaches to Study the Cancer-Associated Immune System. *Front. Immunol.* **2021**, *12*, 716860. [CrossRef]
17. Dunn, G.P.; Old, L.J.; Schreiber, R.D. The Three Es of Cancer Immunoediting. *Annu. Rev. Immunol.* **2004**, *22*, 329–360. [CrossRef]
18. Munhoz, R.R.; Postow, M.A. Recent Advances in Understanding Antitumor Immunity. *F1000Research* **2016**, *5*, 2545. [CrossRef]
19. Markov, O.V.; Mironova, N.L.; Vlasov, V.V.; Zenkova, M.A. Molecular and Cellular Mechanisms of Antitumor Immune Response Activation by Dendritic Cells. *Acta Naturae* **2016**, *8*, 17–30. [CrossRef]
20. Elmusrati, A.; Wang, J.; Wang, C.-Y. Tumor Microenvironment and Immune Evasion in Head and Neck Squamous Cell Carcinoma. *Int. J. Oral Sci.* **2021**, *13*, 24. [CrossRef]
21. Wan, Y.Y. Regulatory T Cells: Immune Suppression and Beyond. *Cell. Mol. Immunol.* **2010**, *7*, 204–210. [CrossRef] [PubMed]
22. Pan, Y.; Yu, Y.; Wang, X.; Zhang, T. Tumor-Associated Macrophages in Tumor Immunity. *Front. Immunol.* **2020**, *11*, 583084. [CrossRef] [PubMed]
23. Yang, Y.; Li, C.; Liu, T.; Dai, X.; Bazhin, A.V. Myeloid-Derived Suppressor Cells in Tumors: From Mechanisms to Antigen Specificity and Microenvironmental Regulation. *Front. Immunol.* **2020**, *11*, 1371. [CrossRef] [PubMed]
24. Solomon, B.; Young, R.J.; Rischin, D. Head and Neck Squamous Cell Carcinoma: Genomics and Emerging Biomarkers for Immunomodulatory Cancer Treatments. *Semin. Cancer Biol.* **2018**, *52*, 228–240. [CrossRef] [PubMed]
25. Galluzzi, L.; Vitale, I.; Warren, S.; Adjemian, S.; Agostinis, P.; Martinez, A.B.; Chan, T.A.; Coukos, G.; Demaria, S.; Deutsch, E.; et al. Consensus Guidelines for the Definition, Detection and Interpretation of Immunogenic Cell Death. *J. Immunother. Cancer* **2020**, *8*, e000337. [CrossRef] [PubMed]
26. Kepp, O.; Senovilla, L.; Vitale, I.; Vacchelli, E.; Adjemian, S.; Agostinis, P.; Apetoh, L.; Aranda, F.; Barnaba, V.; Bloy, N.; et al. Consensus Guidelines for the Detection of Immunogenic Cell Death. *Oncoimmunology* **2014**, *3*, e955691. [CrossRef] [PubMed]
27. Galluzzi, L.; Vitale, I.; Aaronson, S.A.; Abrams, J.M.; Adam, D.; Agostinis, P.; Alnemri, E.S.; Altucci, L.; Amelio, I.; Andrews, D.W.; et al. Molecular Mechanisms of Cell Death: Recommendations of the Nomenclature Committee on Cell Death 2018. *Cell Death Differ.* **2018**, *25*, 486–541. [CrossRef]
28. Limagne, E.; Nuttin, L.; Thibaudin, M.; Jacquin, E.; Aucagne, R.; Bon, M.; Revy, S.; Barnestein, R.; Ballot, E.; Truntzer, C.; et al. MEK Inhibition Overcomes Chemoimmunotherapy Resistance by Inducing CXCL10 in Cancer Cells. *Cancer Cell* **2022**, *40*, 136–152.e12. [CrossRef]
29. Jung, A.C.; Moinard-Butot, F.; Thibaudeau, C.; Gasser, G.; Gaiddon, C. Antitumor Immune Response Triggered by Metal-Based Photosensitizers for Photodynamic Therapy: Where Are We? *Pharmaceutics* **2021**, *13*, 1788. [CrossRef]
30. Pozzi, C.; Cuomo, A.; Spadoni, I.; Magni, E.; Silvola, A.; Conte, A.; Sigismund, S.; Ravenda, P.S.; Bonaldi, T.; Zampino, M.G.; et al. The EGFR-Specific Antibody Cetuximab Combined with Chemotherapy Triggers Immunogenic Cell Death. *Nat. Med.* **2016**, *22*, 624–631. [CrossRef]
31. Park, S.-J.; Ye, W.; Xiao, R.; Silvin, C.; Padget, M.; Hodge, J.W.; van Waes, C.; Schmitt, N.C. Cisplatin and Oxaliplatin Induce Similar Immunogenic Changes in Preclinical Models of Head and Neck Cancer. *Oral Oncol.* **2019**, *95*, 127–135. [CrossRef] [PubMed]
32. Tissue-Specific Transcription Factor Pit-1/GHF-1 Binds to the c-Fos Serum Response Element and Activates c-Fos Transcription. Molecular Endocrinology. Oxford Academic. Available online: https://academic.oup.com/mend/article/13/5/742/2741697 (accessed on 27 July 2022).
33. Gottardi, C.J.; Dunbar, L.A.; Caplan, M.J. Biotinylation and Assessment of Membrane Polarity: Caveats and Methodological Concerns. *Am. J. Physiol.-Ren. Physiol.* **1995**, *268*, F285–F295. [CrossRef] [PubMed]
34. Obeid, M.; Tesniere, A.; Ghiringhelli, F.; Fimia, G.M.; Apetoh, L.; Perfettini, J.-L.; Castedo, M.; Mignot, G.; Panaretakis, T.; Casares, N.; et al. Calreticulin Exposure Dictates the Immunogenicity of Cancer Cell Death. *Nat. Med.* **2007**, *13*, 54–61. [CrossRef]
35. Blanchet, A.; Bourgmayer, A.; Kurtz, J.-E.; Mellitzer, G.; Gaiddon, C. Isoforms of the P53 Family and Gastric Cancer: A Ménage à Trois for an Unfinished Affair. *Cancers* **2021**, *13*, 916. [CrossRef] [PubMed]
36. Di Agostino, S.; Sorrentino, G.; Ingallina, E.; Valenti, F.; Ferraiuolo, M.; Bicciato, S.; Piazza, S.; Strano, S.; del Sal, G.; Blandino, G. YAP Enhances the Pro-Proliferative Transcriptional Activity of Mutant P53 Proteins. *EMBO Rep.* **2016**, *17*, 188–201. [CrossRef] [PubMed]

37. Donehower, L.A.; Soussi, T.; Korkut, A.; Liu, Y.; Schultz, A.; Cardenas, M.; Li, X.; Babur, O.; Hsu, T.-K.; Lichtarge, O.; et al. Integrated Analysis of TP53 Gene and Pathway Alterations in The Cancer Genome Atlas. *Cell Rep.* **2019**, *28*, 1370–1384.e5. [CrossRef]
38. Gaiddon, C.; Lokshin, M.; Ahn, J.; Zhang, T.; Prives, C. A Subset of Tumor-Derived Mutant Forms of P53 Down-Regulate P63 and P73 through a Direct Interaction with the P53 Core Domain. *Mol. Cell. Biol.* **2001**, *21*, 1874–1887. [CrossRef]
39. Miller, J.J.; Gaiddon, C.; Storr, T. A Balancing Act: Using Small Molecules for Therapeutic Intervention of the P53 Pathway in Cancer. *Chem. Soc. Rev.* **2020**, *49*, 6995–7014. [CrossRef]
40. Miller, J.J.; Blanchet, A.; Orvain, C.; Nouchikian, L.; Reviriot, Y.; Clarke, R.M.; Martelino, D.; Wilson, D.; Gaiddon, C.; Storr, T. Bifunctional Ligand Design for Modulating Mutant P53 Aggregation in Cancer. *Chem. Sci.* **2019**, *10*, 10802–10814. [CrossRef]
41. Apetoh, L.; Ghiringhelli, F.; Tesniere, A.; Obeid, M.; Ortiz, C.; Criollo, A.; Mignot, G.; Maiuri, M.C.; Ullrich, E.; Saulnier, P.; et al. Toll-like Receptor 4–Dependent Contribution of the Immune System to Anticancer Chemotherapy and Radiotherapy. *Nat. Med.* **2007**, *13*, 1050–1059. [CrossRef]
42. Tokunaga, R.; Zhang, W.; Naseem, M.; Puccini, A.; Berger, M.D.; Soni, S.; McSkane, M.; Baba, H.; Lenz, H.-J. CXCL9, CXCL10, CXCL11/CXCR3 Axis for Immune Activation—A Target for Novel Cancer Therapy. *Cancer Treat. Rev.* **2018**, *63*, 40–47. [CrossRef] [PubMed]
43. Sung, F.L.; Poon, T.C.W.; Hui, E.P.; Ma, B.B.Y.; Liong, E.; To, K.F. Antitumor Effect and Enhancement of Cytotoxic Drug Activity by Cetuximab in Nasopharyngeal Carcinoma Cells. *In Vivo* **2005**, *9*, 237–245.
44. Son, D.J.; Hong, J.E.; Ban, J.O.; Park, J.H.; Lee, H.L.; Gu, S.M.; Hwang, J.Y.; Jung, M.H.; Lee, D.W.; Han, S.-B.; et al. Synergistic Inhibitory Effects of Cetuximab and Cisplatin on Human Colon Cancer Cell Growth via Inhibition of the ERK-Dependent EGF Receptor Signaling Pathway. *BioMed Res. Int.* **2015**, *2015*, e397563. [CrossRef] [PubMed]
45. Jiang, N.; Wang, D.; Hu, Z.; Shin, H.; Qian, G.; Rahman, M.; Zhang, H.; Amin, A.; Nannapaneni, S.; Wang, X.; et al. Combination of Anti-HER3 Antibody MM-121/SAR256212 and Cetuximab Inhibits Tumor Growth in Preclinical Models of Head and Neck Squamous Cell Carcinoma. *Mol. Cancer Ther.* **2014**, *13*, 1826–1836. [CrossRef]
46. Hientz, K.; Mohr, A.; Bhakta-Guha, D.; Efferth, T. The Role of P53 in Cancer Drug Resistance and Targeted Chemotherapy. *Oncotarget* **2017**, *8*, 8921–8946. [CrossRef]
47. Zhou, G.; Liu, Z.; Myers, J.N. TP53 Mutations in Head and Neck Squamous Cell Carcinoma and Their Impact on Disease Progression and Treatment Response. *J. Cell. Biochem.* **2016**, *117*, 2682–2692. [CrossRef]
48. Jiang, Z.; Liu, Z.; Li, M.; Chen, C.; Wang, X. Immunogenomics Analysis Reveals That TP53 Mutations Inhibit Tumor Immunity in Gastric Cancer. *Transl. Oncol.* **2018**, *11*, 1171–1187. [CrossRef]
49. Zhang, H.; Huang, Z.; Song, Y.; Yang, Z.; Shi, Q.; Wang, K.; Zhang, Z.; Liu, Z.; Cui, X.; Li, F. The TP53-Related Signature Predicts Immune Cell Infiltration, Therapeutic Response, and Prognosis in Patients with Esophageal Carcinoma. *Front. Genet.* **2021**, *12*, 607238. [CrossRef]
50. Guo, G.; Yu, M.; Xiao, W.; Celis, E.; Cui, Y. Local Activation of P53 in the Tumor Microenvironment Overcomes Immune Suppression and Enhances Antitumor Immunity. *Cancer Res.* **2017**, *77*, 2292–2305. [CrossRef]
51. Deb, S.P.; Muñoz, R.M.; Brown, D.R.; Subler, M.A.; Deb, S. Wild-Type Human P53 Activates the Human Epidermal Growth Factor Receptor Promoter. *Oncogene* **1994**, *9*, 1341–1349.
52. Ludes-Meyers, J.H.; Subler, M.A.; Shivakumar, C.V.; Munoz, R.M.; Jiang, P.; Bigger, J.E.; Brown, D.R.; Deb, S.P.; Deb, S. Transcriptional Activation of the Human Epidermal Growth Factor Receptor Promoter by Human P53. *Mol. Cell. Biol.* **1996**, *16*, 6009–6019. [CrossRef] [PubMed]
53. Sauer, L.; Gitenay, D.; Vo, C.; Baron, V.T. Mutant P53 Initiates a Feedback Loop That Involves Egr-1/EGF Receptor/ERK in Prostate Cancer Cells. *Oncogene* **2010**, *29*, 2628–2637. [CrossRef] [PubMed]
54. Huang, S.; Benavente, S.; Armstrong, E.A.; Li, C.; Wheeler, D.L.; Harari, P.M. P53 Modulates Acquired Resistance to EGFR Inhibitors and Radiation. *Cancer Res.* **2011**, *71*, 7071–7079. [CrossRef] [PubMed]
55. Bouali, S.; Chrétien, A.-S.; Ramacci, C.; Rouyer, M.; Marchal, S.; Galenne, T.; Juin, P.; Becuwe, P.; Merlin, J.-L. P53 and PTEN Expression Contribute to the Inhibition of EGFR Downstream Signaling Pathway by Cetuximab. *Cancer Gene Ther.* **2009**, *16*, 498–507. [CrossRef]
56. Faridoni-Laurens, L.; Tourpin, S.; Alsafadi, S.; Barrois, M.; Temam, S.; Janot, F.; Koscielny, S.; Bosq, J.; Bénard, J.; Ahomadegbe, J.-C. Involvement of N-Terminally Truncated Variants of P73, DeltaTAp73, in Head and Neck Squamous Cell Cancer: A Comparison with P53 Mutations. *Cell Cycle Georget. Tex* **2008**, *7*, 1587–1596. [CrossRef]
57. Gwosdz, C.; Balz, V.; Scheckenbach, K.; Bier, H. P53, P63 and P73 Expression in Squamous Cell Carcinomas of the Head and Neck and Their Response to Cisplatin Exposure. In *Advances in Oto-Rhino-Laryngology*; Bier, H., Ed.; KARGER: Basel, Switzerland, 2004; pp. 58–71. ISBN 978-3-8055-7789-2.
58. Knickelbein, K.; Tong, J.-S.; Chen, D.; Wang, Y.-J.; Misale, S.; Bardelli, A.; Yu, J.; Zhang, L. Restoring PUMA Induction Overcomes KRAS-Mediated Resistance to Anti-EGFR Antibodies in Colorectal Cancer. *Oncogene* **2018**, *37*, 4599–4610. [CrossRef]
59. Rocco, J.W.; Leong, C.-O.; Kuperwasser, N.; DeYoung, M.P.; Ellisen, L.W. P63 Mediates Survival in Squamous Cell Carcinoma by Suppression of P73-Dependent Apoptosis. *Cancer Cell* **2006**, *9*, 45–56. [CrossRef]
60. Rocco, J.W. p63 and p73: Life and Death in Squamous Cell Carcinoma. *Cell Cycle* **2006**, *5*, 936–940. [CrossRef]

61. Panaretakis, T.; Kepp, O.; Brockmeier, U.; Tesniere, A.; Bjorklund, A.-C.; Chapman, D.C.; Durchschlag, M.; Joza, N.; Pierron, G.; van Endert, P.; et al. Mechanisms of Pre-Apoptotic Calreticulin Exposure in Immunogenic Cell Death. *EMBO J.* **2009**, *28*, 578–590. [CrossRef]
62. Martins, I.; Kepp, O.; Schlemmer, F.; Adjemian, S.; Tailler, M.; Shen, S.; Michaud, M.; Menger, L.; Gdoura, A.; Tajeddine, N.; et al. Restoration of the Immunogenicity of Cisplatin-Induced Cancer Cell Death by Endoplasmic Reticulum Stress. *Oncogene* **2011**, *30*, 1147–1158. [CrossRef]
63. Sims, G.P.; Rowe, D.C.; Rietdijk, S.T.; Herbst, R.; Coyle, A.J. HMGB1 and RAGE in Inflammation and Cancer. *Annu. Rev. Immunol.* **2010**, *28*, 367–388. [CrossRef] [PubMed]
64. Sistigu, A.; Yamazaki, T.; Vacchelli, E.; Chaba, K.; Enot, D.P.; Adam, J.; Vitale, I.; Goubar, A.; Baracco, E.E.; Remédios, C.; et al. Cancer Cell–Autonomous Contribution of Type I Interferon Signaling to the Efficacy of Chemotherapy. *Nat. Med.* **2014**, *20*, 1301–1309. [CrossRef] [PubMed]
65. Judd, N.P.; Allen, C.T.; Winkler, A.E.; Uppaluri, R. Comparative Analysis of Tumor Infiltrating Lymphocytes in a Syngeneic Mouse Model of Oral Cancer. *Octolaryngol.-Head Neck Surg.* **2012**, *147*, 493–500. [CrossRef] [PubMed]
66. Garrido, G.; Rabasa, A.; Sánchez, B.; López, M.V.; Blanco, R.; López, A.; Hernández, D.R.; Pérez, R.; Fernández, L.E. Induction of Immunogenic Apoptosis by Blockade of Epidermal Growth Factor Receptor Activation with a Specific Antibody. *J. Immunol. Baltim. Md 1950* **2011**, *187*, 4954–4966. [CrossRef]
67. Galluzzi, L.; López-Soto, A.; Kumar, S.; Kroemer, G. Caspases Connect Cell-Death Signaling to Organismal Homeostasis. *Immunity* **2016**, *44*, 221–231. [CrossRef]
68. Wu, J.; Waxman, D.J. Immunogenic Chemotherapy: Dose and Schedule Dependence and Combination with Immunotherapy. *Cancer Lett.* **2018**, *419*, 210–221. [CrossRef]
69. Tatarova, Z.; Blumberg, D.C.; Korkola, J.E.; Heiser, L.M.; Muschler, J.L.; Schedin, P.J.; Ahn, S.W.; Mills, G.B.; Coussens, L.M.; Jonas, O.; et al. A Multiplex Implantable Microdevice Assay Identifies Synergistic Combinations of Cancer Immunotherapies and Conventional Drugs. *Nat. Biotechnol.* **2022**, 1–11. [CrossRef]

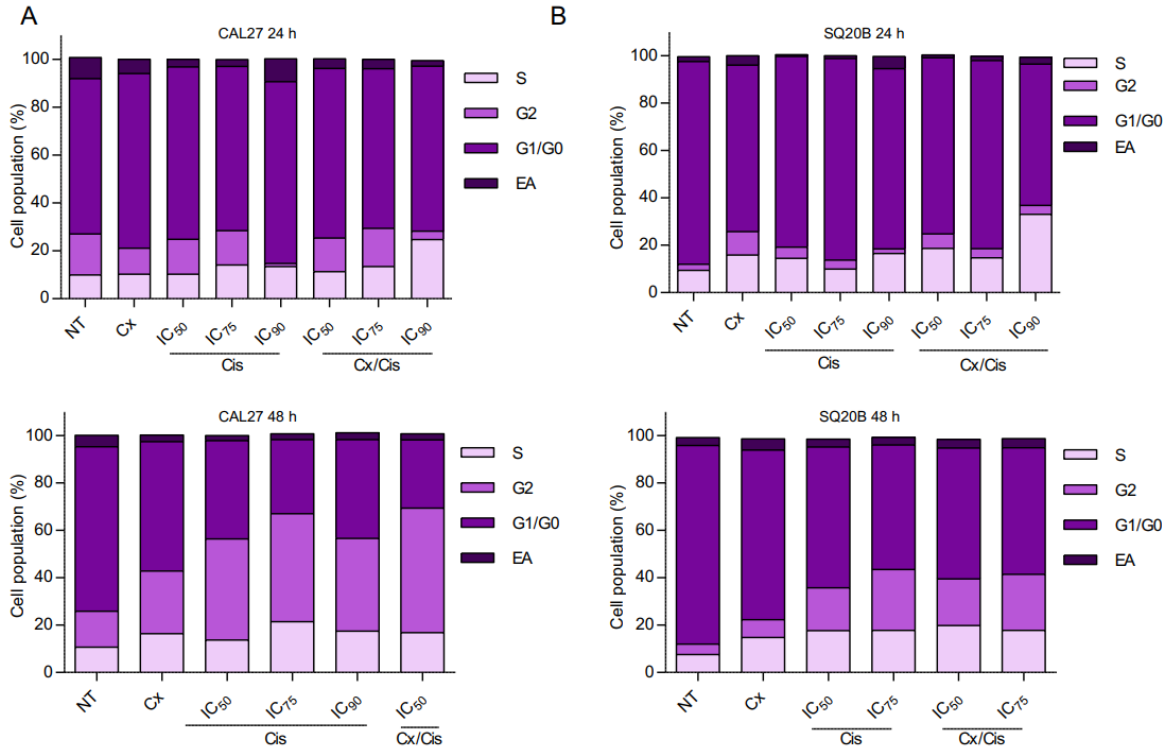

Figure S1. A,B. Quantification of the cell cycle distribution data of CAL27 (A) and SQ20B (B) cells treated 24 h (upper histograms) and 48 h (lower histograms) with cetuximab (Cx), cisplatin (Cis) at the IC50 and IC75 and the Cx/Cis combination. The histograms show the mean number of percentages of cells in S, G2, G1/G0, and early apoptosis (EA; i.e., sub-G1).;.

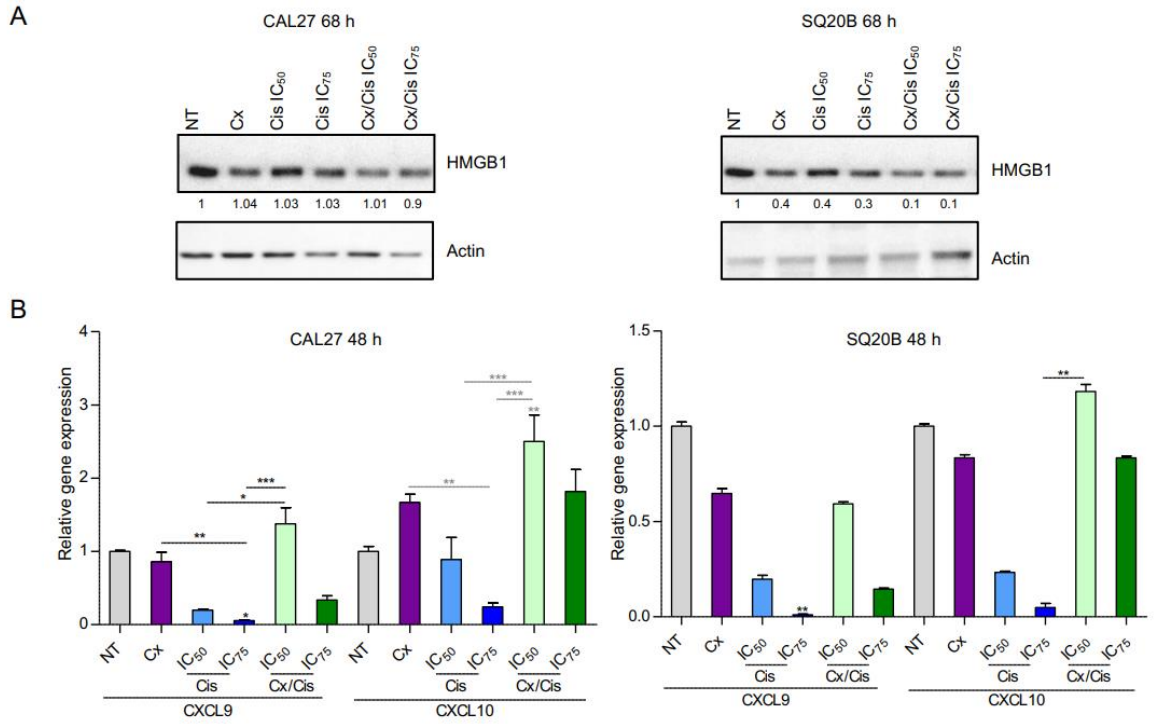

Figure S2. A. Western blot analysis of the HMGB1 expression in the supernatant from CAL27 (left panels) and SQ20B (right panels) cell cultures

harvested 68 h after with cetuximab (Cx), cisplatin (Cis) at the IC50 and IC75 and the Cx/Cis combination. Signals were quantified respectively to the actin loading Cells 2022, 11, x FOR PEER REVIEW 21 of 24 control and normalized with respect to the non-treated control (quantification results are shown). The blots that are shown are re Apresentative examples of three independent experiments. Additional independent biological replicates are shown in supporting documents. B. Analysis of the expression of CXCL9 and CXCL10 by RT-qPCR in CAL27 (left histographs) and SQ20B (right histographs) cells treated for 48 h with cetuximab (Cx), cisplatin (Cis) at the IC50 and IC75 and the Cx/Cis combination. Data are represented as the mean from one independent experiment +SEM;.

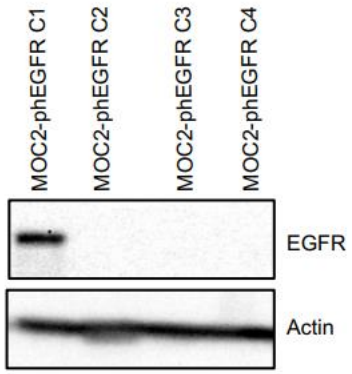

Figure S3. Western blot analysis of EGFR expression in whole-cell protein extracts from MOC-2 cells transduced with a pBABE-hEGFR expression plasmid after selection of clones on puromycin. EGFR expression is observed in the MOC2-phEGFR C1 clone. The blots that are shown are representative examples of three independent experiments;.

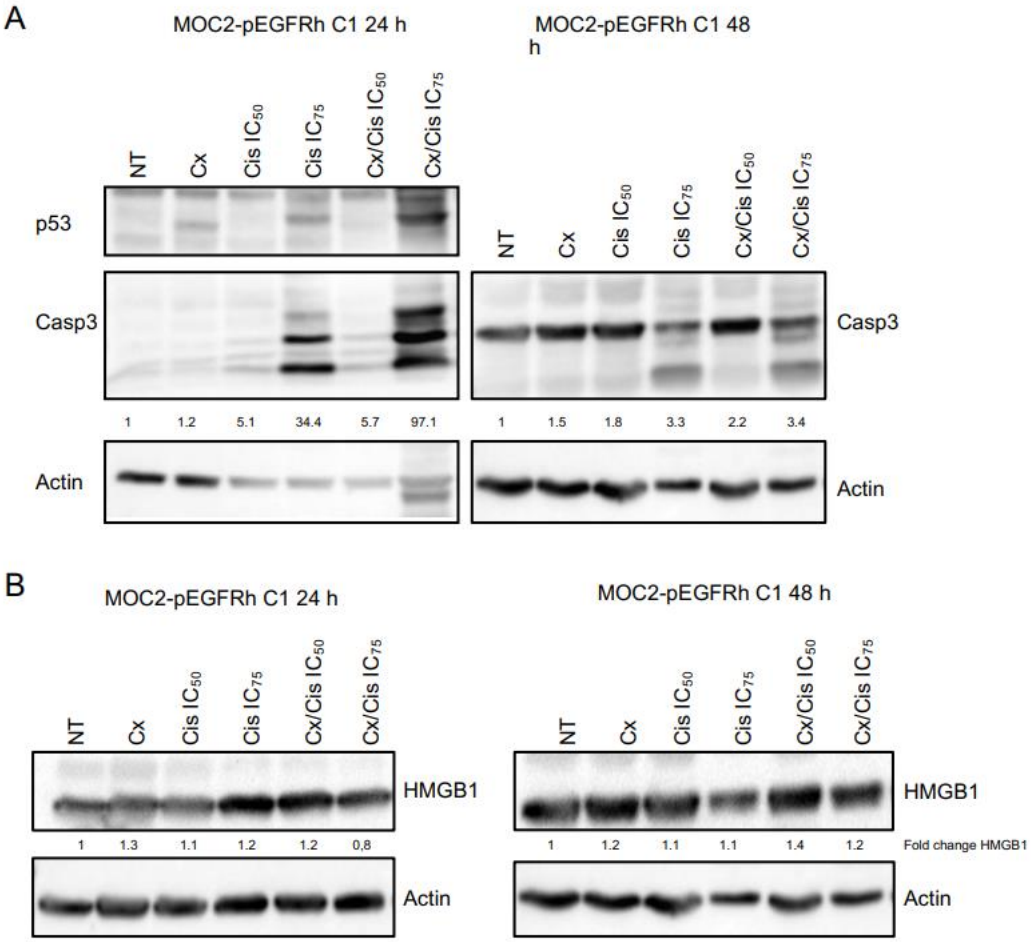

Figure S4. A. Western blot analysis of p53 and cleaved caspase-3 (Casp3) expression in whole protein extracts from MOC2-phEGFR C1 cells treated with cetuximab (Cx), cisplatin (Cis) at the IC50, IC75, and IC90, and the Cx/Cis combination for 24 h (left panels) and 48 h (right panels). Casp3 signals were quantified respectively to the actin loading control and normalized with respect to the non-treated control (quantification results are shown). B. Western blot analysis of the HMGB1 expression in whole protein extracts from MOC2-phEGFR C1 cell cultures treated for 24 h (left panels) and 48 h (right panels) with cetuximab (Cx), cisplatin (Cis) at the IC50, and IC75 and the Cx/Cis combination. Signals were quantified respectively to the actin loading control and normalized with respect to the non-treated control (quantification results are shown). Blots. shown are representative examples of two independent experiments. Additional independent biological replicates are shown in supporting documents.;.

Supplementary tables

Table S1. List of oligonucleotides primers used for RT-qPCR gene expression assays

Gene name	Forward primer (5'-3')	Reverse primer (5'-3')
DDB2	TGGCATCAGTTCGCTTAATG	ACTTCCGTGTCCTGGCTTC
FDRX2	TCCTACTGACCCCACCTGAG	TCGACTCTGCCTCAGTACACC
RPS27L	CAGATCGCTTGCAGCTTG	TCTTCCAAGGACGGATGTAGTAA
ZMAT3	GCCAGGAAAGAAGGGAATG	GCGGGGATTGAAGTAAGGAC
RPLPO	GAAGGCTGTGGTGCTGATGG	CCGGATATGAGGCAGCAGTT
GAPDH	GCACAAGAGGAAGAGAGAGACC	AGGGGAGATTCAGTGTGGTG

Gene names, forward and reverse primer sequences are shown

Table S2. List of TaqMan assays used for RT-qPCR gene expression assays

Gene name	TaqMan gene expression assay ID
CXCL9	Hs00171065_m1
CXC10	Hs00171042_m1
TBP	Hs00427620_m1

Gene names and TaqMan gene expression assay ID are shown

Table S3. List of antibodies used for western blot analysis

Protein	Provider	Antibody dilution
Cleaved caspase-3	Asp175 Cell signaling	1/1000
p53	DO-1 Santa cruz	1/1000
p63	4A4 Abcam	1/1000
p73	EP436Y Abcam	1/1000
Calreticulin	D3E6 Cell signaling	1/1000
EGFR	D38B1 Cell signaling	1/2000
HMGB1	1856 abcam	1/1000 (supernatant) 1/5000 (whole cell extract)
Actin	C4	1/10 000
GAPDH	House made	1/000
BSA	B2901 sigma	1/1000

Protein names, antibody providers and used antibody dilutions are shown.

Complementary Results

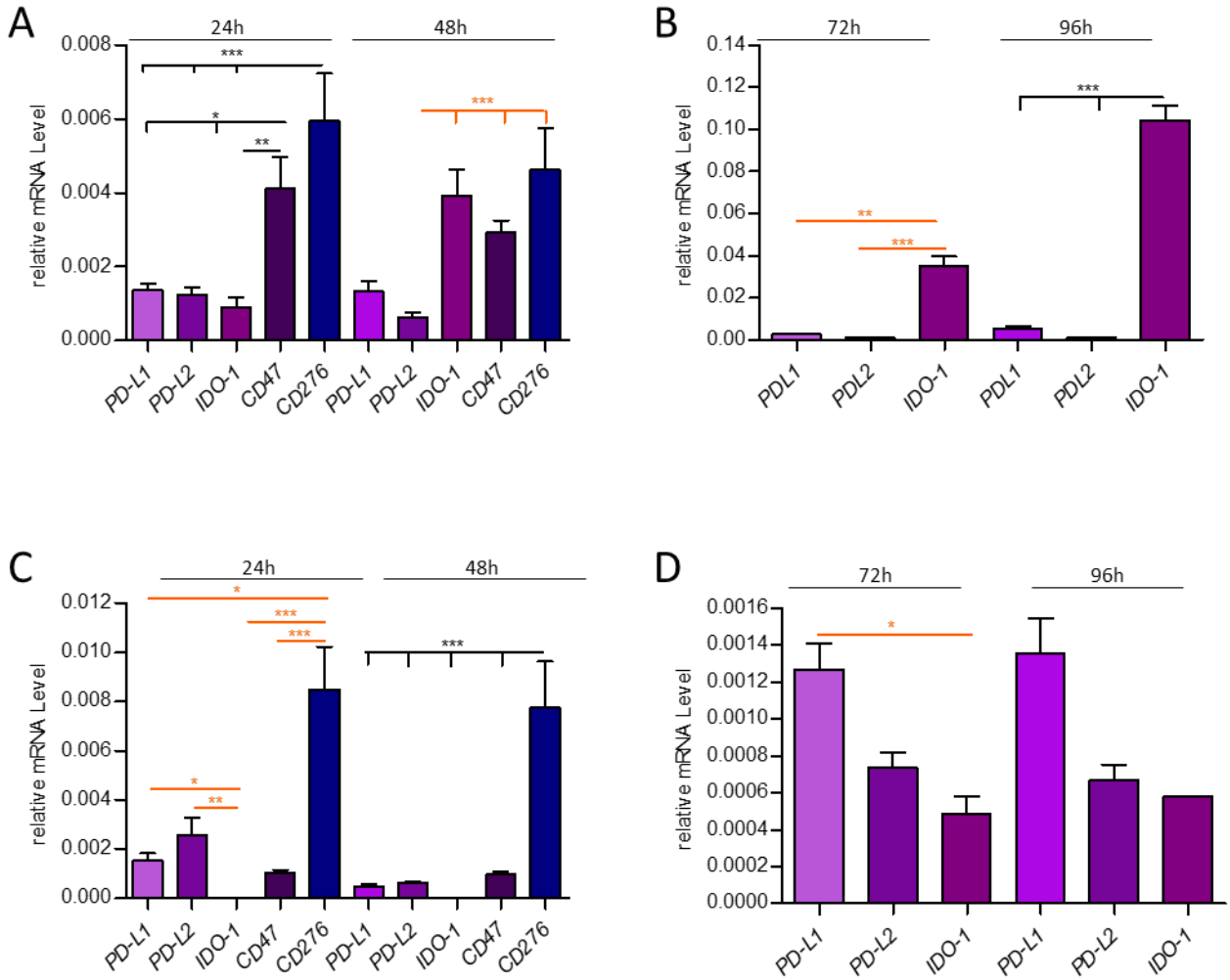

Figure 10: Complementary results 1

Analysis of the expression of the *PD-L1, PD-L2, IDO-1, CD47*, and *CD276*, genes by RT-qPCR in CAL27 (A-B) and SQ20B (C-D) cells incubated from 24h to 86h (3 days). Data is represented as mean from three independent experiments +SEM. The observed differences are statistically significant when: *<p=0.05,**<p=0.01,***<p=0.001 (Anova and post-test Tuckey or Kruskal Wallis and post-test Dunn).

A. Results

ICP are ligand/receptor couples whose function is to regulate the immune system. Tumors hijack this system by expressing inhibitory ICPs in order to escape the immune response and inhibit the cytotoxic activity of T cells. Here, we studied the endogenous gene expression of five ICPs in two head and neck cancer cell lines (Cal27 and SQ20B).

CD276 and CD47 are highly expressed in both cell lines

Cells were cultured according to regular conditions, harvested 24h and 48h after seeding, and RNA was extracted. Thus we measured the basal expression levels of ICPs and their evolution over culture time, and in function of cell confluency. To analyze the expression of PD-L1, PD-L2 and IDO-1 we incubated Cal27 and SQ20B cells for a longer period of time to 3 days and 4 days after seeding. Total RNA was extracted and gene expression was assessed using a RT-qPCR approach and relative gene expression quantification using the $2^{\wedge-\Delta ct}$ method. *CD276* was found to be the ICP gene with the highest expression in both cell lines, and its expression seems stable over time (Fig 10A-D). The second most expressed ICP encoding gene is *CD47*, which is more expressed in Cal27 than in SQ20B (Fig 10A; 10C). Similar to *CD276*, the expression level of CD47 is not modified over time. The relative expression of both *PD-L1* and *PD-L2* was weaker in both lines after 24h of culture and further decreased after 48h, especially in SQ20B cells (Fig 10B; 10C). *IDO-1* is the ICP-encoding gene that displayed the greatest change in expression, with a 2-fold increase after 48h of culture in Cal27 cells (Fig 10A-B). *IDO-1* expression was not detected in SQ20B cells (Fig 10C). In the Cal27 cell line, the relative expression of *PD-L1* is increased by 2-fold and 3-fold after 72h and 86h of culture, respectively (Fig 10B), whereas the relative expression of *PD-L2* is stable (Fig 10B). In contrast, *IDO-1* expression increases to 0.04-fold after 72 h and its expression continues to increase to 0.10-fold after 86 h (Fig 10B). On the contrary, in the SQ20B cell line, *PD-L2* relative expression decreases slightly and *PD-L1* expression does not change (Fig 10D). IDO-1 is detectable after 72h of incubation but at a lower level than the other ICPs (Fig 10D).

Next, we studied the impact of treatments on the expression of these ICPs. Cells were treated with cetuximab (2.5µg/ml) alone, cisplatin alone at IC_{50} or IC_{75}, and with a cetuximab/cisplatin co-treatment at IC_{50} or IC_{75}. Cells were harvested after 6h or 24h of treatment, total RNAs were extracted, and gene expression was analyzed by RT-qPCR. In both lines, the expression of *CD276* and *CD47* was not affected by treatments. After 6h, treatments had no significant effect on the expression of *PD-L1, PD-L2,* and *IDO-1* (Fig 13; Fig 14).

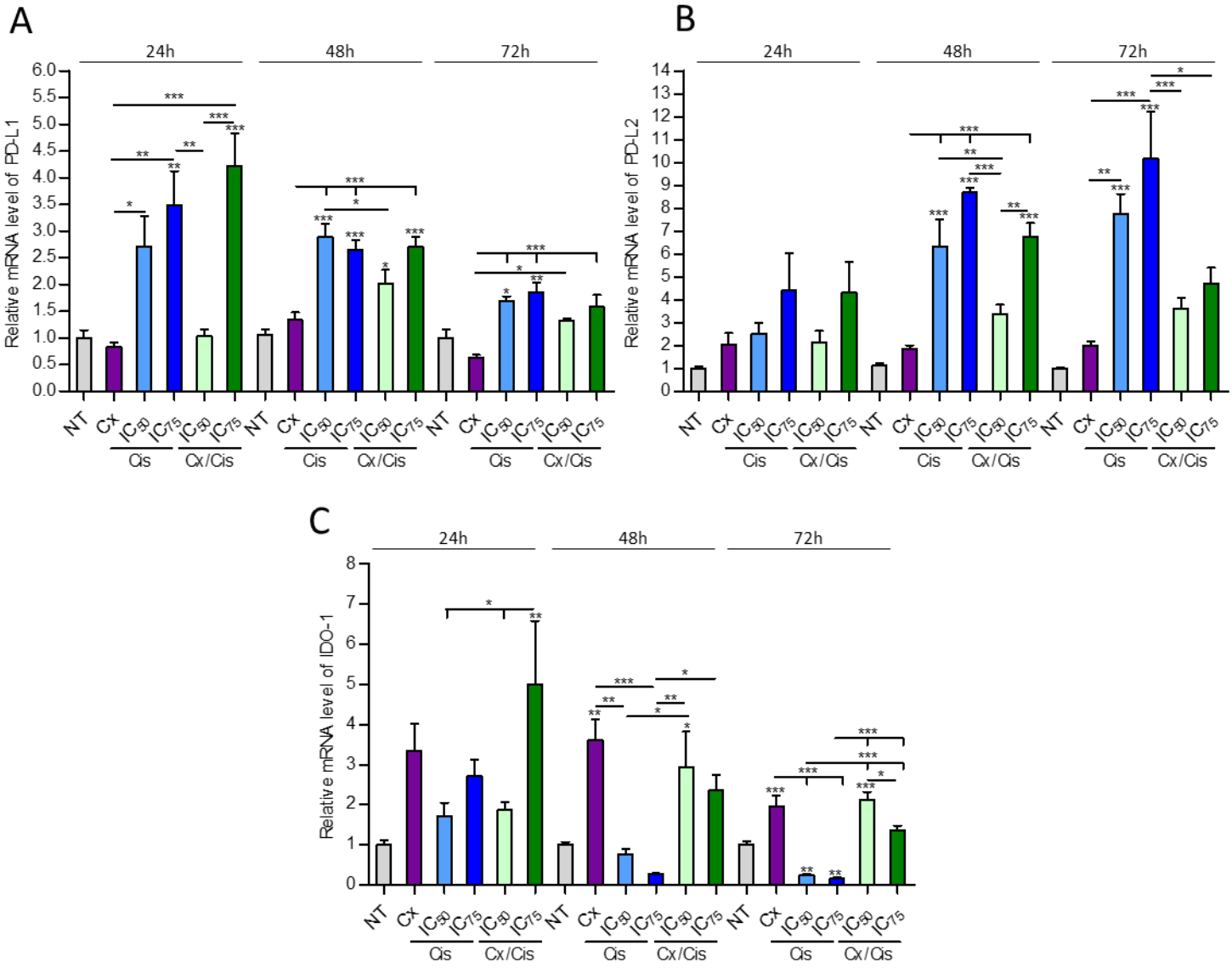

Figure 11: Complementary results 2

Analysis of the expression of the PD-L1 (A), PD-L2 (B), and IDO-1 (C) genes by RT-qPCR in CAL27 cells treated for 24h, 48h, and 72h, with cetuximab (Cx), cisplatin (Cis) at the IC_{50} and IC_{75} and the Cx/Cis combination. Data is represented as mean from three independent experiments +SEM. The observed differences are statistically significant when: *<p=0.05,**<p=0.01,***<p=0.001 (Anova and post-test Tuckey).

Cetuximab/cisplatin combination increased ICPs genes expression

We, therefore, decided to continue this analysis with a longer treatment only in the Cal27 cell line because this cell line shows a higher expression of *PD-L1*, *PD-L2*, and *IDO-1* during long incubation. Treatment with cetuximab had no effect on *PD-L1* expression, and cisplatin alone increased *PD-L1* expression after 24h and 48h of treatment. Co-treatment at IC_{75} increases PD-L1 expression at 24h and 48h of treatment and co-treatment at IC_{50} increases *PD-L1* expression only at 48h of treatment. Co-treatment has no effect on *PD-L1* expression after 72h of treatment (Fig1 1A). Cetuximab slightly increased the expression *PD-L2 (~2 fold),* although this increase was not significant. The impact of cisplatin is more important on *PD-L2* expression than on *PD-L1* expression. The greatest increase in *PD-L2* (~9 fold) expression is obtained after treatment with cisplatin IC_{75}. The only effect of co-treatment on *PD-L2* expression was observed at IC_{75} at 48h of treatment with a 7-fold increase and, as for *PDL1*, co-treatment has no effect on *PD-L2* after 72h (Fig 11B). *IDO-1* expression showed a significant increase upon 48h and 72h of treatment with cetuximab of 4-fold and 3-fold respectively. Cisplatin decreased statistically *IDO-1* expression after 72h of treatment. Co-treatment at IC_{75} increased *IDO-1* expression after 24h of treatment but only the IC_{50} increased *IDO-1* expression after 48h and 72h of treatment (Fig 11C).

Cetuximab has an inverse effect on PD-L1 protein expression depending on the cell line

We subsequently analyzed the expression of the PD-L1 protein, which is the target of the immunotherapy authorized since 2017 for the treatment of HNSCC cancer. Cetuximab has an opposite effect depending on the cell line. Indeed, cetuximab treatment decreased PD-L1 protein expression in Cal27 cells whereas it was increased in SQ20B cells. This effect is particularly striking 24h and 48 h after treatment (Fig 12A;12B). The cetuximab/cisplatin co-treatment had the same impact as cetuximab alone on Cal27 cells (Fig 12A) but decreased PD-L1 expression upon 48h of treatment (but not 24h and 72h) in SQ20B cells (Fig 12B). Cisplatin treatment showed a dose-dependent effect: in Cal27 cells, the IC_{50} of cisplatin increased PD-L1 protein expression after 24h and 48h of treatment, but not after 72h; increased expression was observed upon 72h of treatment with the IC_{75} of cisplatin (Fig 12A). In the SQ20B line, cisplatin alone has little effect on PD-L1 protein expression (Fig 12B).

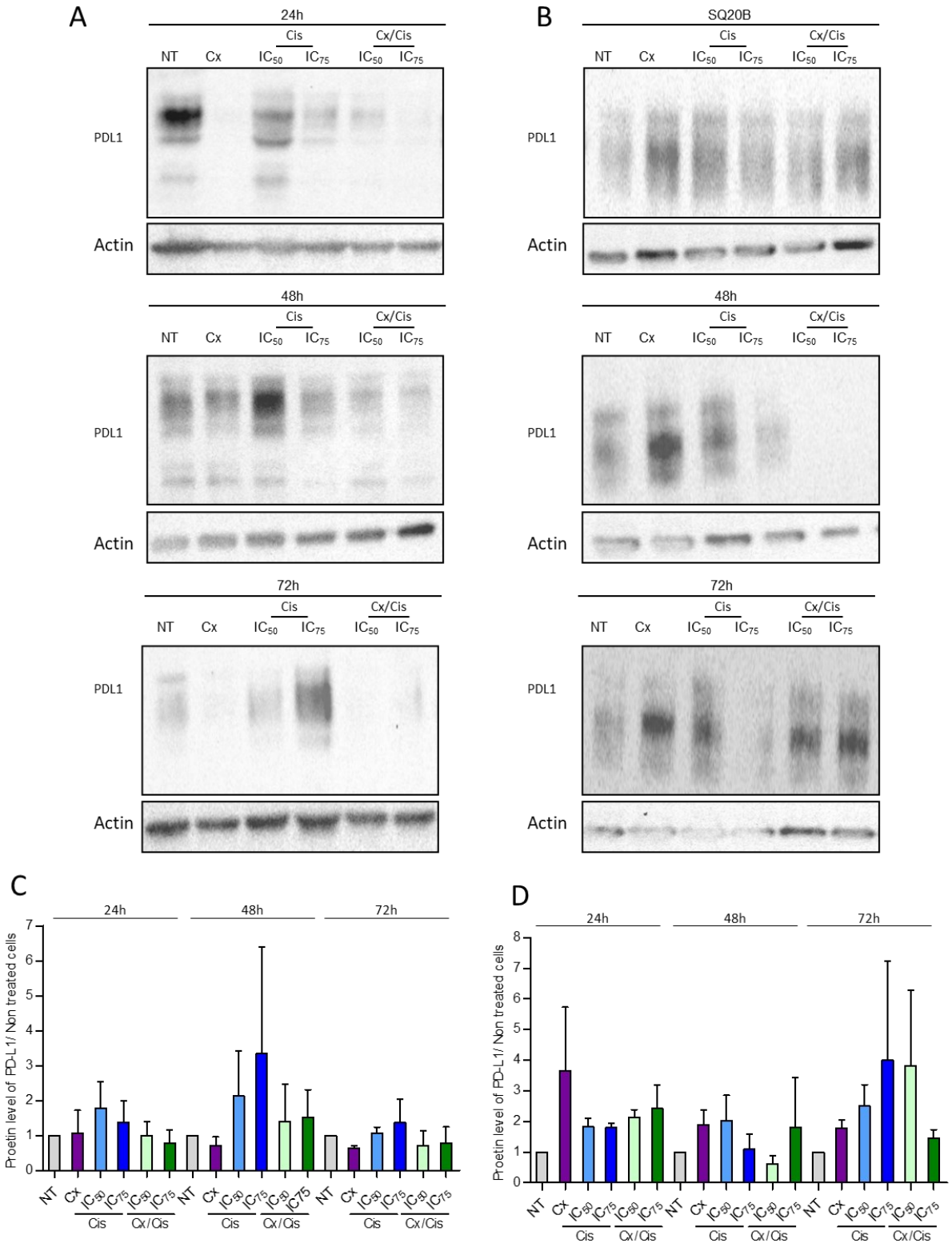

Figure 12: Complementary results 3

Western blot analysis of PD-L1 expression in whole protein extracts from CAL27 (A) and SQ20B (B) cells treated with cetuximab (Cx), cisplatin (Cis) at the IC50, and IC75, and the Cx/Cis combination for 24h, 48h, and 72h. Quantitative analysis of PD-L1 signal obtained by western blot in Cal27 (C) and SQ20B (D) cells. Data is represented as mean from three independent experiments

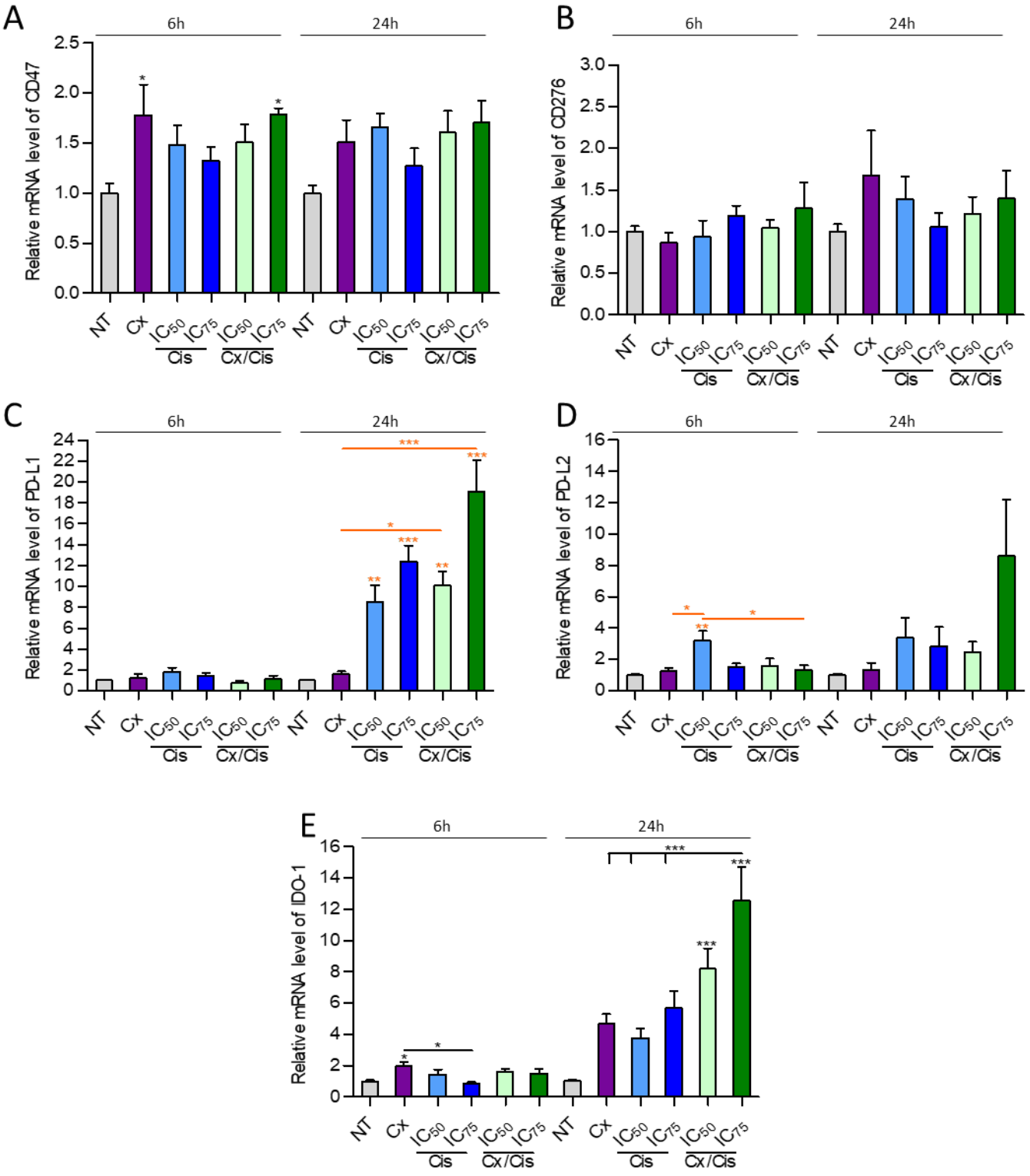

Figure 13: Complementary results 4

Analysis of the expression of the CD47 (A), CD276 (B), PD-L1 (C), and PD-L2 (D) genes by RT-qPCR in SQ20B cells treated for 6h, and 24h, with cetuximab (Cx), cisplatin (Cis) at the IC50 and IC75 and the Cx/Cis combination. Data is represented as mean from three independent experiments +SEM. The observed differences are statistically significant when: *<p=0.05,**<p=0.01,***<p=0.001 (Kruskal Wallis and post-test Dunn).

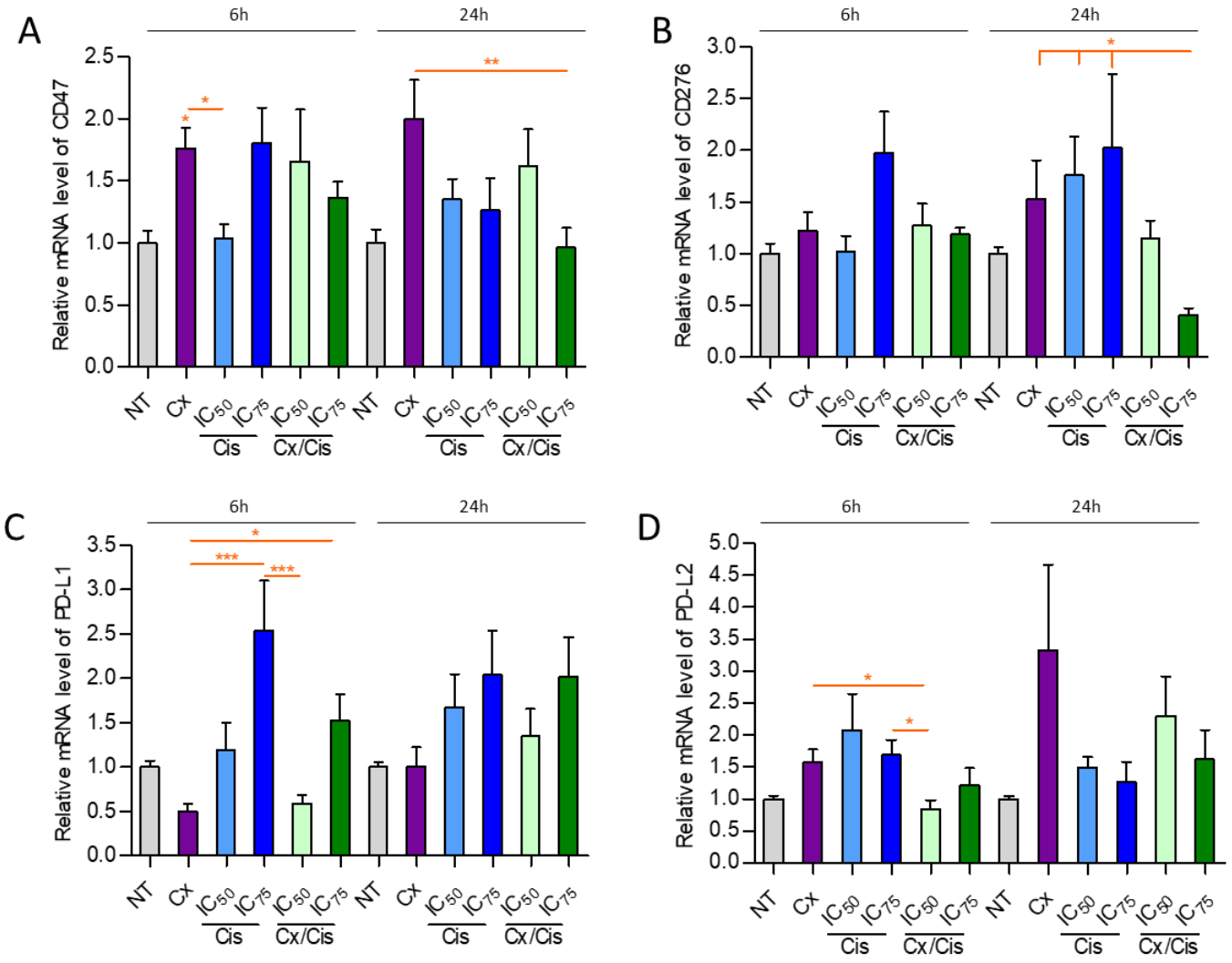

Figure 14: Complementary results 5

Analysis of the expression of the CD47 (A), CD276 (B), PD-L1 (C), and PD-L2 (D) genes by RT-qPCR in SQ20B cells treated for 6h, and 24h, with cetuximab (Cx), cisplatin (Cis) at the IC50 and IC75 and the Cx/Cis combination. Data is represented as mean from three independent experiments +SEM. The observed differences are statistically significant when: *<p=0.05,**<p=0.01,***<p=0.001 (Kruskal Wallis and post-test Dunn).

B. Material and methods

Gene expression assays

Gene expression assays on cultured cells were performed by extracting total RNA from pelleted cells using a standard TRIZol procedure (TRI Reagent®: TR 118 Molecular Research Center), according to the manufacturer's instructions. RNA was retro-transcribed using the High-Capacity cDNA reverse transcription system (Applied Biosystems™), and real-time quantitative PCR was performed using the QuantStudio 3 Real-Time PCR system (Applied Biosystems™). *CD47*, *CD276*, *IDO-1, PD-L1,* and *PD-L2* expression was measured with pairs of specific primers (see Table S5)The expression of genes of interest was normalized to the expression of *TBP*, used as a reference gene, with the $2^{-\Delta\Delta Ct}$ method.

SDS-PAGE and western blot analysis

Total protein extraction was carried out by homogenizing $1E^{06}$ cells in 100µL of 1X Laemmli lysis buffer [6.25mM Tris (pH 6.8), 1%SDS, 1%DTT, protease and phosphatase inhibitors, Sigma]. 20 or 30µg of total proteins were resolved by 6%-15% SDS-PAGE (depending on protein molecular weight) according to standard methods. For the analysis of HMGB1 release in the extracellular medium, 40µL of cells culture supernatant, diluted in SDS-PAGE sample buffer (2X Laemmli lysis buffer, 2X DTT), were resolved by 10% SDS-PAGE. Proteins were detected with primary antibodies raised against PD-L1 (1/1000, cell signaling, E1L3N) or actin (1/10 000, C4). Depending on the host species, blots were probed with secondary antibodies (1/10 000 anti-mouse IgG-HRP linked antibody, Cell Signaling 7076S; 1/10 000 anti-rabbit IgG-HRP linked antibody, Cell Signaling 7074S) Proteins were visualized with enhanced chemiluminescence using the Clarity™ ECL Western blotting Substrate Bio-Rad reagent, according to the manufacturer instructions. Signals were acquired on a Pxi Imager (Syngene®) and were quantified with the ImageJ software.

Table 1 :Complementary: List of oligonucleotides primers used for RT-qPCR gene expression assays

Gene name	**Forward primer (5'-3')**	**Reverse primer (5'-3')**
CD47	ATTGCATGGCCCTCTTCTGA	TCTTTGAATGCATTAAGGGGTTCCT
CD276	CACTGTGGTTCTGCCTCACA	GTCCTGGCCCTCAGCAAAG
IDO-1	TGGCCAGCTTCGAGAAAGAG	TGGCAAGACCTTACGGACATC
PD-L1	CCATACAGCTGAATTGGTCATC	CAGAATTACCAAGTGAGTCCTTTCA
PD-L2	ATTGCAGCTTCACCAGATAGC	AAAGTTGCATTCCAGGGTCAC
RPLPO	GAAGGCTGTGGTGCTGATGG	CCGGATATGAGGCAGCAGTT

Gene names, forward and reverse primer sequences are shown

Discussion

Now… Bring me that horizon.
Captain Jack Sparrow, Pirates of the Caribbean.

HNSCC have a strong infiltration of immune cells in their microenvironment. Unfortunately, the anti-tumor response induced by the immune system can be inhibited by immunosuppressive mechanisms such as the expression of immune checkpoints (ICP) on the surface of tumor cells. These mechanisms allow the tumor to escape the immune system and promote its progression. Restoration of anti-tumor immunity can be achieved by two methods: induction of immunogenic cell death (ICD) or removal of immune checkpoint inhibition by blocking ligand-receptor binding.

ICD makes tumors more immunogenic and activates immune responses. Cetuximab is a therapy targeting EGFR, expressed in 90% of HNSCC, and is used in the treatment of HNSCC. Pozzi *et al* demonstrated the ability of cetuximab to induce ICD in colon cancer.

A. Impact of the EXTREME regimen on HNSCC cell immunogenicity through DAMPs emission and the induction of ICD

Calreticulin exposure was observed in Difi cells after 4h of treatment with cetuximab and we obtained similar results in the same condition in our HNSCC cell lines. Pozzi et al used immunocytofluorecence to detect the membrane translocation of calreticulin using the Abcam2907 anti-calreticulin antibody. We initially used the same antibody using an immunocytofluorescent approach of Cal27 and SQ20B cells. However, confronted with the lack of reproducibility of our results, we evaluated the specificity of this antibody by analyzing the calreticulin expression by a western blot analysis of whole cell protein extracts of Cal27 and SQ20B cells transfected with anti-CRT siRNA. Intriguingly the obtained signal was not lost or diminished after siRNA-mediated gene expression downregulation. We concluded that this antibody was not specific and made several attempts with alternative anti-calreticulin antibodies validated by a siRNA method and selected a monoclonal antibody (data not shown). In addition, we decided to use an alternative detection method based on the purification of plasma membrane protein allowing us to quantify the translocation of calreticulin. Furthermore, we demonstrated the capacity of the combination to induce calreticulin exposure as well.

We demonstrated that cetuximab alone or combined with cisplatin was also able to induce ICD in vivo by vaccination in HNSCC. Pozzi et al generated cetuximab that was unable to induce ADCC and thus demonstrated that this mechanism is not responsible for the induced immune response but rather for the ICD. We did not pursue our research as far in our study of vaccination, but it would be interesting to see if cetuximab induces ICD by the same mechanism, and so independently of ADCC, in HNSCC like in colon cancer. Interestingly, and contrary to the literature, low-dose cisplatin (IC_{50}) alone is also able to induce ICD in HNSSC. The incapacity of cisplatin to induce calreticulin translocation suggested that cisplatin can't induce ICD [155]. But a recent study on HNSCC shows that a high dose of cisplatin, IC_{90},

was able to induce weak ICD with only 2/10 mice vaccinated [154]. In our study, a lower dose of cisplatin (IC_{50}) didn't induce calreticulin exposure but induced other DAMPs and ultimately vaccinate 8/12 mice.

Unexpectedly, a stronger dose (IC_{75}) of cisplatin alone or combined with cetuximab didn't induce ICD while inducing DAMPs expression. It seems that ICD mediated by cisplatin is dose-dependent and is better with low dose (IC_{50}) than with high dose (IC_{90}) [154].

This could be explained by the fact that caspase-3 cleaved is induced at higher levels upon treatment with the IC_{75} of cisplatin and could explain the impact on ICD induction. Actually, caspase-3 can inhibit DAMP like IL-33 cytokine but also inhibits the intracellular responsible for the expression of type-I IFN. Furthermore, caspase-3 activation stimulates the expression of prostaglandin E2 which has an immunosuppressive function on the immune system, and the exposure of phosphatidylserine (PS) on the outer leaflet of cells' plasma membrane. PS is recognized by specific PS receptors and stimulates phagocytosis of apoptotic bodies by macrophages, which delivers an anti-inflammatory signal (see [156] and references therein). Thus, our observations suggest that the intensity of the induction of caspase-3-related cell death could correlate with the modulation of the immunogenicity of cancer cells upon cytotoxic treatment. Therefore, there might be a subtle balance between treatment-induced cell death, which potentially prevents cancer cell immunogenicity via immunomodulatory, and treatment-induced stress, which could result in the improvement of cancer cell immunogenicity. Previous reports show that the impact of chemotherapy drugs on the immunogenicity of a cancer cell depends on the dose used [157]: indeed, to provide a high cytotoxic effect, drugs are often used at their maximum tolerated dose, whereas an anti-tumor effect via the stimulation of the immune system had been observed with suboptimal doses.

B. Impact of the EXTREME regimen on HNSCC cell immunogenicity through the regulation of the expression of ICP

However, the induction of ICD is likely to be ineffective if malignant cells express a high level of ICP. Indeed, the immune response triggered by DAMPs emission and mediated by immune cells such as dendritic cells (DC) and especially the activated T lymphocytes will be inhibited in contact with tumor cells expressing ICP. We, therefore, studied, in parallel to the induction of ICD, the expression of different ICP and their modulation by treatments *in vitro*. We focused on the expression of CD276, CD47, and Indoleamine2,3-dioxygenase (IDO-1), which are not much studied in the HNSCC context, but also on more characterized ICP, like PD-L1 and its homolog PD-L2.

First, we assessed the expression of each ICP, at the transcriptional level, in two HNSCC cell lines, Cal27 and SQ20B. In both cell lines, CD276 was the ICP gene with the highest expression, and with stable expression over cell culture time, consistently with the detection of CD276 in HNSCC patient samples by single cells RNA-seq [158]. CD276 is a type I membrane protein with an extracellular domain similar to PD-L1 and is exclusively expressed on immune cells in physiologic conditions [159]. However, we were able to detect the expression of CD276 at the transcriptional level, suggesting the ability of tumor cells to hijack the expression of ICP to escape the immune system. Indeed, CD276 is known to induce an immunosuppressive response through the inactivation of T cells, or through the reduction of IFN-γ implicated in macrophage activation [160]. The receptors of CD276 haven't been identified yet. One potential candidate CD276 receptor however is the Triggering Receptor Expressed on Myeloid cell (TREM)-like transcript (TLT-2). The binding of CD276 to TLT-2 enhances $CD8^+$ activity in co-culture between mast cell and $CD8^+$ cell, suggesting a stimulatory effect of CD276 [161]. However, this interaction has not been demonstrated in other studies [162]. On the counterpart, CD276 demonstrated inhibitory function in mice immune cells [163], so CD276 function remains controversial. Regardless of its function, CD276 DNA copy number variation and mRNA overexpression in tumor cells compared to healthy tissue has been reported in patients with HNSCC [164] and in a cohort of 18 HNSCC used to perform single-cell RNA-seq [72] the expression of CD276 correlated with shorter OS [158]. Furthermore, CD276 correlated with advanced clinical stage and increased tumor size suggesting its implication in the disease progression [162]. The expression of CD276 in cancer stems cells was proposed to allow HNSCC to escape immune response during cancer initiation, development, and metastasis progression, and is therefore proposed to support tumor progression [165].

The second most expressed ICP is CD47, which is more expressed in Cal27 cells than in SQ20B cells and isn't impacted during cell culture time. CD47 is a transmembrane glycoprotein expressed on normal cells and tissues and inhibits immune response [166]. By binding to Thrombospondin-1, CD47 inactivates T cells [167] but most importantly inhibits macrophages and DC via binding with Signal regulatory protein alpha (SIRPα) [166]. CD47/SIRP-α induces phosphorylation of the ITM domain of SIRP-α and so the recruitment of the SH2 domain-containing phosphatase-1/2. The CD47/SIRP-α sequence is incomplete but the consequence is a deactivation of myosin, a motor protein, and decreased phagocytosis activity [168]. Through this interaction and signalization CD47 act as a "don't eat me" signal that inhibits phagocytosis by the macrophage or DC [167]. The high expression of CD47 in Cal27 and SQ20B may explain the failure of cetuximab-mediated phagocytosis of cancer cells by macrophages *in vitro* phagocytosis assays: most importantly, despite the calreticulin exposure triggered upon treatment with cetuximab, no increased cancer cell uptake by THP-1 macrophages was observed in an *in vitro*

phagocytosis assay (Data not shown). One hypothesis is that CD47 expressed by Cal27 and SQ20B prevents phagocytose even in the presence of calreticulin. Calreticulin binds to a lipoprotein-receptor-related protein (LRP), also called CD91, and induces phagocytosis. But this interaction is counteracted by the expression of CD47, as tumor cells expressing calreticulin can upregulate CD47 to escape phagocytosis. Interestingly, CD47 blockade alone isn't sufficient to restore phagocytosis, which remains dependent on calreticulin exposure [169]. This implicates that anti-CD47 therapy should be combined with phagocytosis inducers but also that the level of CD47 should be taken into consideration in the case of ICD-inducing therapies since calreticulin-dependent phagocytosis has an essential role in immune system activation.

Since our study aimed to determine the impact of cetuximab on ICP expression and so the impact on tumor immunogenicity, and since treatments with cetuximab, cisplatin, and the combination had no impact on the expression of CD276 and CD47 mRNAs in Cal27 and SQ20B cells, no further experiments dedicated to the study of these two ICPs were carried out. However, we cannot rule out at this point that the treatment we used has no impact on the protein expression of these two ICPs.

IDO-1 is only detected at the transcriptional level in the Cal27 cell line, and its expression increased with cell culture time. In HNSCC, IDO-1 is overexpressed compared to normal tissues [170] and is associated with the worst survival when expressed in the tumor[171]. IDO-1 is a rate-limiting enzyme implicated in tryptophan metabolism [172] that is secreted by immune cells and tumors but not expressed by normal tissues [170]. IDO-1 catalyzes the oxidation of tryptophan to kynurenine creating a local tryptophan deficiency leading to T cells inhibition and activation of General Control Nonrepressible 2 (GCN2), a regulator kinase that plays a crucial role in the amino-acid starvation response and that promotes Treg differentiation [172]. In our hands, IDO-1 mRNA expression is increased by cetuximab alone or combined with cisplatin, after prolonged treatment (48h and 72h) and could be due to cetuximab's capacity to induce ICD. IDO-1 gene expression is induced by a danger signal such as type-I IFN, thought IFNAR activation, and inflammation *in vivo* in mice skin [173], and we demonstrated that cetuximab and the co-treatment can trigger the emission of three DAMPs including type-I IFN. It remains to be determined whether the emission of DAMPs and the inflammation created we observed in Cal27 and S20B cells upon treatments is functionally able to regulate the expression of IDO-1, and whether this could modulate the immunogenicity of cancer cells. Interestingly, OSCC patients treated with the Nimotuzumab anti-EGFR antibody display an increase of IDO-1 expression [171]. Therefore, the increase of IDO-1 expression upon treatment of cetuximab with or without cisplatin could induce a resistance mechanism to ICP blockade. Whether this hypothesis applies to HNSCC has still to be determined though. In contrast, treatment with cisplatin alone didn't increase IDO-1 expression levels but decreased IDO-1 expression after 72h.

Chemotherapy is thought to induce IDO-1 expression via stress induction and dying cell-associated DAMPs [171], but it has also been shown that chemotherapy induces IDO-1 mRNA in circulating tumor cells of HNSCC patients [17]. Here, cisplatin didn't induce IDO-1 expression may be due to lower levels of DAMP emission, unlike cetuximab and the co-treatments with cisplatin. In the HNSCC context, IDO-1 immunotherapeutic role needs further characterization [171].

Finally, we focused on the PD-L1 and PD-L2 ICPs. PD-L1 and PD-L2 are types I transmembrane proteins containing a signal domain, the IgV-like domain, and present the same mechanism of action. The binding to their receptor PD-1 induces the phosphorylation of ITIM and ITSM domains which recruit SHP-1/2 and deliver an inhibitory signal to T cells [103] but also regulate Treg differentiation by inducing FOXP3 [172]. In physiological conditions, PD-L2 is only expressed by DC and macrophages [174]. Thus, the detection of PD-L2 expression in SQ20B and Cal27 cells suggests that cancer cell lines from the larynx and tongue can hijack ICPs. In contrast, PD-L1 is expressed by immune cells but also by non-immune tissues including in the heart, lung, placenta, and liver [103].

We found PD-L1 to be expressed at higher levels than PD-L2 in Cal27 and SQ20B cells, unlike previous observations made in HNSCC patients, where PD-L2 is classically more expressed [174], [175]. PD-L2 expression is associated with the worst OS and has immunosuppressive function favoring tumors apparition [174], [176]. In our study, PD-L2 was upregulated upon 48h and 72h of treatment with both the IC_{50} and IC_{75} of cisplatin. In OSCC, cisplatin induces the upregulation of PD-L2 expression through STAT1/3 pathways, as suggested by the fact that an inhibitor of STAT1, fludarabine, and an inhibitor of STAT3, cryptotanshinone, inhibits the cisplatin effect on PD-L2 [176]. At present, it is difficult to hypothesize which signaling pathways are directly triggered by cisplatin and result in the activation of PD-L2 expression. Indeed, the mechanism of the regulation of the expression of PD-L2 has not yet been fully elucidated. For the time being, the STAT3 [177] and STAT6 [178] transcription factors have been identified as required for PD-L2 expression. In addition, the NFκ-B pathway has been shown to regulate the DNA binding abilities of STAT6 [178]. Yet, PD-L2 modulation needs further characterization. On the contrary, PD-L1 expression regulation is better characterized and involves the EGFR signaling pathways. The principal pathway involved in the modulation of PD-L1 expression in HNSCC is JAK2/STAT1 induced by IFN-γ and EGF [179]. The binding between ligand and receptor causes a transphosphorylation of Janus Kinase (JAK) protein kinase. Once activated JAK forms a dock for STAT by binding and phosphorylation of the receptor. Phosphorylated STAT dissociates from JAK and forms hetero or -homodimer and translocates in the nucleus to activate genes transcription like *PD-L1* on Hodgkin lymphoma [180]. EGFR is overexpressed in 80-90% of HNSCC tumors, which may be accompanied by overactivation of downstream pathways [1], notably the JAK/STAT pathways that could explain the impact on PD-L1

expression. Cal27 and SQ20B cells could be good models to test this hypothesis, as they express high levels of EGFR (Data not shown).

Moreover, PD-L1 expression is detected in 60% of HNSCC tumors in a cohort of 134 patients[181] but the association of PD-L1 expression with survival or prognostic is controversial due to variation of PD-L1 expression between studies, but also the variety of thresholds used to stratify PD-L1 expressing tumors as “high-“ or “low-expressing” [182].

Our study shows the different impacts of treatments on PD-L1 expression depending on the cell lines. In Cal27, we observed an increase at the transcription level and on the protein level of PD-L1 with cisplatin treatment alone. We can hypothesize that this could be due to the induction of STAT1 by cisplatin [183] leading to an increase of PD-L1 expression. On the same cell line, we also observe no effect of cetuximab at the transcript level of PD-L1 but we observed a decrease of PD-L1 protein expression. One hypothesis to explain this observation is that the inhibition of the EGFR pathways by cetuximab could block the JAK/STAT pathways, therefore, decreasing PD-L1 expression. Further functional analyses are required to validate these hypotheses.

On the contrary, cetuximab increased the PD-L1 protein level in the SQ20B cell line. SQ20B cell line is more resistant to cetuximab compared to Cal27, and this could be explained by the stabilization of the Hypoxia Inducible Factor 2 (HIF2) transcription factor upon treatment with cetuximab [184]. In normoxic conditions, HIF is degraded by the proteasome but the lack of oxygen in hypoxic conditions inhibits this degradation, allowing HIF to translocate to the nucleus where its transcription factor activity regulates the expression of VEGF to create new vessels. In addition, HIF also regulates a shift in metabolism to aerobic glycolysis, allowing cells to adapt and survive in hypoxia [185]. HIF binds to Hypoxia Element Response on gene promoters and it has been demonstrated that PD-L1 promoter contains these elements [186]. Furthermore, studies show an upregulation of PD-L1 protein under hypoxic conditions suggesting the implication of HIF in the modulation of PD-L1 gene expression [187]. The increase of HIF2 in SQ20B cells mediated by cetuximab treatment could lead to an increase of PD-L1 expression. A functional analysis of the role of HIF2 using siRNA-mediated expression downregulation could be undertaken to challenge this hypothesis.

The experiment using cetuximab and cisplatin co-treatment yielded contradictory results: indeed, we observed an increase of PD-L1 transcript expression and a decrease of PD-L1 protein expression in Cal27 cell lines. In the SQ20B cell line, PD-L1 protein level is increased at 24h and 72h of treatment but decreases at 48h.

Taken together our data shows that the most highly expressed ICP in Cal27 and SQ20B cell lines are CD276 and CD47, which could suggest a strong inhibition of T cells activities and phagocytose respectively. However, the expression of these ICPs is not impacted by treatments in contrast to IDO-1 expression which is increased by cetuximab and cisplatin alone or combined treatment. Cetuximab alone induces an increase of PD-L1 protein in SQ20B only and has the opposite effect on Cal27 with a diminution of PD-L1 proteins. Finally, PD-L1 and PD-L2 expression is increased after 48h and 72h of cisplatin treatment. However, our study has some limitations. The protein expression of CD276 and CD47 were not analyzed, especially the membrane expression of these ligands. This information would allow us to evaluate their potential impact on the immune response. In the case of CD47, a co-culture experiment with macrophages would allow us to see its real impact on phagocytosis, and particularly the co-treatment of cetuximab and anti-CD47 would clearly establish the role of CD47 in ICD. To perform its inhibitory action PD-L1 must be available for ligand access, so it must be located at the cell membrane. We tried to analyze the expression of PD-L1 at the cell membrane by immunocytofluorescent labeling, but only one experiment out of three attempts yielded satisfactory results. This single analysis confirmed the effects observed in the western blot analysis but could not be reproduced (Data not shown). The impact of the immune cell composition of the tumor microenvironment will also play a key role in the response to cetuximab, whether it is the induction of ICD or ADCC. The composition of the TME was analyzed by immnuohistofluorescence but for now, it did not reveal a clear message about the modulation of the TME (Data not shown).

C. General conclusions

Nivolumab and pembrolizumab, two humanized IgG4 mAbs targeting PD-1, are the only immunotherapies approved by the FDA for the management of patients with recurrent/metastatic (R/M) HNSCC [188]. Nivolumab is used after cisplatin therapies without consideration for PD-L1 expression [189], and pembrolizumab is recommended in combination with cisplatin in advanced HNSCC, but pembrolizumab can also be used as monotherapy for patients overexpressing PD-L1 [182]. Our results reinforce the rationale for combining these two immunotherapies with cisplatin since cisplatin increases the expression of PD-L1 and thus increases its PD-1 receptor, suggesting that the immunosuppression in place is mainly through the PD-L1/PD-1 axis. In addition, cisplatin increases PD-L2, which would be responsible for the response to anti-PD1 immunotherapies observed in patients who do not express PD-L1 [174]. Unfortunately, the objective tumor rate response of these two therapies is 15% in HNSCC [182] but it could improve by the induction of ICD mediated by cetuximab. We demonstrated the capacity of cetuximab to induce ICD and so an anti-tumoral response in HNSCC. This response could be a boost to the immune system in the addition of ICP blocked. The impact of cetuximab on PD-L1 is negligible since

patients not expressing PD-L1 also respond to anti-PD-1 and cetuximab could increase PD-L2 to improve the response to anti-PD-1 [182]. To date, a clinical trial combining pembrolizumab and cetuximab is in phase II [189]. However, this immune response may be attenuated or even prevented by CD47 expression. Thus, the relevance to use an antagonist of CD47 in addition to cetuximab remains an open question.

In conclusion, cetuximab is able to modulate HNSCC cell immunogenicity through both the induction of an ICD and the activation of an anti-cancer immune response in pre-clinical models, as well as through the modulation of the expression of immune checkpoints. Through these two mechanisms, cetuximab could influence the immune landscape of the HNSCC microenvironment via the recruitment and/or activation of anti-tumor immune cells. Further studies using syngeneic mice models are necessary to confirm this effect. Cetuximab could also make the tumors more sensitive to immunotherapies through and increased PD-L1 and PD-L2 expression. Interestingly, we found Cetuximab to induce ICD when combined with lower-dose cisplatin. The EXTREME protocol (i.e. cetuximab and cisplatin combination), which is currently used for the management of patients with R/M HNSCC could therefore be able to induce ICD and modulate cancer cell immunogenicity. It remains to be validated whether both the EXTREME protocol and ICP blocking immunotherapies proposed in a therapeutic sequence during patient management confirm to have a potential synergy. This synergy could potentially improve the rate of patients who show long-term tumor response to immunotherapies that target PD-1.

Bibliography

[1] D. E. Johnson, B. Burtness, C. R. Leemans, V. W. Y. Lui, J. E. Bauman, et J. R. Grandis, « Head and neck squamous cell carcinoma », *Nat. Rev. Dis. Primer*, vol. 6, nº 1, Art. nº 1, nov. 2020, doi: 10.1038/s41572-020-00224-3.

[2] F. Bray, J. Ferlay, I. Soerjomataram, R. L. Siegel, L. A. Torre, et A. Jemal, « Global cancer statistics 2018: GLOBOCAN estimates of incidence and mortality worldwide for 36 cancers in 185 countries », *CA. Cancer J. Clin.*, vol. 68, nº 6, p. 394-424, nov. 2018, doi: 10.3322/caac.21492.

[3] F. Faraji *et al.*, « The Genome-Wide Molecular Landscape of HPV-Driven and HPV-Negative Head and Neck Squamous Cell Carcinoma », in *Molecular Determinants of Head and Neck Cancer*, B. Burtness et E. A. Golemis, Éd. Cham: Springer International Publishing, 2018, p. 293-325. doi: 10.1007/978-3-319-78762-6_11.

[4] J.-L. Lefebvre et D. Chevalier, « Épidémiologie des cancers des voies aérodigestives supérieures », *EMC - Oto-Rhino-Laryngol.*, vol. 7, nº 2, p. 1-11, juin 2012, doi: 10.1016/S0246-0351(12)41900-6.

[5] E. Alsahafi *et al.*, « Clinical update on head and neck cancer: molecular biology and ongoing challenges », *Cell Death Dis.*, vol. 10, nº 8, p. 540, juill. 2019, doi: 10.1038/s41419-019-1769-9.

[6] P. Economopoulou, R. de Bree, I. Kotsantis, et A. Psyrri, « Diagnostic Tumor Markers in Head and Neck Squamous Cell Carcinoma (HNSCC) in the Clinical Setting », *Front. Oncol.*, vol. 9, p. 827, août 2019, doi: 10.3389/fonc.2019.00827.

[7] D. M. Gress *et al.*, « Principles of Cancer Staging », in *AJCC Cancer Staging Manual*, M. B. Amin, S. B. Edge, F. L. Greene, D. R. Byrd, R. K. Brookland, M. K. Washington, J. E. Gershenwald, C. C. Compton, K. R. Hess, D. C. Sullivan, J. M. Jessup, J. D. Brierley, L. E. Gaspar, R. L. Schilsky, C. M. Balch, D. P. Winchester, E. A. Asare, M. Madera, D. M. Gress, et L. R. Meyer, Éd. Cham: Springer International Publishing, 2017, p. 3-30. doi: 10.1007/978-3-319-40618-3_1.

[8] D. Reisman et W. T. Loging, « Transcriptional regulation of the p53 tumor suppressor gene », *Semin. Cancer Biol.*, vol. 8, nº 5, p. 317-324, janv. 1998, doi: 10.1006/scbi.1998.0094.

[9] C. R. Leemans, P. J. F. Snijders, et R. H. Brakenhoff, « The molecular landscape of head and neck cancer », *Nat. Rev. Cancer*, vol. 18, nº 5, p. 269-282, mai 2018, doi: 10.1038/nrc.2018.11.

[10] G. Zhou, Z. Liu, et J. N. Myers, « TP53 Mutations in Head and Neck Squamous Cell Carcinoma and Their Impact on Disease Progression and Treatment Response », *J. Cell. Biochem.*, vol. 117, nº 12, p. 2682-2692, déc. 2016, doi: 10.1002/jcb.25592.

[11] M. Fischer, « Census and evaluation of p53 target genes », *Oncogene*, vol. 36, nº 28, p. 3943-3956, juill. 2017, doi: 10.1038/onc.2016.502.

[12] Y. Zhang *et al.*, « Ferredoxin reductase is critical for p53-dependent tumor suppression via iron regulatory protein 2 », *Genes Dev.*, vol. 31, nº 12, p. 1243-1256, juin 2017, doi: 10.1101/gad.299388.117.

[13] C. Gwosdz, V. Balz, K. Scheckenbach, et H. Bier, « p53, p63 and p73 Expression in Squamous Cell Carcinomas of the Head and Neck and Their Response to Cisplatin Exposure », in *Advances in Oto-Rhino-Laryngology*, H. Bier, Éd. Basel: KARGER, 2004, p. 58-71. doi: 10.1159/000082473.

[14] A. Blanchet, A. Bourgmayer, J.-E. Kurtz, G. Mellitzer, et C. Gaiddon, « Isoforms of the p53 Family and Gastric Cancer: A Ménage à Trois for an Unfinished Affair », *Cancers*, vol. 13, nº 4, p. 916, févr. 2021, doi: 10.3390/cancers13040916.

[15] K. Inoue et E. A. Fry, « Chapter: Alterations of p63 and p73 in human cancers », *Subcell. Biochem.*, vol. 85, p. 17-40, 2014, doi: 10.1007/978-94-017-9211-0_2.

[16] A. Jedlinski, A. Ansell, A.-C. Johansson, et K. Roberg, « EGFR status and EGFR ligand expression influence the treatment response of head and neck cancer cell lines: EGFR status influences treatment response », *J. Oral Pathol. Med.*, vol. 42, nº 1, p. 26-36, janv. 2013, doi: 10.1111/j.1600-0714.2012.01177.x.

[17] S. Job *et al.*, « Preferential Response of Basal-Like Head and Neck Squamous Cell Carcinoma Cell Lines to EGFR-Targeted Therapy Depending on EREG-Driven Oncogenic Addiction », *Cancers*, vol. 11, nº 6, p. 795, juin 2019, doi: 10.3390/cancers11060795.
[18] S. Nair, J. A. Bonner, et M. Bredel, « EGFR Mutations in Head and Neck Squamous Cell Carcinoma », *Int. J. Mol. Sci.*, vol. 23, nº 7, p. 3818, mars 2022, doi: 10.3390/ijms23073818.
[19] T. M. Brand, M. Iida, et D. L. Wheeler, « Molecular mechanisms of resistance to the EGFR monoclonal antibody cetuximab », *Cancer Biol. Ther.*, vol. 11, nº 9, p. 777-792, mai 2011, doi: 10.4161/cbt.11.9.15050.
[20] S. Bouali *et al.*, « P53 and PTEN expression contribute to the inhibition of EGFR downstream signaling pathway by cetuximab », *Cancer Gene Ther.*, vol. 16, nº 6, Art. nº 6, juin 2009, doi: 10.1038/cgt.2008.100.
[21] C. H. Chung *et al.*, « Molecular classification of head and neck squamous cell carcinomas using patterns of gene expression », *Cancer Cell*, vol. 5, nº 5, p. 489-500, mai 2004, doi: 10.1016/S1535-6108(04)00112-6.
[22] V. Walter *et al.*, « Molecular subtypes in head and neck cancer exhibit distinct patterns of chromosomal gain and loss of canonical cancer genes », *PloS One*, vol. 8, nº 2, p. e56823, 2013, doi: 10.1371/journal.pone.0056823.
[23] Cancer Genome Atlas Network, « Comprehensive genomic characterization of head and neck squamous cell carcinomas », *Nature*, vol. 517, nº 7536, p. 576-582, janv. 2015, doi: 10.1038/nature14129.
[24] B. Bakir, A. M. Chiarella, J. R. Pitarresi, et A. K. Rustgi, « EMT, MET, Plasticity, and Tumor Metastasis », *Trends Cell Biol.*, vol. 30, nº 10, p. 764-776, oct. 2020, doi: 10.1016/j.tcb.2020.07.003.
[25] L. De Cecco *et al.*, « Head and neck cancer subtypes with biological and clinical relevance: Meta-analysis of gene-expression data », *Oncotarget*, vol. 6, nº 11, p. 9627-9642, mars 2015.
[26] P. M. Glumac et A. M. LeBeau, « The role of CD133 in cancer: a concise review », *Clin. Transl. Med.*, vol. 7, p. 18, juill. 2018, doi: 10.1186/s40169-018-0198-1.
[27] J. Muzaffar, S. Bari, K. Kirtane, et C. H. Chung, « Recent Advances and Future Directions in Clinical Management of Head and Neck Squamous Cell Carcinoma », *Cancers*, vol. 13, nº 2, p. 338, janv. 2021, doi: 10.3390/cancers13020338.
[28] « Understanding the Staging of Head and Neck Cancer », *Cancer Treatment Centers of America*, 10 août 2018. https://www.cancercenter.com/cancer-types/head-and-neck-cancer/stages (consulté le 25 avril 2022).
[29] M.-K. N. D. Hutchinson, M. Mierzwa, et N. J. D'Silva, « Radiation resistance in head and neck squamous cell carcinoma: dire need for an appropriate sensitizer », *Oncogene*, vol. 39, nº 18, Art. nº 18, avr. 2020, doi: 10.1038/s41388-020-1250-3.
[30] T. Bos, J. A. Ratti, et H. Harada, « Targeting Stress-Response Pathways and Therapeutic Resistance in Head and Neck Cancer », *Front. Oral Health*, vol. 2, p. 676643, 2021, doi: 10.3389/froh.2021.676643.
[31] I. Brook, « Late side effects of radiation treatment for head and neck cancer », *Radiat. Oncol. J.*, vol. 38, nº 2, p. 84-92, juin 2020, doi: 10.3857/roj.2020.00213.
[32] J.-P. Machiels, C. René Leemans, W. Golusinski, C. Grau, L. Licitra, et V. Gregoire, « Squamous cell carcinoma of the oral cavity, larynx, oropharynx and hypopharynx: EHNS–ESMO–ESTRO Clinical Practice Guidelines for diagnosis, treatment and follow-up », *Ann. Oncol.*, vol. 31, nº 11, p. 1462-1475, nov. 2020, doi: 10.1016/j.annonc.2020.07.011.
[33] A. B. Griso, L. Acero-Riaguas, B. Castelo, J. L. Cebrián-Carretero, et A. Sastre-Perona, « Mechanisms of Cisplatin Resistance in HPV Negative Head and Neck Squamous Cell Carcinomas », *Cells*, vol. 11, nº 3, p. 561, févr. 2022, doi: 10.3390/cells11030561.
[34] W. Yu *et al.*, « Cisplatin generates oxidative stress which is accompanied by rapid shifts in central carbon metabolism », *Sci. Rep.*, vol. 8, nº 1, p. 4306, déc. 2018, doi: 10.1038/s41598-018-22640-y.

[35] P. Mukhopadhyay *et al.*, « Mitochondrial-targeted antioxidants represent a promising approach for prevention of cisplatin-induced nephropathy », *Free Radic. Biol. Med.*, vol. 52, nº 2, p. 497-506, janv. 2012, doi: 10.1016/j.freeradbiomed.2011.11.001.
[36] K. Mashhour et W. Hashem, « Cisplatin Weekly Versus Every 3 Weeks Concurrently with Radiotherapy in the Treatment of Locally Advanced Head and Neck Squamous Cell Carcinomas: What Is the Best Dosing and Schedule? », *Asian Pac. J. Cancer Prev. APJCP*, vol. 21, nº 3, p. 799-807, mars 2020, doi: 10.31557/APJCP.2020.21.3.799.
[37] A.-M. Florea et D. Büsselberg, « Cisplatin as an Anti-Tumor Drug: Cellular Mechanisms of Activity, Drug Resistance and Induced Side Effects », *Cancers*, vol. 3, nº 1, p. 1351-1371, mars 2011, doi: 10.3390/cancers3011351.
[38] K. Engeland, « Cell cycle regulation: p53-p21-RB signaling », *Cell Death Differ.*, mars 2022, doi: 10.1038/s41418-022-00988-z.
[39] G. Peng, « Exploiting the homologous recombination DNA repair network for targeted cancer therapy », *World J. Clin. Oncol.*, vol. 2, nº 2, p. 73, 2011, doi: 10.5306/wjco.v2.i2.73.
[40] S. Dasari et P. Bernard Tchounwou, « Cisplatin in cancer therapy: Molecular mechanisms of action », *Eur. J. Pharmacol.*, vol. 740, p. 364-378, oct. 2014, doi: 10.1016/j.ejphar.2014.07.025.
[41] W. Kim *et al.*, « Cellular Stress Responses in Radiotherapy », *Cells*, vol. 8, nº 9, Art. nº 9, sept. 2019, doi: 10.3390/cells8091105.
[42] J.-Y. Hong *et al.*, « Computational modeling of apoptotic signaling pathways induced by cisplatin », *BMC Syst. Biol.*, vol. 6, nº 1, p. 122, déc. 2012, doi: 10.1186/1752-0509-6-122.
[43] H. Kalkavan et D. R. Green, « MOMP, cell suicide as a BCL-2 family business », *Cell Death Differ.*, vol. 25, nº 1, p. 46-55, janv. 2018, doi: 10.1038/cdd.2017.179.
[44] R. Perez, T. Crombet, J. de Leon, et E. Moreno, « A view on EGFR-targeted therapies from the oncogene-addiction perspective », *Front. Pharmacol.*, vol. 4, p. 53, avr. 2013, doi: 10.3389/fphar.2013.00053.
[45] A. G. Sacco et F. P. Worden, « Molecularly targeted therapy for the treatment of head and neck cancer: a review of the ErbB family inhibitors », *OncoTargets Ther.*, vol. 9, p. 1927-1943, avr. 2016, doi: 10.2147/OTT.S93720.
[46] J. B. Vermorken *et al.*, « Platinum-Based Chemotherapy plus Cetuximab in Head and Neck Cancer », *N. Engl. J. Med.*, vol. 359, nº 11, p. 1116-1127, sept. 2008, doi: 10.1056/NEJMoa0802656.
[47] P. Specenier et J. B. Vermorken, « Optimizing treatments for recurrent or metastatic head and neck squamous cell carcinoma », *Expert Rev. Anticancer Ther.*, vol. 18, nº 9, p. 901-915, sept. 2018, doi: 10.1080/14737140.2018.1493925.
[48] H. Picon et A. K. Guddati, « Mechanisms of resistance in head and neck cancer », p. 10.
[49] P. Wee et Z. Wang, « Epidermal Growth Factor Receptor Cell Proliferation Signaling Pathways », *Cancers*, vol. 9, nº 5, p. 52, mai 2017, doi: 10.3390/cancers9050052.
[50] A. Kiyota *et al.*, « Anti-Epidermal Growth Factor Receptor Monoclonal Antibody 225 Upregulates $p27^{KIP1}$ and $p15^{INK4B}$ and Induces G1 Arrest in Oral Squamous Carcinoma Cell Lines », *Oncology*, vol. 63, nº 1, p. 92-98, 2002, doi: 10.1159/000065726.
[51] B. Vincenzi, G. Schiavon, M. Silletta, D. Santini, et G. Tonini, « The biological properties of cetuximab », *Crit. Rev. Oncol. Hematol.*, vol. 68, nº 2, p. 93-106, nov. 2008, doi: 10.1016/j.critrevonc.2008.07.006.
[52] F. B. Ozgeris, M. S. Keles, E. Balkan, A. Kara, et N. Kurt, « The Impact of Cetuximab on Apoptotic and Autophagic Gene Expression in Metastatic Colorectal Cancer Cells », p. 12.
[53] B. Liu, M. Fang, M. Schmidt, Y. Lu, J. Mendelsohn, et Z. Fan, « Induction of apoptosis and activation of the caspase cascade by anti-EGF receptor monoclonal antibodies in DiFi human colon cancer cells do not involve the c- jun N-terminal kinase activity », *Br. J. Cancer*, vol. 82, nº 12, p. 1991-1999, juin 2000, doi: 10.1054/bjoc.2000.1201.

[54] M. Mandal, L. Adam, J. Mendelsohn, et R. Kumar, « Nuclear targeting of Bax during apoptosis in human colorectal cancer cells », *Oncogene*, vol. 17, nº 8, p. 999-1007, août 1998, doi: 10.1038/sj.onc.1202020.
[55] G. Tortora *et al.*, « Cooperative inhibitory effect of novel mixed backbone oligonucleotide targeting protein kinase A in combination with docetaxel and anti-epidermal growth factor-receptor antibody on human breast cancer cell growth », *Clin. Cancer Res. Off. J. Am. Assoc. Cancer Res.*, vol. 5, nº 4, p. 875-881, avr. 1999.
[56] J. Heidemann *et al.*, « Angiogenic effects of interleukin 8 (CXCL8) in human intestinal microvascular endothelial cells are mediated by CXCR2 », *J. Biol. Chem.*, vol. 278, nº 10, p. 8508-8515, mars 2003, doi: 10.1074/jbc.M208231200.
[57] S.-M. Huang, J. Li, et P. M. Harari, « Molecular inhibition of angiogenesis and metastatic potential in human squamous cell carcinomas after epidermal growth factor receptor blockade », *Mol. Cancer Ther.*, vol. 1, nº 7, p. 507-514, mai 2002.
[58] J. Kurai *et al.*, « Antibody-Dependent Cellular Cytotoxicity Mediated by Cetuximab against Lung Cancer Cell Lines », *Clin. Cancer Res.*, vol. 13, nº 5, p. 1552-1561, mars 2007, doi: 10.1158/1078-0432.CCR-06-1726.
[59] H. Kimura, K. Sakai, T. Arao, T. Shimoyama, T. Tamura, et K. Nishio, « Antibody-dependent cellular cytotoxicity of cetuximab against tumor cells with wild-type or mutant epidermal growth factor receptor », *Cancer Sci.*, vol. 98, nº 8, p. 1275-1280, août 2007, doi: 10.1111/j.1349-7006.2007.00510.x.
[60] W. Wang, A. K. Erbe, J. A. Hank, Z. S. Morris, et P. M. Sondel, « NK Cell-Mediated Antibody-Dependent Cellular Cytotoxicity in Cancer Immunotherapy », *Front. Immunol.*, vol. 6, p. 368, juill. 2015, doi: 10.3389/fimmu.2015.00368.
[61] X. Yang, X. Zhang, E. D. Mortenson, O. Radkevich-Brown, Y. Wang, et Y.-X. Fu, « Cetuximab-mediated Tumor Regression Depends on Innate and Adaptive Immune Responses », *Mol. Ther.*, vol. 21, nº 1, p. 91-100, janv. 2013, doi: 10.1038/mt.2012.184.
[62] Z. Wang, H. Zhang, Y. Zhai, F. Li, X. Shi, et M. Ying, « Single-Cell Profiling Reveals Heterogeneity of Primary and Lymph Node Metastatic Tumors and Immune Cell Populations and Discovers Important Prognostic Significance of CCDC43 in Oral Squamous Cell Carcinoma », *Front. Immunol.*, vol. 13, p. 843322, mars 2022, doi: 10.3389/fimmu.2022.843322.
[63] A. Elmusrati, J. Wang, et C.-Y. Wang, « Tumor microenvironment and immune evasion in head and neck squamous cell carcinoma », *Int. J. Oral Sci.*, vol. 13, nº 1, p. 24, août 2021, doi: 10.1038/s41368-021-00131-7.
[64] A. K. Palucka et L. M. Coussens, « The Basis of OncoImmunology », *Cell*, vol. 164, nº 6, p. 1233-1247, mars 2016, doi: 10.1016/j.cell.2016.01.049.
[65] W.-W. Lin et M. Karin, « A cytokine-mediated link between innate immunity, inflammation, and cancer », *J. Clin. Invest.*, vol. 117, nº 5, p. 1175-1183, mai 2007, doi: 10.1172/JCI31537.
[66] K. J. Hiam-Galvez, B. M. Allen, et M. H. Spitzer, « Systemic immunity in cancer », *Nat. Rev. Cancer*, vol. 21, nº 6, Art. nº 6, juin 2021, doi: 10.1038/s41568-021-00347-z.
[67] H. Gonzalez, C. Hagerling, et Z. Werb, « Roles of the immune system in cancer: from tumor initiation to metastatic progression », *Genes Dev.*, vol. 32, nº 19-20, p. 1267-1284, oct. 2018, doi: 10.1101/gad.314617.118.
[68] C. A. Janeway, *Immunobiology: the immune system in health and disease*. New York: Garland, 2005.
[69] S. McComb, A. Thiriot, B. Akache, L. Krishnan, et F. Stark, « Introduction to the Immune System », in *Immunoproteomics*, vol. 2024, K. M. Fulton et S. M. Twine, Éd. New York, NY: Springer New York, 2019, p. 1-24. doi: 10.1007/978-1-4939-9597-4_1.

[70] L. Zitvogel, A. Tesniere, et G. Kroemer, « Cancer despite immunosurveillance: immunoselection and immunosubversion », *Nat. Rev. Immunol.*, vol. 6, nº 10, Art. nº 10, oct. 2006, doi: 10.1038/nri1936.
[71] Z. Qi, T. Barrett, A. S. Parikh, I. Tirosh, et S. V. Puram, « Single-cell sequencing and its applications in head and neck cancer », *Oral Oncol.*, vol. 99, p. 104441, déc. 2019, doi: 10.1016/j.oraloncology.2019.104441.
[72] S. V. Puram *et al.*, « Single-Cell Transcriptomic Analysis of Primary and Metastatic Tumor Ecosystems in Head and Neck Cancer », *Cell*, vol. 171, nº 7, p. 1611-1624.e24, déc. 2017, doi: 10.1016/j.cell.2017.10.044.
[73] Z.-D. Huang *et al.*, « Molecular Subtypes Based on Cell Differentiation Trajectories in Head and Neck Squamous Cell Carcinoma: Differential Prognosis and Immunotherapeutic Responses », *Front. Immunol.*, vol. 12, p. 791621, déc. 2021, doi: 10.3389/fimmu.2021.791621.
[74] C. H. L. Kürten *et al.*, « Investigating immune and non-immune cell interactions in head and neck tumors by single-cell RNA sequencing », *Nat. Commun.*, vol. 12, p. 7338, déc. 2021, doi: 10.1038/s41467-021-27619-4.
[75] E. F. Davis-Marcisak *et al.*, « Differential variation analysis enables detection of tumor heterogeneity using single-cell RNA-sequencing data », *Cancer Res.*, vol. 79, nº 19, p. 5102-5112, oct. 2019, doi: 10.1158/0008-5472.CAN-18-3882.
[76] S. M. Y. Chen, A. L. Krinsky, R. A. Woolaver, X. Wang, Z. Chen, et J. H. Wang, « Tumor immune microenvironment in head and neck cancers », *Mol. Carcinog.*, vol. 59, nº 7, p. 766-774, juill. 2020, doi: 10.1002/mc.23162.
[77] Gonzalez-Rodriguez, Villa-Álvarez, Sordo-Bahamonde, Lorenzo-Herrero, et Gonzalez, « NK Cells in the Treatment of Hematological Malignancies », *J. Clin. Med.*, vol. 8, nº 10, p. 1557, sept. 2019, doi: 10.3390/jcm8101557.
[78] I. Osińska, K. Popko, et U. Demkow, « Perforin: an important player in immune response », *Cent.-Eur. J. Immunol.*, vol. 39, nº 1, p. 109-115, 2014, doi: 10.5114/ceji.2014.42135.
[79] M. Bots et J. P. Medema, « Granzymes at a glance », *J. Cell Sci.*, vol. 119, nº 24, p. 5011-5014, déc. 2006, doi: 10.1242/jcs.03239.
[80] X. Yu, Y. A. Chen, J. R. Conejo-Garcia, C. H. Chung, et X. Wang, « Estimation of immune cell content in tumor using single-cell RNA-seq reference data », *BMC Cancer*, vol. 19, p. 715, juill. 2019, doi: 10.1186/s12885-019-5927-3.
[81] « KLRD1 killer cell lectin like receptor D1 [Homo sapiens (human)] - Gene - NCBI ». https://www.ncbi.nlm.nih.gov/gene?Db=gene&Cmd=ShowDetailView&TermToSearch=3824 (consulté le 4 mai 2022).
[82] S. K. Bisheshar, E. J. De Ruiter, L. A. Devriese, et S. M. Willems, « The prognostic role of NK cells and their ligands in squamous cell carcinoma of the head and neck: a systematic review and meta-analysis », *Oncoimmunology*, vol. 9, nº 1, p. 1747345, avr. 2020, doi: 10.1080/2162402X.2020.1747345.
[83] T. Kurosaki, K. Kometani, et W. Ise, « Memory B cells », *Nat. Rev. Immunol.*, vol. 15, nº 3, Art. nº 3, mars 2015, doi: 10.1038/nri3802.
[84] T. Chu, Z. Wang, D. Pe'er, et C. G. Danko, « Cell type and gene expression deconvolution with BayesPrism enables Bayesian integrative analysis across bulk and single-cell RNA sequencing in oncology », *Nat. Cancer*, vol. 3, nº 4, p. 505-517, 2022, doi: 10.1038/s43018-022-00356-3.
[85] M. Norouzian, F. Mehdipour, S. Balouchi Anaraki, M. J. Ashraf, B. Khademi, et A. Ghaderi, « Atypical Memory and Regulatory B Cell Subsets in Tumor Draining Lymph Nodes of Head and Neck Squamous Cell Carcinoma Correlate with Good Prognostic Factors », *Head Neck Pathol.*, vol. 14, nº 3, p. 645-656, sept. 2020, doi: 10.1007/s12105-019-01095-1.
[86] Z. Qi *et al.*, « Single-Cell Deconvolution of Head and Neck Squamous Cell Carcinoma », *Cancers*, vol. 13, nº 6, p. 1230, mars 2021, doi: 10.3390/cancers13061230.

[87] R. Förster, A. C. Davalos-Misslitz, et A. Rot, « CCR7 and its ligands: balancing immunity and tolerance », *Nat. Rev. Immunol.*, vol. 8, nº 5, Art. nº 5, mai 2008, doi: 10.1038/nri2297.
[88] Y. Wang *et al.*, « Dendritic cell biology and its role in tumor immunotherapy », *J. Hematol. Oncol.J Hematol Oncol*, vol. 13, nº 1, p. 107, déc. 2020, doi: 10.1186/s13045-020-00939-6.
[89] A. Gardner et B. Ruffell, « Dendritic Cells and Cancer Immunity », *Trends Immunol.*, vol. 37, nº 12, p. 855-865, déc. 2016, doi: 10.1016/j.it.2016.09.006.
[90] J. Zhou, Z. Tang, S. Gao, C. Li, Y. Feng, et X. Zhou, « Tumor-Associated Macrophages: Recent Insights and Therapies », *Front. Oncol.*, vol. 10, 2020, Consulté le: 6 mai 2022. [En ligne]. Disponible sur: https://www.frontiersin.org/article/10.3389/fonc.2020.00188
[91] C. Zhang, M. Yang, et A. C. Ericsson, « Function of Macrophages in Disease: Current Understanding on Molecular Mechanisms », *Front. Immunol.*, vol. 12, 2021, Consulté le: 6 mai 2022. [En ligne]. Disponible sur: https://www.frontiersin.org/article/10.3389/fimmu.2021.620510
[92] D. Hirayama, T. Iida, et H. Nakase, « The Phagocytic Function of Macrophage-Enforcing Innate Immunity and Tissue Homeostasis », *Int. J. Mol. Sci.*, vol. 19, nº 1, p. 92, déc. 2017, doi: 10.3390/ijms19010092.
[93] « M1 and M2 Macrophages Polarization via mTORC1 Influences Innate Immunity and Outcome of Ehrlichia Infection », *J. Cell. Immunol.*, vol. 2, nº 3, juin 2020, doi: 10.33696/immunology.2.029.
[94] J. M. Hu *et al.*, « CD163 as a marker of M2 macrophage, contribute to predict aggressiveness and prognosis of Kazakh esophageal squamous cell carcinoma », *Oncotarget*, vol. 8, nº 13, p. 21526-21538, févr. 2017, doi: 10.18632/oncotarget.15630.
[95] A. T. Kumar *et al.*, « Prognostic Significance of Tumor-Associated Macrophage Content in Head and Neck Squamous Cell Carcinoma: A Meta-Analysis », *Front. Oncol.*, vol. 9, p. 656, juill. 2019, doi: 10.3389/fonc.2019.00656.
[96] V. Golubovskaya et L. Wu, « Different Subsets of T Cells, Memory, Effector Functions, and CAR-T Immunotherapy », *Cancers*, vol. 8, nº 3, p. 36, mars 2016, doi: 10.3390/cancers8030036.
[97] R. Bacchetta, E. Gambineri, et M.-G. Roncarolo, « Role of regulatory T cells and FOXP3 in human diseases », *J. Allergy Clin. Immunol.*, vol. 120, nº 2, p. 227-235, août 2007, doi: 10.1016/j.jaci.2007.06.023.
[98] H. Raskov, A. Orhan, J. P. Christensen, et I. Gögenur, « Cytotoxic CD8+ T cells in cancer and cancer immunotherapy », *Br. J. Cancer*, vol. 124, nº 2, Art. nº 2, janv. 2021, doi: 10.1038/s41416-020-01048-4.
[99] S. Maleki Vareki, « High and low mutational burden tumors versus immunologically hot and cold tumors and response to immune checkpoint inhibitors », *J. Immunother. Cancer*, vol. 6, p. 157, déc. 2018, doi: 10.1186/s40425-018-0479-7.
[100] Z. Mei, J. Huang, B. Qiao, et A. K. Lam, « Immune checkpoint pathways in immunotherapy for head and neck squamous cell carcinoma », *Int. J. Oral Sci.*, vol. 12, nº 1, Art. nº 1, mai 2020, doi: 10.1038/s41368-020-0084-8.
[101] G. Gaud, R. Lesourne, et P. E. Love, « Regulatory mechanisms in T cell receptor signalling », *Nat. Rev. Immunol.*, vol. 18, nº 8, Art. nº 8, août 2018, doi: 10.1038/s41577-018-0020-8.
[102] V. Sivaganesh, N. Promi, S. Maher, et B. Peethambaran, « Emerging Immunotherapies against Novel Molecular Targets in Breast Cancer », *Int. J. Mol. Sci.*, vol. 22, nº 5, Art. nº 5, janv. 2021, doi: 10.3390/ijms22052433.
[103] S. Ceeraz, E. C. Nowak, et R. J. Noelle, « B7 family checkpoint regulators in immune regulation and disease », *Trends Immunol.*, vol. 34, nº 11, p. 556-563, nov. 2013, doi: 10.1016/j.it.2013.07.003.
[104] M.-L. Alegre, K. A. Frauwirth, et C. B. Thompson, « T-cell regulation by CD28 and CTLA-4 », *Nat. Rev. Immunol.*, vol. 1, nº 3, p. 220-228, déc. 2001, doi: 10.1038/35105024.
[105] N. Joller et V. K. Kuchroo, « Tim-3, Lag-3, and TIGIT », *Curr. Top. Microbiol. Immunol.*, vol. 410, p. 127-156, 2017, doi: 10.1007/82_2017_62.
[106] L. Chocarro *et al.*, « Understanding LAG-3 Signaling », *Int. J. Mol. Sci.*, vol. 22, nº 10, p. 5282, mai 2021, doi: 10.3390/ijms22105282.

[107] Anfray, Ummarino, Andón, et Allavena, « Current Strategies to Target Tumor-Associated-Macrophages to Improve Anti-Tumor Immune Responses », *Cells*, vol. 9, nº 1, p. 46, déc. 2019, doi: 10.3390/cells9010046.
[108] J. M. Bauml, C. Aggarwal, et R. B. Cohen, « Immunotherapy for head and neck cancer: where are we now and where are we going? », *Ann. Transl. Med.*, vol. 7, nº Suppl 3, p. S75, juill. 2019, doi: 10.21037/atm.2019.03.58.
[109] L. Galluzzi *et al.*, « Consensus guidelines for the definition, detection and interpretation of immunogenic cell death », *J. Immunother. Cancer*, vol. 8, nº 1, p. e000337, mars 2020, doi: 10.1136/jitc-2019-000337.
[110] T. L. Aaes et P. Vandenabeele, « The intrinsic immunogenic properties of cancer cell lines, immunogenic cell death, and how these influence host antitumor immune responses », *Cell Death Differ.*, vol. 28, nº 3, p. 843-860, mars 2021, doi: 10.1038/s41418-020-00658-y.
[111] Z. Asadzadeh *et al.*, « Current Approaches for Combination Therapy of Cancer: The Role of Immunogenic Cell Death », *Cancers*, vol. 12, nº 4, p. 1047, avr. 2020, doi: 10.3390/cancers12041047.
[112] S. Gebremeskel et B. Johnston, « Concepts and mechanisms underlying chemotherapy induced immunogenic cell death: impact on clinical studies and considerations for combined therapies », *Oncotarget*, vol. 6, nº 39, p. 41600-41619, déc. 2015, doi: 10.18632/oncotarget.6113.
[113] M. P. Chao *et al.*, « Calreticulin Is the Dominant Pro-Phagocytic Signal on Multiple Human Cancers and Is Counterbalanced by CD47 », *Sci. Transl. Med.*, vol. 2, nº 63, p. 63ra94-63ra94, déc. 2010, doi: 10.1126/scitranslmed.3001375.
[114] T. Panaretakis *et al.*, « The co-translocation of ERp57 and calreticulin determines the immunogenicity of cell death », *Cell Death Differ.*, vol. 15, nº 9, Art. nº 9, sept. 2008, doi: 10.1038/cdd.2008.67.
[115] M. Obeid *et al.*, « Calreticulin exposure dictates the immunogenicity of cancer cell death », *Nat. Med.*, vol. 13, nº 1, p. 54-61, janv. 2007, doi: 10.1038/nm1523.
[116] I. Martins *et al.*, « Restoration of the immunogenicity of cisplatin-induced cancer cell death by endoplasmic reticulum stress », *Oncogene*, vol. 30, nº 10, p. 1147-1158, mars 2011, doi: 10.1038/onc.2010.500.
[117] M. Obeid *et al.*, « Ecto-calreticulin in immunogenic chemotherapy », *Immunol. Rev.*, vol. 220, p. 22-34, déc. 2007, doi: 10.1111/j.1600-065X.2007.00567.x.
[118] J. Dunn et M. H. Grider, « Physiology, Adenosine Triphosphate », in *StatPearls*, Treasure Island (FL): StatPearls Publishing, 2022. Consulté le: 11 mai 2022. [En ligne]. Disponible sur: http://www.ncbi.nlm.nih.gov/books/NBK553175/
[119] O. Kepp *et al.*, « Consensus guidelines for the detection of immunogenic cell death », *Oncoimmunology*, vol. 3, nº 9, p. e955691, déc. 2014, doi: 10.4161/21624011.2014.955691.
[120] M. R. Elliott *et al.*, « Nucleotides released by apoptotic cells act as a find-me signal for phagocytic clearance », *Nature*, vol. 461, nº 7261, p. 282-286, sept. 2009, doi: 10.1038/nature08296.
[121] M. Michaud, X. Xie, J. M. Bravo-San Pedro, L. Zitvogel, E. White, et G. Kroemer, « An autophagy-dependent anticancer immune response determines the efficacy of melanoma chemotherapy », *OncoImmunology*, vol. 3, nº 7, p. e944047, juill. 2014, doi: 10.4161/21624011.2014.944047.
[122] J. Sprooten et A. D. Garg, « Type I interferons and endoplasmic reticulum stress in health and disease », *Int. Rev. Cell Mol. Biol.*, vol. 350, p. 63-118, 2020, doi: 10.1016/bs.ircmb.2019.10.004.
[123] Y.-M. Kim et E.-C. Shin, « Type I and III interferon responses in SARS-CoV-2 infection », *Exp. Mol. Med.*, vol. 53, nº 5, Art. nº 5, mai 2021, doi: 10.1038/s12276-021-00592-0.
[124] L. Galluzzi *et al.*, « Molecular mechanisms of cell death: recommendations of the Nomenclature Committee on Cell Death 2018 », *Cell Death Differ.*, vol. 25, nº 3, Art. nº 3, mars 2018, doi: 10.1038/s41418-017-0012-4.

[125] L. Galluzzi, A. Buqué, O. Kepp, L. Zitvogel, et G. Kroemer, « Immunogenic cell death in cancer and infectious disease », *Nat. Rev. Immunol.*, vol. 17, nº 2, p. 97-111, févr. 2017, doi: 10.1038/nri.2016.107.
[126] S. Lee, M. Kwak, S. Kim, et J. Shin, « The Role of High Mobility Group Box 1 in Innate Immunity », *Yonsei Med. J.*, vol. 55, p. 1165-76, sept. 2014, doi: 10.3349/ymj.2014.55.5.1165.
[127] F. Radogna et M. Diederich, « Stress-induced cellular responses in immunogenic cell death: Implications for cancer immunotherapy », *Biochem. Pharmacol.*, vol. 153, p. 12-23, juill. 2018, doi: 10.1016/j.bcp.2018.02.006.
[128] R. Tokunaga *et al.*, « CXCL9, CXCL10, CXCL11/CXCR3 axis for immune activation - a target for novel cancer therapy », *Cancer Treat. Rev.*, vol. 63, p. 40-47, févr. 2018, doi: 10.1016/j.ctrv.2017.11.007.
[129] P. Pelegrin, « P2X7 receptor and the NLRP3 inflammasome: Partners in crime », *Biochem. Pharmacol.*, vol. 187, p. 114385, mai 2021, doi: 10.1016/j.bcp.2020.114385.
[130] E. Rivas-Yáñez *et al.*, « P2X7 Receptor at the Crossroads of T Cell Fate », *Int. J. Mol. Sci.*, vol. 21, nº 14, p. 4937, juill. 2020, doi: 10.3390/ijms21144937.
[131] W. Ren, P. Rubini, Y. Tang, T. Engel, et P. Illes, « Inherent P2X7 Receptors Regulate Macrophage Functions during Inflammatory Diseases », *Int. J. Mol. Sci.*, vol. 23, nº 1, p. 232, déc. 2021, doi: 10.3390/ijms23010232.
[132] D. Myrtek et M. Idzko, « Chemotactic activity of extracellular nucleotideson human immune cells. », *Purinergic Signal.*, vol. 3, nº 1-2, p. 5-11, mars 2007, doi: 10.1007/s11302-006-9032-0.
[133] D. Klaver et M. Thurnher, « Control of Macrophage Inflammation by P2Y Purinergic Receptors », *Cells*, vol. 10, nº 5, p. 1098, mai 2021, doi: 10.3390/cells10051098.
[134] M. J. Lamberti, A. Nigro, F. M. Mentucci, N. B. Rumie Vittar, V. Casolaro, et J. Dal Col, « Dendritic Cells and Immunogenic Cancer Cell Death: A Combination for Improving Antitumor Immunity », *Pharmaceutics*, vol. 12, nº 3, p. 256, mars 2020, doi: 10.3390/pharmaceutics12030256.
[135] H. Mao, L. Xie, et X. Pi, « Low-Density Lipoprotein Receptor-Related Protein-1 Signaling in Angiogenesis », *Front. Cardiovasc. Med.*, vol. 4, p. 34, mai 2017, doi: 10.3389/fcvm.2017.00034.
[136] P. A. Roche et P. Cresswell, « Antigen Processing and Presentation Mechanisms in Myeloid Cells. », *Microbiol. Spectr.*, vol. 4, nº 3, juin 2016, doi: 10.1128/microbiolspec.mchd-0008-2015.
[137] T. Liu, L. Zhang, D. Joo, et S.-C. Sun, « NF-κB signaling in inflammation », *Signal Transduct. Target. Ther.*, vol. 2, nº 1, Art. nº 1, juill. 2017, doi: 10.1038/sigtrans.2017.23.
[138] H. L. Pahl, « Activators and target genes of Rel/NF-κB transcription factors », *Oncogene*, vol. 18, nº 49, Art. nº 49, nov. 1999, doi: 10.1038/sj.onc.1203239.
[139] C. Hetz, K. Zhang, et R. J. Kaufman, « Mechanisms, regulation and functions of the unfolded protein response », *Nat. Rev. Mol. Cell Biol.*, vol. 21, nº 8, p. 421-438, août 2020, doi: 10.1038/s41580-020-0250-z.
[140] M. G. Metcalf, R. Higuchi-Sanabria, G. Garcia, C. K. Tsui, et A. Dillin, « Beyond the cell factory: Homeostatic regulation of and by the UPR ^{ER} », *Sci. Adv.*, vol. 6, nº 29, p. eabb9614, juill. 2020, doi: 10.1126/sciadv.abb9614.
[141] H. Hu, M. Tian, C. Ding, et S. Yu, « The C/EBP Homologous Protein (CHOP) Transcription Factor Functions in Endoplasmic Reticulum Stress-Induced Apoptosis and Microbial Infection », *Front. Immunol.*, vol. 9, 2019, Consulté le: 12 mai 2022. [En ligne]. Disponible sur: https://www.frontiersin.org/article/10.3389/fimmu.2018.03083
[142] O. Kepp *et al.*, « Viral subversion of immunogenic cell death », *Cell Cycle*, vol. 8, nº 6, p. 860-869, mars 2009, doi: 10.4161/cc.8.6.7939.
[143] T. Panaretakis *et al.*, « Mechanisms of pre-apoptotic calreticulin exposure in immunogenic cell death », *EMBO J.*, vol. 28, nº 5, p. 578-590, mars 2009, doi: 10.1038/emboj.2009.1.
[144] M. Hansen, D. C. Rubinsztein, et D. W. Walker, « Autophagy as a promoter of longevity: insights from model organisms », *Nat. Rev. Mol. Cell Biol.*, vol. 19, nº 9, Art. nº 9, sept. 2018, doi: 10.1038/s41580-018-0033-y.

[145] L. Wang et J. J. Ou, « Hepatitis C virus and autophagy », *Biol. Chem.*, vol. 396, nº 11, p. 1215-1222, nov. 2015, doi: 10.1515/hsz-2015-0172.
[146] L. Galluzzi, O. Kepp, et G. Kroemer, « Enlightening the impact of immunogenic cell death in photodynamic cancer therapy », *EMBO J.*, vol. 31, nº 5, p. 1055-1057, mars 2012, doi: 10.1038/emboj.2012.2.
[147] P.-E. Joubert, I. P. Grégoire, G. Meiffren, C. Rabourdin-Combe, et M. Faure, « Autophagie et pathogènes - « Bon appétit Messieurs ! » », *médecine/sciences*, vol. 27, nº 1, Art. nº 1, janv. 2011, doi: 10.1051/medsci/201127141.
[148] S. Kim, Y. Joe, Y.-J. Surh, et H. Chung, « Differential Regulation of Toll-Like Receptor-Mediated Cytokine Production by Unfolded Protein Response », *Oxid. Med. Cell. Longev.*, vol. 2018, p. 1-8, avr. 2018, doi: 10.1155/2018/9827312.
[149] Y.-J. Wang, R. Fletcher, J. Yu, et L. Zhang, « Immunogenic effects of chemotherapy-induced tumor cell death », *Genes Dis.*, vol. 5, nº 3, p. 194-203, mai 2018, doi: 10.1016/j.gendis.2018.05.003.
[150] H. Liu, Z. He, et H.-U. Simon, « The Role of Autophagy in Cancer and Chemotherapy », in *Autophagy: Cancer, Other Pathologies, Inflammation, Immunity, Infection, and Aging*, Elsevier, 2016, p. 253-265. doi: 10.1016/B978-0-12-802937-4.00014-4.
[151] C. Pozzi *et al.*, « The EGFR-specific antibody cetuximab combined with chemotherapy triggers immunogenic cell death », *Nat. Med.*, vol. 22, nº 6, p. 624-631, juin 2016, doi: 10.1038/nm.4078.
[152] X. Wang *et al.*, « An Immunogenic Cell Death-Related Classification Predicts Prognosis and Response to Immunotherapy in Head and Neck Squamous Cell Carcinoma », *Front. Immunol.*, vol. 12, p. 781466, nov. 2021, doi: 10.3389/fimmu.2021.781466.
[153] P. Economopoulou *et al.*, « Surrogates of immunologic cell death (ICD) and chemoradiotherapy outcomes in head and neck squamous cell carcinoma (HNSCC) », *Oral Oncol.*, vol. 94, p. 93-100, juill. 2019, doi: 10.1016/j.oraloncology.2019.05.019.
[154] S.-J. Park *et al.*, « Cisplatin and oxaliplatin induce similar immunogenic changes in preclinical models of head and neck cancer », *Oral Oncol.*, vol. 95, p. 127-135, août 2019, doi: 10.1016/j.oraloncology.2019.06.016.
[155] M. Obeid *et al.*, « Ecto-calreticulin in immunogenic chemotherapy », *Immunol. Rev.*, vol. 220, nº 1, p. 22-34, déc. 2007, doi: 10.1111/j.1600-065X.2007.00567.x.
[156] L. Galluzzi, A. López-Soto, S. Kumar, et G. Kroemer, « Caspases Connect Cell-Death Signaling to Organismal Homeostasis », *Immunity*, vol. 44, nº 2, p. 221-231, févr. 2016, doi: 10.1016/j.immuni.2016.01.020.
[157] J. Wu et D. J. Waxman, « Immunogenic chemotherapy: Dose and schedule dependence and combination with immunotherapy », *Cancer Lett.*, vol. 419, p. 210-221, avr. 2018, doi: 10.1016/j.canlet.2018.01.050.
[158] W. Lin *et al.*, « Multi-Omics Data Analyses Identify B7-H3 as a Novel Prognostic Biomarker and Predict Response to Immune Checkpoint Blockade in Head and Neck Squamous Cell Carcinoma », *Front. Immunol.*, vol. 12, 2021, Consulté le: 16 mai 2022. [En ligne]. Disponible sur: https://www.frontiersin.org/article/10.3389/fimmu.2021.757047
[159] L. Ni et C. Dong, « New B7 family checkpoints in human cancers », *Mol. Cancer Ther.*, vol. 16, nº 7, p. 1203-1211, juill. 2017, doi: 10.1158/1535-7163.MCT-16-0761.
[160] W.-T. Zhou et W.-L. Jin, « B7-H3/CD276: An Emerging Cancer Immunotherapy », *Front. Immunol.*, vol. 12, 2021, Consulté le: 16 mai 2022. [En ligne]. Disponible sur: https://www.frontiersin.org/article/10.3389/fimmu.2021.701006
[161] M. Hashiguchi, H. Kobori, P. Ritprajak, Y. Kamimura, H. Kozono, et M. Azuma, « Triggering receptor expressed on myeloid cell-like transcript 2 (TLT-2) is a counter-receptor for B7-H3 and enhances T cell responses », *Proc. Natl. Acad. Sci. U. S. A.*, vol. 105, nº 30, p. 10495-10500, juill. 2008, doi: 10.1073/pnas.0802423105.

[162] S. Yang, W. Wei, et Q. Zhao, « B7-H3, a checkpoint molecule, as a target for cancer immunotherapy », *Int. J. Biol. Sci.*, vol. 16, nº 11, p. 1767-1773, mars 2020, doi: 10.7150/ijbs.41105.
[163] W.-K. Suh *et al.*, « The B7 family member B7-H3 preferentially down-regulates T helper type 1–mediated immune responses », *Nat. Immunol.*, vol. 4, nº 9, Art. nº 9, sept. 2003, doi: 10.1038/ni967.
[164] L. Mao *et al.*, « Selective blockade of B7-H3 enhances antitumour immune activity by reducing immature myeloid cells in head and neck squamous cell carcinoma », *J. Cell. Mol. Med.*, vol. 21, nº 9, p. 2199-2210, sept. 2017, doi: 10.1111/jcmm.13143.
[165] C. Wang *et al.*, « CD276 expression enables squamous cell carcinoma stem cells to evade immune surveillance », *Cell Stem Cell*, vol. 28, nº 9, p. 1597-1613.e7, sept. 2021, doi: 10.1016/j.stem.2021.04.011.
[166] T. Qu, B. Li, et Y. Wang, « Targeting CD47/SIRPα as a therapeutic strategy, where we are and where we are headed », *Biomark. Res.*, vol. 10, p. 20, avr. 2022, doi: 10.1186/s40364-022-00373-5.
[167] L. Wu *et al.*, « Anti-CD47 treatment enhances anti-tumor T-cell immunity and improves immunosuppressive environment in head and neck squamous cell carcinoma », *OncoImmunology*, vol. 7, nº 4, p. e1397248, avr. 2018, doi: 10.1080/2162402X.2017.1397248.
[168] M. E. W. Logtenberg, F. A. Scheeren, et T. N. Schumacher, « The CD47-SIRPα immune checkpoint », *Immunity*, vol. 52, nº 5, p. 742-752, mai 2020, doi: 10.1016/j.immuni.2020.04.011.
[169] M. P. Chao *et al.*, « Calreticulin is the dominant pro-phagocytic signal on multiple human cancers and is counterbalanced by CD47 », *Sci. Transl. Med.*, vol. 2, nº 63, p. 63ra94, déc. 2010, doi: 10.1126/scitranslmed.3001375.
[170] M. Liu *et al.*, « Targeting the IDO1 pathway in cancer: from bench to bedside », *J. Hematol. Oncol.J Hematol Oncol*, vol. 11, p. 100, août 2018, doi: 10.1186/s13045-018-0644-y.
[171] D. J. Lin *et al.*, « The immunotherapeutic role of indoleamine 2,3-dioxygenase in head and neck squamous cell carcinoma: A systematic review », *Clin. Otolaryngol. Off. J. ENT-UK Off. J. Neth. Soc. Oto-Rhino-Laryngol. Cervico-Facial Surg.*, vol. 46, nº 5, p. 919-934, sept. 2021, doi: 10.1111/coa.13794.
[172] Y. Wang, Y. Wang, Y. Ren, Q. Zhang, P. Yi, et C. Cheng, « Metabolic modulation of immune checkpoints and novel therapeutic strategies in cancer », *Semin. Cancer Biol.*, p. S1044579X22000311, févr. 2022, doi: 10.1016/j.semcancer.2022.02.010.
[173] A. J. Muller *et al.*, « Chronic inflammation that facilitates tumor progression creates local immune suppression by inducing indoleamine 2,3 dioxygenase », *Proc. Natl. Acad. Sci.*, vol. 105, nº 44, p. 17073-17078, nov. 2008, doi: 10.1073/pnas.0806173105.
[174] Y. Qiao *et al.*, « PD-L2 based immune signature confers poor prognosis in HNSCC », *Oncoimmunology*, vol. 10, nº 1, p. 1947569, doi: 10.1080/2162402X.2021.1947569.
[175] Y. Xu *et al.*, « PD-L2 glycosylation promotes immune evasion and predicts anti-EGFR efficacy », *J. Immunother. Cancer*, vol. 9, nº 10, p. e002699, oct. 2021, doi: 10.1136/jitc-2021-002699.
[176] S. Sudo *et al.*, « Cisplatin-induced programmed cell death ligand-2 expression is associated with metastasis ability in oral squamous cell carcinoma », *Cancer Sci.*, vol. 111, nº 4, p. 1113-1123, avr. 2020, doi: 10.1111/cas.14336.
[177] A. Garcia-Diaz *et al.*, « Interferon Receptor Signaling Pathways Regulating PD-L1 and PD-L2 Expression », *Cell Rep.*, vol. 19, nº 6, p. 1189-1201, mai 2017, doi: 10.1016/j.celrep.2017.04.031.
[178] E. N. Rozali, S. V. Hato, B. W. Robinson, R. A. Lake, et W. J. Lesterhuis, « Programmed Death Ligand 2 in Cancer-Induced Immune Suppression », *Clin. Dev. Immunol.*, vol. 2012, p. 656340, 2012, doi: 10.1155/2012/656340.
[179] F. Concha-Benavente, B. Kansy, J. Moskovitz, J. Moy, U. Chandran, et R. L. Ferris, « PD-L1 Mediates Dysfunction in Activated PD-1 $^{+}$ NK Cells in Head and Neck Cancer Patients », *Cancer Immunol. Res.*, vol. 6, nº 12, p. 1548-1560, déc. 2018, doi: 10.1158/2326-6066.CIR-18-0062.

[180] X. Hu, J. Li, M. Fu, X. Zhao, et W. Wang, « The JAK/STAT signaling pathway: from bench to clinic », *Signal Transduct. Target. Ther.*, vol. 6, nº 1, Art. nº 1, nov. 2021, doi: 10.1038/s41392-021-00791-1.
[181] F. Concha-Benavente *et al.*, « Identification of the cell-intrinsic and extrinsic pathways downstream of EGFR and IFNγ that induce PD-L1 expression in head and neck cancer », *Cancer Res.*, vol. 76, nº 5, p. 1031-1043, mars 2016, doi: 10.1158/0008-5472.CAN-15-2001.
[182] X. Qiao *et al.*, « The Evolving Landscape of PD-1/PD-L1 Pathway in Head and Neck Cancer », *Front. Immunol.*, vol. 11, 2020, Consulté le: 16 mai 2022. [En ligne]. Disponible sur: https://www.frontiersin.org/article/10.3389/fimmu.2020.01721
[183] N. C. Schmitt, S. Trivedi, et R. L. Ferris, « STAT1 Activation is Enhanced by Cisplatin and Variably Affected by EGFR Inhibition in HNSCC Cells », *Mol. Cancer Ther.*, vol. 14, nº 9, p. 2103-2111, sept. 2015, doi: 10.1158/1535-7163.MCT-15-0305.
[184] P. Coliat, L. Ramolu, J. Jégu, C. Gaiddon, A. C. Jung, et E. Pencreach, « Constitutive or Induced HIF-2 Addiction is Involved in Resistance to Anti-EGFR Treatment and Radiation Therapy in HNSCC », *Cancers*, vol. 11, nº 10, p. E1607, oct. 2019, doi: 10.3390/cancers11101607.
[185] Y. Huang, D. Lin, et C. M. Taniguchi, « Hypoxia inducible factor (HIF) in the tumor microenvironment: friend or foe? », *Sci. China Life Sci.*, vol. 60, nº 10, p. 1114-1124, oct. 2017, doi: 10.1007/s11427-017-9178-y.
[186] M. Z. Noman *et al.*, « PD-L1 is a novel direct target of HIF-1α, and its blockade under hypoxia enhanced MDSC-mediated T cell activation », *J. Exp. Med.*, vol. 211, nº 5, p. 781-790, mai 2014, doi: 10.1084/jem.20131916.
[187] K. Hudson, N. Cross, N. Jordan-Mahy, et R. Leyland, « The Extrinsic and Intrinsic Roles of PD-L1 and Its Receptor PD-1: Implications for Immunotherapy Treatment », *Front. Immunol.*, vol. 11, 2020, Consulté le: 18 mai 2022. [En ligne]. Disponible sur: https://www.frontiersin.org/article/10.3389/fimmu.2020.568931
[188] B. Patel et N. F. Saba, « Current Aspects and Future Considerations of EGFR Inhibition in Locally Advanced and Recurrent Metastatic Squamous Cell Carcinoma of the Head and Neck », *Cancers*, vol. 13, nº 14, p. 3545, juill. 2021, doi: 10.3390/cancers13143545.
[189] M. Fasano *et al.*, « Head and neck cancer: the role of anti-EGFR agents in the era of immunotherapy », *Ther. Adv. Med. Oncol.*, vol. 13, p. 1758835920949418, janv. 2021, doi: 10.1177/1758835920949418.

Article annex

I developed the phagocytosis experiment that showed the involvement of ΔNp63 in the regulation of the immune response (Figure 5). Thus, we were able to demonstrate that p63 promotes phagocytosis of cancer cells. This article has been submitted to the journal EMBO.

Université de Strasbourg

Prénom NOM

TITRE de la thèse

École doctorale Sciences de la vie et de la santé | ED 414 Université de Strasbourg

Résumé

Les carcinome épidermoïdes de la tête et du cou (CETC) se développent dans la cavité buccale, le pharynx et le larynx et ont un faible taux de survie à 5 ans d'environ 40% en raison de la résistance des cellules cancéreuses aux thérapies utilisées. L'utilisation d'une thérapie ciblée, le cetuximab, n'a permis qu'un gain modeste en termes de survie des patients. Une nouvelle alternative thérapeutique, appelée immunothérapies, vise à lever le frein que les cellules cancéreuses exercent sur les cellules immunitaires. Dans les essais cliniques, les immunothérapies ont montré une grande efficacité, mais chez peu de patients (environ 20%). L'activation de la mort cellulaire spécifique, appelée mort cellulaire immunogène (MCI), active le système immunitaire et pourrait augmenter la proportion de patients chez qui les immunothérapies sont efficaces. Le cetuximab aurait la capacité de déclencher la MCI dans certains cancers, et donc d'activer le système immunitaire.

Au cours de mon travail de thèse, j'ai pu démontrer que le cetuximab seul ou en combinaison induisait l'émission de signaux de danger représentant la première étape du MCI. J'ai également validé in-vivo l'induction de la MCI par le cetuximab.

Ainsi, j'ai démontré que le cetuximab peut moduler l'immunogénicité des cellules cancéreuses en impactant l'expression des points de contrôle immunitaires et en induisant la MCI.

Cancer de la tête et du cou ; cetuximab ; mort cellulaire immunitaire ; immunothérapies.

Résumé en anglais

HNSCC cancers develop in the oral cavity, pharynx and larynx and have a low 5-year survival rate of approximately 40% due to the resistance of cancer cells to the therapies used. The use of a targeted therapy, cetuximab, has resulted in only a modest gain in patient survival. A new therapeutic alternative, called immunotherapies, aims to remove the brake that cancer cells exert on immune cells. In clinical trials, immunotherapies have shown great efficacy, but in few patients (about 20%). Activation of specific cell death, called immunogenic cell death (ICD), activates the immune system and may increase the proportion of patients in whom immunotherapies are effective. Cetuximab is thought to have the ability to trigger ICD in certain cancers, and thus activate the immune system.

During my thesis work, I was able to demonstrate that cetuximab alone or in combination induced the emission of danger signals representing the first step of ICD. I also validated in-vivo the induction of ICD by cetuximab.

So, I demonstrated that cetuximab can modulate the immunogenicity of cancer cells by impacting the expression of immune checkpoints and inducing ICD.

Head and neck cancer; cetuximab; immune cell death; immunotherapies.